

Lecture Notes in Mechanical Engineering

Henrique A. Almeida  
Joel C. Vasco *Editors*

# Progress in Digital and Physical Manufacturing

Proceedings of ProDPM'19

 Springer

# **Lecture Notes in Mechanical Engineering**

**Lecture Notes in Mechanical Engineering (LNME)** publishes the latest developments in Mechanical Engineering - quickly, informally and with high quality. Original research reported in proceedings and post-proceedings represents the core of LNME. Volumes published in LNME embrace all aspects, subfields and new challenges of mechanical engineering. Topics in the series include:

- Engineering Design
- Machinery and Machine Elements
- Mechanical Structures and Stress Analysis
- Automotive Engineering
- Engine Technology
- Aerospace Technology and Astronautics
- Nanotechnology and Microengineering
- Control, Robotics, Mechatronics
- MEMS
- Theoretical and Applied Mechanics
- Dynamical Systems, Control
- Fluid Mechanics
- Engineering Thermodynamics, Heat and Mass Transfer
- Manufacturing
- Precision Engineering, Instrumentation, Measurement
- Materials Engineering
- Tribology and Surface Technology

To submit a proposal or request further information, please contact the Springer Editor in your country:

**China:** Li Shen at [li.shen@springer.com](mailto:li.shen@springer.com)

**India:** Dr. Akash Chakraborty at [akash.chakraborty@springernature.com](mailto:akash.chakraborty@springernature.com)

**Rest of Asia, Australia, New Zealand:** Swati Meherishi at [swati.meherishi@springer.com](mailto:swati.meherishi@springer.com)

**All other countries:** Dr. Leontina Di Cecco at [Leontina.dicecco@springer.com](mailto:Leontina.dicecco@springer.com)

To submit a proposal for a monograph, please check our Springer Tracts in Mechanical Engineering at <http://www.springer.com/series/11693> or contact [Leontina.dicecco@springer.com](mailto:Leontina.dicecco@springer.com)

**Indexed by SCOPUS. The books of the series are submitted for indexing to Web of Science.**

More information about this series at <http://www.springer.com/series/11236>

Henrique A. Almeida · Joel C. Vasco  
Editors

# Progress in Digital and Physical Manufacturing

Proceedings of ProDPM'19

 Springer

*Editors*

Henrique A. Almeida  
Polytechnic Institute of Leiria  
Marinha Grande, Portugal

Joel C. Vasco  
Escola Superior de  
Tecnologia e Gestão  
Leiria, Portugal

ISSN 2195-4356                      ISSN 2195-4364 (electronic)  
Lecture Notes in Mechanical Engineering  
ISBN 978-3-030-29040-5            ISBN 978-3-030-29041-2 (eBook)  
<https://doi.org/10.1007/978-3-030-29041-2>

© Springer Nature Switzerland AG 2020

This work is subject to copyright. All rights are reserved by the Publisher, whether the whole or part of the material is concerned, specifically the rights of translation, reprinting, reuse of illustrations, recitation, broadcasting, reproduction on microfilms or in any other physical way, and transmission or information storage and retrieval, electronic adaptation, computer software, or by similar or dissimilar methodology now known or hereafter developed.

The use of general descriptive names, registered names, trademarks, service marks, etc. in this publication does not imply, even in the absence of a specific statement, that such names are exempt from the relevant protective laws and regulations and therefore free for general use.

The publisher, the authors and the editors are safe to assume that the advice and information in this book are believed to be true and accurate at the date of publication. Neither the publisher nor the authors or the editors give a warranty, expressed or implied, with respect to the material contained herein or for any errors or omissions that may have been made. The publisher remains neutral with regard to jurisdictional claims in published maps and institutional affiliations.

This Springer imprint is published by the registered company Springer Nature Switzerland AG  
The registered company address is: Gewerbestrasse 11, 6330 Cham, Switzerland

# Preface

The “Progress in Digital and Physical Manufacturing” book contains keynotes and papers presented at the first International Conference on Progress in Digital and Physical Manufacturing (ProDPM’19), organized by the School of Technology and Management (ESTG) of the Polytechnic Institute of Leiria (IPLeiria), from October 2 to 4, 2019.

This international conference aims to provide a major international forum for the scientific exchange of multi-disciplinary and inter-organizational aspects performed by academics, researchers, and industrial partners in order to exchange ideas in the field of digital and physical manufacturing and related areas. It represents a significant contribution to the current advances in industrial digital and physical manufacturing issues as it contains topical research in this field.

The ProDPM’19 conference expects to foster networking and collaboration among participants to advance the knowledge and identify major trends in the field. The conference addresses to industrial challenges focused on current market demands and actual technological trends, such as mass customization, new business, and industrial models or predictive engineering. Its contribution in science and technology developments leads to more suitable, effective, and efficient products, materials, and processes, generating added value for the industry and promoting the awareness of the role and importance of the digital and physical manufacturing development in the society.

This book is, therefore, an essential reading for all of those working on digital and physical manufacturing, promoting better links between the academia and the industry. The conference papers will cover a wide range of important topics like additive manufacturing, biomanufacturing, advanced and smart manufacturing technologies, rapid tooling, micro-fabrication, virtual environments, simulation and 3D CAD and data acquisition, materials, and collaborative design.

We are deeply grateful to the keynote speakers, authors, participants, reviewers, the International Scientific Committee, session chairs, student helpers and administrative assistants, for contributing to the success of this conference.

Henrique Almeida  
Joel Vasco  
Conference Co-chairs

# Conference Committees

## Conference Co-chairs

Henrique de Amorim Almeida	Mechanical Engineering Department, School of Technology and Management, Polytechnic Institute of Leiria, Leiria, Portugal henrique.almeida@ipleiria.pt
Joel Oliveira Correia Vasco	Mechanical Engineering Department, School of Technology and Management, Polytechnic Institute of Leiria, Leiria, Portugal joel.vasco@ipleiria.pt

## Organizing Committee

Anabela Gonçalves Rodrigues Marto  
Carlos Alexandre Bento Capela  
Dino Miguel Fernandes Freitas  
Flávio Gabriel da Silva Craveiro  
Helena Maria Coelho da Rocha Terreiro Galha Bártolo  
Luis Manuel de Jesus Coelho  
Mário António Simões Correia  
Milena Maria Nogueira Vieira  
Rui Miguel Barreiros Ruben

## Scientific Committee

Alain Bernard	École Centrale de Nantes, France
Andrew Boydston	University of Washington, USA
António Augusto Magalhães Cunha	University of Minho, Portugal
António Pouzada	University of Minho, Portugal



Bopaya Bidanda	University of Pittsburgh, USA
Dachamir Hotza	Federal University of Santa Catarina, Brazil
David Rosen	Georgia Institute of Technology, USA
Eujin Pei	Brunel University, UK
Fernando Moreira da Silva	University of Lisbon, Portugal
Ian Campbell	Loughborough University, UK
Igor Drstvensek	University of Maribor, Slovenia
Jan T. Sehr	Ruhr University Bochum, Germany
Jean-Yves Hascoet	Ecole Centrale de Nantes, France
João Manuel R. S. Tavares	University of Porto, Portugal
Joaquim de Ciurana	University of Girona, Spain
Jorge Vicente Lopes da Silva	CENPRA, Brazil
Jorge Vilanova	EADS, Spain
José Carlos Caldeira	INESC TEC, Porto, Portugal
José Carlos Lino	University of Minho, Portugal
José Pinto Duarte	Pennsylvania State University, USA
José Simões	Escola Superior de Artes e Design, Portugal
José Rui Marcelino	University of Lisbon, Portugal
Jukka Tuomi	Helsinki University of Technology, Finland
Júlio César Viana	University of Minho, Portugal
Lihui Wang	KTH Royal Institute of Technology, Sweden
Luigi Galantucci	Politecnico di Bari, Italy
Mario Domingo Monzón Verona	University of Las Palmas de Gran Canaria, Spain
Nickolas Sapidis	University of Western Macedonia, Greece
Omar Fergani	Siemens, Germany
Paulo Bártolo	University of Manchester, UK
Paulo Fernandes	Instituto Superior Técnico, Portugal
Paulo Lisboa	Liverpool John Moores University, UK
Patrik Ohldin	Freemelt, Sweden
Pedro Filipe do Carmo Cunha	Polytechnic Institute of Setubal, Portugal
Pedro Miguel Gomes Januário	University of Lisbon, Portugal
Renato Manuel Natal Jorge	University of Porto, Portugal
Ricardo Jardim-Gonçalves	GRIS - Uninova, Portugal
Richard Bibb	Loughborough University, UK
Rita Assoreira Almendra	University of Lisbon, Portugal
Ryan Wicker	University of Texas at El Paso, USA
Steinar Killi	Oslo School of Architecture and Design, Norway
Tahar Laoui	King Fahd University of Petroleum and Minerals, Saudi Arabia
Tatjana Spahiu	Polytechnic University of Tirana, Albania
Terry Wohlers	Wohlers Associates, USA
Tugrul Ozel	Rutgers University, USA

## Acknowledgments and Sponsors

The editors and conference co-chairs wish to acknowledge for the support and sponsorship given in the organization of the *ProDPM'19 – International Conference on Progress in Digital and Physical Manufacturing*:

### Main Sponsors



### Event Sponsors



### Institutional Sponsors



# Invited Lectures

The conference had the privilege of including in the scientific program the following world-renown speakers:

## **Alain Bernard, École Centrale de Nantes, France**

Prof. Alain Bernard, 1960, graduated in 1982, PhD in 1989, was Associate Professor, from 1990 to 1996 in Centrale Paris. In 1996, he got Full Professor position in University Nancy I, in the “Integrated Design and Manufacturing” team, and moved to Centrale Nantes in 2001 where he was Dean for Research (2007–2012). He is Researcher in Digital Sciences Laboratory (LS2N-UMR CNRS 6004) in the “Systems Engineering” (IS3P) team. Recent research topics are KBE applied to computer-aided decision-making systems for additive manufacturing. He is Vice-President of the French Additive Manufacturing Association (AFPR), CIRP Fellow and Member of the French National Academy of Technologies.

## **Bruno Romero, HP Inc.**

Bruno Romero is the Iberia 3D Printing Applications Engineer of HP’s 3D Printing Jet Fusion Business. This position includes supporting Spain and Portugal sales team and transferring HP’s 3D Printing knowledge to partners and customers. Main team is based in Barcelona, Spain. Bruno joined HP in 2017 in the 3D Printing Sales organization and Applications Development team. In this position he is connected to Business Development, Sales, Marketing and R&D teams but also to the WW Applications Development team.

## **Carlos Mougueira, TRUMPF, Portugal**

Carlos Mougueira has been Employee at TRUMPF Portugal since 2015 as Sales Engineer responsible for Laser Division in Aerospace, Automotive and Metalworking sectors. He graduated in Mechatronic Engineering from Universidade de Évora and has gained experience in Laser Technology and Systems in Portuguese and Spanish industries during more than 10 years.

**Eujin Pei, Brunel University London, UK**

Dr. Eujin Pei is Director for Postgraduate Research and Program Director for the BSc Product Design and BSc Product Design Engineering programs at Brunel University London. He is a Chartered Engineer (CEng) and a Technological Product Designer (CTPD) with the Institution of Engineering Designers. He is Convenor of the International Organization for Standardization ISO/TC261/WG4 committee that is responsible for Data Transfer and Design Standards for Additive Manufacturing and Chair for the British Standards Institute BSI/AMT/008 for Additive Manufacturing. His research interest centers on functionally graded additive manufacturing and 4D printing.

**Igor Drstvensek, University of Maribor, Slovenia**

Prof. Dr. Igor Drstvensek is Lecturer at University of Maribor, Faculty of Mechanical Engineering, where he is lecturing production technologies and maintenance. His research work in the last 15 years is dedicated to additive manufacturing and especially to medical applications of Additive Manufacturing. He is Head of the Additive Manufacturing Laboratory at the Faculty of Mechanical Engineering, University of Maribor. In 2006, he has initiated the first implant production by the use of layered technologies in Slovenia and in last 10 years conducted 30 projects of cranial and maxillofacial implant production that ended with successful implantation of 27 PMMA and 3 Ti64 implants, owning several patent applications.

**Inma Vazquez, Stratasys**

Inma Vazquez is Channel Manager France and Iberia for Stratasys. She is one of the European women with more experience in additive manufacturing. Worked 11 years in 3DSystems, 2 years in HP division 3Dprinting and 4 years in Stratasys as Sales Manager. Speaks 6 languages and is an expert in introducing new products in several European markets focusing on applications to improve manufacturing processes in various industries.

**Jaume Homs, HP Inc., Spain**

Jaume Homs is the Iberia Channel and Sales Manager of HP's 3D Multi-Jet Fusion Business. This position includes Spanish and Portugal responsibility of channel recruitment, management, and sales of HP's 3D Printing Multi-Jet Fusion line of solutions. Main team is based in Barcelona, Spain. He joined HP in 2002 in the R&D organization as Software Engineer and Project Manager. Since then, he has held different positions in R&D, marketing, sales, and business management. Prior to his current position, he was the Indigo Commercial Business Manager for Europe Middle East and Africa. Previously, he had a sales position in Iberia in the Indigo business and prior to that in the DesignJet business. He has a proven track over-achieving all business goals. He holds a Master in Computer Science from

Universitat Autònoma de Barcelona, a Master in IT Management, and an Executive MBA by la Salle.

### **Joana de Medina, Stratasys**

Joana Mayeur de Medina is a Chemical Engineer with over 20 years' experience in technical sales and key account management. Born in Rio de Janeiro, Joana has moved to France in 2001 and has built a successful career growing businesses at different levels for companies such as ExxonMobil, Xerox, Canon, Experian and HP. In 2016, Joana has embraced the challenge of building up the 3D printing business for HP in France. Since 2018 at Stratasys, she is the Strategic Account Manager for France and Iberia, working actively with the main industries to develop and implement additive manufacturing solutions that will transform the Industry.

### **Omar Fergani, Siemens, Germany**

Dr. Fergani is Strategic Software Technology Manager at Siemens digital industries software. His main focus is to deliver cutting-edge software technology to industrialize additive manufacturing (AM). Some of his topics of interest are print first-time-right processes, the closed-loop solution to achieve the autonomous machines as well as the smart factory. Previously, he oversaw developing the first AM process simulation to complete Siemens digital twin offering. He is a holder of a Ph.D. in mechanical engineering and a double master's degree in manufacturing and materials from the Georgia Institute of Technology and the Norwegian University of Science and Technology. He is selected as one of the outstanding young manufacturing engineers and was previously selected as 30 under 30, future leaders of manufacturing by the Society of Manufacturing Engineers.

### **Paulo Bártolo, University of Manchester, UK**

Paulo Bártolo is Professor of Advanced Manufacturing and Head of the Manufacturing Group at the School of Mechanical, Aerospace and Civil Engineering, University of Manchester. He is the University's Industry 4.0 Academic Lead, Team Leader of the Industry 4.0 societal challenge at Digital Futures, and sits on the Management Board of the EPSRC & MRC Centre for Doctoral Training in Regenerative Medicine. He is Professor at the Advanced Manufacturing Group at the Tecnológico de Monterrey, at Nanyang University, and Member of CIAUD (at University of Lisbon). He is Fellow of CIRP, Advisor of the Brazilian Institute of Biofabrication and several UK and International Funding Agencies, and received a commendation and public recognition from the Portuguese Government. He is Founding Editor of Virtual and Physical Prototyping Journal and Editor-in-Chief of Biomanufacturing Reviews.

**Terry Wohlers, Wohlers Associates Inc., USA**

Terry Wohlers is President of Wohlers Associates, Inc., an independent consulting firm he founded 32 years ago. He has authored more than 421 books, articles, and technical papers on product development and manufacturing and has given 155 keynote presentations on five continents. In 2004, he received an Honorary Doctoral Degree of Mechanical Engineering from Central University of Technology in Bloemfontein, South Africa. In 2005, he became Fellow of the Society of Manufacturing Engineers (SME). In 2016, he became Adjunct Professor at RMIT University in Melbourne, Australia. For 24 years, he has been Principal Author of the Wohlers Report, an annual worldwide publication focused on additive manufacturing and 3D printing.

**Ulric Ljungblad, Freemelt**

Dr. Ulric Ljungblad is CEO and co-founder of Freemelt. After his PhD at University of Gothenburg, he worked for 10 years in the semiconductor industry. From 2006 he has been working in additive manufacturing focusing on systems development and innovation. He holds more than 20 patents. He co-founded Freemelt in 2017 aiming to launch an open source electron beam AM system to promote much faster development of processing parameters for new metal materials. He worked as R&D manager at Freemelt during the development of the Freemelt ONE system that was launched in 2018 and he became the CEO of Freemelt in 2019.

# **Keynotes**

# HP 3D Printing: Accuracy and Repeatability in Digital Manufacturing

Bruno Romero Azorin

HP Inc., Sant Cugat, 08174 Barcelona, Spain  
bruno.romero.azorin@hp.com

**Abstract.** HP Multi Jet Fusion is a 3D Printing technology with a high rate of penetration into real manufacturing environments. This aspect is pushing HP to deliver products and solutions more robust, more profitable, with higher productivity, and more precise and accurate. Recently, HP has introduced the new printer Jet Fusion 5200 and the software HP 3D Process Control that will allow to produce high volume of parts at the lowest cost and with tolerances matching ISO 286 IT13 grade and repeatability with Cp CpK over 1.

**Keywords:** Multi Jet Fusion • Additive Manufacturing • Process capacity • OEE

## 1 Process Capacity and OEE in Digital Manufacturing

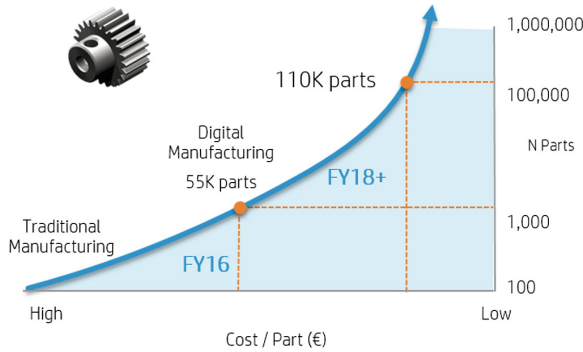
### 1.1 HP Multi Jet Fusion Approach to Process Capacity and OEE

Nowadays there are many 3D Printing technologies available in the market. Each technology presents advantages for certain applications, namely, prototyping, jigs and fixtures or tooling and in some cases true final parts. However, manufacturing final parts in big volumes with consistency, repeatability, part quality and cost effectiveness it is only available for few technologies.

HP's Multi Jet Fusion (MJF), first introduced in 2016, is a technology ready for manufacturing environments capable to compete with plastic injection molding and CNC machining in terms of material properties and isotropy, cost per part and productivity. The factors that increase the breakeven point of MJF vs. injection molding or CNC machining are part size, part design complexity and expected production volume. For instance, a gear of 30 cm<sup>3</sup> up to 100,000 units it would be more economic to be manufactured using MJF than with injection molding (Fig. 1). The first HP 3D Printer, Jet Fusion 4200, has proofed the big penetration in several markets and in many of the cases to produce true final parts.

Recently HP has introduced a new MJF platform: the HP Jet Fusion 5200. The hardware architecture and several software modules of this 3D Printer have been designed to maximize the accuracy and repeatability of printed parts, while increasing the OEE (overall equipment effectiveness).





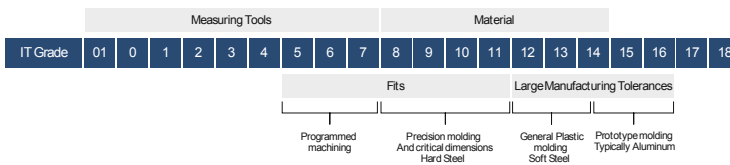
**Fig. 1.** Cost per Part breakeven point MJF vs. Injection Molding.

In terms of accuracy and repeatability, most of the printers in the market make trade-offs in mechanical properties and achievable dimensional tolerances depending on part orientation, part location on the build platform resulting in low process capacity ( $C_p$  and  $C_{pK}$ ). Thanks to the software HP 3D Process Control and complex algorithms running from HP’s Cloud System, the users are able to create parts with consistent dimensions and tolerances independently of the build location and build after build achieving high process capacity ( $C_p$  and  $C_{pK}$ ).

The OEE is a metric that integrates the tracking and control of the entire end-to-end manufacturing process, enabling the detection of deviations that might appear at any stage of the process. The HP 3D Printers are designed to bring the highest OEE among the printers in the market.

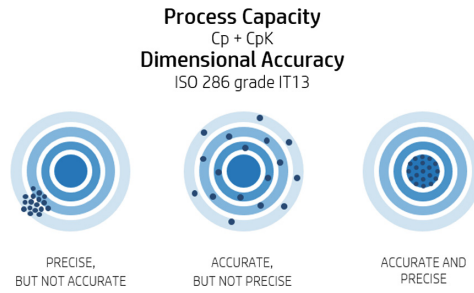
**1.2 HP 3D Process Control**

HP 3D Process Control it is a cloud-based software developed by HP that will allow to print parts consistently with a tolerance in the range of grade IT13- IT14 according to ISO 286 (Fig. 2).



**Fig. 2.** ISO 286 IT grades description.

Con conversationally IT13-IT14 grades are well known tolerance ranges achievable by injection molding with aluminum molds and soft steel molds (Fig. 3).



**Fig. 3.** Visual description of Precision and Accuracy.

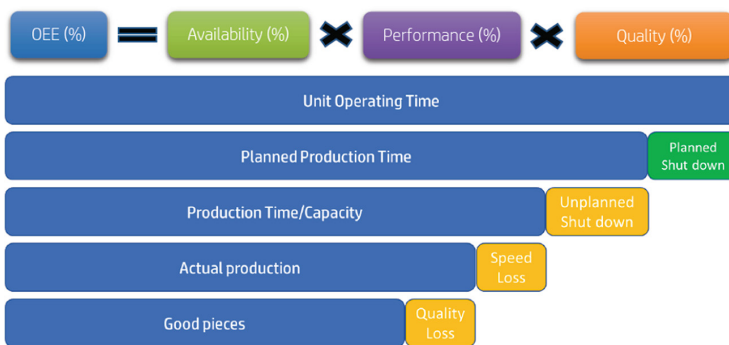
Additionally, HP 3D Process Control enables dimensions consistency across the build and build after build by defining a Cp/CpK for a given set of critical dimensions in a given part.

Basically, 3D Process Control operates creating a profile of the build platform compensating the dissimilar material contractions all over the build volume acting at several levels:

- MJF technology singularities and aspects
- Printer by printer deviations
- Part by part geometry singularities

### 1.3 Overall Equipment Effectiveness

The OEE is calculated by multiplying the manufacturing process availability, quality and performance (Fig. 4).



**Fig. 4.** OEE (overall equipment effectiveness) definition.

Availability factor refers to unexpected waiting times. HP strategy to maximize this factor is:

- 3D Printers are designed modular to maximize the operability and throughput;
- Printer components and systems are tested to determine end of life and to proactively suggest predictive maintenance;
- Components known to fail in a higher rate are redundant to avoid stops during manufacturing process;
- Basic HP Service Support includes remote support and next business day on-site support.

Performance factor refers to deviations to expected process time. HP strategy to maximize this factor is:

- 3D Printers are designed modular to maximize the operability and throughput;
- The printing module does several subsystems pre-checks and calibration before starting the printing process. These operations are most of the parallel to shorten the time. Once the print is finished the build platform can be extracted and the printer immediately ready to print a new build.

Quality refers to parts that are out of specifications, mainly in dimensions. HP strategy to maximize this factor is:

- Define a clear expectation of achievable dimensional tolerances according to ISO 286;
- Provide and adjust repeatability and accuracy thanks to HP Process Control;
- Thanks to HP Service Support react to any deviations to help customers to get back to quality parameters.

# Laser Metal Deposition and Laser Metal Fusion

Carlos Mougueira

TRUMPF Portugal  
Lagoas Park, Edifício 11, Piso 1, 2740-270 Porto Salvo, Portugal  
www.trumpf.com

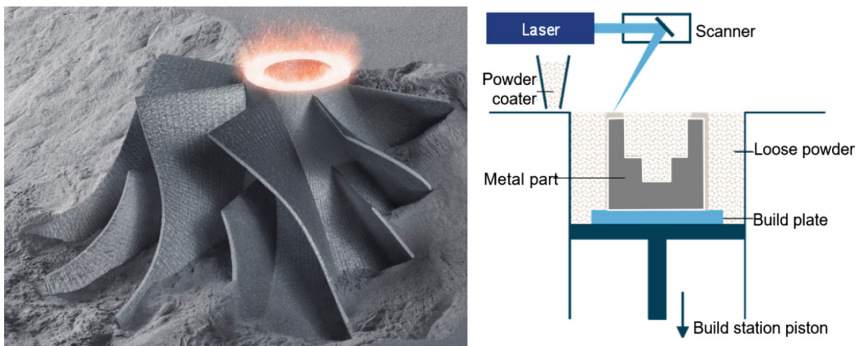
**Abstract.** Additive Manufacturing: the benefits of the Laser Metal Fusion and Laser Metal deposition in application areas where conventional production reaches its limits.

**Keywords:** Additive Manufacturing · 3D Printing · Laser Metal Fusion

## 1 Additive Manufacturing Process

### 1.1 Laser Metal Fusion

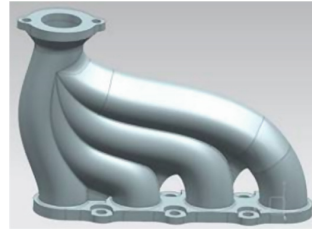
Powder Bed Based laser melting (Laser Metal Fusion, LMF) is often referred to as metallic 3D printing, Powder Bed Fusion or Selective Laser Melting. The laser builds up the workpiece layer by layer from a bed of powder. The blueprint is provided by a CAD model. Tools are not required. The powder is applied to a platform, and the laser beam melts the powder with high precision, according to the CAD data, connecting defined locations with the layer below. The laser then repeats this process until the metallic component is ready. The workpiece now possesses the properties of the material that was used in powder form. A large number of metallic materials in powder form can be used for this method, including steel, aluminum, or titanium (Figs. 1 and 2).



**Fig. 1.** Powder Bed Based laser melting (Laser Metal Fusion, LMF).

**Example: Exhaust Manifold:**

- Material: Titanium
- N° of layers: 2 915 | 60  $\mu\text{m}$
- Time of processing: 26 h 33 min
- Objective: Design optimization



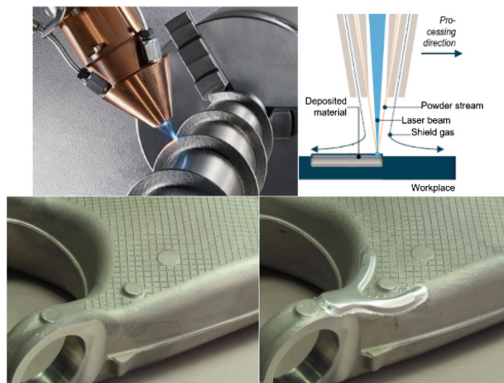
**Fig. 2.** Optimization design of a manifold.

**1.2 Laser Metal Deposition**

Laser Metal Deposition – or LMD for short – is also known as Direct Energy Deposition or Laser Cladding. The process is simple to explain. The laser creates a melt pool on the surface of the component, and metallic powder is automatically fed in through a nozzle. Interconnected weld beads are thus formed which form structures on existing substrates or even create entire components (Fig. 3).

**Example: Wishbone**

- Material: Aluminum
- Time of processing: aprox. 20s
- Objective: costs and time production reduction



**Fig. 3.** Laser metal deposition on a wishbone component.

**Reference**

1. TRUMPF Laser-und Systemtechnik GmbH

# Digital Manufacturing Is a Reality with HP 3D Printing: Introducing the New HP 3D Jet Fusion 5200 Printing Solution

Jaume Homs

Sales Manager HP 3D Print Iberia  
HP Inc., Sant Cugat, 08174 Barcelona, Spain  
jaume@hp.com

**Abstract.** HP Multi Jet Fusion it is a 3D Printing technology with a high rate of penetration into real manufacturing environments. This aspect is pushing HP to deliver products and solutions more robust, more profitable, with higher productivity, and more precise and accurate. Recently, HP has introduced the new printer Jet Fusion 5200 and the software HP 3D Process Control that will allow to produce high volume of parts at the lowest cost and with tolerances matching ISO 286 IT13 grade and repeatability with Cp Cpk over 1.

**Keywords:** Multi Jet Fusion · Additive Manufacturing · Mass production

## 1 Unleash New Growth and Scale Production with HP's Most Advanced Plastics 3D Printing Solution

### 1.1 Introducing the New HP 3D Jet Fusion 5200 Printing Solution

HP has recently announced the release of its new Jet Fusion 5200 Series 3D printing solution, introduced a new TPU material, launched its Digital Manufacturing Network and expanded on strategic partnerships within various industries.

The major announcements broaden the company's AM operations in a big way and enable HP customers to truly exploit digital manufacturing. As Christoph Schell, President of 3D Printing and Digital Manufacturing at HP, explained: "*The Fourth Industrial Revolution is one of the most transformative forces in our lifetime. New technology innovations will be required, new partnership models will emerge and new modes of doing business will unfold*".

HP is committed to helping customers with diverse manufacturing needs turn change into opportunity by delivering the most innovative solutions portfolio and comprehensive ecosystem of industry-leading partners. The broadening of our portfolio with the new Jet Fusion 5200 Series 3D printing system, coupled with

expanded industrial alliances and our new Digital Manufacturing network, are important accelerators of our digital manufacturing journey.

The new Jet Fusion 5200 Series expands upon HP's existing Multi Jet Fusion portfolio, which also includes the Jet Fusion 300/500 Series for functional prototyping applications and the Jet Fusion 4200 Series, for short runs and production. The new 3D printer series adds to the portfolio, offering a solution for volume production.

The hardware comes with a number of improvements and upgrades which enable users to benefit from higher productivity, accuracy, consistency and efficiency. Other advantages of the new series include increased flexibility, improved uptime, streamlined workflows and simplified fleet management.

The new system effectively moves the center of the operation from a two-pass mode to a one-pass mode. This approach is enabled by the presence of a more powerful lamp and allows for a higher degree of productivity compared to HP's other MJF systems. Further, the more powerful lamp also creates opportunities for working with high-temperature materials down the line.

The Jet Fusion 5200 Series also integrates a more sophisticated thermal imaging system (with five times the resolution of the 4200 Series), providing better precision and tighter process control.

The new 3D printing system also comes with a new cooling module, which further streamlines and automates the production process. The low-cost cooling unit essentially sits on top of the build unit and once the printing process is complete, the still hot parts are automatically transferred into the cooling boxes so that the build unit is liberated for the next job. This is highly advantageous for customers requiring high productivity and that operate multiple build units.

The 5200 Series comprises of three 3D printer models: the Jet Fusion 5200, Jet Fusion 5210 and Jet Fusion 5210 Pro. The latter two models offer better economic value than the 5200 for larger volume production. The 5210 models are also more conducive for industrial applications because they enable manufacturers to see the status of the machine from a distance.

## 1.2 Improved Software and New Materials

To accompany the new hardware, HP has also introduced two new software suites: **3D Process Control** and **HP 3D Center**. The former helps to optimize the dimensional accuracy and consistency of part geometries. HP 3D Center, for its part, gives users the tools to optimize their whole factory. Finally, HP also launched the HP 3D Parts Assessment Service, which helps customers to identify and assess what parts can be 3D printed.

Excitingly, HP has also taken this opportunity to launch a new material for its Jet Fusion 5200 Series technology: **ULTRASINT**, a TPU thermoplastic polyurethane material developed by BASF. The new material is well suited for the automotive, industrial and consumer goods sectors for applications that require good shock absorbance, energy return and flexibility.

A number of companies are already utilizing the new material and HP's Jet Fusion 5200 systems for production applications (Fig. 1).



**Fig. 1.** HP 3D Jet Fusion 3D Printing Solution.



# The Digital Twin of Production, the Ultimate Tool to Achieve First-Time-Right in Metal Additive Manufacturing

Omar Fergani

Siemens Digital Industries, Manufacturing Engineering Software, Berlin, Germany  
omar.fergani@siemens.com

**Abstract.** The concept of digital twin is at the core of the digital transformation happening in manufacturing industries. The digital twin of the production process is an effective technology that allows the use of data-driven or physics-based model to simulate the process and optimize the process parameters to achieve the best quality product. In the context of additive manufacturing, the scrap rate is high compared to more traditional process. Due to the full digital nature of AM processes, the concept of digital twin of the process, also referred to as the process simulation is used in this presentation as a test bed to demonstrate the usefulness of the digital twin of the production.

**Keywords:** Additive Manufacturing · Digital twin · Process simulation

## 1 Introduction

A digital twin is a virtual representation of a physical product or process, used to understand and predict the physical counterpart's performance characteristics. Digital twins are used throughout the product lifecycle to simulate, predict, and optimize the product and production system before investing in physical prototypes and assets. By incorporating multi-physics simulation, data analytics, and machine learning capabilities, digital twins are able to demonstrate the impact of design changes, usage scenarios, environmental conditions, and other endless variables – eliminating the need for physical prototypes, reducing development time, and improving quality of the finalized product or process. To ensure accurate modelling over the entire lifetime of a product or its production, digital twins use data from sensors installed on physical objects to determine the objects' real-time performance, operating conditions, and changes over time. Using this data, the digital twin evolves and continuously updates to reflect any change to the physical counterpart throughout the product lifecycle, creating a closed-loop of feedback in a virtual environment that enables companies to continuously optimize their products, production, and performance at minimal cost. The potential applications for a digital twin depend on what stage of the product lifecycle it models. Generally

speaking, there are three types of digital twin – Product, Production, and Performance, which are explained below. The combination and integration of the three digital twins as they evolve together is known as the digital thread. The term “thread” is used because it is woven into, and brings together data from, all stages of the product and production lifecycles.

In the context of additive manufacturing, Fig. 1 demonstrate the capabilities encapsulated in each digital twin in one integrated solution. To support the end user, solve multiple challenges related to the industrialization of additive manufacturing. From a system level, the data integrity and consistency are key to deliver the highest quality product and the end to end platform is an answer to this challenge.

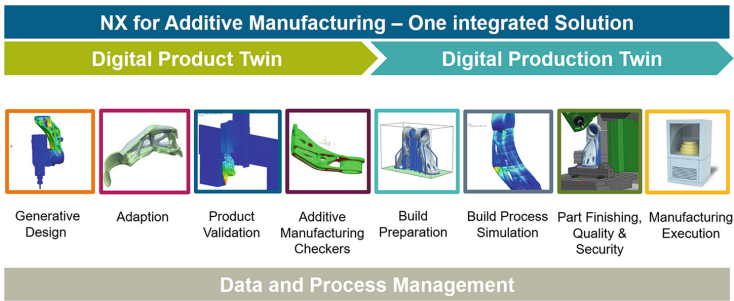


Fig. 1. Concept of the digital twin applied for additive manufacturing.

Moreover, the end to end solution deliver key technologies to solve other manufacturing issues such as the scrap rate. In additive manufacturing, and due to the complex thermos-mechanical process involved, the scrap rate is quite high (estimated at 30%) mainly due to challenges as described in Fig. 2.

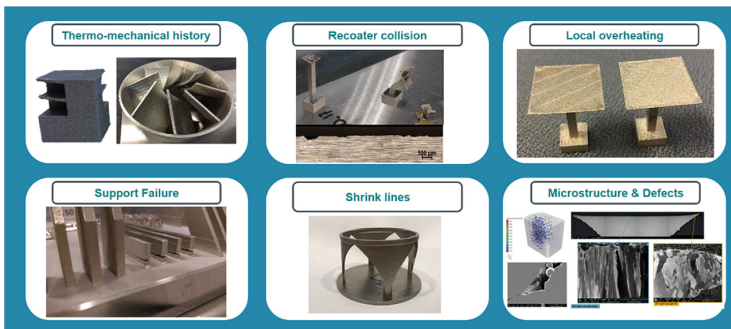


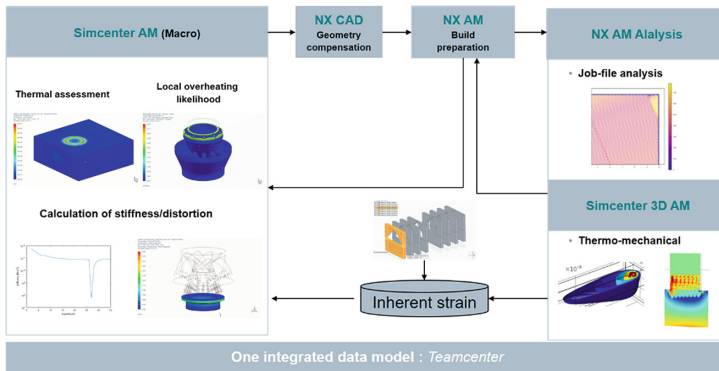
Fig. 2. The different root causes leading to the high scrap rate in metal additive manufacturing.

As discussed previously, the concept of the digital twin provides multiple technologies integrated in one platform to address the most pressing manufacturing problems. In the next section, we will describe how the digital twin of the production process provides a strong physics-based tool to analyses the AM process at multiple level, from macro to micro scale identifying and correcting potential manufacturing challenges upfront in a cost-effective manner.

## 2 Methodology and Approach

The process simulation also digital twin of the manufacturing process provides a guided workflow to the user that allows for the assessment of distortions, the prediction of recoater collisions, prediction of areas of overheating, and other important feedback about the print process. The AM Process Simulation solution offers the ability to iterate on a solution between the design and build tray setup steps of the workflow, and the simulation step. This closed feedback loop is possible due to the tightly integrated nature of the CAD, CAM, CAE and the machine controller. The simulation data created feeds into the digital thread of information which informs each step of the printing process. This digital backbone enables the system to develop pre-compensated models and, more importantly, to feed those seamlessly back into the model design and manufacturing processes without additional data translation. This high level of integration is what customers need today in order to be successful in industrializing additive manufacturing.

Figure 3, describes the architecture of the finite element-based solution that was implemented for this purpose.



**Fig. 3.** Architecture of a finite element-based process simulation solution.

### 3 Results and Discussions

This technology was implemented and investigated in multiple use cases. We demonstrate here a complex gas turbine component. This part was designed thanks to additive manufacturing capabilities. The original part was an assembly of 27 parts that were consolidated to one in this case. The complexity of the geometry led to a number of manufacturing challenges. These issues were predicted thanks to the technology described previously and corrected upfront in a cost-effective way. Figure 4 describes the obtained results compared to the 3D scan.

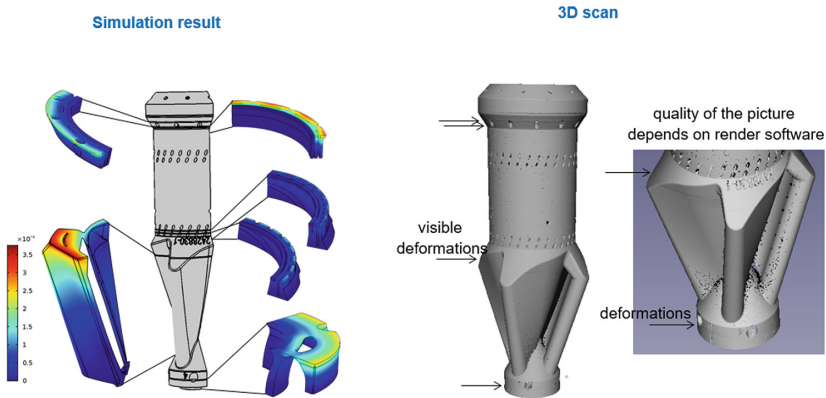


Fig. 4. Simulation results compared to 3D scans.

Multiple simulation demonstrated that the usage of the physics-based simulation to predict overheating, distortion and other challenges like residual stress is beneficial for the designer to make changes at an early stage. Also, it is demonstrated through experiments, that the process simulation is a key step to reduce machine failures, thanks to capabilities like prediction of recoater crash and the optimization of the job file. The ultimate objective of such technology is to achieve a zero scrap rate and deliver the promise of a fully digital manufacturing technology. Although the progress is impressive, efforts are needed to develop more technologies for additive manufacturing where the power of physics is combined with the insight from the data. Most of the future capabilities of Siemens digital twin will be based on this new paradigm.

# Contents

## Advanced Manufacturing Technologies

<b>Additive Manufacturing Was the Answer, but What Is the Question? . . . . .</b>	<b>3</b>
Steinar Killi and William Kempton	

<b>Expectations of Additive Manufacturing for the Decade 2020–2030 . . . . .</b>	<b>10</b>
Henrique Almeida and Joel Vasco	

<b>Additive Technologies in the Medical Field for 2030 . . . . .</b>	<b>20</b>
Emanuel Serrano, Liliana Vitorino, and Henrique A. Almeida	

<b>Technological and Economic Comparison of Additive Manufacturing Technologies for Fabrication of Polymer Tools for Injection Molding . . . . .</b>	<b>28</b>
Achim Kampker, Bruno Alves, and Peter Ayvaz	

<b>Novel Robotic 3D Printing Technology for the Manufacture of Large Parts . . . . .</b>	<b>40</b>
Uwe Klaeger and Andriy Telesh	

## Green and Digital Manufacturing Environments and Simulation Systems

<b>Implementing RAMI4.0 in Production - A Multi-case Study . . . . .</b>	<b>49</b>
Elder Hernández, Pedro Senna, Daniela Silva, Rui Rebelo, Ana C. Barros, and César Toscano	

<b>Assessing Industry 4.0 Readiness of Portuguese Companies . . . . .</b>	<b>57</b>
Hélder F. Castro, Alexandre R. F. Carvalho, Fátima Leal, and Helena Gouveia	

<b>Exploring the Linkages Between the Internet of Things and Planning and Control Systems in Industrial Applications . . . . .</b>	<b>65</b>
Ricardo Soares, Alexandra Marques, Reinaldo Gomes, Luís Guardão, Elder Hernández, and Rui Rebelo	
<b>Virtual Workstations Applied to the Mould Industry - A Case Study . . . . .</b>	<b>73</b>
Fabiana Guarda, Luís Marrazes, and Mário Afonso	
<b>To Simulate or Not to Simulate? Challenges in Digitally Prototyping HMI Interactive Technologies . . . . .</b>	<b>82</b>
Sevcan Yardim Sener and Owain Pedgley	
<b>Study on the On-line Support System for Welder . . . . .</b>	<b>89</b>
Satoru Asai, Yosuke Ogino, Kazufumi Nomura, and Kazunori Hattori	
<b>Development of a Supporting System of Pass Design in Multi-pass Welding Based on GMAW Weld Pool Simulation . . . . .</b>	<b>96</b>
Yosuke Ogino, Toshihiro Fujiwara, Satoru Asai, Kosuke Tamura, and Shin-ichi Sakamoto	
<b>Integration of BIM and Generative Design for Earthbag Projects . . . . .</b>	<b>102</b>
Deborah M. Santos and José Nuno Beirão	
<b>Potential of Natural Ventilation and Vegetation for Achieving Low-Energy Tall Buildings in Tropical Climate: An Overview . . . . .</b>	<b>110</b>
Humera Mughal and José Nuno Beirão	
<b>Design</b>	
<b>Improve Engineering Skills in Digital Manufacturing for New Products . . . . .</b>	<b>119</b>
C. Relvas and A. Ramos	
<b>Geometry-Based Process Adaption to Fabricate Parts with Varying Wall Thickness by Direct Metal Deposition . . . . .</b>	<b>125</b>
Daniel Eisenbarth, Fabian Soffel, and Konrad Wegener	
<b>Design and Printing Parameters Effect on PLA <i>Fused Filament Fabrication</i> Scaffolds . . . . .</b>	<b>131</b>
R. Baptista and M. Guedes	
<b>Strategies for Obtaining Porous Media Through the Process Planning in Material Extrusion Additive Manufacturing . . . . .</b>	<b>137</b>
Marcelo Okada Shigueoka, Elis Cassiana Nakonetchnei, and Neri Volpato	
<b>Programming 4D Printed Parts Through Shape-Memory Polymers and Computer-Aided-Design . . . . .</b>	<b>143</b>
Eujin Pei, Giselle Hsiang Loh, Seok Woo Nam, and Ezrin Faten Azhar	

## **CAD and 3D Data Acquisition Technologies**

### **Modeling and Simulation of a Novel Functional Brace for Large Bone Defects** . . . . . 155

Mohammed S. Alqahtani, Abdalla M. Omar, Glen Cooper, and P. J. Bartolo

### **AM Tooling for the Mouldmaking Industry** . . . . . 162

João Carreira, Joel Vasco, and Henrique Almeida

### **3D Printing: An Innovative Technology for Customised Shoe Manufacturing** . . . . . 171

Tatjana Spahiu, Erald Piperi, Andrea Ehrmann, Henrique A. Almeida, Rita M. T. Ascenso, and Liliana C. Vitorino

## **Materials**

### **Polymer Matrix Nanocomposites for 3D Printing** . . . . . 183

Mylene S. Cadete, Tiago E. P. Gomes, Alfredo Costa, Maria Fonseca, João Dias-de-Oliveira, and Victor Neto

### **Morphology and Thermal Behaviour of New Mycelium-Based Composites with Different Types of Substrates** . . . . . 189

Rafael M. E. Alves, M. L. Alves, and Maria J. Campos

### **Developing Sustainable Materials for Marine Environments: Algae as Natural Fibers on Polymer Composites** . . . . . 198

Gleiciane dos Santos Silva, Carlos Capela, and Marcelo Gaspar

### **On the Effect of Deposition Patterns on the Residual Stress, Roughness and Microstructure of AISI 316L Samples Produced by Directed Energy Deposition** . . . . . 206

Gabriele Piscopo, Alessandro Salmi, Eleonora Atzeni, Luca Iuliano, Mattia Busatto, Simona Tusacciu, Manuel Lai, Sara Biamino, Mostafa Toushekhah, Abdollah Saboori, and Paolo Fino

### **A Novel Specimen Geometry for Fatigue Crack Growth in Vacuum** . . . . . 213

L. M. S. Santos, C. Capela, F. V. Antunes, J. A. M. Ferreira, J. D. Costa, and R. Branco

### **Fatigue Life Prediction in Selective Laser Melted Samples Under Variable Amplitude Loading Based on Two Constant-Amplitude Tests** . . . . . 219

L. Santos, R. Branco, J. D. Costa, C. Capela, and J. A. Martins Ferreira

### **Study of Laser Metal Deposition (LMD) as a Manufacturing Technique in Automotive Industry** . . . . . 225

F. Q. Ramalho, M. L. Alves, M. S. Correia, L. M. Vilhena, and A. Ramalho

## Applications

<b>Photocurable Alginate Bioink Development for Cartilage Replacement Bioprinting</b> .....	243
H. Mishbak, Enes Aslan, Glen Cooper, and P. J. Bartolo	
<b>Composite Scaffolds for Large Bone Defects</b> .....	250
Evangelos Daskalakis, Enes Aslan, Fengyuan Liu, Glen Cooper, Andrew Weightman, Bahattin Koç, Gordon Blunn, and P. J. Bartolo	
<b>Bi-material Electrospun Meshes for Wound Healing Applications</b> .....	258
Enes Aslan, Cian Vyas, Carl Diver, Gavin Humphreys, and P. J. Bartolo	
<b>Fabrication of Cellulose Hydrogel Objects Through 3D Printed Sacrificial Molds</b> .....	265
Hossein Najaf Zadeh, Tim Huber, Freya Dixon, Conan Fee, and Don Clucas	
<b>3D Printed Geometries on Textile Fabric for Garment Production</b> .....	271
Tatjana Spahiu, Erald Piperi, Andrea Ehrmann, Ermira Shehi, and Dudina Rama	
<b>Moving Forward to 3D/4D Printed Building Facades</b> .....	277
Flávio Craveiro, José P. Duarte, Helena Bártolo, and Paulo Bártolo	
<b>Author Index</b> .....	283



# **Advanced Manufacturing Technologies**



# Additive Manufacturing Was the Answer, but What Is the Question?

Steinar Killi<sup>(✉)</sup> and William Kempton

Oslo School of Architecture and Design, Oslo, Norway  
steinar.killi@aho.no

**Abstract.** At its core, this paper forms a discussion around the popular uptake of technologies such as AM, and why technologies such as these are not pursued with equal interest in industry as they have been in popular culture. More specifically, it asks – Why is AM still hard to sell into the manufacturing industry? As an ongoing work this paper is an attempt to construct a vision and roadmap to how AM could be implemented in any businesses dealing with physical, manufactured products. Using design tools and techniques from systemic design, service design and industrial design, this paper argues for a broader and more holistic approach to AM. We see this qualitative emphasis on design through the lenses of client/designer/producer relations that are becoming increasingly complex, in their approach to business models and relations with costumers.

**Keywords:** Product design · Design process · Technology development · Additive manufacturing

## 1 Introduction

### 1.1 Background

The starting point of this paper is a question which those engaged in research on AM are constantly asked, namely, “could you manufacture this [pointing at artefact] any cheaper or faster through AM than you would through conventional methods?” The answer to this question is most usually ‘no’. However, from a design perspective such a reply needs to be followed up by questions of *why* such a product should be made through AM, or even *how* a design can be altered to make it possible. In other words, there is a need for design practice to reflect on the technical, economical and emotional aspects of AM’s commercial uptake.

For years now the AM industry [1], popular journals [2] and TV shows [3] have been selling in AM as the answer to wide-ranging social and political issues [4]. Not only has Additive Manufacturing been lauded as an alternative to mass-manufacturing production techniques [5], it is bringing to relevance topics such as local production (peer production, sustainability; [6]), re-shoring (bringing back industry from low-wage countries) and bespoke products (customization [7]) to mention a few. And, of course, the AM industry is growing and maturing. It may not do so at the speed previously anticipated by for instance Gartners hype cycles and not in areas one would expect.

For instance, the vision of having a 3D printer in every household seems only more distant today than it did 10 years ago, when desktop-friendly 3D printers were first made available. The reasons for the slow implementation both in the industry and as a home appliance are many and complex.

The focus of this paper is to discuss some of the possible reasons for the implementation of AM being different to what it was initially perceived as. Specifically, this paper aims to direct discussions towards a growing interest in design thinking, designerly practice and doing [8] as an overarching strategy and approach to reflecting on AM technology.

## 1.2 Technological Obstacles and Opportunities

Many research journals are devoted to the topic of AM technology, such as *Rapid Prototyping Journal* and *Additive Manufacturing*. Additionally, conferences and festivals which celebrate possibilities and challenges in different AM areas of use have been held all over the world (such as TED, AMUG and the TCT show). The underlying theme, which is reflected in many of these arenas, is the fact that technical processes such as SLS and DLS (Carbon 3D) need to constantly improve/optimize to have any hope of being implemented by a company. From this perspective, a design needs to conform and adapt to the intended production technology, which would influence both function and aesthetics. For example, electromedical devices found in a hospital's Intensive Care Unit (ICU) may need to comply with more stringent flammability requirements, which is only possible through a handful of flame retardant AM materials. So far so good, but there are other obstacles at hand.

At the other end of the spectrum, one might reflect on how a company adapts its business model to its products. For instance, a company selling razors might sell its razors at a rather low price, while the overhead comes from the razorblades themselves. In contrast, a technology company selling their smartphone at a premium could be competitive by providing cloud and streaming services at limited costs. But what happens when third party providers start to break apart such existing relationships?

Through these examples, we point to the fact that business models may be disrupted by new and competitive services. Furthermore, in relation to AM, it would be relevant to imagine the consequences of introducing AM to industries that are heavily oriented on manufacturing processes such as CNC milling or casting, such as the Oil & Gas industry.

The point to make is that internally in companies as in Oil & Gas, huge investments have been made in manufacturing machinery and on relevant human resources. In such an environment, the introduction of new technologies could create friction or even resistance. Other issues could be if a company simply assembles a solution, buying parts from different sub-contractors. Do they have any interest in using AM, even if they do not see any immediate benefits?

Common for all these issues and several others, is that you need to understand the company, how it works, where they make their income, and even how it is organized. We now see an emerging complex structure that will differ for every company that plans to implement AM. In other words, there is no master plan for implementing AM.

For this, however, we will point towards examples where new technologies and the design of a product meet.

### 1.3 New Technology or New Ways to Work

Seen in retrospect, new technology appears very often to lead to innovative new ways of manufacturing, as well as the products themselves. For example, the introduction of CAD drawing and CNC machining is arguably an important contributor to automotive design [9]. Whereas molds had traditionally been handmade and therefore also voluptuous in shape, more minimalistic, single curved surfaces were introduced during the 1970s. One reason for this change of style may have been the more precise mold making techniques brought forth by CNC/CAD. However, the initial implementation of such technologies proved challenging in terms of recreating the same double curved surfaces of previous decades. Soon, the technology caught up, and more organic shapes were once again introduced in cars during the 1980s.

Sticking to the automotive industry, there are yet more examples of how a change of mentality could be disruptive. The whole concept of lean manufacturing, introduced by the Japanese car industry with Toyota in the front seat, was just as disruptive as contemporary technical advancements. Just as the moving assembly line had been organized the same way since Henry Ford introduced it in 1913 [10], Taiichi Ohno and Eiji Toyoda introduced lean manufacturing, Toyota reorganized the assembly line starting in the 1970s, to become a competitive advantage soon to be adapted by the whole automotive industry.

It could seem, that if AM is going to be the disruptive change in the manufacturing industry so many have anticipated, there are bound to be new changes in mentality which are not obvious for us today.



**Fig. 1.** The two brand logos for Adidas. To the left, the trefoil today used for products designed before 1996, but still sold today. To the right, the three stripes logo, for all products made after 1996, today's main logo for Adidas. Picture courtesy Adidas.

## 2 Design as Disruption

### 2.1 Design Tools and Methods

In the recent decade, design and management concepts such as design thinking [11] have become industry buzz words. It trickles out to companies not typically linked to design, such as banks and hospitals, as well as on executive levels in car companies. Although new enterprises now embrace approaches such as design thinking, service design, systemic design and user experience design, the core approach to a design practice still remains the same. From the early contributions by Bruce Archer [12] in the mid-1960s, to companies selling sports- or interior products such as Adidas and Ikea include design tools and invoke design processes deeply into their organization. Others, such as the design consultancy IDEO develops and share resources for doing field research and prototyping through their online designkit [13].

In short, a design process typically involves four distinct phases – (1) gathering insight about the context of inquiry, (2) documenting and analyzing that insight, (3) synthesizing a new project brief and (4) executing the project. Because of its inquisitive nature, design is typically preceded by engineering and sales phases. Therefore, in a product development process, design typically focuses on the front-end of a process – gathering insight about possible users and use environments, analyzing findings gathered from field studies, before starting to conceptualise and materialise new solutions or proposals.

Particularly relevant design methods for looking at new opportunities and relations is Gigamapping [14] and user journey maps [15]. While the user journey map is oriented on describing the journey of a user by representing different touchpoints that characterize a service's interactions, the gigamapping is more overarching and concerned with previously hidden relations.

## 3 A Tentative Analysis

Companies engaged in product development usually have two directions in their portfolio of products – heritage products and new products (those not yet designed). Heritage products could be necessary for spare parts and maintenance. Some companies such as Adidas even celebrate their heritage by re-introducing heritage products. These products, called originals, may be upgraded with respect to new production methods, materials and aesthetic detailing. For Adidas, these products are sold under the old brand signature which is the *trefoil*. New products are sold under the new logo, known as the *three stripes*. (see Fig. 1). When the shift was made in 1997 [16], all products before that date were labeled with the old logo. This occurs even though the product is slightly redesigned and produced in 2016.



**Fig. 2.** Left: The Vintage Adidas Gazelle from the 1970s. Right: The Adidas Gazelle original from 2016. The whole production line for the original was reorganized, new blue prints were made etc. The Trefoil logo can be seen on the heel. Photo: Complex.com

Heritage product such as these might for yet other companies be a major source of income, through continued maintenance and the sale of spare parts. Consequently, such companies could have a back catalogue of thousands of parts. For instance, the digital printer manufacturer EPSON has an extensive back catalogue of heritage products. While they don't produce spare parts, they do however provide software upgrades for them [17].

If we see the heritage part library from an AM point of view, we could divide that catalogue into two parts. On one hand, there are those parts that need to be exact copies of the originals. In this case, materials, visual and haptic representations have to be replicated. On the other, there are those part of the catalogue which could benefit from a redesign. Specifically, they might benefit from optimising its structure both for AM production as well as for its functional purpose. In the design of completely new products, optimization for AM production would be integral for the refinement functional purpose.

If we look at Adidas again, their heritage products would fit into the group where both visual aesthetics and user experience need to be catered for. Today's designers who work with the originals make adjustments in materials and smaller details, but a Gazelle model from the 1970s should be recognized in the same way as a Gazelle produced in 2016 (See Fig. 2).

Interestingly, Adidas are today working on shoe designs produced using AM. The product, titled Futurecraft 4D, can potentially be customized and optimized for its users through unique adaptations to the AM manufactured sole.

## 4 Discussion and Conclusion

Given the complexity of a company, how they develop products, how it's produced, back catalogues and so forth it is quite obviously a wicked task to analyze it with regards to AM. Up to now companies have been using AM in product development, for prototyping, for small test series or some employees have tried to sell in AM as

possible production tools. So far this is going slow and as mentioned earlier; a lot of obstacles lies in the path. The tentative research proposal this paper intend to be is to use design methods to get a more holistic understanding of a company's DNA. A tentative question to start the mapping could then be; what could AM do?

- Companies are diverse and complex, they often have back catalogues of products as well as having new products in the pipeline. It wouldn't make any sense to make generalisations about how, when and where AM should be used. That being said, there is a tradition for AM being a part of a product development process, for making prototypes, initial test series, and increasingly so as a sub-component in a larger product assembly, such as in the automotive and aeronautical industry.
- The task would then be developing gigamaps addressing the complexity and diversity of when engaged with a company, where the delivery would be a blueprint of where AM might be implemented on different levels.

## References

1. Wohlers, T.: Wohlers Report 2010: Additive Manufacturing State of the Industry Annual Worldwide Progress Report. Wohlers Associates, Fort Collins (2010)
2. Markillie, P.: Manufacturing: The Third Industrial Revolution (2012). <http://www.economist.com/node/21553017>
3. TED-ed: Printing a Human Kidney - Anthony Atala (2013)
4. Stein, J.: The political imaginaries of 3D printing: prompting mainstream awareness of design and making. *Des. Cult.* **9**, 1–25 (2017)
5. Hopkinson, N., Hague, R., Dickens, P.: *Rapid Manufacturing: An Industrial Revolution for the Digital Age*. John Wiley & Sons, West Sussex (2006)
6. Woern, A.L., McCaslin, J.R., Pringle, A.M., Pearce, J.M.: RepRapable recyclebot: open source 3-D printable extruder for converting plastic to 3-D printing filament. *Hardware* **4**, e00026 (2018)
7. Bertling, J., Rommel, S.: A critical view of 3D printing regarding industrial mass customization versus individual desktop fabrication. In: Ferdinand, J.-P., Petschow, U., Dickel, S. (eds.) *The Decentralized and Networked Future of Value Creation*, pp. 75–105. Springer, Switzerland (2016)
8. Cross, N.: Designerly ways of knowing: design discipline versus design science. *Des. Issues* **17**, 49–55 (2001)
9. Tumminelli, P.: *Car design*. TeNeues (2004)
10. Ford, H., Crowther, S.: *My Life and Work: An Autobiography of Henry Ford*. BN Publishing, New York (2008)
11. Cross, N.: *Design Thinking: Understanding How Designers Think and Work*. Berg Publishers, Oxford (2011)
12. Archer, L.B.: *Systematic Method for Designers*. Council of Industrial Design, London (1965)
13. IDEO.org: Design Kit. <http://www.designkit.org/>
14. Sevaldson, B.: *GIGA-Mapping: Visualisation for Complexity and Systems Thinking in Design*. Nordes, Charleston (2011)

15. ServiceDesign Tools: Customer Journey Map|Service Design Tools. <http://www.servicedesigntools.org/tools/8>
16. Logoorange: Logo design history - Famous Brands Glossary. <https://logoorange.com/logo-design-a/>
17. Epson: New & Back Catalogue Products. <https://www.epson.com.au/products/back-catalogue.asp>





# Expectations of Additive Manufacturing for the Decade 2020–2030

Henrique Almeida<sup>1,2,3</sup>  and Joel Vasco<sup>1,2,3</sup> 

<sup>1</sup> School of Technology and Management,  
Polytechnic Institute of Leiria, Leiria, Portugal  
henrique.almeida@ipleiria.pt

<sup>2</sup> CIIC, Polytechnic Institute of Leiria, Leiria, Portugal

<sup>3</sup> Institute for Polymers and Composites,  
University of Minho, Guimarães, Portugal

**Abstract.** Additive manufacturing became one of the most important manufacturing technologies in the last three decades. The freeform building capacity plays a relevant role on industrial applications where conventional manufacturing approaches are not technically or even not economically feasible. The development of advanced materials for AM is an ongoing process, providing a new competitive edge to AM technologies. Nowadays, AM plays an important role on the production of complex geometries for products of several domains, such as aerospace, automotive, medical among others, supported by high performance materials and increased efficiency AM processes. Distributed manufacturing supply chain also became a reality, enabling new business models and bridging the gap between product designers and end-users. Additionally, high levels of manufacturing automation, incorporating AM equipment as well as smart factories are emerging. At the middle of the 2020s decade, standardisation for materials, material testing and manufacturing processes started its appearance to establish ground-breaking standards to harmonize the use of additive manufacturing technologies worldwide. Now, on the edge of a new decade, a bright future for AM technologies can be foreseen. This paper presents the AM prospects for the next decade and its prospective impact on business and industrial production models.

**Keywords:** Additive manufacturing · Technologies · Trends · Business models

## 1 Introduction

The freeform building capacity of the additive manufacturing approach plays a quite relevant role on several domains, such as medical industry, automotive industry and tooling industry, among others, where conventional manufacturing approaches are not technically feasible due to geometrical complexity. The bottom-up approach enables almost every geometry possible while the top-down approach is highly dependent on tool geometry and the required degrees of freedom for tool access (Weller et al. 2015; Watson and Taminger 2018).

Concerning the AM processing technologies, different definitions and terminology have emerged that are ambiguous and confusing, requiring the development of specific

standards for AM processes and materials (Monzón et al. 2015). During the two last decades, several different AM processes have emerged and became available on the market and its feasibility is not clear in terms of application (Guo and Leu 2013; Gao et al. 2015; Lee et al. 2017a).

These AM processes have been classified by the joint technical committees ASTM F42/ISO TC 261 into seven different categories, according to the processing principles used in each category, defined on the ISO 17296-2:2015 standard (ISO 2015):

- Vat Photopolymerization;
- Material Jetting;
- Binder Jetting;
- Material Extrusion;
- Powder Bed Fusion;
- Sheet Lamination;
- Directed Energy Deposition.

These categories group the AM processes by their interaction with the processed material and, therefore, are focused on the technology. However, technological novelties on AM appeared after such classification and new materials arise every day to comply with market requirements. This paper presents an overview on the technological developments at the verge of 2020s concerning AM industrialization and industry digitalisation. This trend analysis enables to foresee what can be expected in the following decade, driven by market needs, providing a useful insight that can be adopted by domestic end-users, product designers, process engineers and decision-makers.

## 2 Production of Complex Components

The bottom-up manufacturing approach provided by AM processes not only allows the possibility of producing components in single or multiple materials, but also allows full design freedom, enabling new functionalities or part optimization for lightweight applications (Chen et al. 2015; Weller et al. 2015; Ngo et al. 2018). Concerning aerospace, aeronautical and, in particular, automotive industries, lightweight components are a very significant factor for vehicle's efficiency, regardless of its motion type (Peters et al. 2014). The weight reduction can be achieved through component's topological optimization provided by generative design (Riss et al. 2014; Zegard and Paulino 2016; Rohde et al. 2019). The topological optimization of a typical component may create complex geometries that are not technically possible to produce by conventional technologies, such as subtractive manufacturing technologies or formative technologies (Yang and Zhao 2015). Therefore, AM is the most appropriate answer to these manufacturing challenges, although it may require additional post-processing operations, depending on the final application specifications (Rickenbacher et al. 2013; Löber et al. 2013).

## 2.1 Design for Additive Manufacturing (DfAM)

Similar to other conventional manufacturing technologies, AM also requires process-specific design rules and guidelines as discussed by Thompson et al. (2016). The increased use of AM for industrial purposes and final products has also promoted the adoption of a Generic Design for Manufacturing Concept for AM, since a product may be fabricated by more than one technology according to its requirements. This design methodology aims to analyse component's specifications, optimize its geometry considering the additive manufacturing approach and validation of the final geometry considering the manufacturing constraints (Vayre et al. 2012; Thompson et al. 2016).

## 2.2 4D Printing and Smart Materials

Smart materials are emerging, showing the capacity of transforming its geometry by reacting to an external physical or chemical stimulus such as temperature, humidity, light, acidity level, electric or magnetic (Pei et al. 2017). The bottom-to-top manufacturing approach provided by AM is perfectly suitable to process these smart materials and to provide them the geometrical features required for a given application. By combining AM with these smart materials, process called 4D printing, the printed structures are no longer static but active, with the capability of changing state such as folding, curling, expanding, contracting and other transformations (Pei et al. 2017; Khoo et al. 2015; Lee et al. 2017b).

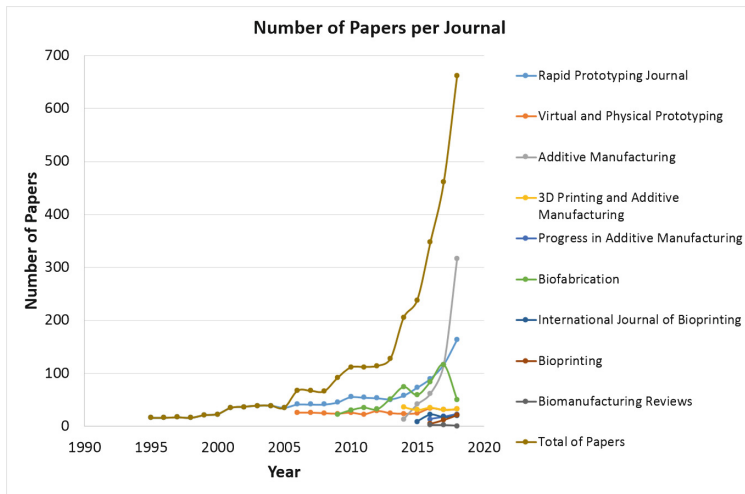
## 2.3 Functionally Graded Additive Manufacturing

Functionally graded additive manufacturing is an integrated design approach and a technological framework to model, analyse and fabricate components that contain property gradation. These parts achieve their multifunctional status by mapping the single or multiple performance requirements and allocating material and structural properties throughout the component's volume (Pei et al. 2017; Oxman, 2011). This approach focuses on material-centric fabrication by emphasising the structure-property relationship (Pei et al. 2017). The design of functionally graded components may be of two types, namely single or multiple material based. In the single material based approach, the gradient design is fully structural based, while in the multiple material based approach, the gradient design may be obtained either by varying the material mixtures or by varying the structural properties or both along the component's volume.

# 3 AM Technological Trends

The beginning of the next decade will witness several technological advances that will make AM competitive enough to dispute a market share with injection moulding, die casting, conventional medical device productions or other classic manufacturing technologies. Regarding the scientific field for instance, after consulting the SCOPUS platform, one of the largest abstract and citation databases of peer-reviewed literature, a research of the main journals of the AM field and the number of papers was performed

per year. From the figure it is possible to observe the continuous increase of publications in the field along with the increase of journals related to the field (Fig. 1).



**Fig. 1.** Number of publications per year per journal relevant to the additive manufacturing field.

The technological trends for AM processes are summarized here, under each previously defined category of the ISO 17296-2:2015 standard:

1. **Vat Photopolymerization:** one of the latest industrial development for this category was presented by Carbon with its CLIP<sup>TM</sup> (Continuous Liquid Interface Production) technology. This technology derives from DLP but offers a continuous build operation and remarkable material properties (Mendes-Felipe et al. 2019). Another relevant developments are the layer freezing for support structures which is under research at the Fraunhofer Institute for Laser Technology (ILT) under the designation TwoCure (Jackson 2018) and manufacturing a layer-free part by rotating a photopolymer in a dynamically evolving light field, under research at UC Berkeley (Kelly et al. 2019).
2. **Material Jetting:** the PolyJet technology represents the highest potential on this category, showing high resolution and multimaterial building capacity (Lee et al. 2017b);
3. **Binder Jetting:** one of the most recent and ongoing developments is the HP's MultiJet Fusion process, capable of processing both polymer and metal materials (Connor et al. 2018);
4. **Material Extrusion:** building rate is the key answer for non-metallic materials to overcome injection moulding along with introduction of carbon fibre onto the filament increasing their mechanical properties up to metal behaviour. (Tekinalp et al. 2014; Ning et al. 2015; Melenka et al. 2016). On metallic materials, the competitive edge rely on the non-dependence of laser to fuse the metal powder but the challenge

is still focused on the decrease of the overall processing time since it is a multi-step process (Desktop Metal 2018);

5. **Powder Bed Fusion:** building speed increased whether by the increase of building chamber volume and multi-laser processing or based on laser-distributed processing is the new competitive edge (Masoomi et al. 2017). Additionally, the industry of specialized post-processing equipment for SLM parts is growing as well as new equipment incorporating both processing units and post-processing operations is making its appearance on the market (Salonitis et al. 2016; Sames et al. 2016); Powder-based processes include novel materials and processing technologies on their portfolio, opening up new applications and increased productivity (Lee et al. 2017b). Concerning R&D of novel metal powders, Freemelt AB (Sweden) developed the Freemelt One, an open source PBF equipment equipped with a 6 kW electron gun and open source software for beam scanning paths and energy deposition control (Peels 2019).
6. **Sheet Lamination:** this category gained a new processing technology – STEP 3D, from Evolve, that claims to be 50x faster than any other AM process (Goehrke 2019).
7. **Directed Energy Deposition:** the technology is well-defined concerning the building concept. Open-source materials, however, are available and open for innovative applications such as multimaterial building (Brueckner et al. 2017; Koopmann et al. 2019).

Besides the process categories already mentioned, new technologies arise that may fall out this classification, such as the cold spray technique (Sova et al. 2013; MacDonald et al. 2017). It is still under development, however, the first commercial equipment has already reached a status that enables process commercialization on the market and it was produced at SPEE3D (Melbourne, Australia).

## 4 New Production and Business Models

The up growing digitalisation of industry creates new business concepts, enabling distributed production of end-user consumer products. The conventional supply chain is shifting from centralized large and typical factories that require high level of stocks management to globally distributed manufacturing centres working upon customer demand (Cozmei and Caloian 2012; Matt et al. 2015).

This decentralized manufacturing model, however, requires on-site experts to run these smaller and flexible production units. Prospectively, human resources must possess adequate digital skills as well as know-how and experience to handle AM equipment and to operate it under suitable conditions. New training offers should arise to provide support to this new market need (Roos and Fusco 2014).

### 4.1 Key-Enabling Technologies for New Production and Business Models

Artificial intelligence (AI) is playing an important role due to the autonomy introduced on manufacturing equipment, enabling automatic and informed decisions concerning

manufacturing strategies, production sequences and priorities, building parameters deviation, among others (Dopico et al. 2016).

The digitalization of industrial processes provides several advantages, from initial product sketch to the final and real product. A digital environment provides the necessary means to create digital twins, for the product, its components and for the manufacturing technologies involved (Chen et al. 2015; Agustí-Juan and Habert 2017).

The product's digital twin can be virtually tested to comply with its application requirements through numerical analysis. These data provide feedback to product design, enabling multi-objective modelling (Knapp et al. 2017).

The production process may also have a digital twin, enabling production risks assessment on an early stage and optimization of production process itself (Debroy et al. 2017).

Digitalisation also brings inline process control, which plays an important role on metal AM processes. Distorted parts or fractures may occur upon unsuitable processing conditions and real-time monitoring of the process provides both technical and economic advantages (Grünberger and Domröse 2014).

The digital environment gathers data and enables feedback of virtual product behaviour, virtual production risks and bottlenecks and real product performance under real operating conditions, enabling a continuous improvement ecosystem (Gardan 2017).

## 4.2 Green Production Models

Additive manufacturing machines are usually small, therefore they can be easily located nearby any existing market, consequently reducing the logistics of moving products around the world. The raw materials for AM systems are also quite common leading to a net reduction in transportation costs (Almeida and Correia, 2016; Gibson et al., 2015; Gibson, 2011). According to several authors (Sreenivasan et al. (2010), Reeves (2009) and Bourell et al. (2009)), there are five main environmental and sustainable benefits in adopting these technologies, allowing AM technologies to have a reduced carbon footprint:

- More efficient and reduced usage of raw materials required in the supply chain. Hence, reduced need to mine and process primary material ores within our natural resources.
- Displacing of energy-inefficient and wasteful manufacturing processes, such as casting or processes like CNC machining that requires cutting fluids.
- Ability to design more efficient products with improved operational performance that are more efficient than conventionally manufactured components by incorporating conformal cooling and heating channels and gas flow paths, etc.
- Ability to eliminate fixed asset tooling, allowing for manufacture to occur at any geographic location such as nearby to the customer, reducing transportation costs within the supply chain, contributing to diminishing the carbon footprint.
- Lighter weight parts, which when used in transport products such as aircraft increase fuel efficiency and reduce carbon emissions.

## 5 Conclusions

The decade 2020–2030 is revealing to be quite promising concerning AM technological developments. Key issues like productivity and sustainability are being overcome with the increase of building chamber volume, the increase of building chamber's quantity, the increase of processing units on a single building chamber and the reduction of the carbon footprint of these technologies. Such approach enables the reduction of product's time-to-market, keeping in mind another important goal, which is the mass customization of components and products. This also allows to heat a chamber once for the production of several components, which at the moment is only possible with smaller products. Having bigger production chambers, indeed increases the time to heat it up for production, but it will also allow to produce more parts per heating.

However, AM still lacks maturity. It has trailed a long path since the 1980s, from the rapid prototyping concept towards the full industrialization of AM on the shop floor for final products and tools. It is well known the disappointment period verified right after the market hype at the end of the 1990s decade. For instance, one of the first LOM manufacturing companies, Helisys Inc. terminated its activity in 2000. But by the turn of the century, AM technologies began again to grow and increase its industrial, academic, scientific, economic and social impact.

AM does not push away completely conventional manufacturing. Although the supply chain is seriously simplified by the fact that few AM processes can ensure a suitable surface finishing or an adequate mechanical behaviour. Therefore, post-processing processes are required for multi-step processes. Comparing to formative processes, there are major AM breakthroughs, trying to overcome the productivity and repeatability of the injection moulding process.

Considering the production issues mentioned earlier, whether for identifying problems that require early detection or product's time-to-market decrease intention, the current industrial digitalization will provide the proper ecosystem for AM processes to continue to grow and develop and fully succeed in the market worldwide.

## References

- Agustí-Juan, I., Habert, G.: Environmental design guidelines for digital fabrication. *J. Cleaner Prod.* **142**, 2780–2791 (2017). <https://doi.org/10.1016/j.jclepro.2016.10.190>. Elsevier Ltd
- Almeida, H.A., Correia, M.S.: Sustainability impact evaluation of support structures in the production of extrusion based parts. In: Muthu, S.S., Savalani, M.M. (eds.) *Handbook of Sustainability in Additive Manufacturing*, vol. I, Springer (ISBN 978-981-10-0549-7), pp. 7–30 (2016). [https://doi.org/10.1007/978-981-10-0549-7\\_2](https://doi.org/10.1007/978-981-10-0549-7_2)
- Almeida, H.A., Oliveira, E.S.G.: Sustainability based on biomimetic design models. In: Muthu, S.S., Savalani, M.M. (eds.) *Handbook of Sustainability in Additive Manufacturing*, vol. II, Springer (ISBN 978-981-10-0604-3), pp. 65–84 (2016). [https://doi.org/10.1007/978-981-10-0606-7\\_3](https://doi.org/10.1007/978-981-10-0606-7_3)
- Bourell, D.L., Leu, M.C., Rosen, D.W.: *Roadmap for Additive Manufacturing: Identifying the Future of Freeform Processing*. The University of Texas at Austin, Austin (2009)

- Brueckner, F., Riede, M., Mueller, M., Marquardt, F., Knoll, M., Willner, R., Seidel, A., Lopez, E., Leyens, C., Beyer, E.: Fabrication of metallic multi-material components using Laser Metal Deposition. *Solid Free Fabr Symp* 2530–2538 (2017)
- Chen, D., et al.: Direct digital manufacturing: definition, evolution, and sustainability implications', *Journal of Cleaner Production*, p. 107 (2015). <https://doi.org/10.1016/j.jclepro.2015.05.009>
- Connor, H.J.O., Dickson, A.N., Dowling, D.P.: Evaluation of the mechanical performance of polymer parts fabricated using a production scale multi jet fusion printing process. *Add. Manuf. Elsevier* **22**, 381–387 (2018). <https://doi.org/10.1016/j.addma.2018.05.035>
- Cozmei, C., Caloian, F.: Additive manufacturing flickering at the beginning of existence. *Procedia Econ. Financ.* **3**, 457–462 (2012). [https://doi.org/10.1016/S2212-5671\(12\)00180-3](https://doi.org/10.1016/S2212-5671(12)00180-3)
- Debroy, T., et al.: Scripta materialia building digital twins of 3D printing machines ☆. *Scripta Materialia, Acta Materialia Inc.*, 135, pp. 119–124 (2017)
- Desktop Metal: Exploring metal finishing methods for 3D-printed parts Metal finishing Part one. Burlington, MA, USA (2018). <https://www.desktopmetal.com/white-paper/metal-finishing-methods/>
- Dopico, M., Gomez, A., De la Fuente, D., et al.: A vision of industry 40 from an artificial intelligence point of view. *Int Conf Artif Intell (ICAI) Steer Comm world Congr Comput Sci Comput Eng Appl Comput* 407–413 (2016). [https://doi.org/10.1016/s0140-6736\(05\)63547-7](https://doi.org/10.1016/s0140-6736(05)63547-7)
- Franchetti, M., Kress, C.: An economic analysis comparing the cost feasibility of replacing injection molding processes with emerging additive manufacturing techniques. *Int. J. Adv. Manuf. Technol.* **88**, 2573–2579 (2017). <https://doi.org/10.1007/s00170-016-8968-7>
- Gao, W., et al.: The status, challenges, and future of additive manufacturing in engineering. *Comput.-Aided Des.* **69**, 65–89 (2015). <https://doi.org/10.1016/j.cad.2015.04.001>. Elsevier Ltd
- Gardan, J.: Additive manufacturing technologies: state of the art and trends. *Addit. Manuf. Handb. Prod. Dev. Def. Ind.* **7543**, 149–168 (2017). <https://doi.org/10.1201/9781315119106>
- Gibson, I.: Is additive manufacturing a sustainable technology?'. In: *Proceedings of SIM2011 Sustainable Intelligent Manufacturing*, Bártolo, H., et al (Eds.), IST Press, 583–589 (2011)
- Gibson, I., Rosen, D., Stucker, B.: *Additive Manufacturing Technologies – 3D Printing, Rapid Prototyping and Direct Digital Manufacturing*, 2nd edn. Springer, New York (2015)
- Goehrke, S.A.: *Evolve Additive Solutions Emerges from Stealth with 50x Faster 3D Printing for Production* (2019). <https://3dprint.com/208742/evolve-additive-solutions/>
- Grünberger, T., Domröse, R.: Optical in-process monitoring of direct metal laser sintering (DMLS). *Laser Technik J.* **11**, 40–42 (2014)
- Guo, N., Leu, M.C.: Additive manufacturing: technology, applications and research needs. *Front. Mech. Eng.* **8**(3), 215–243 (2013). <https://doi.org/10.1007/s11465-013-0248-8>
- ISO: *Additive manufacturing - General principles - Part 2: Overview of process categories and feedstock*, ISO 17296-2:2015 (E), 2015, pp. 1–5 (2015)
- Jackson, B.: Fraunhofer's TwoCure technology realized in industry-ready 3D printer, *3D Printing Industry* (2018a). <https://3dprintingindustry.com/news/fraunhofers-twocure-technology-realized-in-industry-ready-3d-printer-141429/>. Accessed 4 Mar 2019
- Jackson, B.: Fraunhofer's TwoCure technology realized in industry-ready 3D printer, *3D Printing Industry* (2018b)
- Kelly, B.E., et al.: Volumetric additive manufacturing via tomographic reconstruction. *Science* **363**(6431), 1075–1079 (2019). <https://doi.org/10.1126/science.aau7114>
- Khoo, Z.X., et al.: 3D printing of smart materials: A review on recent progresses in 4D printing. *Virtual Phys. Prototyping* **10**(3), 103–122 (2015). <https://doi.org/10.1080/17452759.2015.1097054>



- Knapp, G.L., et al.: Building blocks for a digital twin of additive manufacturing. *Acta Mater.* **135**, 390–399 (2017). <https://doi.org/10.1016/j.actamat.2017.06.039>
- Koopmann, J., Voigt, J., Niendorf, T.: Additive manufacturing of a steel-ceramic multi-material by selective laser melting. *Metall. Mat. Trans. B Process Metall. Mat. Process Sci.* **50**, 1042–1051 (2019). <https://doi.org/10.1007/s11663-019-01523-1>
- Lee, J.Y., An, J., Chua, C.K.: Fundamentals and applications of 3D printing for novel materials. *Appl. Mat. Today* **7**, 120–133 (2017a). <https://doi.org/10.1016/j.apmt.2017.02.004>. Elsevier Ltd
- Lee, J.Y., An, J., Chua, C.K.: ‘Fundamentals and applications of 3D printing for novel materials. *Appl. Mat. Today* **7**, 120–133 (2017b). <https://doi.org/10.1016/j.apmt.2017.02.004>. Elsevier Ltd
- Löber, L., Flache, C., Petters, R., et al.: Comparison of different post processing technologies for SLM generated 316 l steel parts. *Rapid Prototyp. J.* **19**, 173–179 (2013). <https://doi.org/10.1108/13552541311312166>
- MacDonald, D., Fernández, R., Delloro, F., Jodoin, B.: Cold spraying of armstrong process titanium powder for additive manufacturing. *J. Therm. Spray Technol.* **26**, 598–609 (2017). <https://doi.org/10.1007/s11666-016-0489-2>
- Masoomi, M., Thompson, S.M., Shamsaei, N.: Quality part production via multi-laser additive manufacturing. *Manuf. Lett.* **13**, 15–20 (2017). <https://doi.org/10.1016/J.MFGLET.2017.05.003>. Elsevier
- Matt, D.T., Rauch, E., Dallasega, P.: Trends towards distributed manufacturing systems and modern forms for their design. *Procedia CIRP* **33**, 185–190 (2015). <https://doi.org/10.1016/j.procir.2015.06.034>
- Melenka, G.W., et al.: Evaluation and prediction of the tensile properties of continuous fiber-reinforced 3D printed structures. *Compos. Struct.* **153**, 866–875 (2016). <https://doi.org/10.1016/j.compstruct.2016.07.018>. Elsevier Ltd
- Mendes-Felipe, C., et al.: State-of-the-art and future challenges of UV curable polymer-based smart materials for printing technologies. *Adv. Mat. Technol.* **1800618**, 1–16 (2019). <https://doi.org/10.1002/admt.201800618>
- Monzón, M.D., et al.: Standardization in additive manufacturing: activities carried out by international organizations and projects. *Int. J. Adv. Manuf. Technol.* **76**(5–8), 1111–1121 (2015). <https://doi.org/10.1007/s00170-014-6334-1>
- Ngo, T.D., et al.: Additive manufacturing (3D printing): a review of materials, methods, applications and challenges. *Compos. Part B.* **143**, 172–196 (2018). <https://doi.org/10.1016/j.compositesb.2018.02.012>. Elsevier
- Ning, F., et al.: Additive manufacturing of carbon fiber reinforced thermoplastic composites using fused deposition modeling. *Compos. Part B: Eng.* **80**, 369–378 (2015). <https://doi.org/10.1016/j.compositesb.2015.06.013>. Elsevier Ltd
- Oxman, N.: Variable property rapid prototyping. *Virtual Phys. Prototyping* **6**(1), 3–31 (2011)
- Peels, J.: Interview with Patrik Ohldin of Open Source Metal 3D Printing Company Freemelt, 3D Print.com (2019). <https://3dprint.com/233218/interview-with-patrik-ohldin-of-open-source-metal-3d-printing-company-freemelt/>. Accessed 8 July 2019
- Pei, E., Loh, G.H., Harrison, D., Almeida, H.A., Verona, M.D.M., Paz, R.: A study of 4D printing and functionally graded additive manufacturing. *Assembly Autom.* **37**(2), 147–153 (2017). <https://doi.org/10.1108/AA-01-2017-012>
- Peters, S., et al.: Automotive manufacturing technologies – an international viewpoint. *Manuf. Rev.* **1**, 10 (2014). <https://doi.org/10.1051/mfreview/2014010>
- Reeves, P.: Additive manufacturing – a supply chain wide response to economic uncertainty and environmental sustainability. In: *International Conference on Industrial Tools and Material Processing Technologies*, Ljubljana, Slovenia (2009)

- Rickenbacher, L., Spierings, A., Wegener, K.: An integrated cost-model for selective laser melting (SLM). *Rapid Prototyp. J.* **19**, 208–214 (2013). <https://doi.org/10.1108/13552541311312201>
- Riss, F., Schilp, J., Reinhart, G.: Load-dependent optimization of honeycombs for sandwich components-new possibilities by using additive layer manufacturing. *Phys. Procedia* **56**, 327–335 (2014). <https://doi.org/10.1016/j.phpro.2014.08.178>
- Rohde, J., et al.: Standardised product development for technology integration of additive manufacturing. *Virtual Phys. Prototyp.* **14**(2), 141–147 (2019). <https://doi.org/10.1080/17452759.2018.1532801>
- Roos, G., Fusco, M.: Strategic implications of additive manufacturing (AM) on traditional industry business models. In: *Proceedings of Additive Manufacturing with Powder Metallurgy Conference, Orlando* (2014)
- Salonitis, K., et al.: Additive manufacturing and post-processing simulation: laser cladding followed by high speed machining. *Int. J. Adv. Manuf. Technol.* **85**(9–12), 2401–2411 (2016). <https://doi.org/10.1007/s00170-015-7989-y>
- Sames, W.J., et al.: The metallurgy and processing science of metal additive manufacturing. *Int. Mat. Rev. Taylor & Francis* **61**(5), 315–360 (2016). <https://doi.org/10.1080/09506608.2015.1116649>
- Sova, A., Grigoriev, S., Okunkova, A., Smurov, I.: Potential of cold gas dynamic spray as additive manufacturing technology. *Int. J. Adv. Manuf. Technol.* **69**, 2269–2278 (2013). <https://doi.org/10.1007/s00170-013-5166-8>
- Sreenivasan, R., Goel, A., Bourell, D.L.: Sustainability issues in laser-based additive manufacturing. *LANE 2010. Phys. Procedia* **5**, 81–90 (2010)
- Tekinalp, H.L., et al.: Highly oriented carbon fiber-polymer composites via additive manufacturing. *Compos. Sci. Technol.* **105**, 144–150 (2014). <https://doi.org/10.1016/j.compscitech.2014.10.009>. Elsevier Ltd
- Thompson, M.K., et al.: Design for additive manufacturing: trends, opportunities, considerations, and constraints. *CIRP Ann.* **65**(2), 737–760 (2016). <https://doi.org/10.1016/J.CIRP.2016.05.004>. Elsevier
- Vayre, B., Vignat, F., Villeneuve, F.: Designing for additive manufacturing. *Procedia CIRP* **3**(1), 632–637 (2012). <https://doi.org/10.1016/j.procir.2012.07.108>
- Watson, J.K., Taminger, K.M.B.: A decision-support model for selecting additive manufacturing versus subtractive manufacturing based on energy consumption. *J. Cleaner Prod.* **176**, 1316–1322 (2018). <https://doi.org/10.1016/j.jclepro.2015.12.009>. Elsevier Ltd
- Weller, C., Kleer, R., Piller, F.T.: Economic implications of 3D printing: market structure models in light of additive manufacturing revisited. *Int. J. Prod. Econ.* **164**, 43–56 (2015). <https://doi.org/10.1016/j.ijpe.2015.02.020>. Elsevier
- Yang, S., Zhao, Y.F.: Additive manufacturing-enabled design theory and methodology: a critical review. *Int. J. Adv. Manuf. Technol.* (2015). <https://doi.org/10.1007/s00170-015-6994-5>
- Zegard, T., Paulino, G.H.: Bridging topology optimization and additive manufacturing. *Struct. Multi. Optim.* **53**(1), 175–192 (2016). <https://doi.org/10.1007/s00158-015-1274-4>



# Additive Technologies in the Medical Field for 2030

Emanuel Serrano<sup>1</sup>, Liliana Vitorino<sup>1(✉)</sup>, and Henrique A. Almeida<sup>1,2</sup>

<sup>1</sup> School of Technology and Management - ESTG,  
Polytechnic Institute of Leiria, Leiria, Portugal

2162093@my.ipleiria.pt, {liliana.vitorino,  
henrique.almeida}@ipleiria.pt

<sup>2</sup> Research Center for Information Technology and Communications - CIIC,  
Polytechnic Institute of Leiria, Leiria, Portugal

**Abstract.** Additive technologies are by definition technologies capable of producing products in a layer-by-layer fashion. Due to the specific characteristics of these technologies, the products can be produced in multi-materials and without any geometric limitations. By associating the use of biocompatible materials, it has become an excellent technology to develop products and/ or devices for the medical field. Additive manufacturing technologies within the medical field have created a specific technological field, namely biomanufacturing which is capable of producing medical devices with the combination of biomaterials, drugs and growth factors and the use of cells for the production of biomedical implants. Additive manufacturing and biomanufacturing technologies have thus shown to be capable of meeting the requirements demanded by the medical sector. However, the significance of these technologies can't be based only on the current context, but also need to be assessed in the future context.

Given the growth and diversity that these technologies have achieved, this study aims to examine the future impact of additive manufacturing technologies in the medical field for the year 2030. To meet this goal, we used the Delphi method which is a technique that involves the application of questionnaires to experts in the field, until reaching the relative consensus of the predictions of these technologies.

**Keywords:** Additive manufacturing systems · Bio manufacturing systems · Biomedical technologies and medical applications · Delphi method

## 1 Introduction

Over the past few years have emerged various manufacturing and processing technologies that have revolutionized the production of customized products. These technologies have exceeded the limits and geometric design limitations that existed previously in conventional manufacturing technologies. However, these technologies have emerged into areas where the requirements are constantly more demanding such as in the medical sector. Additive manufacturing technologies are capable of producing medical devices and implants with several types of specifications, such as biocompatible, anatomically shaped, biomaterial-based, cell-based, pharmaceutical-based,

functionally graded, etc. [1]. In the case of medical devices, examples that interact directly with patients are orthosis and exoskeletons [1]. In the case of medical implants, they may be of two types, namely externally to the body and internally to the body. Examples of external implants are prosthesis for the leg, foot, hand, eye, etc. [1]. Regarding internal implants, they may also be divided in two additional categories, namely permanent and temporary. Examples of internal permanent implants are metallic implants such as hip and knee prostheses etc. [1]. Examples of internal temporary implants are scaffolds which are used for either hard or soft tissue engineering and regenerative medicine applications where they are absorbed by the body during their degradation and tissue regeneration [1].

Additive manufacturing processes for medical applications comprise the following techniques [2–4]:

1. Vat photopolymerization (e.g., stereolithography, SLA) – an additive manufacturing process in which a liquid photopolymer in a vat is selectively cured by light-activated polymerization.
2. Material jetting (e.g., Polyjet) – an additive manufacturing process in which droplets of build material are selectively deposited.
3. Binder jetting (e.g., 3D printers using powder and binder) – an additive manufacturing process in which a liquid bonding agent is selectively deposited to join powder materials.
4. Material extrusion (e.g., FDM) – an additive manufacturing process in which material is selectively dispensed through a nozzle.
5. Powder bed fusion (e.g., SLS) – an additive manufacturing process in which thermal energy selectively fuses regions of a powder bed.
6. Sheet lamination (e.g., Sheet Forming) – an additive manufacturing process in which laminated sheets of material are consecutively cut and added to the previous layer.
7. Directed energy deposition (e.g., laser cladding) – an additive manufacturing process in which material is fused and added during the production of the part.

Thus, additive manufacturing technologies, biomanufacturing, bioprinting have demonstrated being able to meet the demands of the medical sector [1]. In Fig. 1, the field of additive technologies in the health sector is visible. However, responses to the needs can't only be based on the current context. A reflection about the future of these technologies is needed to determine its applicability, ethics and potential within the medical field.

Additive manufacturing technologies have to be able to meet several demands. But will these technologies be able to do it in the future? Which will be the technological route of these technologies? Will additive technologies be prevented from advancing in the medical field due to either ethical and/or regulatory issues? Or will it force a change in current health legislation worldwide? In short, what is the impact of additive manufacturing technologies in the medical sector in the future? To be able to answer these questions, we developed this research study and we used the Delphi methodology which is presented in the next section.



**Fig. 1.** Examples of medical devices and implants produced with the aid of additive technologies (adapted from Almeida et al. 2018).

## 2 Methodology

### 2.1 Study Design

To meet the proposed objectives, the study began with a literature review to understand the additive manufacturing technologies and biomanufacturing technologies. The next step was to choose a methodology that would be able to help predict the impact of these technologies in the medical field, particularly for the year 2030. For this specific case, it was found that the best technique to apply was the Delphi method. Once the topic has global impact, it was decided to invite international researchers to give their contribution in the study.

### 2.2 Delphi Method

The Delphi method consists to survey an expert opinion and reach a consensus group response through several rounds [5]. Opinions, beliefs, and judgments are collected and organized in a systematic method that focuses primarily on the consensus and divergent ideas [6]. The main scope of the method begins with individual feedback regarding a given topic or questionnaire, then the answers are assessed, and a group's global judgement is obtained. The next round regards the rating of the answers and all the experts involved revise their views and opinions. This process only ends with a positive or negative consensus opinion is achieved.

**2.2.1 First Round**

In first stage of Delphi method, the criteria inclusion to select the experts were:

1. Number of publications in the area, combining both additive manufacturing and medical applications;
2. Number of patents in the area, combining both additive manufacturing and medical applications, and;
3. And number of research projects combining both additive manufacturing and medical applications.

Once established the preliminary list of participants, two participants from each continent were chosen and invited to be part of the study and participate in the first round. As mentioned, the first round is a questionnaire composed with a list of questions that focus on general aspects of the PEST analysis, this is political, economic, social and technological issues. The questions are listed in the following table:

The first round presented to be the most demanding due to the fact that not all selected participants were willing to participate. Therefore, as they answered positively or negatively, new participants were required to be evaluated and invited to be part of the study. This process continued until achieving 2 participants per continent. In the end, 7 experts were involved in this stage (Tables 1 and 2).

**Table 1.** List of questions according to the PEST topics.

Political issues	<ol style="list-style-type: none"> <li>1. How will additive technologies influence intellectual property policies?</li> <li>2. How will additive technologies influence the issues of accountability and ethics?</li> <li>3. How do you define the barrier between customized and replicated products?</li> <li>4. What advantages do you think additive technologies can bring to manufacturing companies?</li> <li>5. Will additive technologies impact labour laws in countries?</li> <li>6. With the development of bio-printing increasingly focused on the printing of tissues and organs, what are the major discussions on ethical issues, considering stem cells? Is this process considered as organ cloning? Or is it a more and more demanding need because of the shortage of organs?</li> </ol>
Economic issues	<ol style="list-style-type: none"> <li>1. Will it be increasingly important to invest in technology teaching, creating further development and progress in additive manufacturing? How can one create more enthusiasm for this sector?</li> <li>2. Will additive manufacturing have an impact on unemployment or economic recessions?</li> <li>3. Developed countries are expected to have enormous economic potential with the growth of additive manufacturing, but developing countries may find it difficult to keep up with this progress. What type of structures can one create for developing countries?</li> <li>4. Homemade additive manufacturing already has many successful cases. Will it add value to the development of this technology or present danger to its future that is approaching? Can this home-grown production contribute or harm additive technologies in the health sector? How can you guard against all the dangers that may arise?</li> </ol>

*(continued)*

**Table 1.** (continued)

	<p>5. Do you consider that there will be an increase in GDP with the use of additive manufacturing in health or will it just be an additional expense for governments?</p> <p>6. Do you think 4D printing will be a major breakthrough for additive manufacturing in medicine? What are the fields where they are applied and what will be the forecast for their application in the global market?</p>
Social issues	<p>1. What kind of changes will additive technologies influence consumer behaviour and demand?</p> <p>2. What kind of changes will additive technologies influence the behaviour of new product offerings?</p> <p>3. What is your opinion on the corporate social responsibility of companies with additive manufacturing technologies in the health sector?</p> <p>4. Additive technologies have also shown a positive impact in ecological terms. Do you consider this a critical topic for applications of additive manufacturing technologies in the medical sector?</p>
technological issues	<p>1. Additive manufacturing in medicine is very much focused on bioprinting. What are the most promising developments that are to be implemented in the market and how should they be implemented?</p> <p>2. One of the limitations in additive manufacturing is the lack of multi-material structures or functional gradients that will make a breakthrough for the technology. Which ones will revolutionize the market and where is there more lack of these advances?</p> <p>3. How do you consider the time of approval by the FDA with the development of technologies and materials for medical devices and products?</p> <p>4. Do you consider that additive manufacturing technologies can already process any material with or without pharmaceuticals, bioactive agents and cells for medical applications?</p> <p>5. It is well known that additive manufacturing will be the next industrial revolution, but one of its limitations is the lack of versatility and printing time. Why has this technology failed to overcome these barriers?</p> <p>6. Do you think that additive manufacturing technologies will have their potential in the production of medical devices and implants or in the production of tissues and organs? Which will be the area with the most promising results social and economically?</p> <p>7. Additive manufacturing already has great work developed for pre-surgical studies of complex operations. What will be the next step of this technology in surgery?</p> <p>8. What are the potential threats of additive manufacturing in the medical sector?</p> <p>9. One of the next advances of additive manufacturing will be the production distribution of personalized pharmaceuticals in pharmacies. Do you consider this a critical step that should be taken for additive manufacturing? If so, how is it justified that this progress has not yet taken hold and what are the barriers to overcome?</p>

### 2.2.2 Second Round

The next stage consisted in analysing the results obtained in the first round and identifying a set of key issues that would be considered as metrics for the second round of evaluation. These items are then rated with a Likert Seven-point scale to assess the importance of each item. In order to increase the significance of the study, in this second, additional participants were added to the process.

**Table 2.** List of topics for each question within the PEST topics.

Political issues	
Question	Item
What level do you agree or disagree that Additive Manufacturing Technologies will have a high impact in the medical sector in 2030?	New legislations/regulations
	New pharmaceutical legislations/ regulations
	Accountability and ethics
	Infringements
	Standardized medical procedures and process certifications
	Local FDA approval time and its internal regulations
	Protecting patient information
No effects on political/legal/ethical issues	
Economic issues	
Question	Item
What level do you agree or disagree that Additive Manufacturing Technologies will have a high impact in the medical sector in the year 2030?	Competitors
	Market
	Provider/Customer Relationship
	Partnerships
	Customized products
	Company Benefits
	Impact on GDP
	Training
	Employment
	Incentives
	Ecological impact in the health sector
	Economic impact in the pharmaceutical sector
No effects on economic issues	
Social issues	
Question	Item
What level do you agree or disagree that Additive Manufacturing Technologies will have a high impact in the medical sector in the year 2030?	Technological literacy
	Cultural issues
	Technology acceptance
	Corporate social responsibility of companies
	No effects on social issues

(continued)



**Table 2.** (continued)

Political issues	
Question	Item
Technological issues	
Question	Item
What level do you agree or disagree that Additive Manufacturing Technologies will have a high impact in the medical sector in the year 2030?	Intellectual property
	New shape design
	New materials
	Composite materials and/or multi-material structures
	Products/Devices with functional gradients
	Donor organ reduction
	Tissue engineering and regeneration
	Pharmaceutical sector
	Medical devices and products
	Medical Technology Development
	Availability of Additive Manufacturing
No effects on technological issues	
Other issues	
Question	Item
What level do you agree or disagree that are the potential threats of additive manufacturing in the medical sector?	Failure to fund clinical trials to demonstrate improved outcomes
	Failure to acknowledge improved outcomes with reliable reimbursement
	Safety issues
	Lack of knowledge about the additive manufacturing technologies
	Regulatory control and inertia of the current system
	Lack of time for health professionals to master these technologies
	Oversimplification of devices or the mis-design because people without an in-depth knowledge feel they have the capacity
	Cybersecurity
	Cost
	Material Strength
	Toxicity issues

Each metric of each question was graded with one of the following seven options:

- Entirely Disagree
- Mostly Disagree
- Somewhat Disagree

- Neither Agree nor Disagree
- Somewhat Agree
- Mostly Agree
- Entirely Agree

Within the Technological Issues, two additional open questions were asked where the participants were requested to give their opinion according to the same grades previously mentioned. The questions are the following:

- Regarding Bioprinting, do you agree or disagree that it will overcome its research domain towards its industrialization in healthcare for the year 2030?
- Regarding the technological barriers of additive manufacturing, do you agree or disagree that it will overcome its current technological barriers for the year 2030?

### 3 Conclusions

Additive manufacturing technologies and biomanufacturing have shown to be able to meet the demands of the medical sector. These technologies tend to grow exponentially, and users also tend to rely on them in the future. This research study aims to predict the impact of additive manufacturing technologies to the horizon of the year 2030 worldwide. The study is still ongoing, which means that there are still no concrete conclusions, but it is already possible to verify that this study will present relevant results towards the medical and scientific community regarding the impacts of the usage of these technologies in the future.

### References

1. Almeida, H.A., Costa, A.F.D., Ramos, C.A.R., Torres, C., Minondo, M., Bartolo, P.J.S., Nunes, A.A., Takanori, D.K., da Silva, J.V.L.: Additive Manufacturing Systems for Medical Applications: Case Studies Additive Manufacturing - Developments in Training and Education. In: Pei, E., Verona, M.M., Bernard, A. (eds.), Springer (ISBN: 978-3-319-76083-4 (Print) 978-3-319-76084 1 (Online)), 187–209 (2018)
2. Almeida, H.A., Correia, M.S.: Sustainability impact evaluation of support structures in the production of extrusion based parts. In: Muthu, S.S., Savalani, M.M. (eds.) Handbook of Sustainability in Additive Manufacturing vol. I, Springer (ISBN 978-981-10-0549-7), pp. 7–30 (2016). [https://doi.org/10.1007/978-981-10-0549-7\\_2](https://doi.org/10.1007/978-981-10-0549-7_2)
3. Gao, W., Zhang, Y., Ramanujan, D., Ramani, K., Chen, Y., Williams, C.B., Wang, C.C.L., Shin, Y.C., Zhang, S., Zavattieri, P.D.: The status, challenges, and future of additive manufacturing in engineering. *Comput.-Aided Des.* **69**, 65–89 (2015)
4. Gibson, I., Rosen, D., Stucker, B.: Additive Manufacturing Technologies – 3D Printing, Rapid Prototyping and Direct Digital Manufacturing, 2nd edn. Springer, New York (2015)
5. Burt, C.G., Cima, R.R., Koltun, W.A., Littlejohn, C.E., Ricciardi, R., Temple, L.K., et al.: Developing a research agenda for the American society of colon and rectal surgeons: results of a delphi approach. *Dis. Colon Rectum* **52**, 898–905 (2009)
6. Steurer, Johann: The delphi method: an efficient procedure to generate knowledge. *Skeletal Radiol.* **40**, 959–961 (2001). <https://doi.org/10.1007/s00256-011-1145-z>



# Technological and Economic Comparison of Additive Manufacturing Technologies for Fabrication of Polymer Tools for Injection Molding

Achim Kampker<sup>1</sup>, Bruno Alves<sup>2</sup>, and Peter Ayvaz<sup>1</sup> 

<sup>1</sup> RWTH Aachen University, Templergraben 55, 52062 Aachen, Germany

p. ayvaz@pem.rwth-aachen.de

<sup>2</sup> Ford Motor Company, Wernigerode, Germany

**Abstract.** This paper investigates the technological and economic potential of 10 different AM materials manufactured with four different AM technologies for the use of tool production for injection molding in small series applications. Therefore, experimental trials with three different injection molding materials with increasing manufacturing difficulty in terms of resulting tool loads are conducted. Tool wear, resulting part quality and tool manufacturing cost are taken into account for potential evaluation. A concrete selection of the most suitable materials for further investigation is given.

**Keywords:** Additive tooling · Injection molding · Rapid tooling

## 1 Introduction

The increasing market dynamic, competition and an uncertain environment poses challenges for manufacturing companies [1]. Shorter product lifecycles and more product variants with an increasing technical complexity require shorter and more frequent product development and ramp-up phases [2]. For all tool-bound manufacturing processes this leads to demanding requirements for tool manufacturing as costs and time-to-market need to be reduced consistently [3–5]. New process technology combinations, such as additive tooling for injection molding are used to decrease costs and shorten time-to-market of polymer components [6].

Over the last two decades, the concept of additive manufactured polymer injection molding tools has been further developed to meet these new requirements of increased product variety and decreased lead times in polymer part production within product development [7, 8]. There are generally two approaches to integrate additive manufacturing into tool production within product development [9, 10]: Indirect tooling makes use of additive manufacturing for master pattern production to manufacture the tool in a subsequent second production step, mostly some form of casting. Direct tooling makes use of additive manufacturing to produce the tool immediately without a second manufacturing step except some form of post processing for quality enhancement. Comparing the process chains of these two approaches, it is evident, that the

direct approach generally requires less process steps and hence offers an inherent benefit in terms of lead times which is why this paper focuses on the direct approach.

Prior case studies on the use of additive manufactured polymer tools for injection molding have investigated the technological potential with respect to resulting part quality as well as tool life of different tooling materials in comparison to conventionally manufactured tools for different applications. Reference [11] shows, that the PolyJet-Material Fullcure 720 is able to withstand 20 cycles compared to 10 cycles of an Al<sub>2</sub>O<sub>3</sub> filled epoxy resin during injection molding using a PLA. The potential use of resin coated 3D printed polymer tools using the PolyJet Material “Digital ABS” was demonstrated in [12]. Another investigation of “Digital ABS” as tool material showed, that the dimensional stability and the surface roughness of the printed tool remained stable over a period of 50 cycles using PP as injection material [13]. Further, the resulting mechanical part material properties deviated little compared to the material properties from parts manufactured in a conventional steel tool [13]. The thermal conductivity behavior of “Digital ABS” as tool material was found suitable for small series production of nucleated PLA resulting in similar thermomechanical part material properties as in temperature controlled steel tools for mass production [14]. “Digital ABS” as tool material once more was investigated in a comparative study using PP as injection material. Compared to a conventional steel tool and a direct metal sintered tool, the PolyJet tool lasted significantly less cycles and resulting parts showed higher shrinkage and crystallinity values [15]. Tool life, general surface quality and especially impact on micro feature characteristics such as edge sharpness, hole diameter and thermal performance evaluation of a DLP insert were extensively investigated in [16, 17].

Further extensive work on the influence of part morphology and crystallinity was done by HARRIS et al. In [18] they showed a doubling of the shrinkage of a PA66 molded in a stereolithography (SL) tool compared to the same geometries from an aluminium (AL) tool. The difference in shrinkage behavior was linked primarily to the different processing conditions namely due to the different cooling behavior caused by the different tool material thermal conductivities. Further, a difference in shrinkage using amorphous ABS could not be observed suggesting special caution for shrinkage compensation when semi crystalline or crystalline polymers are used. [19] therefore proposed two approaches to control crystallinity behavior in parts from SL tools. First melt temperature alteration was used to lower the possible melt temperature resulting in a lower crystallinity in PA66 parts from SL tools. Due to the fast cooling in AL tools, the zone in which crystallinity can be influenced is passed to fast, hence melt temperature alteration did not affect crystallinity in parts from AL tools. Second, the use of a nucleating agent provides parts with a consistent crystallinity regardless of the cooling rate resulting in parts with a crystallinity in between the values of parts from SL and AL tools without using a nucleating agent. [20] further showed that the lower thermal conductivity of the polymer tools increases the degree of crystallization of semi-crystalline PA66 injection molded parts, which also increases the shrinkage potential of the injection molded parts. Compared to parts from AL tools, parts from a SL tool developed approx. 30% more crystallinity resulting in a total crystalline difference of approx. 6%. [21] show how the low thermal conductivity of a SL tool can be used to produce fully crystalline PEEK parts at much lower process parameters compared to a conventional steel. It was possible to produce a small number of parts at a

tool temperature of 23 °C and with an injection pressure of 25 bar using a SL tool. According to [21], a tool temperature of approx. 200 °C and an injection pressure of 500 bar would be required using a steel tool to achieve parts with a similar crystalline structure. In addition to that, [22] conclude, that a good heat conducting tool material causes thick boundary layers and small spherulites whereas a poor heat conducting material results in thin boundary layers and large spherulites. Larger spherulites show correlation with increased yield stress of the parts whereas a poor surface quality lowers mechanical properties due to the notch effect.

Besides purely technological analyses, case studies with a focus on economic comparison of the different tool manufacturing routes were also conducted. [23] shows a possible tooling cost reduction of 80%–90% when using polymer based AM to manufacture injection molding tools for two different reference parts within product development phase. Further, a cost effectiveness for the production of up to 3400 units for the smaller reference part and up to 500 units for the bigger reference part were confirmed during a break even analysis. Based on these results, the authors present in [24], how a detailed cost estimation model, considering the AM and injection molding part of the process chain can look like, promoting the idea to use AM as synergistic addition in combination with traditional manufacturing processes. [25] compares the suitability of two different PolyJet materials, “Digital ABS” and “RGD450” for the use of tool production. More than 120 parts of a reference geometry in ABS material were produced successfully. A technological comparison with an aluminum tool as reference showed, that overall form accuracy of the resulting molded part could be reached while required surface roughness could not reach the roughness of parts from the aluminum tool [25]. An economic comparison showed, that for the investigated use case a 10% and 15% saving in overall cost for “Digital ABS” and “RGD450” respectively could be achieved, while lead time could only be reduced by 13% using the “RGD450” tool [25].

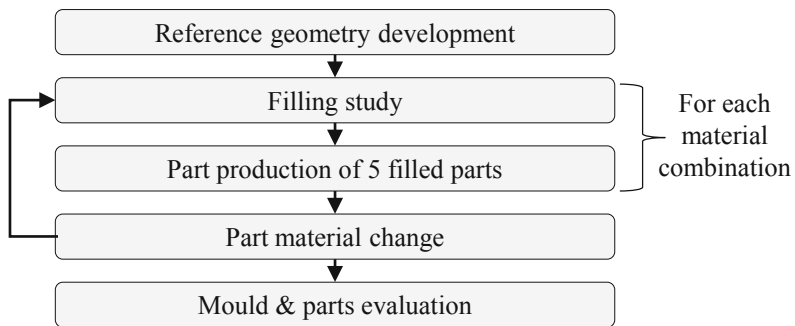
The literature shows, that studies focusing on single application fields already investigated printed polymer tools – namely “Digital ABS” material with respect to its suitability as tool material. Further, extensive research to the effect on resulting part material characteristics such as morphology and crystallinity were conducted to help explain the difference in mechanical behavior. However, the increasing number of available materials for polymer additive manufacturing requires a broader study on the suitability of distinct materials for the use of tool production. This paper provides a technological and economic comparison of 10 different additive manufacturing materials with respect to their potential for the use of injection molding tool production, thus serving as an orientation for tool material selection for design engineers.

## 2 Methodology

### 2.1 General Trial Procedure

The conducted trials follow the procedure displayed in Fig. 1. After reference geometry and tool design, the tool is tested with different injection molding materials. First, a filling study for the material combination is done to determine the filling parameters resulting in completely filled parts. Filling studies for all tool materials are done

following the same procedure. Starting from initial injection molding parameters, a first shot at 90% of calculated part volume is done. Subsequent parameter adaption is done with respect to observed filling behavior of the part. Thereby final parameters for full volumetric filling of the parts vary between the tool materials. Filling parameters are held constant to produce five volumetric fully filled parts with the same tool. Once five parts with each injection molding material are produced or tool failure occurs, the tool is changed and no further cycles are conducted with this tool material. Technical comparison of the tools after the trials is done by determining the produced number of parts per material combination and via optical inspection of tool wear to assess the possibility to produce further parts. Additionally, weight of the resulting molded parts is compared to determine part quality. Tool manufacturing cost allows for an economic comparison. A conventionally milled steel tool served as a reference.



**Fig. 1.** General trial methodology

## 2.2 Reference Geometry and Tool Design

Injection molded parts span a broad area of geometric variety starting from parts only a few grams in weight to whole car exterior components or big disposal containers weighing several kilograms. To examine the potential of different tool materials, a preliminary limitation in part size is undertaken in order to keep the tool loads within expected bearable limits. A size limitation to roughly 100 mm in diameter should allow producing parts with every tool material without immediate tool failure. The resulting reference geometry and corresponding tool can be seen in Fig. 2. The geometry covers typical geometric features commonly available in injection molding parts such as holes, ribs and pins in both the part itself and the resulting tool. Tool thickness is 20 mm on the injection and 27 mm on the ejection side to reduce possible clamping of the ejector pins.

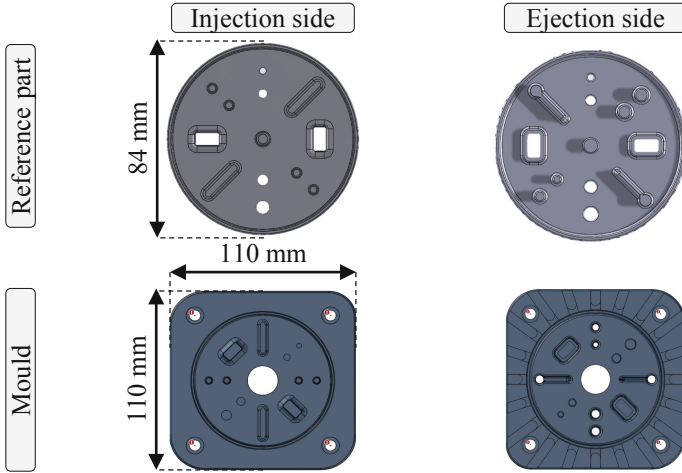


Fig. 2. Reference part and tool geometry

### 2.3 Tool and Machine Setup

Experience from previous trials as well as [15, 25] state, polymer tools should be incorporated into a standard metal tool frame for both, reducing necessary print volume as well as increasing mechanical stability against thermal and mechanical load during injection molding processes. Figure 3 shows the used tool mounting during the trials. An ejection system was used to remove the parts from the tools without putting additional loads on the tools. Trials were performed using a hydraulic 1600 kN injection molding machine (ENGEL victory 160). Active cooling was not used due to poor thermal conductivity of the printed tools.

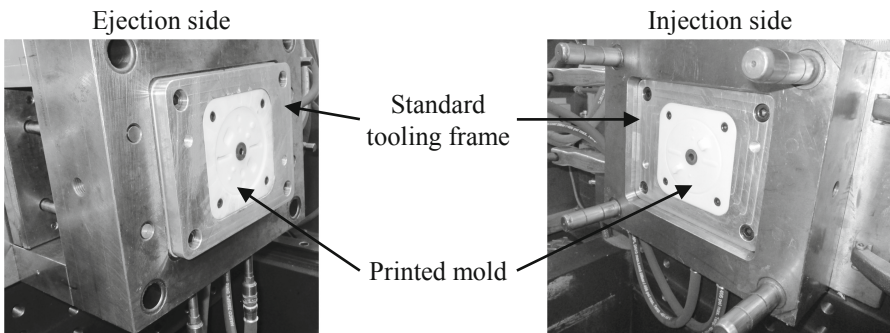


Fig. 3. Tool setup at injection molding machine

## 2.4 Tested Tool and Part Materials

Overall 10 different additive manufacturing (AM) materials from PolyJet, stereolithography, CLIP and selective laser sintering were each tested with three different part materials (PP, PA6, PA6 + GF30%) of increasing difficulty in terms of mechanical and thermal loads on the tools during injection phases. Available material data for AM materials is very scarce and mostly restricted to single values instead of comprehensive material data sets due to the novelty of the materials and the expenditure of required material tests. Further, values for material characteristics are not always measured under same test conditions making comparisons between different AM materials difficult. Nonetheless, material pre-selection needs to be done based on comparable measures. Therefore, the most reliable material characteristics values for the selection of suitable AM materials pose tensile strength (R), elongation at break ( $\epsilon$ ), heat deflection temperature (HDT) and glass transition temperature ( $T_g$ ). Thermal conductivity would offer another valuable insight but is not available for most of the materials. Table 1 summarizes the tested AM materials for tool production with the key material characteristics available.

**Table 1.** Tested tool material characteristics

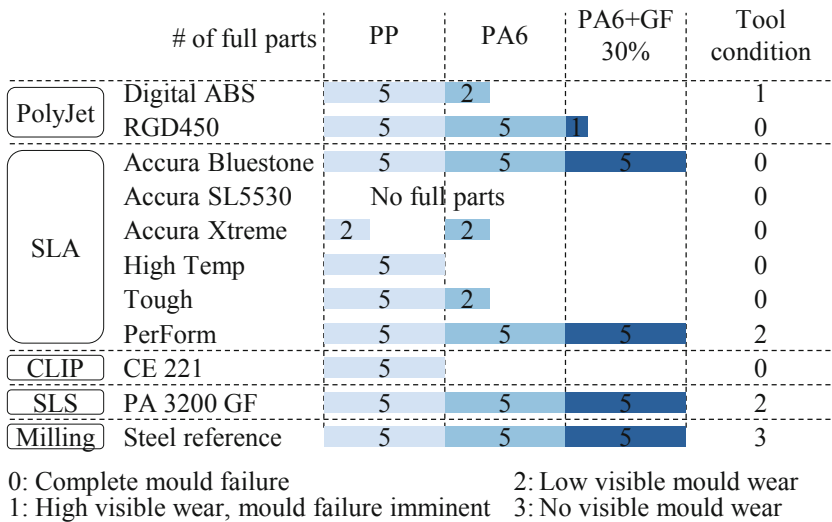
Material	R [MPa]	$\epsilon$ [%]	HDT@0.45 MPa [°C]	HDT@1.8 MPa [°C]	$T_g$ [°C]
Digital ABS	55–60	25–40	92–95	51–55	47–53
RGD450	40–45	20–35	49–54	45–50	48–52
Accura bluestone	66–68	1.4–2.4	267–284	65	51
Accura SL5530	57–63	3.8–4.4	68	56	82
Accura Xtreme	38–44	14–22	62	54	70–74
High temp	51.1	2	289	130	–
Tough	55.7	24	48.5	45.9	–
PerForm	80	1.2	268	119	81
CE221	79–105	–	231	201	–
PA 3200 GF	47–51	5.5–9	157	96	–

## 3 Trial Results

Out of the 10 tested AM materials, only three materials (PerForm, PA3200GF, Accura Bluestone) allowed to produce five fully filled parts of each injection molding material. Out of those three only PerForm and PA3200GF were not completely destroyed upon trial ending. While most of the AM tool materials were able to withstand the molding trials with PP part material, PA6 injection molding material posed a challenge mostly due to the higher injection temperature of  $\sim 280$  °C compared to  $\sim 220$  °C for PP. Most prominent tool failure mechanism is the breaking of sharp edges or small ribs due to a combination of thermal and mechanical load during injection. Accura Blue-stone broke completely into four parts despite not being the most brittle material



according to values for elongation at break, see Table 1. However, it was still possible to manufacture all required parts. Accura SL5530 and Accura Xtreme both performed very poorly breaking either immediately or after very few cycles, allowing to produce no full parts at all or just very few. The PolyJet material “RGD450” allowed to produce PP and PA66 parts with no major damages to the tool. Upon injecting PA66 + GF30% the material deteriorated very quickly allowing to produce only 1 fully filled part. The materials “Digital ABS”, “Tough” and “High Temp” all allowed to produce PP parts with no major damages to the tool, but all failed to produce 5 fully filled parts from PA66, where the material “High Temp” deteriorated immediately upon injection PA66 material. Figure 4 summarizes the results.



**Fig. 4.** Trial results – number of fully filled parts and tool condition after trials

Looking at the average weights of the parts produced in Table 2, the performance of the different AM materials with respect to filling behavior can be compared. It becomes evident, that deviation of part weights are smallest for PerForm material for all molded materials while highest deviations can be attributed to PA 3200 GF tool compared to parts from the steel reference tool. The lowest deviation of about 0,7% was achieved when molding PP in a PerForm tool. The highest deviation occurred when molding an PA66 part in a PA 3200 GF tool.

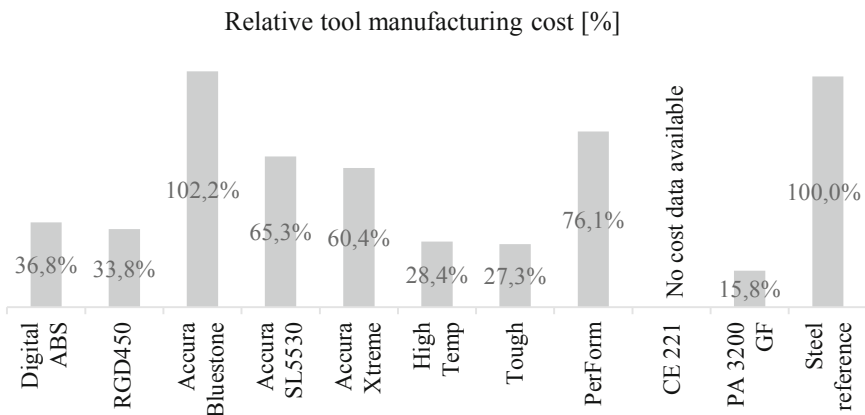
Taking additionally tool surface roughness into account, one explanation for the different filling levels can be given by a significantly weaker effect of holding pressure using a PA 3200 GF tool compared to a PerForm tool due to a poorer surface roughness and thus worse flowing properties of the liquid polymer in the tool. The higher surface roughness effectively hinders the molten material to flow resulting in less dense parts. However, it has to be noted, that different injection molding parameters were used for

**Table 2.** Average weight of the parts produced

Material	PP		PA6		PA6 + GF30%	
	w [g]	dev.[%]	w [g]	dev.[%]	w [g]	dev.[%]
Digital ABS	13,1	-3,7	18,2	-4,7	-	-
RGD450	12,14	-10,7	16,92	-11,4	18,8	-10,0
Accura bluestone	13,5	-0,7	18	-5,8	20,6	-1,4
Accura SL5530	-	-	-	-	-	-
Accura Xtreme	14,4	5,9	17	-11,0	-	-
High temp	14,1	3,7	-	-	-	-
Tough	14,1	3,7	17,04	-10,8	-	-
PerForm	13,7	0,7	18,16	-4,9	20,6	-1,4
CE221	14,1	3,7	-	-	-	-
PA 3200 GF	12,5	-8,1	16,5	-13,6	19,8	-5,3
Steel reference	13,6	0,0	19,1	0,0	20,9	0,0

the tested materials as finding the optimal parameter set was not an objective. Hence, influence of these variations needs to be considered before deriving definitive conclusions.

A tool manufacturing cost comparison offers an economic view on the potential of different materials for tool manufacturing. As costs for different manufacturing technologies vary greatly between companies depending on many factors like machine availability or economies of scale, a relative cost comparison using the milled steel tool as a reference is done. Prices for printed tools are obtained from different on demand manufacturing suppliers and averaged to get a more objective view of the market prices. Except Accura Bluestone material, all printed tools offered a reduction in manufacturing cost. From a perspective of tool manufacturing cost, PA 3200 GF offers the highest economic potential with a cost reduction of 84.2% compared to a steel tool. The PerForm tool offered a 23.9% cost reduction. Figure 5 displays the summarized results.

**Fig. 5.** Tool production cost comparison

## 4 Conclusions

This comparative study provided an overview of the technological and economic potential of 10 different AM materials for the use as injection molding tools. Trials with three different injection molding materials were performed and the resulting part weights and tool wear were evaluated following a standardized methodology.

From a technological point of view, only PerForm and PA 3200 GF are suited to manufacture all three tested materials without suffering from complete tool failure suggesting a higher potential for tool manufacturing. Accura SL5530 and Accura Xtreme were the only AM materials not capable of manufacturing one set of five parts of at least one part material suggesting a poor suitability for the tool manufacturing. For lower melting polymers like PP in this study, a variety of potential AM materials could be used. Comparing the results with the material characteristics from Table 1 the results of the trials can only be explained partially. The poorest performers, namely Accura SL5530 and Accura Xtreme both have a comparably low HDT while at the same time having a low elongation at break, indicating that a combination of low values of those two material characteristics result in poor behavior as injection molding tool. Digital ABS, RGD450 and Tough all also have low HDTs but at the same time, significantly higher values for elongation at break suggesting a more ductile behavior and therefore a possibly higher resistance against breaking upon deformation. Accura Bluestone, Perform, High Temp and CE221 show the highest HDT with at the same time the lowest values for elongation at break suggesting a very brittle material behavior. While indeed, a brittle behavior for Accura Bluestone and Tough could be observed during the trials, failure mechanism for CE221 was a complete malfunction of the mechanical behavior during deforming of PA66. It has to be noted, that the tool from CE221 had to be printed with an inner lattice structure as it was not possible to print the tool as a solid body due to limitations within the manufacturability of CLIP technology. Therefore, it was significantly more likely to fail during trials. PerForm however suffered mild cracks in the surface of the tool but was unaffected by the trials other than that. Surprisingly the PA 3200 GF tool generated good results in terms of number of full parts produced. As material characteristics for this material are in the middle of the extremes, a concrete explanation solely based on the available material characteristics for the performance cannot be given.

From an economic point of view, PA 3200 GF offers the highest cost savings in tool manufacturing. While cost savings seem significant, increased cycle times and decreased tool life needs to be considered to get a comprehensive view of the cost savings potential. Hence, a decision for a concrete material will always be subject to a trade-off between cost, lead time, required part quantity and part finish.

This study offers a first glance at the potential for different AM materials for the use as tool material for injection molding. PerForm and PA 3200 GF offer the highest technological potential even for high melting polymer materials and therefore should be further investigated with priority. Digital ABS, RGD 450, Tough and Accura Bluestone also offer technological benefits and could also be investigated with a secondary priority. Accura SL5530, Accura Xtreme, High Temp and CE221 should not

further be investigated as they offer little to no potential from a technological point of view. Considering the economic evaluation for tool manufacturing as of today, PA 3200 GF offers the highest potential. However, it should be considered, that market prices for AM materials are likely to decline with increasing material development and available supply. Further, achievable surface roughness for PA 3200 GF poses a possible limitation. In [26] a method to reduce surface roughness of SLS parts is introduced. Here, the surface roughness of sintered PA 12 could be effectively reduced to 10  $\mu\text{m}$  Rz by exposing specimens to trifluoroacetic acid for 120 s lifting it on the same level as PerForm material. However, industrial application needs to be verified due to handling issues with the aggressive acid.

Further trials with the proposed AM materials should include a systematic investigation to fathom the achievable geometric limits of possible parts in terms of size and level of detail. It is also of essential importance to better understand the material behavior of printed tools. As this study shows, available AM material data is neither complete, nor coherent, as the observed tool lives during trials could not clearly be attributed to specific material characteristics. Therefore, a specific material model that can be used to simulate the effects of thermal and mechanical loads during injection molding would be extremely helpful to predict tool life. A study on the influence of tool design changes on tool life and part filling behavior is also required. Finally, a comprehensive cost calculation model to integrate tool manufacturing cost as well as occurring cost during injection molding itself, taking into account tool life is essential to determine economic potential of any given AM material for injection molding tool.

## 5 Acknowledgements

This work was conducted within Ford and RWTH joint Alliance research project program.

## References

1. Kampker, A., Burggräf, P., Wesch-Potente, C., Petersohn, G., Krunke, M.: Life cycle oriented evaluation of flexibility in investment decisions for automated assembly systems. *CIRP J. Manuf. Sci. Technol.* **6**(4), 274–280 (2013)
2. Kampker, A., Burggräf, P., Deuskens, C., Maue, A., Förstmann, R.: Integrated product and process development: modular production architectures based on process requirements. *Procedia CIRP* **20**, 109–114 (2014)
3. Altan, T., Lilly, B., Yen, Y.C.: Manufacturing of dies and molds. *CIRP Ann.* **50**(2), 404–422 (2001)
4. Levy, G.N., Schindel, R., Kruth, J.P.: Rapid manufacturing and rapid tooling with layer manufacturing (LM) technologies, state of the art and future perspectives. *CIRP Ann.* **52**(2), 589–609 (2003)
5. Rahmati, S.: Direct rapid tooling. *Compr. Mat. Process.*, 303–344 (2014). Elsevier
6. Kampker, A., Förstmann, R., Kawollek, S., Bride, B.: Additive tooling für kunststoffbasierte urformverfahren. *Lightweight Des.* **9**(2), 38–43 (2016)

7. Segal, J.I., Campbell, R.I.: A review of research into the effects of rapid tooling on part properties. *Rapid Prototyp. J.* **7**(2), 90–99 (2001)
8. Martinho, P.G., Bártolo, P.J., Pouzada, A.S.: Hybrid moulds: effect of the moulding blocks on the morphology and dimensional properties. *Rapid Prototyp. J.* **15**(1), 71–82 (2009)
9. Chua, C.K., Hong, K.H., Ho, S.L.: Rapid tooling technology. Part 1. a comparative study. *Int. J. Adv. Manuf. Technol.* **15**(8), 604–608 (1999)
10. Rosochowski, A., Matuszak, A.: Rapid tooling: the state of the art. *J. Mat. Process. Technol.* **106**(1), 191–198 (2000)
11. Oroszlany, Á., Nagy, P., Kovács, J.G.: Injection molding of degradable interference screws into polymeric mold. *MSF* **659**, 73–77 (2010)
12. Noble, J., Walczak, K., Dornfeld, D.: Rapid tooling injection molded prototypes: a case study in artificial photosynthesis technology. *Procedia CIRP* **14**, 251–256 (2014)
13. Volpato, N., Solis, D.M., Costa, C.A.: An analysis of Digital ABS as a rapid tooling material for polymer injection moulding. *IJMPT* **52**(1/2), 3 (2016)
14. Tábi, T., et al.: Comparison of thermal, mechanical and thermomechanical properties of poly (lactic acid) injection-molded into epoxy-based Rapid Prototyped (PolyJet) and conventional steel mold. *J. Therm. Anal. Calorim.* **123**(1), 349–361 (2016)
15. Mendible, G.A., Rulander, J.A., Johnston, S.P.: Comparative study of rapid and conventional tooling for plastics injection molding. *Rapid Prototyp. J.* **23**(2), 344–352 (2017)
16. Mischkot, M., et al.: performance simulation and verification of vat photopolymerization based, additively manufactured injection molding inserts with micro-features. In: *Industrializing Additive Manufacturing - Proceedings of Additive Manufacturing in Products and Applications – AMPA 2017*, 162–168 (2018)
17. Mischkot, M., et al.: Dimensional accuracy of Acrylonitrile Butadiene Styrene injection molded parts produced in a pilot production with an additively manufactured insert. In: *33rd International Conference of The Polymer Processing Society (PPS-33)* (2018)
18. Harris, R., Newlyn, H., Hague, R., Dickens, P.: Part shrinkage anomalies from stereolithography injection mould tooling. *Int. J. Mach. Tools Manuf* **43**(9), 879–887 (2003)
19. Harris, R.A., Hague, R.J.M., Dickens, P.M.: Crystallinity control in parts produced from stereolithography injection mould tooling. *Proc. Inst. Mech. Eng., Part L: J. Mat.: Des. Appl.* **217**(4), 269–276 (2003)
20. Harris, R.A., Hague, R., Dickens, P.M.: The structure of parts produced by stereolithography injection mould tools and the effect on part shrinkage. *Int. J. Mach. Tools Manuf* **44**(1), 59–64 (2004)
21. Harris, R.A., Hague, R.J.M., Dickens, P.M.: Thermal conditions in stereolithography injection mould tooling and their use for polyether-ether-ketone moulding. *Int. J. Prod. Res.* **42**(1), 119–129 (2004)
22. Michaeli, W., Lindner, F.: Influence of mould materials on the morphological and mechanical properties of injection-moulded prototypes. *Macromol. Mat. Eng.* **286**(4), 232–236 (2001)
23. Charalambis, A., et al.: Economic trade-offs of additive manufacturing integration in injection moulding process chain
24. Charalambis, A., Kerbache, L., Tosello, G., Pedersen, D., Mischkot, M.: Economic analysis of additive manufacturing integration in injection molding process chain. In: *Proceedings on 7th International Conference on Industrial Engineering and Systems Management* (2017)

25. Kampker, A., Triebs, J., Kawollek, S., Ayvaz, P.: Direct polymer additive tooling – verwendung von polymerwerkzeugen für den einsatz im kleinserien spritzguss. In: Kynast, M., Eichmann, M., Witt, G. (eds.): Rapid.Tech + FabCon 3.D – International Trade Show & Conference for Additive Manufacturing 2018, pp. 45–62. Hanser, München (2018)
26. Wiedau, L.C., Meyer, L., Wegner, A., Witt, G.: Chemisches nachbehandeln von laser-sinter-proben – einflussuntersuchung von verschiedenen säuren auf die oberflächentopologie. In: Kynast, M., Eichmann, M. and Witt, G. (eds.) Rapid. Tech + FabCon 3.D – International Trade Show & Conference for Additive Manufacturing 2018, pp 267–282. Hanser, München (2018)



# Novel Robotic 3D Printing Technology for the Manufacture of Large Parts

Uwe Klaeger<sup>(✉)</sup> and Andriy Telesh

Fraunhofer Institute for Factory Operation and Automation IFF,  
Magdeburg, Germany  
{uwe.klaeger, andriy.telesh}@iff.fraunhofer.de

**Abstract.** Additive manufacturing technologies are being used more widely to manufacture complex part geometries. Given the existing space limitations and the substantial time required to build up parts (small layer thicknesses), most 3D printing technologies do not operate cost effectively. When they are combined with industrial robotics, however, they become particularly interesting for the manufacture of large parts. This paper reports on the development of the design of a novel high-production system that can build parts weighing as much as 50 kg and measuring more than 1000 mm.

The innovative solution is based on the build platform's six-axis controller to deposit large quantities of material (5–10 dm<sup>3</sup>/h) with layer thicknesses of 5–10 mm rapidly. The use of three extruders makes it possible to process different thermoplastics such as ABS, PC, PLA or PP in granule form. Both hard-soft materials and different colors can be combined. The VINCENT simulation tool developed by the Fraunhofer IFF is being used to develop the control system for complex manufacturing operations. This new integrative approach to motion planning and event simulation makes it possible to test geometry and function even before the system starts being built.

**Keywords:** 3D printing · Large parts · Multi-material · Simulation

## 1 Introduction

The manufacture of large parts in particular is connected with high production costs in many sectors [1]. Numerous manufacturing processes require models, molds, jigs and gauges that have to be built in elaborate and frequently manual steps. While 3D printing is a promising alternative to manually building such items, it is stymied at present by build space limitations and long manufacturing times resulting from the low build rates of currently available technologies. Our new innovative approach is intended to overcome these shortcomings by combining the advantages of 3D printing with universal industrial robotics in one high-production and cost effective system.

## 2 State-of-the-Art

### 2.1 3D Printing Technologies for Large Sizes

Large-scale 3D printers are based on thermoplastics (granules, filaments). Some projects on overcoming build space limitations have been completed in recent years. Stratasys, the pioneer of Fused Layer Modeling [2], introduced its first large-scale system, the Fortus 900mc, with a build space in the range of 900 mm [3]. Its low build rates with just four adjustable layer thicknesses in the range of 0.5 to 0.18 mm limit its productivity greatly, though. The Voxeljet VX4000 with a build space of  $4000 \times 2000 \times 1000$  mm<sup>3</sup> can process approximately fifty liters per hour at layer thicknesses of 0.2 to 0.4 mm [4]. The drawback of this technology is the very low strength of parts (material: infiltrated quartz sand), which severely limits their uses.

### 2.2 Industrial Robotics for 3D Printing

The use of industrial robots in additive manufacturing has only started attracting attention in recent years. Cranfield University developed Wire+Arc Additive Manufacturing to manufacture large airframe structural components [5]. Robots build up layers with thicknesses of up to 4 mm in a dimensional range of 2000 mm  $\times$  1000 mm. Although this facilitates faster part building, the stresses induced when heat is applied cause parts to warp. Stratasys introduced its “Infinite-Build 3D Demonstrator” together with Boeing, Ford and Siemens at the formnext in Frankfurt [6]. No concrete industrial applications have been reported yet. The University of Nantes built an emergency shelter measuring 3 m  $\times$  3 m  $\times$  3 m in thirty minutes. The part quality obtained is too low for industrial applications, though [7].

German company Gefertec’s 3D metal printing uses CNC robots to arc weld parts [8]. Parts with dimensions of 1000 mm  $\times$  1000 mm  $\times$  1000 mm can be manufactured at build rates of 0.5–1 dm<sup>3</sup>/h (aluminum) and are finished by milling.

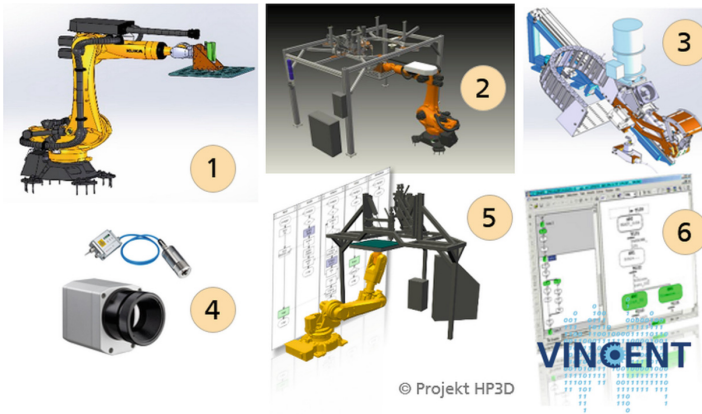
## 3 Large-Scale Printer System Design

### 3.1 System Components

The system developed and its individual subsystems are described in detail below. The prototype demonstrator system includes the following main components:

- an articulated robot that builds and handles parts (1),
- a base frame (gantry) that holds the extruder units (2),
- three extruder units with needle nozzles (3),
- a scanner that measures temperatures (part surface, melt temperature) and captures geometry data (4),
- a robot that machines and positions inserts (5), and
- VINCENT tool for simulations concomitant to development (6)





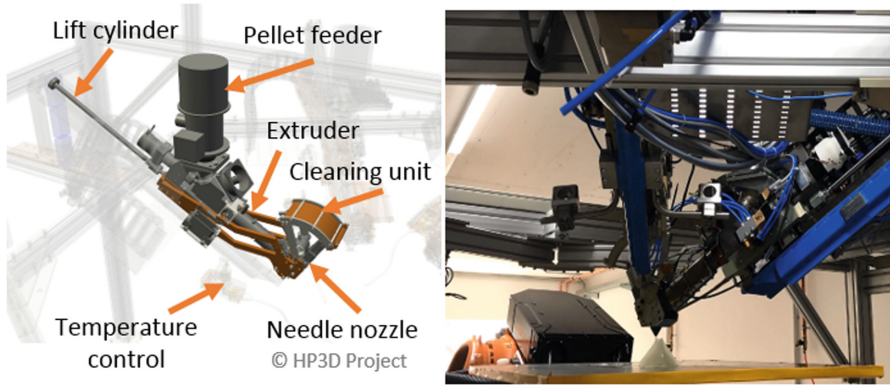
**Fig. 1.** Main components of the complete system

Figure 1 presents the complete system and its main components. The three extruders in the upper section of the gantry are arranged at a  $30^\circ$  angle as a revolving magazine. Every extruder can be moved linearly to the work plane by a pneumatic cylinder. This establishes a safe separation distance to the gantry while simultaneously increasing the robot's operating range. Parts are built up layer-by-layer on a work platform, which is mounted directly on the articulated robot. The build platform's six-axis movement ensures that the point of material deposition is always perpendicular to the extruder nozzle. This greatly reduces anisotropy of part properties. The system design foresees using a second robot to position other (even metallic) components (inserts) in parts so that other functional elements can be integrated automatically [9].

### 3.2 Extruder Development and Dispensing System Testing

An extrusion system that directly processes standard plastic granules was developed for the HP3D process (see Fig. 2). Substituting the filament material presently used in FDM systems resulted in a substantial cost-benefit of as much as a factor of five. That boosts the cost effectiveness of manufacturing, something that ought to open up other uses for this new technology.

The extruder unit was designed for a maximum part build rate of 5 kg/h. Tests have been performed with the materials ABS, SAN, PMMA, PP, PC, PC/ABS, PLA, and PVA to date. The extruder nozzle's diameter can be varied in a range of 1 to 5 mm at present. A modified needle nozzle was installed in the extruder to ensure a continuous and consistent flow of material.



**Fig. 2.** Schematic of the extruder unit and a part being built on the demonstrator

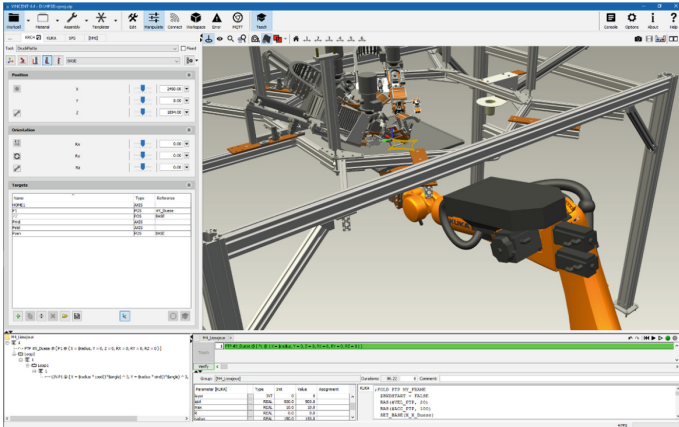
This prevents material from escaping uncontrollably during the build process. The heated build platform is clamped on the six-axis articulated robot, which interacts with the extruders through the control program. At first, the simultaneous opening and closing of the nozzle system caused material defects, especially at the beginnings and ends of seams, when parts were built. This problem was solved by introducing a dwell time (delay). A material-dependent time constant, which correlates extruded volume, temperature and extruder speed, was calculated depending on the material model. This eliminates voids in the needle nozzle caused by the inertia of the melt process.

## 4 Controller Development Using the VINCENT Simulation Tool

The development of the controller for the complete system was a major priority. The controller includes the components of component control, motion planning, machine monitoring and machine controls. Key activities are coupling the simulation with the machine controller (PLC, robot control by a real-time interface) and developing safety specifications that prevent collisions in workspaces (safe machine operation).

Moreover, workpieces and materials are being incorporated in all of the operations and the real-time capability is being demonstrated for the created models under real conditions. The development of the control system for complex manufacturing operations is being supported by the VINCENT simulation tool developed by the Fraunhofer IFF [10]. The simulation results are entering directly into the engineering of the complete system (see Fig. 3).

The software module can be used to design both PLC controlled and robot movements (e.g. variable target position) parametrically. This makes it possible during planning for processes later implemented on the PLC and robot programs to read and write the same parameters. When functions are transferred to the controller (control code generation) the program ensures that these variables are consistently crosschecked between the PLC and the robot by a fieldbus.



**Fig. 3.** Results of VINCENT simulations as the basis for system engineering

The machine's function has to be verified on the virtual model largely offline in order to transfer virtual operations planning to the real PLC or the robot is. Then, the PLC and robot programs can be exported directly from VINCENT. Linking the virtual system model and real controller online makes it possible to identify potential collisions between different system components and a complex part before a task is executed. Both brief movements and complete manufacturing programs lasting several hours can be tested in advance. One of the tool's significant strengths is its rapid collision detection based on 3D CAD data and kinematic structure. This can be used to identify danger zones and automatically generate and verify motion rules for collision testing in real time. Now upgraded with these program components, VINCENT can generate every system component's safety zones automatically at the push of a button. Integrated rules prevent collisions between the individual components as well as with the operator. The use of established standard formats to exchange data ensures operations are defined simply and continuously in the machine. The demonstrator's engineering (gantry design, extruder unit configuration) and the extruder's interaction with the robot and build platform were optimized in several iterative cycles. At the same time, the controller components (PLC) were put through other simulations (motion optimization, part building, path planning) concomitant to design.

## 5 Conclusion

The new technological approach reduces manufacturing times of large-size/large-volume parts significantly. It can save 10–40% of costs over the conventional approach.

The use of robots makes it possible to produce parts with practically unlimited dimensions. Part volumes of 1–10 m<sup>3</sup> are possible depending on the robot's size. The build platform's six degrees of freedom make it possible to manufacture parts with highly complex geometries such as freeforms, support structures and undercuts.

The use of three extruder units shortens non-productive time refilling material, on the one hand, and expands the range of materials to hard-soft components and different colors, on the other. The system was successfully tested under industrial conditions. This is grounds for optimism about widely marketing it. Other tests will involve optimizing the controller design. The materials' thermostability during part building especially has to be improved. This will be done by employing different additives.

Another task will be to optimize the build space's movements as a function of the extruder units' locations. The technical specifications of the electrical components (drives, sensors, control loops, etc.) for the control module have to be improved, as do the safety specifications for the complete system, factoring in every assembly. The most important future research activities will include:

- testing different material compositions with the goal of increasing part strength as layers are built up,
- refining the VINCENT control module to optimize motion paths of robots, extruders and insert handling,
- optimizing the extruder units' mixing and dispensing system to process materials of varying viscosity, and
- improving temperature control during part building.

**Acknowledgement.** This joint project was funded by the German Federal Ministry of Education and Research (BMBF) in its "Innovations for Tomorrow's Production, Services and Work" (funding code 02P14A027).

## References

1. Hohmann, L.: Metav: Durchgängige Prozessketten in der Fertigung-Vision and Wirklichkeit. MM Maschinenmarkt, Vogel Business Media GmbH & Co, KG, Würzburg (2016)
2. Patent No. US5121329 A. Stratasys (1992)
3. mc. <http://www.stratasys.com/de/3d-drucker/production-series/fortus-900mc>
4. Steck, R.: Voxeljet V4000: Größter Sandform-Drucker der Welt. [www.engineeringspot.de/2016/07/voxeljet-vx4000-groesster-sandform-3d-drucker-der-welt](http://www.engineeringspot.de/2016/07/voxeljet-vx4000-groesster-sandform-3d-drucker-der-welt)
5. Innovative Process Model of Ti-6Al-4 V Additive Layer Manufacturing Using Cold Metal Transfer (CMT). International Solid Freeform Fabrication Symposium. Austin (USA) (2015)
6. Knabel, J.: 3druck.com/drucker-and-produkte/stratasys-zeigt-neue-fdm-fertigungsanlage-mit-8-axen-1448149
7. [www.iutnantes.univ-nantes.fr/accueil/une-imprimante-3d-pour-construire-un-habitat-d-urgence-en-20-minutes-1283343.kjsp](http://www.iutnantes.univ-nantes.fr/accueil/une-imprimante-3d-pour-construire-un-habitat-d-urgence-en-20-minutes-1283343.kjsp)
8. Röhrich, T.: Potentials and applications of additive manufacturing with arc and wire (3DMP®) in tool-making industry. Fachtagung Werkstoffe and Additive Fertigung, Potsdam, 25, 26 04 2018
9. Klaeger, U., Steuer, J.: High Performance 3D-3D-Druck mittels Robotertechnik. Vortrag auf dem 5. Mitteldeutschen Forum »3D-Druck in Anwendung«. Jena, 5, September (2018)
10. Juhasz, T: Digital twin - business value and technical implementation confirm industry. In: Workshop and Information Day, Thomond Park Stadium, Limerick, 6 December 2018

# **Green and Digital Manufacturing Environments and Simulation Systems**



# Implementing RAMI4.0 in Production - A Multi-case Study

Elder Hernández<sup>(✉)</sup>, Pedro Senna, Daniela Silva, Rui Rebelo,  
Ana C. Barros, and César Toscano

CESE, INESC TEC, Porto, Portugal  
{elder.hernandez, pedro.senna, daniela.s.silva,  
ana.c.barros, ctoscano}@inesctec.pt,  
rui.d.rebelo@inescte.pt

**Abstract.** The Industry 4.0 (i4.0) paradigm was conceived bearing smart machines enabling capabilities, mostly through real-time communication both between smart equipment on a shop floor and decision-aiding software at the business level. This interoperability is achieved mostly through a reference architecture specifically designed for i4.0, which is aimed at devising the information architecture with real-time capabilities. From such architectures, the Reference Architectural Model for Industrie 4.0 (RAMI 4.0) is considered the preferred approach for implementation purposes, especially within Small and Medium Enterprises (SMEs). Nevertheless, the implementation of RAMI 4.0 is surrounded with great challenges when considering the current industrial landscape, which requires retrofitting of existing equipment and the various communication needs. Through three different case studies conducted within footwear and cork industries, this research proposes a RAMI 4.0 SME implementation methodology that considers the initial stages of equipment preparation to enable smart communications and capabilities. The result is a methodological route aimed for SMEs' implementation of smart machines, based on RAMI 4.0, which considers both the technological aspects as well as the business requirements.

**Keywords:** RAMI4.0 · SMEs · Technology implementation management

## 1 Introduction

The premise of Industry 4.0 (i4.0) is built around the paradigm of smart machines communication through a framework that ensures a constant flow of information throughout the levels of a given company. A backbone to help devise the i4.0 information architectures is the Reference Architectural Model for Industrie 4.0 (RAMI 4.0). However, the implementation of RAMI 4.0 has been challenging, since it relies on various factors which may affect or hinder the final output, such as the current industrial landscape, as well as the multiplicity of equipment within the factory, which have different sources, diverse construction and various communication capabilities [4].

Despite broad implementation in large industries, there is a lack of methodological management when it comes to implementing i4.0-enabled machinery on Small and Medium Enterprises (SMEs). More importantly, SMEs face a lack of resources combined with precise technological maturity assessment regarding relevant solutions, as well as practical business applications [2]. A crucial aspect surrounding these obstacles is the methodological management skills, supported by the lack of standardisation and regulations for technology implementation. Based on case studies conducted in the footwear and cork industries, this research devises a methodology to help SME manufacturers into preparing industrial equipment for a RAMI4.0 architecture [3]. Such methodology is supported by cyber-physical systems designed to integrate computational & physical processes with human interactions, aimed at establishing Key Performance Indicators (KPIs), which drive the Industry 4.0 implementation process [1].

## **2 The Reference Architectural Model for Industrie 4.0 (RAMI 4.0)**

The i4.0 paradigm has brought forth new architectural challenges, which enable a higher degree of i4.0 approaches by the organizations [5–7]. Under the Plattform Industrie 4.0 [9], RAMI 4.0 is proposed to be a guide to support the implementation of i4.0-enabled systems architectures. It is represented as a three-dimensional layer model cube which encases the most important elements of the business and i4.0 technological novelty. RAMI 4.0 proposed architecture consists on having each entity of the business represented as a component, which exposes services, functionalities and communication channels. According to Ferreira et al. [8], there are challenges that arise when designing the i4.0 architecture. The first challenge is due to the necessity of defining the required business entities: how these entities participate during the value creation process can be challenging to map and requires the perception of the real implication within the value chain network. The second challenge pertains systems integration and interoperability. Existing hierarchical architectures based on the ISA 88/95 are the most commonly found throughout the industry [10–12]. Thus, it is necessary to have a clear grasp on how to transform/integrate new systems with existing legacy systems.

The German Engineering Federation has released a Guideline for i4.0 aimed at providing guiding principles for implementing i4.0 within SMEs [13]. A scheduled process coupled with constant feedback is considered crucial for the success of the i4.0 implementation [13]. Despite having produced such guiding principles, there is a lack of implementation studies on the literature that concern i4.0 for SMEs, especially with multiple iterations and a maturity assessment done prior to the implementation process [14]. This assessment must be performed during the business definition stage, and requires a multidisciplinary team that is comprised of business model decision-makers, i4.0 component implementation experts and data analysts, since its purpose is to design a business and technological implementation framework that considers business KPIs, available data gathered from equipment sensors, and retrofitting of machinery.

### 3 Research Methods

The methodology used for this research consists of a literature review and multi-case study analysis aimed at proposing a RAMI 4.0 implementation methodology for SMEs. In order to achieve the above mentioned implementation methodology, an analysis of the current RAMI 4.0 literature on implementation methodology protocols and guidelines focused on SMEs was conducted, which was combined with research on innovation developments regarding i4.0 reference architectures capable of combining technological aspects with business requirements. Moreover, identification of SME-based projects with implementation of RAMI 4.0 driven architectures was carried out.

### 4 RAMI 4.0 SME Implementation Methodology

RAMI 4.0 implementation methodologies have widespread as industries embrace the industry 4.0 paradigm. Most of these methodologies conduct a three layer assessment, business, technology and processes definition, such as business strategy definition, KPI definition, systems modelling, technology maturity, process re-engineering, human-resource training [2, 8, 14]. Based on existing RAMI 4.0 implementation methodologies, and implementation driven case studies, a RAMI 4.0 SME implementation methodology proposal is forwarded (Fig. 1), which maintains the same core objective to support. However, obstacles such as low business preparation, huge variety of existent legacy systems, and multi-disciplinary outsourced teams means that a more flexible and controlled approach during the implementation process must be taken [6, 15].

The proposed methodology provides an overall view of the process, thus enabling the identification of key agents on each step (actors, resources, and drivers), the identification of the different layers that comprise the final solutions, the design of the necessary proof of concept (PoC) to establish a pre-solution validation, as well as the identification of obstacles and possible blocking points.

For SMEs, two types of stakeholders were identified on a RAMI 4.0 implementation project: business stakeholders, and technology & process stakeholders. Business stakeholders provide the project's core goals, objectives and requirements under a business view perspective, sourcing and choosing the required project stakeholders, a project management to meet project goals (project timeframe, budget, and quality), and project evaluation, which oversees the successful development, integration and implementation of each considered solution. On the other hand, technology & process stakeholders are comprised of experts from fields required for the implementation process (e.g.: process, automation, communication). The intent of these stakeholders concerns the analysis, integration and implementation of technological novelty brought by i4.0 premise in the industrial production processes.



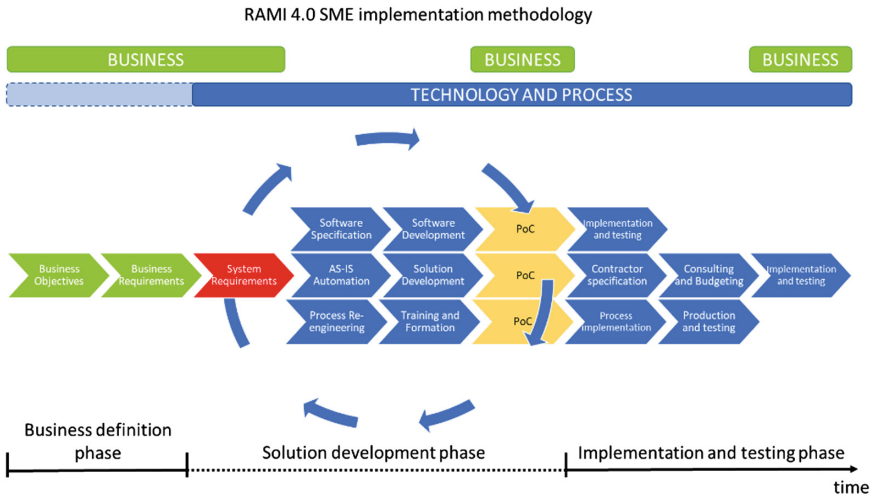


Fig. 1. RAMI 4.0 SME implementation methodology

When compared to previous methodologies, the application of PoC combined with iterative cycles during the solution development process, constitutes the main novelty of the proposed implementation methodology. In terms of approach, the methodology has three phases: business definition; solution development; and, implementation and testing. **Business definition** constitutes the baseline for the project. This phase is driven by the business expert, which embodies the business vision for the project and define the objectives and goals for the RAMI 4.0 implementation project. The choice of the stakeholders for the project, technical team and experts, should be the main objective at this stage. **Solution development** concerns the core of the methodology where the different layers of solution development take part. This phase follows an iterative cyclical approach, beginning with the system requirements definition, in which business experts discuss the business indicators and requirements with other project stakeholders. This discussion is essential as it will bring cohesion within the project with all stakeholders involved. The target of this step is to define a RAMI 4.0 architecture design adapted to the project and solutions. This step serves as a start and revision step during the iterative cycles. Having the stakeholders agreed with the system requirements, the technical development phase takes place for each required solution layer. Each layer develops a PoC of the proposed solutions, and its viability is assessed by both business and technology experts. After all solutions have been validated through a PoC and the RAMI 4.0 architecture agreed upon, the **implementation and testing** phase is initiated, where each of the proposed solutions is implemented and tested accordingly. Project management and business experts validate the final output and close the project. When considering the timeline of the project, it must be considered the length of each of the three phases that constitute this methodology. As it provides an iterative approach the solution provision can be adapted and revised in each cycle according to new information from stakeholders, avoid obstacles or solve roadblocks that could hinder, prolong or in worse scenarios, jeopardize the project timeline.

## 5 Multi-case Study

The following three case studies applied different methodologies to implement RAMI 4.0 driven architectures. In terms of case-study typology, one case was under an industry-driven project targeting a specific industry as a whole, and the other two were business driven and performed as consulting services. A brief presentation of the Case Studies with regards to the target industry, project objectives, methodology applied and implementation stages is portrayed in Table 1.

**Table 1.** Presentation of the Case Studies (CS)

	CS 1	CS 2	CS 3
Industry	Footwear production	Cork transformation	Cork transformation
Project	Industry-driven implementation	Business-driven implementation	Business-driven implementation
Methodology	PoC	Waterfall	PoC and RAMI 4.0 SME Implementation
Implementation	Allowed to establish and consolidate the process on how new technology is implemented within the industry, technical and management requirement, coordination with multi-disciplinary and out-sourced teams.	I - project objectives, time frame, and budget II - business requirements and assessment of the production and support processes III - information on systems, infrastructure and automation levels IV - results from II and III sent to external automation consultant team V - implementation of the architecture proposed in IV VI - test and validation	- Outsourced experts defined the implementation project objectives and pre-determined the project length - Regular meetings to debate and check solution proposals, PoC definition and schedule industrial implementation and testing - PoC of solutions were developed for each layer of the RAMI 4.0 SME

In Case Study 1 (CS 1), a series of PoC was conducted to demonstrate the possible applications of i4.0 enabled architectures, such as RAMI 4.0, and technology in footwear SMEs. This case allowed to stablish and consolidate a general process of how i4.0 technology can be implemented. Also, it demonstrated how the implementation of RAMI 4.0 enabled architectures require parallel solution development cycles in order to tackle the different business, technological and processes layers.

Case Study 2 (CS 2) was conducted on a different company, which brought in teams experts from business and technology backgrounds to support the implementation project. However, these teams worked separately with reduced interaction and integration. The modularity concept of this methodology only had advantages on each phase separately, without an overall implementation view that incorporated both business indicators and technological capabilities. Thus, the company was not able to have feasibility and implementation feedback until the final solution was both proposed and implemented, constituting a major disadvantage since it was considered not viable for the company's initial goals.

In Case Study 3 (CS 3), teams of outsourced experts from business and technology fields were brought in since the start, contributing in defining the implementation project objectives and pre-determining the project length. Regular meetings were arranged and planned to de-bate and check solution proposals, PoC definition and schedule industrial implementation and testing. PoC of solution were developed for each implemented layer of the RAMI 4.0, such as process, automation, communication, information systems.

## 5.1 Discussion

The presented case studies provided inputs to understand the implementation of RAMI 4.0 enabled architectures in SME production settings. CS 1 contributed with the success of the PoC approach since it demonstrated possible implementation solutions of the various RAMI 4.0 layers. Also, this approach allowed multidisciplinary teams to work together with a global intent. CS 2 and CS 3 were similar implementation projects. However, they differ on the methodological approach taken: waterfall methodology (CS 2), and PoC with an industrial implementation objective (CS 3).

As seen in Table 2, the output in terms of qualitative parameters were more controlled and successful in CS 3 when compared with CS 2. A higher interaction among stakeholders and the development of PoC for solutions with iterative cycles provided quick gains and drove the implementation project towards its initial objectives.

**Table 2.** Comparison between Case Studies (CS).

Qualitative parameters	CS 1	CS 2	CS 3
Objectives	Reached	Changed	Adapted and reached
Length	Followed	Overpassed	Followed
Team participation	Start of project	Modular and scarce	Start of project
Team cohesion	Collaborative environment	Low interaction	Collaborative environment
Solution development	Iterative development	Long and unclear direction	Iterative solution, quick wins with peer validation
Solution quality	Proof of Concept (PoC)	Unclear/undefined	PoC validated towards industrial implementation

## 6 Conclusions

The introduction of PoCs as a means to validate the designed i4.0 solutions, which enable scalability capabilities for widespread implementation of i4.0 componentry, is considered the major novelty of the proposed RAMi 4.0 SME implementation methodology. Furthermore, these PoCs are intended to demonstrate the integration between the different RAMI 4.0 layers: asset, integration, communication, information, functional and business.

The correct definition of the KPIs based on the business requirements, while considering technological limitations, ensures that a complete and clear implementation process is agreed upon by all stakeholders of the project, which allow for better expected outputs in terms of RAMI4.0 implementation. The correct understanding of the implementation procedure enables the experts of each solution layer to provide possible and feasible PoC solutions, thus producing the desirable outcome. Another relevant point concerns the overall alignment, where the project objectives and goals must adapt to business requirements and remain technologically feasible to the project management.

Future research on this field may apply the proposed RAMI 4.0 SME implementation methodology on other manufacturing sectors, and service-directed industries, aimed at better evaluating the extension of this implementation methodology. Furthermore, an effort to better assess i4.0 implementation costs and trade-offs with existing machinery is necessary, so that SMEs decision-makers can have better tools and more reliable information when deciding upon implementation actions.

**Acknowledgements.** This work is co-financed by the ERDF – European Regional Development Fund through the Operational Programme for Competitiveness and Internationalisation - COMPETE 2020 under the PORTUGAL 2020 Partnership Agreement, and through the Portuguese National Innovation Agency (ANI) as a part of project «FAMEST: POCI-01-0247-FEDER-024529» and was supported by the Project “TEC4Growth - Pervasive Intelligence, Enhancers and Proofs of Concept with Industrial Impact”, NORTE-01-0145-FEDER-000020, financed by the North Portugal Regional Operational Programme (NORTE 2020), under the PORTUGAL 2020 Partnership Agreement, and through the European Regional Development Fund (ERDF).

## References

1. Barros, A.C., Simões, A.C., Toscano, C., Marques, A., Rodrigues, J.C., Azevedo, A.: Implementing cyber-physical systems in manufacturing. In: CIE47 Proceeding. Lisbon, Portugal (2017)
2. Schröder, C.: The Challenges of Industry 4.0 for Small and Medium-sized Enterprises. Friedrich-Ebert-Stiftung, Bonn (2016)
3. Yin, D.R.K.: Case Study Research: Design and Methods. Sage Publications, Thousand Oaks (2009)
4. Wang, L., Törngren, M., Onori, M.: Current status and advancement of cyber-physical systems in manufacturing. *J. Manuf. Syst.* **37**(Part 2), 517–527 (2015). ISSN 0278-6125

5. Monostori, L., Kádár, B., Bauernhansl, T., Kondoh, S., Kumara, S., Reinhart, G., Ueda, K.: Cyber-physical systems in manufacturing. *CIRP Ann.* **65**(2), 621–641 (2016)
6. Jbair, M., Ahmad, B., Mus' ab H.A., Harrison, R.: Industrial cyber physical systems: a survey for control-engineering tools. In: 2018 IEEE Industrial Cyber-Physical Systems (ICPS), pp. 270–276. IEEE, May 2018
7. Kamble, S.S., Gunasekaran, A., Sharma, R.: Analysis of the driving and dependence power of barriers to adopt industry 4.0 in Indian manufacturing industry. *Comput. Ind.* **101**, 107–119 (2018). ISSN 0166-3615, <https://doi.org/10.1016/j.compind.2018.06.004>
8. Ferreira, F., Faria, J., Azevedo, A., Marques, A.L.: Industry 4.0 as enabler for effective manufacturing virtual enterprises. In: Working Conference on Virtual Enterprises, pp. 274–285. Springer, Cham, October 2016
9. VDI/VDE-Gesellschaft Mess- und Automatisierungstechnik. (2015). Status Report:Reference Architecture Model Industrie 4.0 (RAMI4.0), vol. 0
10. Instrument Society of America (ISA). ISA-88.01 Batch Control Systems, Part 1. Models and Terminology, ISA Standards (1995)
11. Instrument Society of America (ISA): ISA-95.01 Enterprise-control System Integration, Part 1. Models and Terminology, ISA Standards (1999)
12. SCHOLTEN, Bianca. Integrating ISA-88 and ISA-95. ISA EXPO 2007, p. 13 (2007)
13. Anderl, R., Picard, A., Wang, Y., Fleischer, J., Dosch, S., Klee, B., Bauer, J.: Guideline Industrie 4.0 - Guiding principles for the implementation of Industrie 4.0 in small and medium sized businesses. VDMA Forum Industrie 4.0, Frankfurt (2015)
14. Anderl, R.: Industrie 4.0–Digital transformation in product engineering and production. In: 21st International Seminar on High Technology-Smart Products and Smart Production. At Piracicaba (SP), Brazil (2016)
15. Liao, Y., Deschamps, F., Loures, E.D.F.R., Ramos, L.F.P.: Past, present and future of Industry 4.0-a systematic literature review and research agenda proposal. *International Journal of Production* (2017)



# Assessing Industry 4.0 Readiness of Portuguese Companies

Hélder F. Castro<sup>1</sup>(✉), Alexandre R. F. Carvalho<sup>1</sup>, Fátima Leal<sup>1</sup>,  
and Helena Gouveia<sup>2</sup>

<sup>1</sup> Intelligent & Digital Systems, R&Di, Instituto de Soldadura e Qualidade,  
Rua do Mirante, 33, 4415-491 Grijó, Portugal

{hfcastro, arcarvalho, fdleal}@isq.pt

<sup>2</sup> R&Di Programmes, R&Di, Instituto de Soldadura e Qualidade,  
Av. Prof. Dr. Cavaco Silva, 258, Taguspark, 2740-120 Oeiras, Portugal  
hngouveia@isq.pt

**Abstract.** Industry 4.0 (i4.0) has changed the industrial processes. Increasingly, companies have to adapt their processes to follow the technology development which has caused a digital transformation. However, mainly the Small and Medium Enterprises have difficulty to evaluate its i4.0 readiness level and design a strategy that implements the i4.0 concepts. Towards this scenario, we present the SHIFTo4.0 – a self-assessment tool that evaluates the i4.0 readiness level of a company. SHIFTo4.0 is based on a model which contemplates six different dimensions: (i) strategy and organization; (ii) smart factory; (iii) smart operations; (iv) smart products; (v) data-driven services; and (vi) human resources. Each dimension is classified using a scale between 0 and 5. In addition, it provides a report with a set of recommendations, *i.e.*, a roadmap, to guide the company in the i4.0 implementation to achieve a higher readiness level. As result, we present a case study that shows how a company can improve their current i4.0 readiness level by using SHIFTo4.0.

**Keywords:** Industry 4.0 · Portuguese industry 4.0 readiness · Information systems · Modelling

## 1 Introduction

Digital technologies have launched the 4th industrial revolution (i4.0) transforming entire industries and the global economy [7, 9]. Disruptive concepts such as the Internet of Things, Cyber-Physical Systems, Cloud-based or Data-based Services are important within the new i4.0 paradigm and present huge challenges for the Portuguese companies particularly for SME (Small and Medium Enterprises).

Previous studies [13] reported a direct correlation between the size of a company and its i4.0 readiness, inferring that SMEs have low probability of reaching

higher i4.0 levels without the help of partners along the value chain. The importance of i4.0 comes from the fact that, it is a revolution that affects not only the technological level of companies as well as its organizational structure and culture, therefore, influencing their future competitiveness and sustainability. In this scenario, acknowledging the company's preparedness to face i4.0 revolution is critical. The i4.0 readiness assessment and maturity models are methodologies that allow benchmarking and setting up roadmaps for the digital transformation of companies. Considering this urgent need, ISQ has developed a tool (SHIFTo4.0) and a methodology to be applied to the Portuguese companies. This paper presents an empirically grounded model based on the German IMPULS [13] study adapted to the Portuguese companies. It aims to evaluate the current i4.0 readiness level of a company and provides guidelines to achieve a higher readiness level to maximise the benefits of i4.0.

Overall, SHIFTo4.0 formulates questions considering 6 dimensions encompassing strategy and organization, smart factory, smart operations, smart products, data-driven services, and human resources. The presented study examines the Portuguese companies through a wide scope of sectors regarding their i4.0 strategy, understanding what motivates them and what are the main hurdles in its adoption and implementation. As results, we present a case study which show the applicability of SHIFTo4.0 in the Portuguese industry.

This paper is organised as follows. Section 2 reviews the related work on i4.0 self-assessment tools. Section 3 describes the SHIFTo4.0 including the description of the dimensions and the levels. Section 4 presents a case study. Finally, Sect. 5 discusses the outcomes of this work.

## 2 Related Work

The emergence of i4.0 originates different researches for assessing the i4.0 readiness of the industries [5, 10].

Schumacher et al. [13] suggest a maturity index which involves nine dimensions: (*i*) strategy; (*ii*) leadership; (*iii*) customers; (*iv*) products; (*v*) operations; (*vi*) culture; (*vii*) people; (*viii*) governance; (*ix*) technology. Schuh et al. [12] developed a maturity index which considers: (*i*) computerisation; (*ii*) connectivity; (*iii*) visibility; (*iv*) transparency; (*v*) predictability; and (*vi*) adaptability. Geissbauer et al. [4] assessment model incorporates seven dimensions: (*i*) digital business models and customer; (*ii*) digitisation of product and service offerings; (*iii*) digitisation and integration of vertical and horizontal value chains; (*iv*) data analytics as core capability; (*v*) agile IT architecture; (*vi*) compliance security, legal and tax; and (*vii*) organization, employees and digital culture. Lichtblau et al. [8] present the IMPULS – a research which measures the i4.0 readiness in the German mechanical engineering industry. It considers: (*i*) strategy and organization; (*ii*) smart factory; (*iii*) smart operations; (*iv*) smart products; (*v*) data-driven services; and (*vi*) employees.

Considering the literature on self-assessment tools which measure the i4.0 readiness, in this work, we adapt the IMPULS model to the Portuguese

industry reality. SHIFTo4.0 presents 3 essential features recommended by the literature [3]: (i) characterises the i4.0 readiness automatically using a self-assessment tool; (ii) presents an automatic guideline/roadmap to achieve a desired level in a defined time frame; and (iii) it is prepared to perform a comparative benchmark within a representative sample, in this case, of the Portuguese industry reality.

### 3 SHIFTo4.0

SHIFTo4.0 is a self-assessment platform that evaluates the level of i4.0 readiness of the Portuguese SMEs [1,6]. It is based on a questionnaire composed of a set of questions which contemplate 6 dimensions: strategy and organization, smart factory, smart operations, smart products, data-driven services, and human resources. For each dimension, SHIFTo4.0 attributes a level between 0 and 5 to evaluate the degree of i4.0 readiness of the company. Then, the company defines a new improved readiness level by dimension, that intends to achieve in a time-frame of 5 years. Finally, the tool creates a roadmap with an action plan for the company achieving an higher level of i4.0 readiness.

#### 3.1 Dimensions Description

In order to cover the multiple i4.0 concepts and assess the level of i4.0 maturity of a company, the SHIFTo4.0 self-assessment tool is supported by different topics that are related to the 6 exiting dimensions.

**Strategy and organization** define a set of actions to follow in order to successfully implement i4.0 concepts. This dimension analyses: (i) the strategy implemented in the company; (ii) the existing indicators to monitor the i4.0 strategy; (iii) the existing technologies; (iv) the present and future i4.0 related investments; and (v) technology and innovation management.

**Smart factory** is an intelligent production system which employs an integration of manufacturing and services [2]. In this context, this dimension analyses the i4.0 readiness regarding equipment infrastructure and its functions, the level of digitalisation and data collection as well as the IT systems.

**Smart operations** uses technology and intelligence to produce autonomously goods and services. This dimension focuses: (i) internal and external information sharing; (ii) autonomous control of the processes and products; (iii) the IT department organization; (iv) IT security solutions; (v) cloud-based services.

**Smart products** are capable to do computations, store data, communicate, and interact with their environment [11]. In this context, this dimension focuses: (i) ICT functions integrated in the product (*e.g.*, memory, sensors, automatic identification; *etc.*); (ii) the data collected during the use stage and its goal.



**Data-based services** are created using information originated in the production and usage stages. Therefore, this dimension examines: (i) the data-based services; (ii) the relevance of the data-based services in the company revenue; and (iii) the level of utilisation of the collected data.

**Human resources** related to the i4.0 implementation, requiring continuous acquisition of new skills and qualifications. This dimension evaluates the level of existing i4.0 skills and the efforts in acquiring i4.0 competences.

### 3.2 Levels Description

The dimensions are classified between 0 and 5 as follows.

**Level 0** is attributed to the companies that present weak knowledge or consider irrelevant the i4.0 concepts for its activity.

**Level 1** is attributed to the companies that present: (i) i4.0 pilot initiatives in at least one area of the company; (ii) productive processes partially supported by IT; (iii) a limited information sharing between the internal areas of the company; (iv) a plan to integrate IT security solutions; (v) a plan to integrate ICT functions in the products; and (vi) i4.0 skills in few areas of the company.

**Level 2** includes companies that present: (i) an intermediate level in terms of i4.0 strategy as well as an indicators system which evaluates its level of implementation; (ii) relevant i4.0 investments; (iii) some of the collected data is obtained automatically and it is partially analysed; (iv) an infrastructure which does not allow a complete integration of i4.0 concepts; (v) a partial information sharing between the internal areas of the company; (vi) a plan to integrate shared information with business partners; (vii) an adequate IT security solutions; (viii) an initial offer regarding data-driven services; (ix) human resources with enough skills to extend the i4.0.

**Level 3** includes companies that present: (i) a strategy based on i4.0 concepts; (ii) i4.0 investments in multiple areas; (iii) IT systems that support the production processes, collecting data automatically; (iv) infrastructure which allow an integration of i4.0 concepts; (v) enough IT security solutions; (vi) a plan to introduce cloud-based services; (vii) the products includes multiple and interconnected ICT functions enabling the offer of the data-driven services; (viii) data-driven services with a small relevance in the revenues; (ix) efforts to expand the human resources i4.0 skills.

**Level 4** includes companies that present: (i) an i4.0 strategy monitoring it with appropriated indicators; (ii) i4.0 investments in the majority areas of the company; (iii) IT systems that support the majority of the production processes collecting a large amount of data for process optimisation; (iv) information sharing both internal and between the business partners; (v) IT security solutions for the most relevant areas; (vi) limited autonomous products and self-adjusting processes; (vii) products with ICT functions which allow the data collecting and analysis in the use stage; (viii) data-driven services with direct integration between the client and the provider; and (ix) human resources with proper i4.0 skills.

**Level 5** includes companies that present: (i) a i4.0 strategy, monitoring its implementation regularly; (ii) a IT system, collecting relevant data automatically; (iii) an equipment infrastructure that meets the communication requirements providing both internal and external information sharing; (iv) comprehensive security solutions; (v) cloud-based solutions which provides a flexible IT infrastructure; (vi) production areas that use autonomously guided products as well as self-adjusting processes; (vii) products with ICT functions which collect data in use stage; (viii) significant revenue from data-driven services; (ix) i4.0 knowledge in all areas of the company.

### 3.3 Roadmap

SHIFTo4.0 generates a report incorporating a roadmap with a set of recommendations that reflects the current i4.0 challenges per dimension. The recommendations constitute an action plan to increase the i4.0 readiness level of the company. Table 1 summarises the recommendations generated per dimension.

**Table 1.** Recommendations per dimension.

Dimension	Recommendations topics
Strategy and organization	Design, development, and implementation of a i4.0 strategy Define and create a set of indicators Creation and deployment of an investment plan Implementation of an innovation management system
Smart factory	Integration of equipment in IT infrastructure Communication M2M and interoperability Increasing the data collection for digital modelling Data Collecting from processes and equipment Discovering knowledge through data analysis Integrating the multiple areas of the company in IT systems
Smart operations	Information sharing at the departmental and inter-departmental level Information sharing with costumers and providers Introduce autonomous control in the processes Implement IT security measures Implement cloud-based solutions
Smart products	Introduce ICT functions in the products Data collecting in product use stage Data analytics models to create data-based services
Data driven services	Integrate data-based services in the clients Increase the personalisation of the products Expand the data analysis to increase the revenue source Analyse the product performance and the degree of use Extend the data analytics models to offer new services
Human resources	Increase the ICT employees skills Promote workshops or seminars to increase knowledge in i4.0 areas Continuous training in the multiple i4.0 areas

## 4 Case Study

As a case-study, we chose a Portuguese SME company to evaluate the impact of the SHIFTo4.0. The company filled the questionnaire and analysed the importance of the SHIFTo4.0 recommendations in its production process. The analysis was based on the current i4.0 readiness level and the disclosed roadmap aligned with the company's objectives. As result, the recommendations were prioritised, structured, and decomposed in smaller actions. Therefore, the report acts as a support document that, from the beginning, can trigger an improvement in the company's i4.0 readiness assessment, namely in the strategy and organization dimension.

The condition of the company, in conjugation with the output given by the SHIFTo4.0 tool, allowed to identify important actions in several topics associated to the dimensions *strategy and organization* and *smart factory*. Among others, the identified actions are based on the tool recommendations to speed up the benefits from i4.0 adoption by the company. The actions were split in five steps:

**Design, development, and implementation of a i4.0 strategy** which incorporates the *strategy and organization* dimension. The strategy acts as a route for the i4.0 readiness enhancement and must contains the objectives, an action plan, and also a set of indicators to show the progress.

The company in analysis had to create a i4.0 strategy once it was nonexistent. The first step was to organise interdepartmental discussions supported by the report provided by SHIFTo4.0. After several iterations, it was defined a i4.0 strategy which encompasses the current state of the company and its objective in a foreseeable time-frame of 5 years.

**Define and create a set of indicators** which incorporates the *strategy and organization* dimension. The company defined as indicators the process efficiency, product quality, eco-efficiency, and value creation. These indicators allow to evaluate the progress of the i4.0 implementation. At the moment, the process efficiency and product quality indicators are in progress, being supervised permanently.

**Increasing the data collection for digital modelling** which incorporates the *smart factory* dimension. The company presented product quality defects due to the difficulty to identify the correct pieces for the process. The existing control is not automatically monitored originating defects. To solve this problem, it was adopted the Radio Frequency Identification (RFID) technology to identify the piece and provide information about its usage. It allowed to create a digital model for each piece ensuring the process efficiency. In addition, this technology is also important for life-time control as it allows to control the number of times which a piece has been used. As result, the number of defects were minimised, contributing to increase the product quality and process efficiency.

**Data Collecting from processes and equipment** which incorporates the *smart factory* dimension. For this step, the company selected a process considering the impact on the company's i4.0 priorities. It was installed multiple

sensors to obtain additional data and control the process more efficiently. The sensors were integrated using a distributed industrial process measurement and control system, based on IEC 61499 standard [14]. This system allow to deploy multiple algorithms performing a predictive control using machine learning techniques. The process performance was improved with this approach. The methodology was planned to be expanded to other processes of the company.

**Discovering knowledge through data analysis** integrates the *smart factory* dimension. The previous steps allowed to understand where to collect information and which data to use, to discover important knowledge to improve the process. The data analysis has detected relevant variables to be controlled to ensure the product quality. This variables was applied in predictive algorithms for anomaly detection.

As result, this case-study increased its readiness level from 1.14 to 1.78 in a time-frame of 6 months.

## 5 Conclusions

The rapid technology development boosted an industrial revolution. Companies must adapt their processes considering the i4.0 paradigm to follow the digital transformation. However, the i4.0 concepts are difficult to implement requiring a high level of knowledge and a good strategy. In this context, the paper presents SHIFTo4.0 – a self-assessment platform which evaluates the level of i4.0 maturity of a company. The main goal is to guide the companies in i4.0 implementation. In this context, the platform provides a report that incorporates an action plan with a set of recommendations considering six i4.0 dimensions.

As result, we present a case study which shows how a company can improve the i4.0 maturity level using SHIFTo4.0. First, the company designed an action plan based on recommendations provided by SHIFTo4.0. These recommendations not only accelerate the action identification, but also highlight the most important ones. The action plan was split in five steps: (*i*) design, development, and implementation of a i4.0 strategy (*ii*) define, create a set of indicators; (*iii*) increasing the data collection for digital modelling; (*iv*) data collecting from processes and equipment; (*v*) discovering knowledge through data analysis.

These results show that the knowledge obtained by the SHIFTo4.0 tool, *i.e.*, the i4.0 maturity level and the objective-driven roadmap, not only trigger immediate actions but also accelerate the i4.0 implementation in a company. In this context, it is feasible that the company can comply with the proposed objective in a time-frame of 5 years. This case-study can be applied in another Portuguese SME company regardless of the starting i4.0 readiness level and i4.0 objectives. To sum up, the presented tool can help to initiate or accelerate the SME path towards i4.0, reaping its intrinsic benefits along the way.

As future work, we intend to apply a benchmark analysis in order to identify patterns in i4.0 implementation of Portuguese SME.





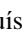


**Acknowledgments.** This work is financed by FEDER funds through COMPETE 2020 in the context of the SIAC system (Collective Actions Support System): 03/SIAC/2016; investment project n° 026752.

## References

1. Castro, H., Carvalho, A.R.F., Leal, F., Gouveia, H.: Importance of i4.0 maturity assessments in promoting its concepts adoption by SMEs (2019, in press)
2. Chen, B., Wan, J., Shu, L., Li, P., Mukherjee, M., Yin, B.: Smart factory of industry 4.0: key technologies, application case, and challenges. *IEEE Access* **6**, 6505–6519 (2018)
3. De Bruin, T., Freeze, R., Kaulkarni, U., Rosemann, M.: Understanding the main phases of developing a maturity assessment model (2005)
4. Geissbauer, R., Vedso, J., Schrauf, S.: Industry 4.0: building the digital enterprise. Retrieved from PwC Website (2016). <https://www.pwc.com/gx/en/industries/industries-4.0/landing-page/industry-4.0-building-your-digital-enterprise-april-2016.pdf>
5. Gökalp, E., Şener, U., Eren, P.E.: Development of an assessment model for industry 4.0: industry 4.0-mm. In: Mas, A., Mesquida, A., O'Connor, R.V., Rout, T., Dorling, A. (eds.) *Software Process Improvement and Capability Determination*, pp. 128–142. Springer, Cham (2017)
6. Leal, F., Castro, H., Carvalho, A.R.F., Gouveia, H.: Data analytics applied to sand casting foundry industries (2019, in press)
7. Liao, Y., Deschamps, F., de Freitas Rocha Loures, E., Ramos, L.F.P.: Past, present and future of industry 4.0 - a systematic literature review and research agenda proposal. *Int. J. Prod. Res.* **55**(12), 3609–3629 (2017). <https://doi.org/10.1080/00207543.2017.1308576>
8. Lichtblau, K.: *Industrie 4.0-readiness*. Impuls-Stiftung (2015)
9. Lu, Y.: Industry 4.0: a survey on technologies, applications and open research issues. *J. Ind. Inf. Integr.* **6**, 1–10 (2017). <http://www.sciencedirect.com/science/article/pii/S2452414X17300043>
10. Mittal, S., Khan, M.A., Romero, D., Wuest, T.: A critical review of smart manufacturing & industry 4.0 maturity models: implications for small and medium-sized enterprises (SMEs). *J. Manuf. Syst.* **49**, 194–214 (2018). <http://www.sciencedirect.com/science/article/pii/S0278612518301341>
11. Schmidt, R., Möhring, M., Härting, R.C., Reichstein, C., Neumaier, P., Jozinović, P.: Industry 4.0 - potentials for creating smart products: empirical research results. In: Abramowicz, W. (ed.) *Business Information Systems*, pp. 16–27. Springer, Cham (2015)
12. Schuh, G., Anderl, R., Gausemeier, J., ten Hompel, M., Wahlster, W.: *Industrie 4.0 maturity index. Managing the digital transformation of companies*. Herbert Utz, Munich (2017)
13. Schumacher, A., Erol, S., Sihni, W.: A maturity model for assessing industry 4.0 readiness and maturity of manufacturing enterprises. *Procedia CIRP* **52**, 161–166 (2016). The Sixth International Conference on Changeable, Agile, Reconfigurable and Virtual Production (CARV2016)
14. Yang, C.H., Vyatkin, V., Pang, C.: Model-driven development of control software for distributed automation: a survey and an approach. *IEEE Trans. Syst. Man Cybern. Syst.* **44**(3), 292–305 (2014)



# Exploring the Linkages Between the Internet of Things and Planning and Control Systems in Industrial Applications

Ricardo Soares<sup>1</sup>  , Alexandra Marques<sup>2</sup> , Reinaldo Gomes<sup>1</sup> ,  
Luís Guardão<sup>2</sup> , Elder Hernández<sup>2</sup> , and Rui Rebelo<sup>2</sup> 

<sup>1</sup> INESC TEC, FEUP – Faculty of Engineering, University of Porto,  
R. Dr. Roberto Frias, 4200-465 Porto, Portugal  
ricardo.s@fe.up.pt

<sup>2</sup> INESC TEC – INESC Technology and Science,  
R. Dr. Roberto Frias, 4200-465 Porto, Portugal

**Abstract.** The potential of the Internet of Things (IoT) and other technologies in the realm of Industry 4.0 to generate valuable data for monitoring the performance of the production processes and the whole supply chain is well established. However, these large volumes of data can be used within planning and control systems (PCSs) to enhance real-time planning and decision-making. This paper conducts a literature review to envisage an overall system architecture that combines IoT and PCS for planning, monitoring and control of operations at the level of an industrial production process or at the level of its supply chain. Despite the extensive literature on IoT implementations, few studies explain the interactions between IoT and the components of PCS. It is expected that, with the increasing digitization of business processes, approaches with PCS and IoT become ubiquitous in the near future.

**Keywords:** Internet of Things · Planning and control systems · Information flow · System architecture

## 1 Introduction

The increasing competitiveness of business environments trigger the need for constant improvement of organizations industrial processes and increase the overall performance of the supply chains. Throughout the years this has been achieved through the development of decision-making tools and algorithms with increasing complexity and effectiveness, such as the production planning and control systems.

Recent advances in sensor technologies and wireless networks have enabled the potential of the Internet of Things (IoT) and Industry 4.0 concepts in industrial applications. Specifically, IoT refers to a network of devices, such as sensors embedded in machinery, that can communicate and interact with others over the Internet, providing relevant information for monitoring the performance of the processes or the value chains in close-to-real-time [18]. Frequently studied aspects include sensors selection, types of data collected, how it is stored, processed and displayed for

decision-makers. The generation of valuable real-time data is now possible and potentiates the improvement of other decision-making processes, beyond performance monitoring. Being an open research topic, there is still little systematic information about the uses of IoT data and its interaction with different decision-making dimensions that are often supported in the planning and control systems.

Planning and Control Systems (PCS) are a broad term to refer to software tools supporting the organisation into planning and forecasting its core processes. Typically referring to production planning and control, both capacity planning and materials requirement planning [19]. For example, beforehand, planning and scheduling the production orders into the machines in order to meet the manufacturing requirements and assuring the optimal occupation of the machines at the minimum costs; and afterwards, controlling the deviations towards the plan [19]. However, in a broad scope, such as the one adopted in this research, it may also apply to supply chain planning and control, hence, considering interlinked operations, especially if performed by different organisations. Examples include the joint planning of production and inbound sourcing, through collaboration between the industry and the third-party logistics providers, followed by the control of actual transported freights and its impact on production planning [20].

This paper aims analyses existing solutions that combine IoT and PCS for planning, monitoring and control of operations at the level of an industrial production process or at the level of its supply chain, in order to: (1) systematize the main components existing in integrated IoT and PCS solutions and its information flows; (2) assess what are the most used techniques and tools for each of these PCS modules when linked with IoT systems. For that purpose, a literature review was performed and the results were analyzed from which a conceptual architecture was envisioned, and the main IoT-PCS interactions were described. Finally, research gaps were found.

The remainder of this paper is as follows. Section 2 presents the adopted methodology for the literature review. Section 3 presents the conceptual framework for IoT and PCS interactions which was drawn in the course of this research and used for classifying the selected publications. Section 4 maps the results of the literature review into the conceptual framework for IoT and PCS interactions and describes the main components and information flows reported in the literature. Finally, Sect. 5 summarises the conclusions and proposes future work.

## 2 Methodology

This research is built in a four-step literature review, adapted from [21]. The first step – literature collection – consists of searches in the Scopus database in January 2019. The search terms were “internet of things” AND “planning” AND (“production” OR “inventory” OR “transportation” OR “logistics”) AND (“control” OR “simulation”). Additional search criteria are only research articles written in the English language and published between 2010 and 2019.

In the second step – descriptive analysis – the formal aspects of the selected publications are analysed, including the publication date, the journal type, the application scope. In the third step – category selection - through an iterative process, the

authors convey to a conceptual framework for IoT and PCS interactions that is used to classify all publications. In the four-step – content analysis – all the authors carefully analyze each paper, seeking to find valuable examples of techniques and tools for each of these PCS components when linked with IoT components, hence, contributing to strengthening the body of knowledge in this domain and identifying possible research gaps.

### 3 A Conceptual Framework for IoT and PCS Interactions

In this research, we consider the three main decision-making dimensions - planning, monitoring and control – each of them can be supported into a specific module or component of the PCS. Planning concerns to the development of optimal operations plans and schedules, which can be applied to different temporal and spatial scales. It usually resorts to the development of optimisation and/or simulation models or heuristic algorithms. Monitoring relates to the collection of real-time information for the assessment of the performance of the on-field operations. The usual support for a monitoring module is a set of dashboards that allow the user to have a holistic perspective of the system's status. The control module builds on the information from the monitoring module by allowing inferences on the level of execution of the plans and schedules, based upon the collected data, and by favouring the interaction of the user. The control module is responsible for communicating any changes to IoT systems, according to the assessments that were made regarding the adequacy of the initial plan.

In respect to the IoT components, we adopt a broad definition that as any resource or set of resources that are used on-field and allow for data collection, be it by sensor technologies or by manual user input. Accordingly, IoT systems can range from highly automated systems (e.g., sensors embedded in the machinery) up to and other web-based applications can also help to manually collect data and interact to the other IoT components.

The possible interactions between PCSs and IoT components are illustrated in Fig. 1, where we also represent the typical information flows one may find between these components.

PCSs are usually fed by a data layer, where essential data is stored. Depending on the systems, there can be independent data layers for each of the PCS modules or a common one; in this paper, we assume the latter option. In the data layer, one may classify data as being static or dynamic, depending on the frequency specific sets of data are updated. Dynamic data is intimately linked with information flows coming from IoT systems, as most of its data is usually advantaged for operations monitoring and control in real-time. The purpose of static data, on the other hand, allows for it to be updated much less frequently, as its purpose is not to be updated/changed as operations execution progresses. Static data may be adjusted by IoT components, usually after collection of several data which has been proven to be deviated from the information stored in databases, thus triggering the need for adjusting such data.



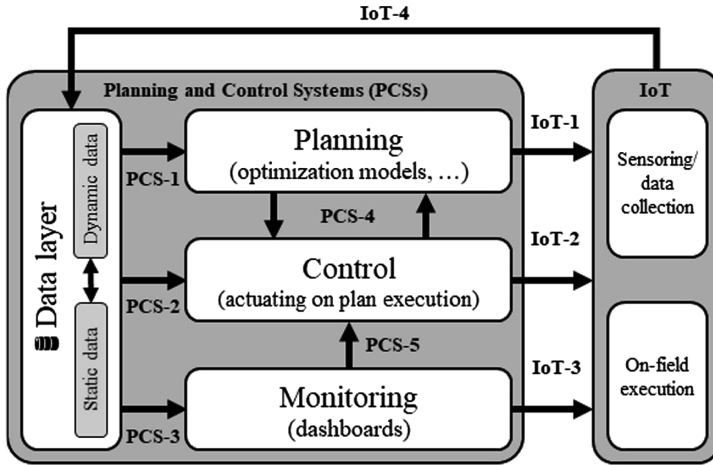


Fig. 1. Possible data flows between components of PCSs and IoT systems

#### 4 Mapping the Results of the Literature Review into the Conceptual Framework for IoT and PCS Interactions

The performed literature review returned a total of 44 articles. From these articles, 27 were excluded based on the abstract analysis since these did not refer to a concrete application IoT with PCS. The total sample of selected publications is 17. The publication dates range from the year 2011 up to 2019, with 2018 having the most published articles (10 occurrences). The vast majority of articles concern applications to manufacturing processes (11 articles).

The components of the conceptual framework that are found in the selected papers are summarised in Table 1. The majority of the selected publications includes all the three components of PCS, namely, planning, control and monitoring which are fed by data provided by the IoT components.

Table 1. Summary of the most frequent components found in the literature review

Components of the conceptual framework	Ref. count	References
Planning + IoT	4	[1–4]
Monitoring + IoT	2	[6, 14]
Planning + Monitoring + IoT	3	[8, 12, 15]
Planning + Control + Monitoring + IoT	8	[5, 7, 9–11, 13, 16, 17]
<b>Total</b>	<b>17</b>	

#### 4.1 PCS with a Monitoring Component Interacting with IoT

In the cases where the PCS consists exclusively in a monitoring module that is fed by real-time data collected by IoT components, the primary purpose of this integrated system is to provide the possibility of analysing in real-time several performance indicators of a given process through the collection and monitoring of relevant dynamic information. The main advantage is its ability to detect exceptions and quickly communicate this information. In recent research work, ref. [14] developed an architecture with similarities to our conceptual framework, which encompasses three layers: (1) IoT-enabled smart shop-floor; (2) critical event & PN-based real-time production performance analysis, and (3) DT-based exception extraction and cause diagnosis. There is a constant process of updating the information coming from the IoT sensors about on-field execution (flow IoT-4), which will feed the monitoring component (flow PCS-3). The information resulting from the monitoring, in the form of performance indicator values, can be sent back to users and used to guide future actions (flow IoT-3), thus, closing this cycle of information flow.

#### 4.2 PCS with a Planning Component Interacting with IoT

Applications with only a planning component linked with IoT can be seldom found. The information flows found in these references consisted in data being fed to the data layer (flow IoT-4) in the form of static data, which are afterwards fed to the planning module (flow PCS-1). These IoT applications used IoT data not for dealing with uncertainty or quality of information issues, but instead performing adaptive adjustment of planning data for subsequent planning iterations. In these applications, IoT data is not fed with new instructions as on-field execution progresses. The applications of this concept ranged from generic production planning [1, 2], where electricity prices or pending customer orders are periodically updated to minimize energy consumption or production makespan, respectively, and even greenhouse planning [3], where several sensor data is collected to infer problem parameters, which in turn are used by the planning module. Contrarily to the references cited above, ref. [4], which applies IoT to a public transportation system, only finds information coming from the planning module to IoT (flow IoT-1) in order to communicate expected arrival times to passengers smartphones.

#### 4.3 PCS with a Planning Component Interacting with IoT

Planning and monitoring merge the previously described approaches and information flows. This approach uses both static data for planning and dynamic data for monitoring, although both modules do not explicitly interact. After planning is performed, monitoring only evaluates the degree of fulfilment of the initial plan. However, it is not possible to actuate in the plan and provide replanning. Applications of this approach were found in the food industry [8], where monitoring of controlled temperature goods is envisaged, as well as in the textile and apparel industry [15] to register and manage abnormalities in product delivery processes in a collaborative environment. An additional application of planning and monitoring was found in the printed circuit board

industry [12] to track equipment and product information in various points of the production process.

#### 4.4 Fully Fledged PCS Interacting with IoT

In this approach, in addition to the previously mentioned flows, there is a loop-flow between the planning component and the control component (flow PCS-4), the latter also receiving information through the data layer (PCS-2), sending the deviations from the initial plan along with the current status of the system (flow IoT-2).

This integrated PCS can act in a decentralised way and re-plan only a part of the system that has been affected by a discrete event [17] or can aggregate the different dimensions of the system and act in the general plan [5, 7, 9–11, 13, 16].

The present architecture is the only one that allows the re-planning process and the constant control of several indicators compared to the initial plan. It is possible to find applications with this concept in various sectors of Industry 4.0, such as manufacturing scheduling [5, 9, 11], the tyre industry [7] and parts manufacturing in the automotive sector [10]. In this latter case, simulation techniques were used in the control component to predict the impact of the deviations in Key Performance Indicators (KPI's). Other sectors where there are already applications with features to this methodology are Smart Cities Traffic Management Systems (TMS) [13] and Supply Chain Trading [16], where the researchers evaluate the potential of a cloud-enabled real-time platform for planning and control in an auction logistics centre.

## 5 Conclusions

This paper allowed to obtain an overview of different applications where planning and control systems are linked with IoT components. The low number of applications with linkages between PCSs and IoT that were found confirm that these concepts are still seldom used. However, the increasing number of publications on this topic suggest an increase in awareness by the research community.

A literature review was performed to characterise different approaches of PCSs linked with IoT systems. To that effect, a conceptual framework was envisaged based on the information flows one may find in different applications. The developed framework can aggregate different dimensions of the production processes, such as real-time monitoring or control and its interaction with other components of the planning system. It is noteworthy that the majority of the papers found combine the four components of the PCS, namely planning, monitoring and control, all fed by a multitude of IoT-based data. However, additional research is needed for a detailed comparison of the functionalities of these components and the standardisation of the data exchange among them and with the IoT. The general adoption of data standards such as ISA-95 can be instrumental for this purpose.

**Acknowledgements.** The first author acknowledges the support of the Ph.D. Grant SFRH/BD/136314/2018, awarded by the Portuguese Science and Technology Foundation (FCT) and financed by the European Social Fund (ESF) and by National Funds of the Ministry of

Science, Technology and Higher Education (MCTES) through the Human Capital Operational Programme (POCH).

This work was also supported by Portugal 2020 project “DM4Manufacturing - Aligning manufacturing decision making with advanced manufacturing technologies”, POCI-01-0145-FEDER-016418, financed by UE/FEDER through the program COMPETE2020.

## References

1. Rubaiee, S., Yildirim, M.B.: An energy-aware multiobjective ant colony algorithm to minimize total completion time and energy cost on a single-machine preemptive scheduling. *Comput. Ind. Eng.* **127**, 240–252 (2019)
2. Saif, U., Guan, Z., Wang, C., He, C., Yue, L., Mirza, J.: Drum buffer rope-based heuristic for multi-level rolling horizon planning in mixed model production. *Int. J. Prod. Res.* **57**, 1–28 (2019). <https://doi.org/10.1080/00207543.2019.1569272>
3. Kang, M., Fan, X.-R., Hua, J., Wang, H., Wang, X., Wang, F.-Y.: Managing traditional solar greenhouse with CPSS: a just-for-fit philosophy. *IEEE Trans. Cybern.* **48**(12), 3371–3380 (2018)
4. Chandra, S., Naik, R.T., Galbeno, L.: Impact assessment of the Internet of Things on feeder transit performance. *Transp. Plan. Technol.* **41**(8), 830–844 (2018)
5. Kang, H.S., Noh, S.D., Son, J.Y., Kim, H., Park, J.H., Lee, J.Y.: The FaaS system using additive manufacturing for personalized production. *Rapid Prototyp. J.* **24**(9), 1486–1499 (2018)
6. Zhang, Y., Ma, S., Yang, H., Lv, J., Liu, Y.: A big data driven analytical framework for energy-intensive manufacturing industries. *J. Clean. Prod.* **197**, 57–72 (2018)
7. Tsai, W.-H., Lu, Y.-H.: A framework of production planning and control with carbon tax under industry 4.0. *Sustainability* **10**(9), 3221 (2018)
8. Tsang, Y.P., Choy, K.L., Wu, C.H., Ho, G.T.S., Lam, H.Y., Tang, V.: An intelligent model for assuring food quality in managing a multi-temperature food distribution centre. *Food Control* **90**, 81–97 (2018)
9. Lin, P., Li, M., Kong, X., Chen, J., Huang, G.Q., Wang, M.: Synchronisation for smart factory - towards IoT-enabled mechanisms. *Int. J. Comput. Integr. Manuf.* **31**(7), 624–635 (2017)
10. Lee, J., Noh, S., Kim, H.-J., Kang, Y.-S.: Implementation of cyber-physical production systems for quality prediction and operation control in metal casting. *Sensors* **18**(5), 1428 (2018)
11. Mourtzis, D., Vlachou, E.: A cloud-based cyber-physical system for adaptive shop-floor scheduling and condition-based maintenance. *J. Manuf. Syst.* **47**, 179–198 (2018)
12. Guo, J.-H.: Applications of the Internet of Things technology in advanced planning systems. *Sens. Mater.* **30**(8), 1723 (2018)
13. Masek, P., et al.: A harmonized perspective on transportation management in smart cities: the novel IoT-driven environment for road traffic modeling. *Sensors* **16**(11), 1872 (2016)
14. Zhang, Y., Wang, W., Wu, N., Qian, C.: IoT-enabled real-time production performance analysis and exception diagnosis model. *IEEE Trans. Autom. Sci. Eng.* **13**(3), 1318–1332 (2016)
15. Shamsuzzoha, A., Toscano, C., Carneiro, L.M., Kumar, V., Helo, P.: ICT-based solution approach for collaborative delivery of customised products. *Prod. Plan. Control.* **27**(4), 280–298 (2016)

16. Kong, X.T.R., Fang, J., Luo, H., Huang, G.Q.: Cloud-enabled real-time platform for adaptive planning and control in auction logistics center. *Comput. Ind. Eng.* **84**, 79–90 (2015)
17. Meyer, G.G., Wortmann, J.C., Szirbik, N.B.: Production monitoring and control with intelligent products. *Int. J. Prod. Res.* **49**(5), 1303–1317 (2011)
18. Ray, P.P.: A survey on Internet of Things architectures. *J. King Saud Univ. Comput. Inf. Sci.* **8**(3), 291–319 (2018)
19. Ellwein, C., et al.: Production planning and control systems – a new software architecture connectivity in target. *Procedia CIRP* **79**(2019), 362–366 (2019)
20. Scholz, J., et al.: Digital technologies for forest supply chain optimization: existing solutions and future trends. *Environ. Manag.* **62**, 1108–1133 (2018)
21. Seuring and Muller: From a literature review to a conceptual framework for sustainable supply chain management. *J. Clean. Prod.* **16**(15), 1699–1710 (2008)



# Virtual Workstations Applied to the Mould Industry - A Case Study

Fabiana Guarda<sup>1(✉)</sup>, Luís Marrazes<sup>2</sup>, and Mário Afonso<sup>3</sup>

<sup>1</sup> Department of Mechanical Engineering, Polytechnic Institute of Leiria,  
Leiria, Portugal

fabiana.guarda@ipleiria.pt

<sup>2</sup> Tecnimoplás - Indústria Técnica de Moldes, Lda, Marinha Grande, Portugal

<sup>3</sup> Lansys - Business IT, Lda, Marinha Grande, Portugal

**Abstract.** Professional CAD/CAM users in the mould making industry count on these environments to design and engineer moulds for the plastic industry. Conventionally this software is accessible through high-powered workstations shared among professionals in closed facilities. Operating in various countries, the access to data and projects, security and real-time collaboration became imperative.

The look for solutions to provide mobility turned Tecnimoplás to virtualization to deliver VDI environments to their commercial, managers and project users.

However, these kind of VDI environments weren't extensively tested yet in the mould making industry, so the company decided to try this solution on their own.

A proof-of-concept was made, and initial conclusions were taken from there leading the project forward. The final solution was tailored and implemented, and users started working only with VDI systems. Tests were then made to achieve the optimal VDI configuration and file time opening, processing times, update times and power consumption measurements took place.

The continues VDI technology update makes this kind of study only a brief approach to this recent technology.

**Keywords:** Virtual workstations · Mould industry · CAD/CAM

## 1 Introduction

The Portuguese mould making industry has been confronted for the past 40 years with an enormous technological evolution not only because of its major client, the automotive industry, but also by the constant changes and updates of software, hardware and machinery that are used in tool manufacturing.

Mould making industry project and design information increased substantially as the result of changing from 2D hand drawings to 3D integrated project which led the companies to increase IT investment over time.

To maintain the competitiveness of the sector and a higher response to market demands, mould manufacturers are compressing production cycles and reducing tool

costs. At the same time, ensuring data and intellectual property security is a paramount concern (NVIDIA Corporation 2018).

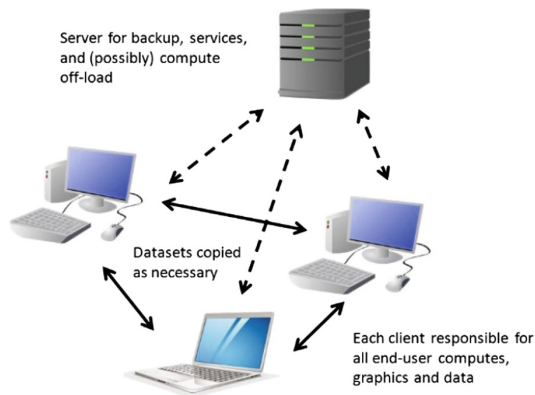
Mobility solutions are also needed to support collaboration between workers, external suppliers, clients and partners to provide them access to mould information in an easy and safe way and very short time (NVIDIA Corporation 2018) (Citrix Systems, Inc. 2013).

Digital transformation brought solutions to support and respond to modern manufacturing processes. Nowadays mould technology and technical aspects are based in structured information stored in IT infrastructure and always available (Kurkure 2018). This leads us to the fourth generation mould.

This mould will be smarter, complex and with multi-functional/multi-process abilities the greater the synergy in adaptation and fusion of technologies/processes in the actual production and business systems.

### 1.1 Traditional Computing Model

Today most CAD (Computer Aided Design) systems run on a computing environment of physical deskside and mobile workstations. Users design, view, model, animate and simulate on their own machines, each responsible for computation, visualization and storage. They do it for one simple reason: it does its job, and it does its job well (Herrera 2018) (Fig. 1).



**Fig. 1.** In the traditional client-side model, each physical workstation is responsible for all end-user computes, graphics and data (Herrera 2018).

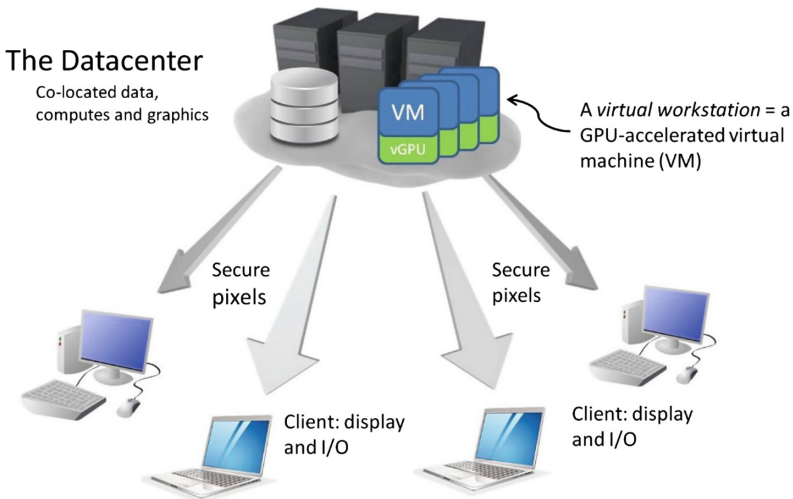
But mould makers are finding challenges with the traditional workstation model, challenges that are increasing over time. They're seeing visualization and computing, starting to creak under this pressure. Mould files are becoming too big and are taking several minutes to open from file server or from hard drives. The risk of security breaches and maintaining that security in a more and more mobile world gets higher while internet is now rooted everywhere. And complex projects are requiring working teams not just from employees, but contractors, clients and consultants who do not

reside in the next workspace. They might be at the factory or out in the field. Yet, they all need access to the same files, from where they are and sure up to date, with no waiting (Herrera 2018).

## 1.2 Virtual Workstations: A New Technology and Infrastructure

For those situations, it's not the abilities of a physical workstation that shows problems, but how they're accessed and shared. A few mould makers are getting the need of a centralized, back-end computing scenario, one that uses platform virtualization technology but with one demanding new addition: the virtualizable GPU (Graphics Processing Unit) (NVIDIA Corporation 2017). Theoretically, virtualization is the capability of a device to host one or more virtual machines (VMs) that each behave like independent machines with their own operating system (OS), all running on the same primary device hardware. To those whose jobs and business depend on interactive 3D graphical computing this became a thunderous solution (NVIDIA Corporation 2017).

With virtual workstations hosted in the datacenter, all compute, data and graphics reside on the server and clients receive only the pixel streams. What is new in the field of platform virtualization, however, is the capability to deliver powerful workstation, GPU-accelerated 3D graphics performance. This allows host servers to now render 3D graphics for multiple hosted machines far faster than a conventional CPU-only server (Herrera 2018) (Fig. 2).



**Fig. 2.** With virtual workstations hosted in the datacenter, all compute, data and graphics reside on the server and clients receive only the pixel streams (Herrera 2018).



## 2 Project Description

Nowadays the use of CAD 3D tools in design and mould development is required and turns to be fundamental to the different manufacturing processes and planning. In the past few years a growing set of operations and components as completed and enriched the tool (mould) project. This growing has significant increased file size causing difficulties and even bottlenecks in processing and treatment of the same.

As this set of operations and mould characteristics are more and more requested by clients, these needs have augmented file opening, edition and processing times. Also due to mould complexity, 3D software has suffered performance issues. Towards response to these new realities, mould making companies have strongly invested in high performance workstation acquisition and local infrastructure expansion and update. This turns out to be a huge investment.

### 2.1 Project Goals

After a careful evaluation it was clear that a different approach to the problem was necessary. The CAD 3D tools support had to be drastically changed. For that managers decided to develop and implement a virtual GPU project (GRID) to support 3D applications.

Five main reasons for the grid were then settled:

- Reduce opening project file time/faster access to data;
- Better application performance and user experience (improving productivity);
- Flexibility, efficiency (reduce power) and ease of management;
- Enhanced security and disaster recovery;
- Mobility to work with 3D applications anywhere on any device.

To achieve these goals Tecnimoplás started looking for Grid Technology Suppliers to access a POC (Proof of Concept) test.

### 2.2 Challenges

In general CAD software suppliers just offer remote support to their applications running in virtualized environments, not ensuring the correct operation and performance of those same applications.

Therefore, not having guarantees or promises of proper functioning of these applications on any virtualized environment, testing the solution became a problem. All the incompatibility between product and grid technology had to be supported.

Added to this difficulty, the need for data storage NAS (Network Attached Storage) or SAN (Storage Area Network) weren't tested or supported by software suppliers.

In this context where the market has not replied, or has very limited and conditioned answers coupled with the absence of industrial practices and evidences in this specific area (design and project moulds for plastic industry), managers decided to start an investigation grid project of his CAD 3D platform.

## 2.3 Project Stages

Some strategic steps were then defined to validate the project. It could only be possible to move on to the next phase if the previous one was confirmed.

### 2.3.1 First Step

The first step of this project was to survey the bottlenecks and constraints of the old solution in the CAD 3D project area.

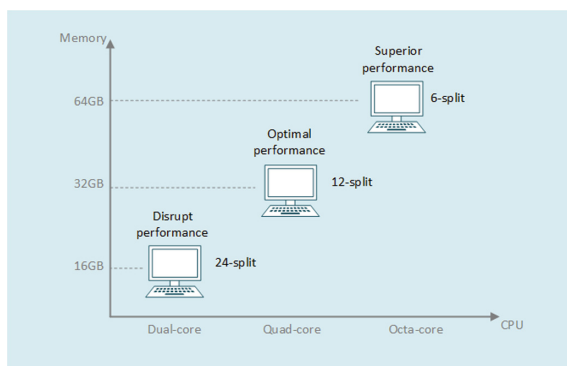
The following was concluded:

- Workstation hardware failure leads the user to be unable to work. That time period can be crucial to ensure on time project;
- All the information could be accessed by anyone who had machine administrator permissions (password breaches);
- Remote file access delay and editing due to network latency once the data is stored in the data center;
- Workers, contractors and suppliers didn't have access to data and design from outside locations;
- Software updates took at least two to three hours for every physical workstation causing losses in productivity.
- Due to the heavy project files, workstations were oversized and not always used at 100%. This leads to large investments without the best outcome.

In this step, it was also made file openings and savings time measurement to compare it with the file times obtained on the GRID solution.

### 2.3.2 Second Step

For one month the POC (Proof-of-Concept) was tested with members from the organization, software and hardware suppliers (Fig. 3).



**Fig. 3.** Virtual machine performed tests and results

To make sure that all users had the right allocation, the organization rolled out a few different virtual client machines: the first virtual-machine had the octa-core CPU

with 64 GB RAM and 6-split GPU, the second one had the Quad-core CPU with 32 GB RAM and 12-split GPU and the third one had the Dual-core CPU with 16 GB RAM and 24-split GPU.

After some test with the end users it was possible to reach the right virtual machine configuration which satisfies all the CAD users needs. The Quad-core, 32 GB RAM, 12-split solution became approved.

### 2.3.3 Implemented Solution

After completed the POC, they moved on to the next step, acquiring the complete solution (Fig. 4).

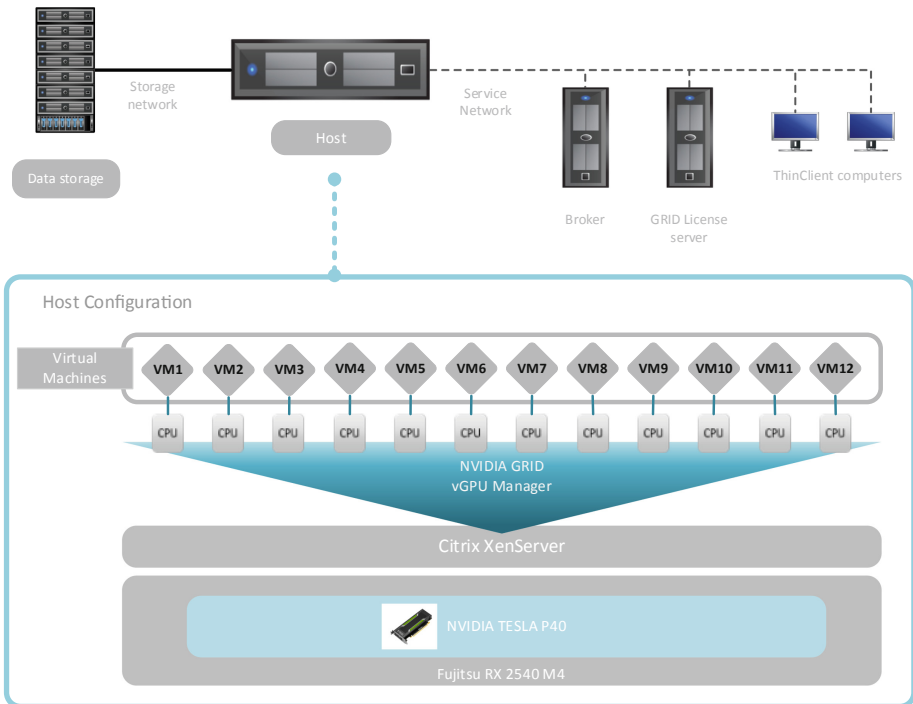


Fig. 4. VDI system configuration solution

This final solution is composed by a server host and a data storage, that gives the physical resources to the virtual machines, processor, memory, storage, graphics and connectivity. The host as two Intel Xeon Gold processors, 512 GB of memory, 10 Gbps Ethernet and NVidia Tesla P40 graphics card. The storage is a fiber channel connected all flash disk array. As for the hypervisor, the option was the Citrix XenServer® Hypervisor.

The XenDesktop® Controller is the server-side component that provide the virtual machines creation and management. It manages the user access, plus brokering and optimizes connections. The NVIDIA GRID® License Manager manages the GRID license usage. Finally, the end user clients with the Citrix Receiver installed to connect to the solution.

### 3 Results

The implemented solution as not yet reached all the goals and it's still under evaluation. However, there are some major conclusions that were already taken:

- Based on test and users experience, calculation times (CPU processing times) looked very similar, but in some few special cases there was an aggravation in processing time due to the CPU server processors lower clock speed. This was the first ensured goal.
- In graphical terms, the users did not noticed any difference between the 2 environments when they applied some CAD functions (rotate, pan zoom in, zoom out, etc.) The goal of keeping graphical performance was ensured.
- All common computer applications necessary for helping users' jobs, are installed and running in their virtual machines with no need to change processes and/or applications.
- Project files open and save are performed significantly faster. In the obtained measurements 10 to 40% of time file opening showed up faster. This was also confirmed in the POC. Despite all the variables the average time of file opening and saving is about 20% faster.
- It is easier and considerable faster to allocate more resources to one user if required. In some bigger projects, the needs for RAM for instance are larger, and with VDI solutions that extra RAM can be delivered in just a matter of minutes.
- With centralized updates all the applications and hardware maintenance are easier and faster.
- Power consumption was significantly decreased in virtualized systems. The thin clients PC's have a lower power consumption (about 95% less) compared to physical workstations.
- Also the noise in project department was reduced from 20 dB per workstation to 2 dB per thin client.
- Mobility that allows the possibility to be in any part of the world and have access to the updated information without need of downloads or access to devices with graphic capacity.

The Table 1 summarizes these results.

**Table 1.** Summary of all main conclusions

	Physical workstation	VDI
Processing times	Excellent	Very Good
Graphical performance	Excellent	Excellent
Common installed applications	Office, Production, etc.	Office, Production, etc.
File opening times	Average 2 min	Average 1,5 min
Allocate resources	2 to 3 days	5 min
Updates	2 h per workstation/update	2 h for 12 VDI/update
Power consumption	225 W	10 W (Thin Client)
Noise at project room	20 dB	2 dB
Mobility	No	Yes

## 4 Conclusions

Tecnimoplás was looking for a virtualized CAD solution to help them on project and designing moulds for the plastic industry.

With this solution they now have faster access to 3D model project files and users can work with large 3D model’s whiteout lag or delay. This translates in increased efficiency and productivity, and it is helping them shorting the time-to-market.

Data protection and intellectual property were an enormous concern. The data was too vulnerable to theft and damage and by centralizing the information in the data center the organization can now better protect it.

Centralizing PLM (product lifecycle management) solutions in the data center provides control over design changes and superior reliability and consolidation of data. Besides, virtualized desktops allow faster access and response times to PLM databases, letting PLM administrators shear seconds off numerous database transactions, which results in time savings.

Mobility and autonomy to the commercial users and suppliers with secure and immediate access to the CAD appliances from any device brought faster collaboration between them decreasing waiting response times.

Data version and update in the data center no longer need to go though all the user’s workstations to update and maintain the applications. This leads to a reduced helpdesk supports and increases efficiency and a lower IT management cost.

If they needed more resources (RAM, HDD, etc.) in a physical workstation they had to purchase and install them but now performance scalability enables resources when they are needed in a matter of minutes.

## References

Citrix Systems, Inc.: XenDesktop with HDX 3D Pro | Customer Case Studies (2013)  
 Herrera, A.: Virtual workstation 101: the whats, whys and hows of a new computing model for professional visual applications. Nvidia (2018)

- NVIDIA Corporation: Customer Success Story | Honda R&D Co., Ltd. Enhancing Productivity With New GPU Virtualization Technology (2017)
- NVIDIA Corporation: Boost Productivity, Enhance Collaboration, and Protect Intellectual Property with NVIDIA Virtual GPU Solutions (2018)
- Kurkure, U., Sivaraman, H.: Virtualized GPUs in high performance datacenters. In: 2018 International Conference on High Performance Computing & Simulation (HPCS), Orleans, France, pp. 887–894. IEEE (2018)



# To Simulate or Not to Simulate? Challenges in Digitally Prototyping HMI Interactive Technologies

Sevcan Yardim Sener<sup>1,2(✉)</sup> and Owain Pedgley<sup>3</sup>

<sup>1</sup> TOBB University of Economics and Technology, 06510 Ankara, Turkey  
sevcanyardim@gmail.com

<sup>2</sup> University of Liverpool, Liverpool L69 3BX, UK

<sup>3</sup> Middle East Technical University, 06800 Ankara, Turkey

**Abstract.** This study of automotive HMI (human-machine interface) design is built around the fact that traditional product modelling and testing tools (i.e. foam-clay mock-ups, working prototypes) are increasingly being replaced by simulation technologies. The development of these technologies creates challenges as well as opportunities for product design teams. This study was carried out as a workshop to understand these challenges. A shortlist of fourteen new in-vehicle interactive technologies was determined through a literature review, followed by recruitment of four experts to evaluate the simulation of these technologies. The evaluation was based on pre-set criteria regarding the suitability, availability of tools and extent of research and development required to simulate the interactive technologies, within a context of new product design and development.

**Keywords:** Interactive technologies · Simulation tools · Feasibility of simulation

## 1 Introduction

This study is woven around developments in simulation and interactive product technologies, carried out in collaboration with an industrial partner (automotive) and a research center (design simulation). The aim of the study is to gather experts' opinions on how (and whether) simulation can be used to digitally prototype technologically advanced in-car interactions with the human-machine interface (HMI) of a vehicle, as part of a feasibility program of R&D. The results of the evaluative workshop [7] are useful for assessing the feasibility of simulating various interactive product technologies with available tools and methods, as well as possibilities for near future scenarios and their anticipated impact.

## 2 Methodology

At the commencement of the study, a large pool of new technologies were researched through online sources (academic studies, technology blogs), and then filtered with the automotive partner regarding their potential for integration into an in-car environment. A shortlist of fourteen technologies was reached, alongside a classification regarding their role in interaction as (i) input (eye tracking, audio fingerprinting, tactile touch displays, biometrics, smell capturing), (ii) input-output (flexible displays, shape changing interfaces, intelligent UI, deformable displays), or (iii) output technologies (texture and softness changing interfaces, see through displays, artificial textures, spatial sound, focused smell). Following the review an extensive document with definitions of the technologies and example product applications was shared with the workshop participants one week prior to the session, to familiarize themselves. During the workshop, the researcher presented the technologies again so as to jog participants' memories. Besides the technologies and definitions, the pre-workshop document also included technology trends and possible locations (fixed, semi-attached, on-body, fully mobile) for the technologies in a driving scenario, as a prompt for participants to keep in mind.

During the workshop participants were requested to independently make a professional assessment of the interactive technologies, under the overarching subject of how to create a simulation of the technologies in a digital environment. They were given individual evaluation sheets for each technology group (input/input-output/output). The criteria to evaluate the technologies were set as: (i) suitability to reality levels, as augmented reality (AR), virtual reality (VR) and augmented virtuality (AV); (ii) availability of hardware/software (bespoke/R&D, commercially existing, or existing at the collaborating organization); (iii) feasibility with regard to R&D time/effort and cost; and (iv) expected impact of a 'successful' simulation of the technology. The independent evaluation process was followed by group discussion about the technologies, with each participant contributing their own perspective. The workshop was video recorded with consent, and then transcribed for analysis.

## 3 Results

The recorded workshop discussions and materials were collated and analyzed, with an aim to identify the collective challenges and potentials of simulating the shortlisted in-car technologies. The results are summarized under three titles: Input Technologies, Input-Output Technologies and Output Technologies.

### 3.1 Input Technologies

These technologies are used to give actions and information to an HMI system corresponding to user tasks and goals. Five input technologies were shortlisted the evaluation of these technologies is summarized in Fig. 1.



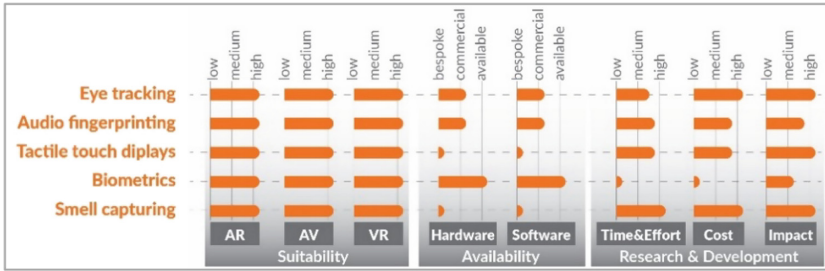


Fig. 1. Evaluation of input technologies

Some input technologies were considered to be possible to simulate, even in the absence of the real-life sensors associated with them, using ‘wizard of oz’ prototyping methods. For example, biometric input for identification is just a single step interaction, which can be mimicked simply by knowing who the user of the simulation is, with the simulation researcher inputting a setting accordingly. On the other hand, if the case was to simulate a product changing its interface according the heartbeat of the user, this would require sensors to continually gather biometric information constantly making the process complicated and costly.

Another important point about the input technologies, in relation to a usage scenario, is the output that is expected to follow or be associated. For example, the input may consist of identifying a certain smell, whilst the corresponding output may for example be a change of interior lighting (a visual response, relatively easy to simulate). Alternatively, the smell sensor may trigger changes in comfort settings of the vehicle seating, requiring more time, effort and cost to simulate. The level of precision or resolution for input sensing emerged as an important point and challenge. Demands for higher precision lead to a necessity for increased time, effort and cost when creating a simulation. For example, if an eye tracking scenario requires precision (e.g. locating small buttons only millimeters apart), workshop participants mentioned it will require longer time (to code and execute) and more capable and expensive eye tracking hardware and software solutions. With less precise demands, for example tracking the changeable focus from one HMI display to another, participants recommended head tracking as being a sufficient input source. Design criteria such as the location of interface controls and technologies places certain demands on simulation possibilities and processes. For example, for tactile touch screens it is easier to simulate tactile elements on a fixed-location screen, but far more challenging to map multimodal elements (visual, tactile) on a mobile screen, especially in mixed reality simulations.

### 3.2 Input-Output Technologies

Input-output technologies combine user actions and the input of information with the output of feedback, through a single underlying means. Four such technologies were shortlisted and the evaluation of these technologies is summarized in Fig. 2.

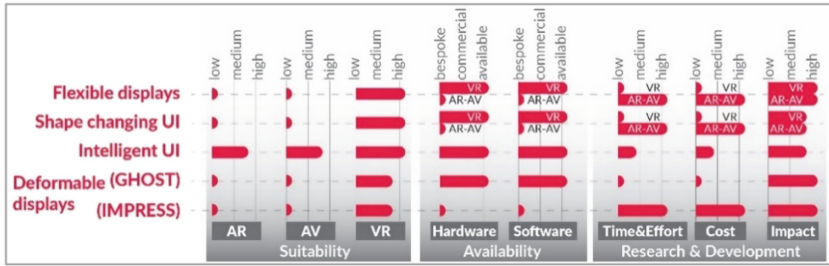


Fig. 2. Evaluation of input-output technologies

Input-output technologies, with their inherent dual functionality created an evaluation challenge for the workshop participants. For example, in flexible displays the input is the flexible materiality of the display caused by a force from the user, requiring haptic feedback from time to time that is notoriously challenging for a VR environment. However, the output is visual, where mapping a changing image onto a flexing surface is not a major challenge in a VR environment. So, the evaluation process demanded more scrutiny and detail on materialistic aspects of the technologies than had been anticipated. The suitability for different simulation environments was a point of major discussion while evaluating these technologies. Some participants regarded the technologies as suitable for VR but not suitable for mixed reality options, thus affecting recommendations for hardware, software, R&D time and effort. Participants suggested that for a detailed assessment of the technologies, it would be better to choose (fix) the simulation environment (AR, AV, VR), since it would focus the discussion on specific requirements and possibilities rather than general comparisons.

The role of particular interactive technologies can change from application to application (e.g. between different interfaces, products, etc.), complicating the evaluation process. This is the case, for example, with the deformable displays exemplified with two different products GHOST [4] (3D representation of information) and IMPRESS [3] (changing content in harmony with the deformation of a display). Even though principally the same technology has been used in both products (display deformation), the end experience is quite different. GHOST changes its shape according to 2D hand movements, which was regarded as relatively easy from a simulation perspective, since it requires tracking of hands only in a planar movement. On the other hand, IMPRESS makes use of the anatomical potential of the hand and requires precise tracking of the hands and fingers to understand exact movements in 3D space. GHOST was considered to fit within the scope of simulation using relatively simple existing equipment and software combinations with little time and effort. However, participants stated that simulation of IMPRESS would require intensive detail about hand position and posture tracking, accompanied by specialist high-precision tracking hardware and software.

### 3.3 Output Technologies

These technologies provide feedback and feedforward information to the user of a product. Five technologies were shortlisted the evaluation of these technologies is summarized in Fig. 3.

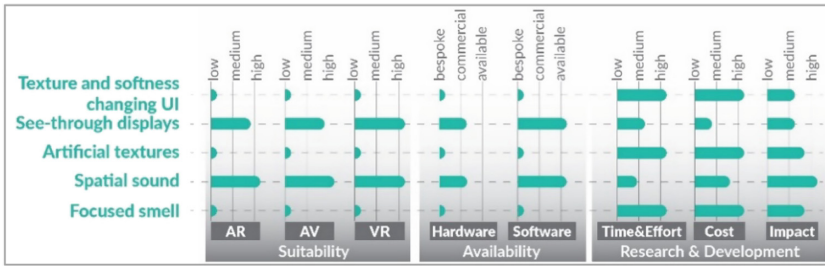


Fig. 3. Evaluation of output technologies

The convincing simulation of output technologies based on modalities other than visual or audible remains difficult to achieve. As simulation environments are heavily built around visual stimuli, visual output as a research area has received the greatest attention and has advanced the most with regard to equipment, software and feasibility. The general observation from the workshop was that although numerous simulation approaches to tactual sensations are possible (touch, haptics, kinaesthetics, proprioception), the associated hardware is often relatively invasive or cumbersome. For these reasons, a perpetual question in the workshop regarding feasibility of non-visual technologies was “is it worth simulating?” instead of “how can we achieve this experience in a simulation?”. For example, in the case of focused smell, experts asked the question “can you VR smell?”. Realizing ‘real smells’ (e.g. leather, deodorants, coffee) into an environment, instead of synthesizing a given smell from a range of ‘smell ingredients’ was regarded as far easier and cheaper. Challenges regarding the simulation of spatial sound (e.g. multiple point sound sources, rather than simple left-right stereo or monoaural) were raised. First the necessary steps for recording spatial sound must be in place, followed by the playback of recordings during simulation. Use of sound in general is relatively simple, with a basic choice between speakers and headphones, but recording of spatial sound requires specific equipment and experience, which makes its implementation in simulations generally more challenging.

Finally, a special note was mentioned regarding see-through displays. Although innovative from a product application point of view, see-through displays were rated as having low impact on simulation possibilities. This is because their simulation is straightforward and without major challenge. It is a case of an interactive technology being far easier to simulate digitally than realize materially in the real world.

## 4 Discussion, Conclusion and Future Work

The evaluation study was productive in surveying what is technically possible regarding the simulation of user-product interactions reliant on emerging interactive technologies. One challenge of the study was to concentrate experts on simulation possibilities other than VR. The majority of collaborating body's experience is in sectors where simulation is carried out using VR solutions. In product and automotive design, the potential for mixed and AR solutions has been repeatedly pointed out, being potentially easier to achieve, compatible as an additional 'layer' onto other modelling methods used in design (e.g. 3D mock-ups, 2D interface mock-ups) and more portable/flexible.

The study revealed a list of points to consider for setting-up a study to evaluate new interactive technologies, regarding their feasibility of simulation for product evaluation purposes. The preset criteria (suitability, availability, R&D) are interconnected. The evaluation of suitability to different levels of reality was made considering available hardware and software. Availability decisions are affected by the intended level of reality, since mimicking a technology in AR requires different equipment than VR, which may or may not be available locally or commercially. R&D evaluation is based not only on the availability of the hardware and software, but on the perceived investment of effort and resources to achieve a successful simulation. More precise follow-up evaluation for all three criteria must take into account contextual factors as follows.

- Details of the usage scenario (in which the interactive technology is applied):
  - the role of the technology (input, output etc.)
  - the properties of the product (mobile, fixed etc.)
  - length of interaction (immediate vs. long-term responses)
  - scenario details (the expected input and output details, user id, open scenario etc.)
  - context of use (daytime, nighttime, alone, collaborative, etc.)
- Level of required simulation precision, as defined by:
  - mapping (mapping visuals on a mobile or fixed element)
  - tracking (tracking one or multiple elements)
  - resolution (visuals on a small or large screen)
- Outside factors:
  - range of available equipment
  - experience level of the participants (participants specialized in VR might overlook or underestimate other options; aim for breadth in expertise)

The study has provided initial answers to the question: to simulate or not to simulate? To obtain results that look more deeply into the feasibility of simulating a particular interactive technology, the above listed points should be brought into the frame. All reality levels have their own challenges and opportunities. For example, mapping of simulations onto elements of the real world can be a challenge for mixed reality, but not for VR. On the other hand, tracking is a significant challenge for VR,


which can be overcome through the use of physical objects in mixed reality. Lastly, workshop participants assessed the impact of successfully simulating most of the shortlisted interactive technologies as medium-to-high. This provides evidence of a common point between communities interested in integrating new interactive technologies into automotive and product designs, and communities interested in simulating such technologies for evaluative and demonstrative purposes. The technologies mentioned in this paper can be rightly regarded as ‘hot topics’ for design and simulation research.

## References

1. Bau, O., Poupyrev, I., Israr, A., Harrison, C.: TeslaTouch: electrovibration for touch surfaces. In: Proceedings of the 23rd Annual ACM symposium on User Interface Software and Technology, UIST 2010, pp. 283–292. ACM, New York (2010)
2. De Amicis, R., Conti, G., Stork, A.: Future shape modelling scenarios. In: De Amicis, R., Conti, G. (eds.) *Future Vision and Trends on Shapes, Geometry and Algebra*, pp. 1–13. Springer, London (2014)
3. Impress - flexible display (2009). <http://www.silkehilsing.de/?projects=impress-flexible-display>. Accessed 30 May 2016
4. Jansen, Y., et al.: Opportunities and challenges for data physicalization. In: Proceedings of the 33rd Annual ACM Conference on Human Factors in Computing Systems, pp. 3227–3236. ACM, New York (2015)
5. Lawson, G., Salanitri, D., Waterfield, B.: VR processes in the automotive industry. In: Kurosu, M. (ed.) *Human-Computer Interaction: Users and Contexts*, pp. 208–217. Springer, Cham (2015)
6. Milleville-Pennel, I., Charron, C.: Driving for real or on a fixed-base simulator: is it so different? An explorative study. *Presence* **24**(1), 74–91 (2015)
7. Stewart, D.W., Shamdasani, P.N., Rook, D.W.: *Focus Groups: Theory and Practice*. SAGE Publications Ltd., Thousand Oaks (2007)
8. Stinson, L.: WIRED, 15 July 2013. <http://www.wired.com/2013/07/this-machine-is-a-camera-for-your-smell-memories/>. Accessed 22 May 2016



# Study on the On-line Support System for Welder

Satoru Asai<sup>1</sup>(✉) , Yosuke Ogino<sup>1</sup>, Kazufumi Nomura<sup>1</sup>,  
and Kazunori Hattori<sup>2</sup>

<sup>1</sup> Osaka University, 2-1, Yamadaoka, Suita, Osaka, Japan  
{asai,ogino,nomura}@mapse.eng.osaka-u.ac.jp

<sup>2</sup> Kuroki Kogyosho Co., Ltd., Kurate-cho, Kurate-gun, Fukuoka, Japan  
hatto@kuroki.co.jp

**Abstract.** In recent years, the shortage of experienced welder has become a problem. Therefore, we are developing online welder support system so that we can demonstrate the performance of experienced welder by providing information to non-skilled welder during welding. This system can be applied to the actual work of welding as well as training only. In this system, the prediction and optimization for welding condition is provided to the welder as acoustic, visual and haptic information during actual work by analyzing the measurement results of welder's behavior and welding condition with molten pool shape, etc. For data analysis, the prediction of penetration shape and optimization of torch movement can be also carried out using numerical simulation by mol-ten pool model. In this paper, in order to develop the on-line support system for welder, a basic investigation was carried out. As a result of the welder gaze measurement test using the smart glass with the proper filtering, it was confirmed that the eye tracking of the skilled welder was more stable than the non-skilled welder. Also, in the TIG manual welding, based on the measurement results of the torch movement by the camera for skilled welder and beginner, the situation of the backbead by numerical simulation was compared. The simulation results agree with the trend of actual welding. It was shown that the application of numerical simulation based molten pool model to simulation manual welding is effective.

**Keywords:** On-line support for welder · Welder behavior · Numerical simulation · Eye tracking · Visual information · Education of welder · TIG welding

## 1 Introduction

In recent years, in Japan, the shortage of skilled welder has become a social problem. Because of this, automatic welding systems using robots have been developed and advanced systems such as intelligent systems using sensors have been promoted.

However, it is difficult to replace all of the work of a skilled welder with the robot, and a lot of work still depend on the welder. Therefore, for the purpose of training welders efficiently, welding training systems have been developed [1], and recently, training systems utilizing virtual reality have been commercialized and applied to

training and education for the welder [2]. However, these systems are limited to the training of welders using simple test pieces, and there is a problem that they cannot be applied to complex welding training such as actual work. On the other hand, as typified by Industry4.0, IoT, which connects production devices to the Internet, analyzes information obtained from sensors and controls it optimally, is attracting attention as a manufacturing revolution [3]. The practical application of a system utilizing IoT is also expected for welding operations. With this background, we are promoting the development of an on-line welder support system so that the performance of a skilled welder can be exhibited by providing information to a non-skilled welder during welding. Here, this online welder support systems are presented and described.

## 2 Outline of Welder Support System

Figure 1 shows the configuration of the welder support system. This system is intended to be applied not only to welder’s education and training but also to actual welding work. In this system, the measurement results of the welder’s behavior, the information obtained from welding and the monitoring results of welding conditions and the condition of the molten pool, etc. can be utilized as the database.

Appropriate welding information is provided through the vision, the tactile sense and the hearing sense. Moreover, as data analysis, the optimization of welding behavior and prediction of the situation of penetration are also performed by using numerical simulation a molten pool model [4]. In tactile information presentation, when the torch motion is unstable, the correction can be automatically carried out by transmitting information through the glove. In visual information presentation, by superimposing a real space image and a virtual image in a mask, it becomes possible to stabilize welding and to control the arc condition more precisely from enlarged image of the molten pool. Also, in addition to the gaze measurement to evaluate where the welder is looking at the molten pool, the behavior of welders and the motion measurement, it will be possible to assess and manage the status of the welder from physical condition information such as blood pressure and pulse of welders.

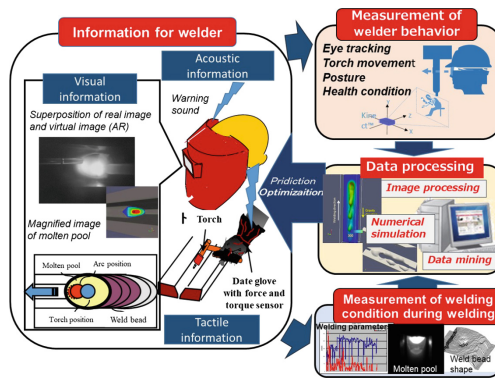


Fig. 1. Constitution of on-line support system for welder

### 3 Measurement Method of Welder Behavior

The measurement method of welder behavior is considered using many cameras as shown in Fig. 2 [5]. In the case of TIG welding, the measurement system is composed of four cameras, computer and display. As cameras, whole view camera for welder's positioning, a small CCD camera equipped to the welding torch for measuring torch movement, a CCD camera for measuring the filler rod feeding behavior and a CCD camera behind the base metal to measure back bead movement were basically used. In addition, CCD and CMOS cameras can be applied for acquisition the quality information. Then, it is possible to obtain a welder behavior as numerical data by image processing of the captured image as shown in Fig. 3. Weaving frequency, weaving width, wire feeding speed and the distance between electrode and tip of filler wire showing filler wire inset position are calculated with image processing of the acquired image using torch fixed CCD camera. Welding speed and molten pool area can be calculated by measuring the movement of back bead with image processing. These seven measuring items are used for analyzing as welder's skill index.

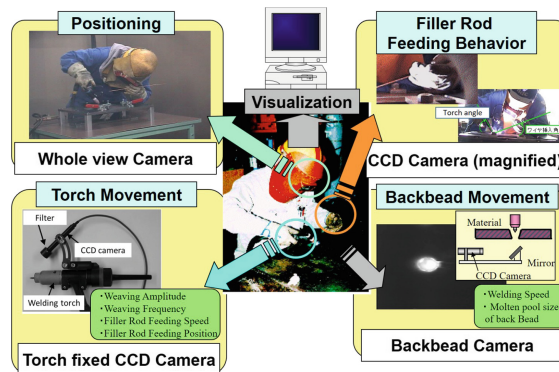


Fig. 2. Measurement system of welder behavior for TIG welding

Another important behavior of welders is gaze. In order to know which position of the molten pool the skilled welder sees, it is necessary to measure the gaze behavior quantitatively. Figure 4 shows a smart glass fitted with a band-pass filter and the ND filter to the scene camera in order to measure the gaze line of welder in the arc.

Figure 5 shows the measurement results of the gaze behavior with different skill levels welder during welding. While the line of sight of the skilled welder is stable and always fixed to the molten pool, beginners find that the fluctuation is large and the line of sight is not stable. Furthermore, it becomes possible to clarify the correlation of skill level and gaze information by molten pool position and time analysis.

As measurement method of welder's behavior, it is possible to measure the three-dimensional behavior of the torch by the acceleration sensor attached to the welding gloves. It is clear that differences in motion patterns due to differences in skill levels are visualized and that monitoring of motion patterns is possible.



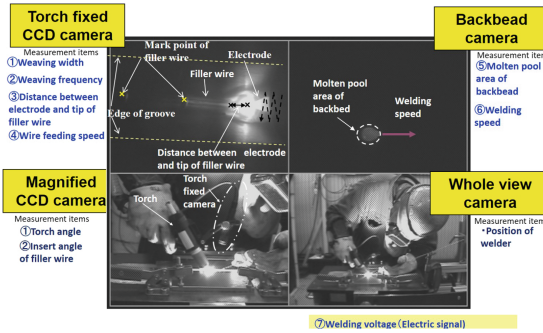


Fig. 3. Images of cameras and measurement items.

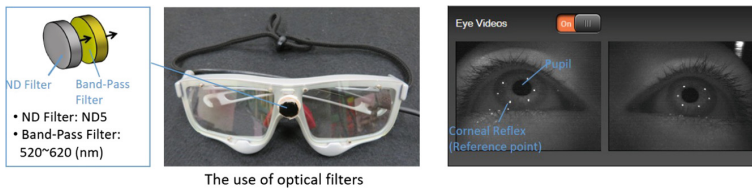


Fig. 4. Smart glass for measuring the gaze behavior of welder.

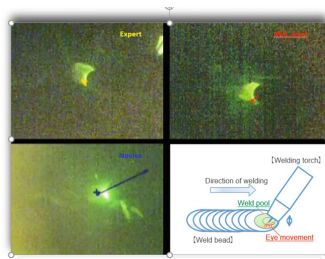
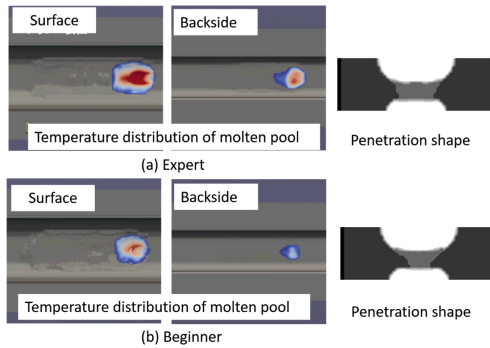


Fig. 5. Measurement results of the gaze behavior during welding

## 4 Analysis of Welder Behavior Using Numerical Simulation

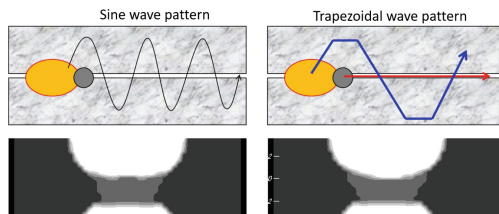
The prediction for the formation of the molten pool and the shape of the molten pool has been performed using numerical simulations with the molten pool formation model [6]. This three dimensional molten pool model considers the flow in the molten pool based on the governing equation and the surface deformation using the VOF method. In this model, a simplified heat source model with a Gaussian distribution as the heat input from the arc is used. Figure 6 shows the simulation results using this model based on the behavior measurement results of the welder as shown in Fig. 2. These shows the temperature distribution of the molten pool on the surface and the back side by comparison with the expert welder and the beginner. Also, the simulation results of

penetration shape are shown. By utilizing numerical simulation, it is possible to predict the molten pool formation conditions by differences of skill level.



**Fig. 6.** Analysis results of welder behavior using numerical simulation

Figure 7 shows the comparison of penetration shape by the difference of weaving pattern between sine wave and trapezoidal wave using numerical simulation. As described above, it is understood that it is possible to optimize the penetration shape and the rod motion pattern of the welder by simulating the characteristic behavior of the welder.



**Fig. 7.** Comparison of penetration shape by the difference of weaving patterns

The information of these simulation results as the database can be presented to a welder during welding in order to optimize the torch motion according to the change of root gap etc. Furthermore, it can be expected to expand the scope of application by improving the simulation accuracy.

## 5 Presentation Method of the Information to Welder

As a method of presenting information on behavior measurement results and numerical simulation results to a welder, there are acoustic presentation, tactile presentation, visual presentation. Acoustic presentation can be provided relatively easily by using a headphone. On the other hand, tactile sense presentation is considered to be applicable

to data glove with force and torque sensors for optimization of the torch motion. Most useful as information presentation is visual presentation, which can provide many informations. Figure 8 shows, a protective mask provided with an information presentation screen using a head mount display on the inner surface as an example of visual information presentation. The results of online analysis of molten pool measurement data from a small camera attached to the torch are presented on the screen, and the welder can perform appropriate welding by obtaining quality evaluation information such as the effectiveness of the motion and the soundness of penetration. Furthermore, by superimposing the real space image and the virtual image obtained from the simulation, it becomes possible to stabilize the welding and to control the arc state more precisely from the molten pool enlarged image. Thus, by presenting information on-line, it becomes possible to always support the welder, and it is considered that sound welding comparable to a skilled welder can be realized.

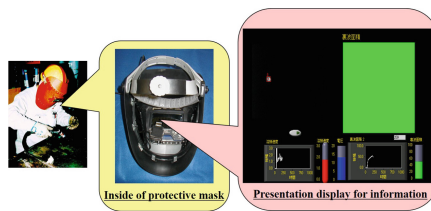


Fig. 8. Protective mask provided with an information presentation

## 6 Conclusion

Online welder support system that can demonstrate the performance of more skilled welders was proposed. In this system, the obtained information can be presented to the welder on-line as acoustic, visual and tactile information by utilizing behavior measurement and numerical simulation. The effectiveness of this system was shown by the example of the numerical simulation result based on the behavior measurement result. Also, visual information presentation in a protective mask is effective as an information presentation method, and further utilization can be expected in the future.


## References

1. IIW CommissionXIV Workshop success: Australasian Welding JactOURNA, vol. 59, Third Quarter (2014)
2. Byrd, A.P., Stone, R.T., Anderson, R.G., Woltjer, K.: The use of virtual welding simulators to evaluate experienced welders. *Weld. J.* **94**(12), 389–395 (2015)
3. Reinhart, G.: *Handbuch Industrie 4.0*. Carl Hanser Verlag (2017)
4. Ogino, Y., et al.: Numerical simulation of WAAM process by a GMAW weld pool model. *Weld. World* **62**, 393–401 (2018)

5. Asai, S., et al.: Visualization and digitization of welder skill for education and training. *Weld. World* **56**(9–10), 26–34 (2012)
6. Ogino, Y., Takabe, Y., Hirata, Y., Asai, S: Numerical model of weld pool phenomena with various joint geometries and welding positions. *Q. J. Jpn. Weld. Soc.* **35**(1), 13–20 (2017). (in Japanese)



# Development of a Supporting System of Pass Design in Multi-pass Welding Based on GMAW Weld Pool Simulation

Yosuke Ogino<sup>1</sup>(✉) , Toshihiro Fujiwara<sup>1</sup>, Satoru Asai<sup>1</sup>,  
Kosuke Tamura<sup>1</sup>, and Shin-ichi Sakamoto<sup>2</sup>

<sup>1</sup> Division of Materials and Manufacturing Science,  
Graduate School of Engineering, Osaka University, Suita, Japan  
{ogino, fujiwara, asai, tamura}@mapse.eng.osaka-u.ac.jp  
<sup>2</sup> Construction Technology Division, Shimizu Corporation, Tokyo, Japan  
saka\_s@shimz.co.jp

**Abstract.** The multi-pass welding process is an indispensable to build a large construction. An automated welding system by a welding robot is desired to realize a high-productive process. Normally, so many welding tests are carried out to determine the optimum welding condition. However, there are many disturbances in the manufacturing site, and the welding quality becomes worse even though the optimum condition is used. Therefore, to realize a high-productive automated welding system, a pass design system which can optimize and correct the welding condition depending on disturbances is required. In this study, a supporting system of pass design in multi-pass welding process is constructed by using numerical simulation of the weld pool.

In this study, the system is applied to the multi-pass groove welding in horizontal position. Weld pool simulation is carried out to obtain the relationship between the welding condition and shape of the weld bead, and make a database of the system. This system can show the optimum welding condition depending on the gap size between the base metals. In addition, the system can correct the welding condition pass by pass depending on the shape of the previous pass. Finally, this system is applied to the experiment and the weld region shows good quality so the gap can be filled without defect. Therefore, the system developed in this study can support to optimize and correct the welding condition depending on the disturbance.

**Keywords:** Multi-pass welding · Numerical simulation · Automated welding · Optimization of welding condition · Correction of welding condition

## 1 Introduction

Arc welding process is an indispensable technology in various fields of industry. For a large construction, the multi-pass welding process is carried out. In this process, welding is carried out on the welding bead until the gap between the base metals are filled out. In order to realize a high-productive process, an automated welding process by using a welding robot is desired. Normally, so many welding tests are carried out to

determine the optimum welding condition such as welding current, voltage, and welding speed. However, there are many disturbances such as the machining accuracy of the base metals, the wind and so on, in the actual manufacturing site, and the welding quality can become worse even though the optimum condition is used. Therefore, to realize a high-productive automated welding system, a pass design system which can optimize and correct the welding condition depending on disturbances is required. In this study, a supporting system of pass design in multi-pass welding process is constructed by using numerical simulation of the weld pool. By using a numerical model, time and costs of the testing before optimizing the welding condition can be reduced.

## 2 Simulation Model

The numerical model used in this study is constructed by authors' research group [1]. Schematic image of the model is shown in Fig. 1. Our numerical model focuses on the weld pool phenomena, and it includes the fluid flow in the molten metal region and surface deformation of the molten metal surface. The flow field in the molten metal region is calculated by following equations:

$$\begin{aligned} \nabla \cdot \vec{v} &= 0 \\ \frac{\partial \vec{v}}{\partial t} + \nabla \cdot (\vec{v}\vec{v}) &= -\frac{1}{\rho}\nabla P + \frac{1}{\rho}\nabla \cdot \boldsymbol{\tau} + \frac{1}{\rho}\vec{F}_{ex} + \vec{g} \end{aligned}$$

where,  $\vec{v}$  is the velocity,  $\rho$  is the density,  $P$  is the pressure,  $\boldsymbol{\tau}$  is the viscous stress tensor,  $\vec{F}_{ex}$  is the external force vector,  $\vec{g}$  is the gravitational acceleration. The surface tension and the arc pressure are considered as the external force in this model. The temperature field in the base metal is calculated by following equation:

$$\frac{\partial H}{\partial t} + \nabla \cdot (\vec{v}H) = -\frac{1}{\rho}\nabla \cdot (-\kappa\nabla T) + \frac{1}{\rho}W$$

where,  $H$  is the enthalpy,  $\kappa$  is the thermal conductivity,  $T$  is the temperature,  $W$  is the internal heat. In this model the internal heat is the heat input from the heat source. The free-surface of the molten metal is tracked by VOF method. In VOF method, the surface shape is expressed by occupancy of the calculation cell:

$$\frac{\partial F}{\partial t} + (\vec{v} \cdot \nabla)F = 0$$

where,  $F$  is the volume fraction of the metal in each calculation cell. These are the governing equations used in the model. Heat input on the surface and arc pressure are given by a simplified heat source model. As shown in Fig. 1, the heat input and arc pressure distributions are flat distribution in this study. The heat input amount, the heat input radius, the peak of the arc pressure, and the arc pressure radius are calculation

parameters to determine the shape of the heat source. The filler material provides on the base metal as molten metal droplet. The size and the temperature of the droplet are the also calculation parameters of the model. These calculation parameters depend on the welding conditions, such as welding current, and have to adjust to reproduce the experimental results.

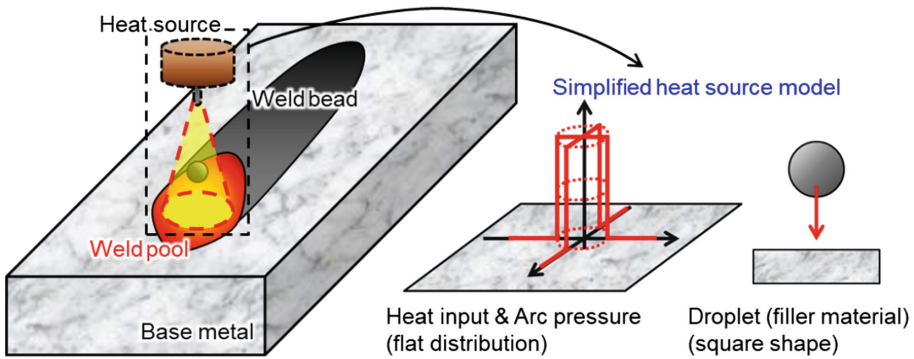


Fig. 1. A schematic image of the numerical model.

### 3 Supporting System of Pass Design in Multi-pass Welding

#### 3.1 Joint Geometry

In this study, the target is the multi-pass groove welding in horizontal position as shown in Fig. 2. This joint is frequently used in the box column of the large construction. The material is mild steel. Normally, this welding carried out by human welders, but an automated welding is strongly demanded. The gap between the base metals can be fluctuated in actual manufacturing site. In addition, the cross-section shape of the weld bead is not same even though the same welding condition is used. If the shape of a certain weld bead changes, the next bead shape also changes. In this study, the change of the gap and the weld bead are treated as the disturbance. In order to obtain the weld bead shape, a laser sensor is used in experiment in this study.

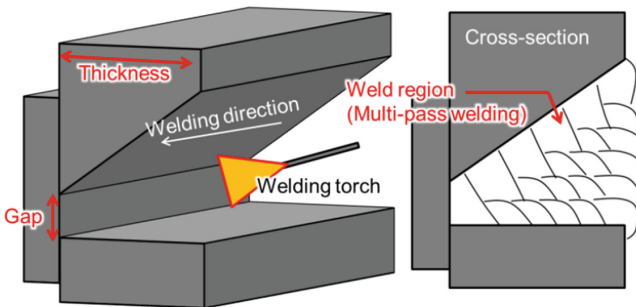
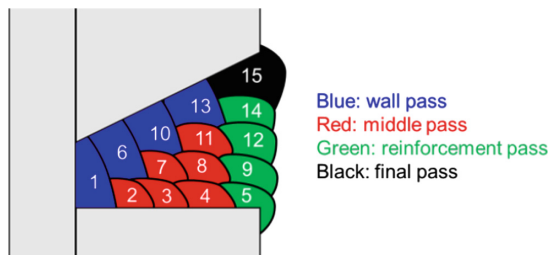


Fig. 2. Joint geometry used in this study.

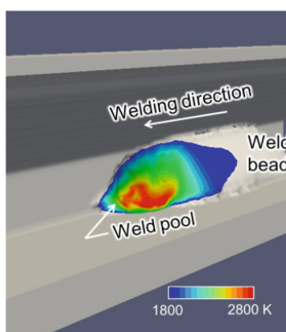
### 3.2 Database of the Supporting System

Firstly, we divide the welding pass into 4 patterns as shown in Fig. 3. The number in the figure is the order of the welding pass. As shown in this figure, the welding is carried out from the bottom side of the gap, and some weld bead become similar shapes. We carried out numerical simulation for each classified pass, and the relationship between the welding condition (the welding speed and the target position) and the weld bead shape are obtained. Here, some fundamental experiments are also carried out in order to adjust the calculation parameters and check the simulation results.



**Fig. 3.** Classification of the welding pass.

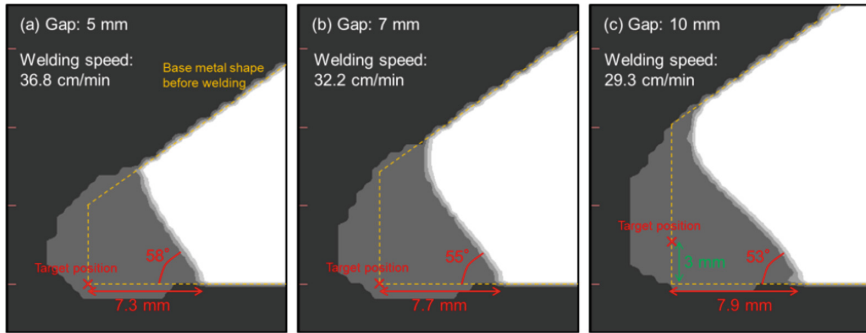
Figure 4 shows the examples of the calculation result. This figure shows the surface temperature distribution of the weld pool. Here, the first pass of the multi-pass welding shown in Fig. 3 is calculated. The gap between the base metals is set to be 7 mm, and welding speed is 32.2 cm/min. Figure 5 shows the calculation results of the cross-section shape of the weld bead when the gap between the base metals is changed. In this simulation, the welding speed and the target position are changed depending on the gap size. On the other hand, other parameters (heat input, feeding rate of filler material and so on) are same. As shown in this figure, the bottom width of the weld bead and the angle of the weld bead are relatively same values. Therefore, the weld bead shape can be controlled by changing the welding speed and the target position. However, of course, the bead shape is not same totally, the welding condition have to correct pass by pass.



**Fig. 4.** Example of the simulation result.



Numerical simulations for other passes are also carried out, and the relationship between the welding conditions and the weld bead shape is obtained.



**Fig. 5.** Cross-section shape of the weld bead with different gap size.

### 3.3 Schematic Diagram of the System

The supporting system of pass design which can determine the welding condition in multi-pass welding is constructed from the obtaining simulation results. By using the relationship between the welding condition and the weld bead shape, a program determining the welding condition from the weld bead shape is constructed. When the system is applied to the experiment, the welding condition is calculated from the bead shape obtained by the laser sensor pass by pass until the gap is filled out.

## 4 Application of the Supporting System

Then, the experimental results using the supporting system are shown. Figure 6 shows the weld bead shape obtained by experiment and the welding condition determined by the system. In this experiment, the thickness of the base metal is 28 mm, and the gap size is 7 mm. The gap between the base metals can be filled out without surface defect as shown in this figure. This result shows the constructed system can set the appropriate welding condition for multi-pass welding process.

Figure 7 shows the experimental result and welding condition in other condition. Here, the thickness of the base metal is 19 mm and the gap size is 9 mm. In this case, the number of the pass decreases due to the base metal thickness, and the welding condition is also changed depending on the gap. As shown, the gap between the base metals also can be filled out without surface defect, and the constructed system can set the appropriate welding condition depending on the base metal thickness and the gap.

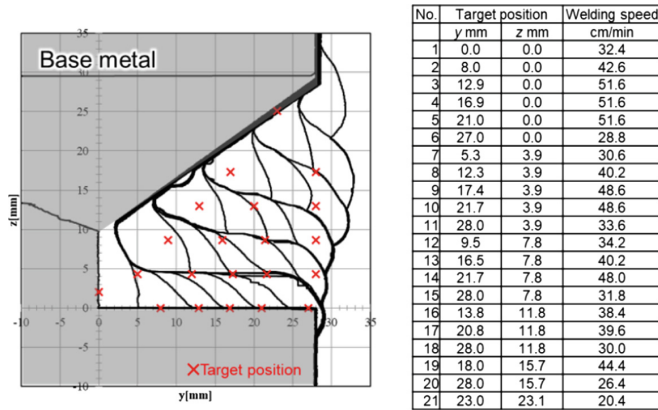


Fig. 6. Weld bead shape in experimental result and welding condition (28 mm, gap 7 mm).

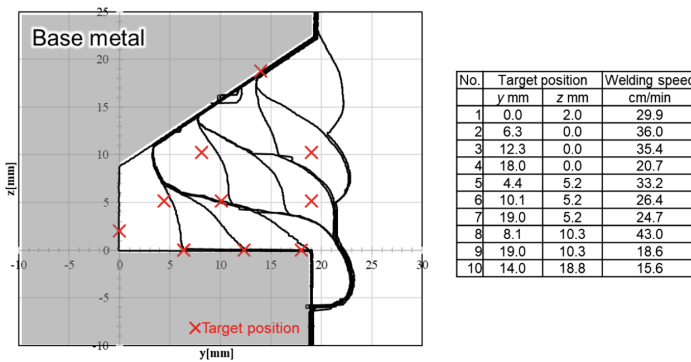


Fig. 7. Weld bead shape in experimental result and welding condition (19 mm, gap 9 mm).

## 5 Conclusion

In this study, a supporting system of pass design for multi-pass welding process is constructed. The relationship between the welding condition and the weld bead shape is obtained from the numerical simulation. The system was applied to the experiment, and the gap between the base metals can be filled out without the surface defect in for a few base metal conditions. Therefore, the system constructed in this study can determine the welding condition for multi-pass welding process depending on the base metal shape.

## Reference

1. Ogino, Y., Asai, S., Hirata, Y.: Numerical simulation of WAAM process by a GMAW weld pool model. *Weld. World* **62**, 393–401 (2018)



# Integration of BIM and Generative Design for Earthbag Projects

Deborah M. Santos<sup>1,2</sup>  and José Nuno Beirão<sup>2</sup> 

<sup>1</sup> Universidade Federal do Cariri, Av. Tenente Raimundo Rocha,  
Juazeiro do Norte, CE, Brazil  
deborah.santos@ufca.edu.br

<sup>2</sup> Faculdade de Arquitetura, CIAUD, Universidade de Lisboa,  
Rua Sá Nogueira, 1349-063 Lisbon, Portugal

**Abstract.** Although earthbag construction is recognizably a low environmental impact solution, existing software tools are limiting factors, since they do not have enough technical data to support its building information model. We propose a visual programming language code to generate earthbag domes inserted in a BIM environment, where these structures can be associated with other design and structural elements, producing the required technical data to inform construction including technical specifications as well as material and task quantification. This research adopted an experimental methodology exploring the advantages of the combination of Building Information modelling with parametric generative design in of the design of earthbag buildings or hybrid constructions involving earthbag walls of different geometries. It was validated resorting to a simulation process where it was possible to redesign and 3D print a scaled model of an existing earthbag building that merges different shapes in the same building, including the automated generation of the associated technical data. The developed tool allows designing different types of earthbag buildings providing a typical BIM model including both geometric model and technical specifications.

**Keywords:** Earthbag · Building Information Modelling (BIM) · Visual programming language

## 1 Introduction

This research adopts an experimental methodology, and addresses the advantages of combining a visual programming language (Grasshopper) with a BIM software (visualArq) to produce earthbag architectural designs.

In 1984, a new earth construction technique was created: the earthbag building. Also known as sandbag, superadobe or superblock technique, it consists in a construction system where the walls are essentially built by staking bags filled with inorganic soil and consolidating them with barbed wire between layers [1–5]. They are durable, strong and climatically efficient. They are more advantageous than other earth building techniques because they do not require formwork, are capable of organic forms, are more resistant in earthquake-prone zones, benefit from lower maintenance

and construction time and are self-supporting up to double storey typologies. This technique is also faster to build than most of other earth construction techniques.

The material of earthbag buildings are almost all natural (earth, clay, water). If a construction becomes obsolete, those materials can return to nature or even be reused to build up another building, guaranteeing a sustainable cycle. The earthbag constructions fill also resilient design principles. Resilience, in context of engineering design, is defined as the ability to provide required capability in the face of adversity, like natural disasters [6]. The earthbag building it is statically strong, durable, and safe even to extraordinary climate conditions and natural calamities like earthquake, flood, wind-storm, storm, and fire [7, 8].

Although earth construction methods are low environmental impact solutions [9–11], existing software tools continue to be limiting factors regarding this type of project and specifically regarding earthbag construction. CICERO (Creative Interface for Constructing Earthbag Resource Objects), is a specific tool developed to generate the volumetric virtual model of earthbag dome shapes, recently created and presented during the conference Sigradi 2017 [12, 13]. However, it is an incomplete tool since earthbag constructions allow the production of other morphological types than domes, namely, compound forms of construction involving several techniques and especially other shapes than domes. Furthermore, the volumetric shape, as was presented in the mentioned article, is not enough to produce all construction documents that should include plans, sections, elevations together with the necessary construction technical specifications, specifically, material descriptions and quantifications required for planning the construction procedures and producing the required and desired qualitative results.

This paper presents the evolution of what was presented at Sigradi 2017, and addresses the last part of a larger research proposing an alternative approach to produce earthbag designs, based on the use of an algorithmic (parametric) approach associated with a building information modeling (BIM) environment.

BIM software can work together with programming languages (scripting or visual) to create generative, parametric models. Since CICERO was previous developed in Grasshopper visual programming language, the BIM environment studied here was visualArq because their integration is already provided by the same supplier.

This research is a part of a larger investigation that encompasses the following steps: 1-Developing a constructive classification of earthbag buildings [14]; 2-Understanding the logic of visual and textual programming languages to define the parametric approach of the experiment [15]; 3-Developing a parametric experiment to support architectural design decision of earthbag building domes using CICERO tool [12, 16]; 4-Presenting a bibliometric analysis that approaches the combination of descriptors BIM and sustainability, concluding that there is no published work involving the development of BIM tools for earthbag construction techniques; 5-Developing a computational experiment, to propose a visual programming language code to generate hybrid earthbag designs including earthbag domes and walls, as an interface to obtain a BIM model of the design.

This paper is focused on step 5. The goal is the improvement of the CICERO tool, integrating the parametric tool in a BIM environment to generate different types of earthbag designs.

## 2 Development

As previously referred earthbag walls are built by staking bags filled with inorganic soil and consolidated with barbed wire between layers. The so called inorganic soiled might be composed by specific amounts of earth (taken from local ground), clay, sand, water, all mixed in proportions capable of producing a stable and durable wall. This wall can be finished with a plaster coating reinforced with the application of chicken fence wire or similar reinforcement. Hence, a BIM technical description of such a wall should be able to provide quantitative descriptions of all the needed materials (1) and respective technical prescriptions describing the details and procedures for the production requirements (2).

### 2.1 Needed Material

The needed materials requiring quantitative calculation from the BIM model are:

Quantity of the compound mixture of earth (taken from local ground), clay, sand and water. This quantity is taken from the geometric model of the wall considering its volume and calculates the amount of each material considering (a) the proportion of each element in the mixture and (b) the increase in volume due to the difference of the materials in supply format (loose) or in the finished compacted form.

Quantity of bags. This quantity takes a bag section based on the wall thickness and calculates (1) the number of layers; (2) a theoretical length per bag (a manageable bag length for manual construction procedures; (3) the amount of extra bag length taken to provide bag closure at each bag's extremes.

Total length of barbed wire considering the application of two parallel threads between layers.

Total surface to plaster. This value is taken to calculate the amounts of materials composing the finishing plaster coating and the surface of chicken fence wire needed to reinforce the plaster. Considering the desired sustainability of the construction we assume the plaster coating to be of a traditional nature, excluding cement as principle, and involving the addition of lime to develop a strong protective and resistant coating. Amounts of chicken wire are given as surface with a 10% increase for overlaps, and plaster coating are given considering (a) the proportion of each element in the mixture and (b) the increase in volume due to the difference of the materials in supply format (loose) or in the finished plastered form.

### 2.2 Technical Prescriptions

Most of the desired technical data for earthbag walls, was generated automatically by VisualArq. Such as style, length, thickness, area (that was renamed as surface area), and volume (that was renamed as volume of compacted earth). However, there was still missing information such as: number of bag layers, barbed wire and bags.

The logic to calculate the layers is based on Hunter and Kiffmeyer empirical studies [17]. They assume that bag layers can variate according to the tamping process and under layers can flatten down after conclusion of higher layers. According to their observation the average measurement is 10 cm, then, for representations and calculus purposes it should be considered a height of 10 cm for each layer.

Because bags are built in rows, the calculus is made in meters measuring the length of the rows. The logic to calculate the total amount of bags is to extract from the model the length of all bag layers, adding at least 20 cm of loose material, for each cut, to tie off the ends [17, 18].

The barbed wire, combined with the woven fabric of the bags, adds a high tensile strength to the wall structure. Some authors point that this application should be made in two parallel threads of 4-point barbed wire for each layer [4, 5, 17, 19]. This premise is put into the calculation of the total barbed wire length.

### 2.3 Inserting the New Material

It is relatively easy to insert a new material in a BIM platform, because they are equipped with user-friendly interfaces to do it. There is a Wall style dialog box (command: `_vaWallStyles`) in VisualArq, where it is possible create a new type of wall, with a new material using the available new style button. Unfortunately, the interface still has some limitations regarding the addition of new variable parameters in materials. For now, it is possible to add just static new parameters. Consulting the assistance, it was said that it is in their plans offer a way to add calculated values in future VisualArq versions. For this new wall style, it was possible to include the following parameters: quantity, style, length, area, wall height and volume. It was expected to include also: layers quantities, barbed wire, bags and surface area. We could include this after the modeling process with the use of the visual programming language, Grasshopper, where this information was calculated following the mathematical model described above and published in our previous paper [12].

In order to transform the parametric dome generated with CICERO into a VisualArq wall, the Grasshopper component for “wallSolid” VisualArq command was added to the CICERO code. This component converts Breps (Boundary representations) into VisualArq walls. In the CICERO tool, the user has just to change the parameters until s/he gets the desired shape. When the parameter is changed, the preview of the model and respective technical data appears in Rhinoceros/VisualArq. After deciding the desired parameters to insert the dome wall, the “bake” command in the wallSolid box is used so that the following design steps may occur in the BIM environment. It might be necessary to have a solid loft dome, with the same dimensions of the walldome, to subtract from the linear earthbag walls generated in the visualArq interface resorting to a typical wall object. This is just an auxiliary process used in the generation of the intersection of the dome with the remaining earthbag walls of the design.

At this time, the only way to insert the desired missing technical data is using Grasshopper. In Grasshopper, it is possible to create a custom parameter and assign a value to the objects, as generated by the software according to the mathematical model calculating materials’ quantities.

After modeling the whole building, the user needs to import the visualArq/Rhinoceros walls into the Grasshopper code, and use the command “bake” in the “setProperty” box. By doing this, the system sends the same walls to VisualArq/Rhinoceros including the technical data that would be missing without following this step.

### 3 Results and Validation

The research resulted in a BIM tool that works using a platform composed of Rhinoceros, plus grasshopper (Visual programming language environment), and VisualArq (BIM plugin of Rhinoceros). In the next paragraphs it is briefly explained how to design earthbag projects with these tools and for the validation process we used a specific earthbag building to check its workability and capacity of generating earthbag designs with compound construction technologies and earthbag wall shapes.

#### 3.1 Procedure to Design Earthbag Projects with Parametric Dome in BIM

The logic to design earthbag buildings in this improved CICERO tool is: first, generate the earthbag domes and solid domes (for subtraction purposes) by changing the numerical parameters in Grasshopper; second, export (using the bake command) to VisualArq, and there insert, the other walls, doors, windows roof, beams, etc.; third, go back to Grasshopper to calculate the missing documentation aspects (those missing in VisualArq); fourth, after the calculation of the new properties, import to VisualArq all the documentation, generate the tables and blueprints (Fig. 1).

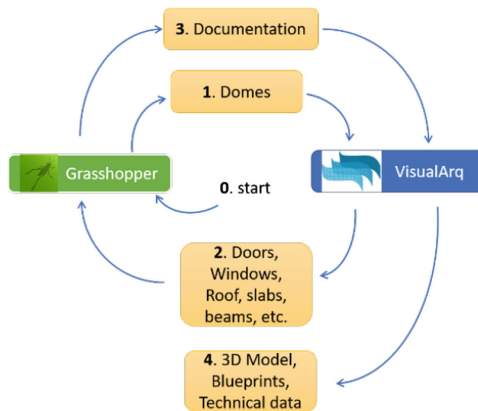
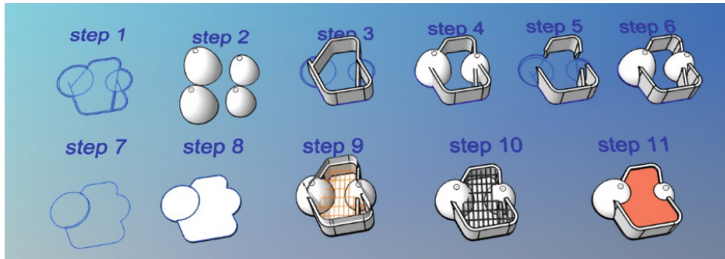


Fig. 1. Logic to design earthbag buildings

#### 3.2 Validation Through Simulation Process

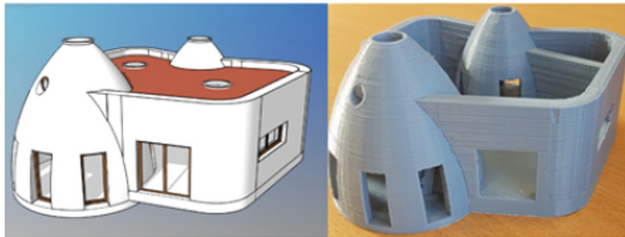
The chosen model for the study case validation was “La casa Vergara”, designed by the architect Andreas Vallejo, and built in Sopó, Cundinamarca, Colômbia in 2011. The project presents 85m<sup>2</sup>, as a self-supporting earthbag linear wall structure and two earthbag domes [20]. Blueprints, pictures of construction and of the building can be easily found in the architect’s personal website [21]. This house was chosen because it is composed by all elements that we wanted to proof to be able to design, in other words, a design with a compound set of construction technologies and several earthbag wall shapes including the dome.

The procedures to model this house are presented in eleven steps in Fig. 2, and include designing the walls, slab, beams and roof, and openings. For each step it was necessary to solve some issues, described in the following sections.



**Fig. 2.** Steps to model “la casa Vergara

The simulation process led us to a final 3D model (Fig. 3) of “La casa Vergara”. It was possible to generate the two domes quickly, by just changing the parameters. It was also straightforward, the process to insert the domes into the BIM software environment. The other walls were generated using the “earthbag wall” material, created for this purpose. In general, the results were quite similar to the existent building.



**Fig. 3.** Final model simulation of “La casa Vergara”. 3D printed model using a FDM printer with PLA filament.

To help the comparative process, it was also made a 3Dprinted scale model (Fig. 3). Many authors wrote about the good impact of elaborating a physical model of the design for the evaluation process, specifically using rapid prototyping [22].

Once the BIM model is done (with associated quantitative data), it was easy to make scaled models through 3D printing and use them in a normal exploratory design process.



## 4 Discussions

With the developed CICERO code and new BIM material, it is possible to design various types of earthbag projects. The proposed interface is able to design earthbag buildings resorting to hybrid construction technologies involving earthbag walls of different shapes including domes. The tool was developed with Grasshopper (visual programming language) and VisualArq components (BIM). After creating the tool, the whole process was tested with an existing case, to check whether the design model could design the features of the real one, with satisfactory results.

Using CICERO, one can quickly generate an earthbag dome by changing some numeric inputs; CICERO constrains results to all the dome known rules pre-defined in the code. The dome models work fine in VisualArq environment, and they can receive the openings using the standard or customized BIM library. A special attention was required to apply the doors and windows in the domes, though. As the domes were generated as “wallSolid”, it was necessary to edit all the numerical data of their cut depth. Otherwise, the software would produce holes in the wall behind.

It was possible to assemble orthogonal walls with the domes, however some more steps were needed than we were expecting. The adopted method was to generate auxiliary dome solids, in addition to the dome walls (step 2, Fig. 2) and subtract its volume from the intersecting walls (steps 4 and 5, Fig. 2). The wall domes were then added (step 6, Fig. 2).

The main contribution was to add technical data regarding the construction of earthbag walls which is produced while modeling the building. This technical data is specific of earthbag construction and constitutes an extension of BIM objects and BIM technical data.

**Funding.** This work was supported by the CNPQ (Brazilian National Council for Scientific and Technological Development) under grant 201904/2015-2.

## References

1. Khalili, E.N. Emergency sandbag shelter (train. 13–14)
2. Geiger, O., Zemskova, K.: Earthbag technology - simple, safe and sustainable. *NEA Technical J.* **XLIII**, 78–90 (2015)
3. Minke, G.: Construction manual for earthquake-resistant houses built of earth (2001)
4. Hart, K.: Earthbag architecture. Hartworks, Lexington (2015). ISBN 9780916289409
5. Wojciechowska, P.: Building with Earth: A Guide to Flexible-form Earthbag Construction. Chelsea Green Publishing Co, White River Junction, United States (2001). ISBN 1890132810
6. Jackson, S.: Principles for resilient design. In: Linkov, I. (ed.) IRGC Resource Guide on Resilience. International Risk Governance Center (2016)

7. Kamal, R., Rahman, S.: A study on feasibility of super adobe technology – an energy efficient building system using natural resources in Bangladesh A study on feasibility of super adobe technology – an energy efficient building system using natural resources in Bangladesh. In: Bui, Q.-B., Cajka, R., Tran, M.-T., Yasar, T.-A., Trinh, A.-U.-H., Wets, G., Woloszyn, M. (eds.) Proceedings of the IOP Conference Series: Earth and Environmental Science, p. 012043. IOPscience, Vietnam (2018)
8. Ross, B.E., Willis, M., Datin, P., Scott, R.: Wind load test of earthbag wall. *Buildings* **3**, 532–544 (2013)
9. Morel, J.C., Mesbah, A., Oggero, M., Walker, P.: Building houses with local materials: Means to drastically reduce the environmental impact of construction. *Build. Environ.* **36**, 1119–1126 (2001)
10. Kumar, R., Sachdeva, S., Kaushik, S.C.: Dynamic earth-contact building: a sustainable low-energy technology. *Build. Environ.* **42**, 2450–2460 (2007)
11. Husain, S.F. Superadobe technology and building systems – a review. In: Proceedings of the International Symposium on Earthen Structures (2018)
12. Santos, D.M., Beirão, J.N.: Generative tool to support architectural design decision of earthbag building domes. In: Proceedings of the SIGraDi 2017, XXI Congreso de la Sociedad Ibero-americana de Gráfica Digital. Blucher, São Paulo, pp. 538–543 (2017)
13. dos Santos, D.M., Beirão, J.N.: CICERO. [www.cicero.earth](http://www.cicero.earth)
14. Santos, D.M., Beirão, J.N.D.C.: Data collection and constructive classification of superadobe buildings. *Rev. Ciência e Sustentabilidade* **2**, 208–226 (2016)
15. Santos, D.M., Pontes, T.B., Leitão, A.M.: Generative design in textual and visual programming languages. In: de Lima, F.T., Borges, M.M., Costa, C.F.R. (eds.) *Digital Techniques Applied to Design Process*, pp. 72–95
16. dos Santos, D.M., Beirão, J.N.: Parametrical design tool and the production of technical data for superadobe domes. *Gestão Tecnol. Proj.* **33**
17. Hunter, K., Kiffmeyer, D.: *Earthbag Building: The Tools, Tricks and Techniques*. New society publishers, Gabriola Island, Canada (2004). ISBN 0865715076
18. Hart, K.: *Earthbag the Complete Step-by-Step Guide*. Magwood, C., Feigin, J. (eds.), 1st edn, New society publishers: Canada (2018). ISBN 978-1-55092-656-9
19. Geiger, O.: *Earthbag building guide; Excellence in natural building series* (2011). ISBN 978-6169093008
20. Vallejo, J.A.: Casa Vergara: Un proyecto de exploración de materiales. *Exkema* **3**, 38–41 (2011)
21. Vallejo, J.A.: Casa Vergara
22. Groat, L.N., Wang, D.: *Architectural Research Methods*. Wiley, New Jersey (2013). ISBN 978-0-470-90855-6



# Potential of Natural Ventilation and Vegetation for Achieving Low-Energy Tall Buildings in Tropical Climate: An Overview

Humera Mughal<sup>1,2</sup>  and José Nuno Beirão<sup>1</sup> 

<sup>1</sup> University of Lisbon, R. Sá Nogueira, 1349-063 Lisbon, Portugal  
humera.mughal@unipa.it, jnb@fa.ulisboa.pt

<sup>2</sup> Palermo University, Piazza Marina, 61, 90133 Palermo, PA, Italy

**Abstract.** Climate change and rise in urban temperatures have further increased the cooling load demands for tall buildings located in hot climatic regions. Cooling loads in tall buildings can be reduced by integrating them with natural ventilation (NV) and building integrated vegetation (BIV) techniques. This study explores the potential of NV and BIV for obtaining low-energy buildings by analyzing ten tall buildings as case studies. Buildings are analyzed for NV, BIV, architecture design parameters, and energy savings. The results show that mixed-mode ventilation is the most commonly employed, and circular building plans have the highest potential for energy savings. Furthermore, the combination of NV with sky-gardens (BIV type) is the best strategy for achieving low-energy tall buildings in the tropical climate. The outcomes show that the application of well-researched building physics rules is in practice for making energy-efficient tall building. These findings may be helpful for designers and planners to develop further strategies and low-cost methods aiming at the development of more sustainable and healthier tall buildings.

**Keywords:** Tall buildings · Ventilation · Vegetation

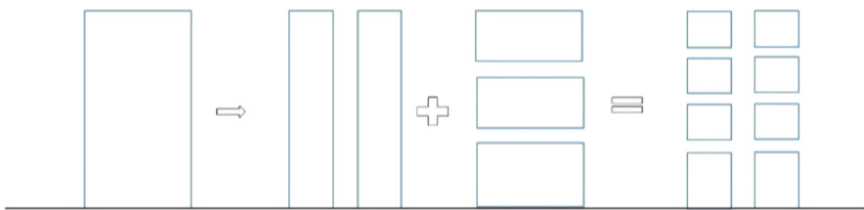
## 1 Introduction

The need of vertical construction due to too rapid urbanization and population rise has led to an increase in the energy use of buildings and higher carbon emissions [1]. Tall buildings are often seen as a viable solution to the increasing demand of construction and as a mean of reducing needs of urban transportation. Despite the advantages associated with tall buildings the higher urban intensity and height of tall building increase the urban heat island (UHI) effect [2]. The UHI effect refers to a higher ambient temperatures that forms in dense urban zones compared to the surrounding suburban or rural areas [3]. This rise in temperature is due to the accumulation of energy in the built surfaces together with the effects caused by sun-light reflection produced by the glazed facades. UHI is especially important for tall buildings situated in hot climatic regions where the interaction of increased outdoor temperatures with high surface areas of building facades results in an increased cooling load demand [4].

Tall buildings are often operated on mechanical systems that are known to be high energy consumers and if not properly managed can result in harmful health impacts on building users [5]. These problems can be solved through the application of sustainable and passive strategies in the design of buildings. Among the various possible sustainable strategies for space design, the application of natural ventilation (NV) can be used for obtaining low-energy healthy buildings [6]. The use of NV in tall buildings is a complex process due to variabilities associated with wind speeds and direction and outdoor urban air quality [5]. Mixed mode systems are often seen as a good replacement of NV and can be used during the time when NV system is ineffective [7]. Building integrated vegetation (BIV) can also improve the effectiveness of NV in tall buildings in addition to improving indoor air quality and buildings ecological footprint [8]. BIV can also help in improving psychological health of users and the system can help meet cooling load demands. It is necessary to develop a proper understanding of energy reduction potential of NV and BIV individually and in combination so that low-energy tall buildings are possible.

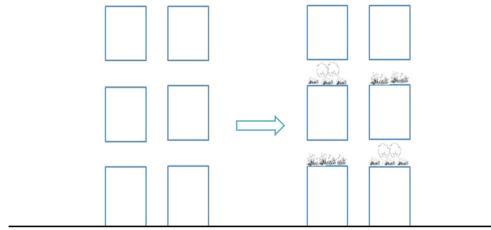
The various factors that can help improving the effectiveness of NV in tall buildings are:

- Building shape/form with least value of drag coefficient. Oval and circular shapes are found to have the least values of drag coefficient and are found to be the best building forms in terms of floor plan for the effectiveness of NV [9]. More over façade pressure is distributed evenly on the façade if building form is twisted and circular [10].
- Since NV requires airflow through the building more permeability along the building façade might bring better results in terms of effectiveness of NV, so the whole buildings can be divided into several parts separated through open spaces. Introduction of this concept is called segmentation that plays a major role where the vertical continuity of the building is broken [11] (Fig. 1).



**Fig. 1.** Integration of segmentation in tall buildings (left to right)

- Furthermore, it has been found that among the various types of BIV systems, incorporating Sky Gardens into the segmentation are found to be a feature, that not only cools down the ambient air coming inside the building but also increases the wind speed by max of 10 m/s affecting NV phenomenon positively [12] (Fig. 2).

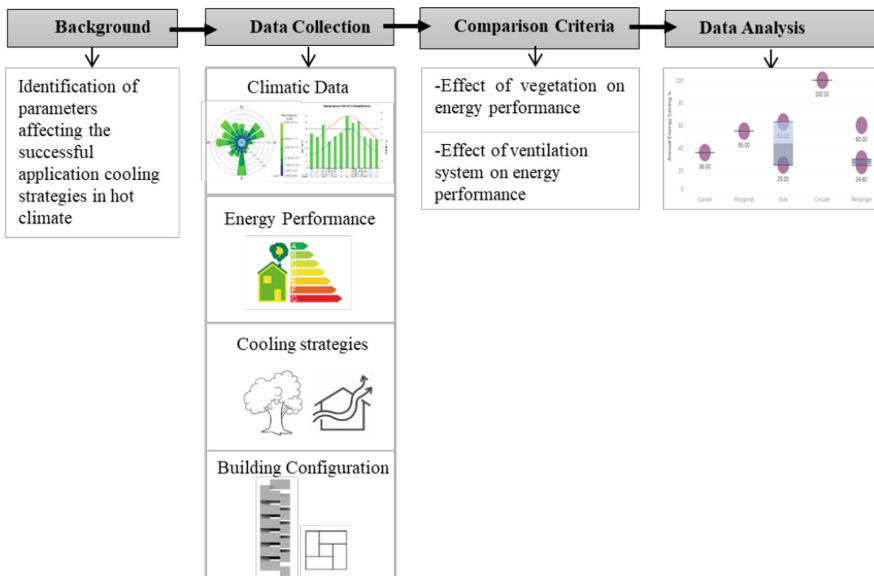


**Fig. 2.** Incorporation of sky gardens in segmentation of tall building

This study developed a data analysis of 10 tall buildings using NV and integrated BIV as cooling techniques. The results from this preliminary study may provide guidelines for designers and planners to improve the development of low-energy and healthier tall buildings. It will also provide an insight into the practical application of already explored factors for improving energy consumption using these strategies.

## 2 Methodology

The main goal of this research is to determine the potential of NV and BIV techniques in reducing the energy consumption in tall buildings located in tropical climates and their adaptation in design. The research followed a three-phase methodology for case studies explained below and shown in Fig. 3.



**Fig. 3.** Research methodology

- Case study Selection: buildings were selected for meeting three criteria: (a) Use: Residential or commercial; (b) Location: Tropical Climate and (c) Cooling Technique: NV and/or BIV
- Comparison Criteria: Keeping the climate data as a constant parameter the case studies were compared based on the type of ventilation system (active or passive), presence of BIV and configuration, correlating these features with the amount of energy saved due to the presence of these cooling systems.
- Results and Discussions: Results obtained from the comparison phase were analysed to determine the application of most important parameters needed to achieve lower energy consumption in tall buildings located in a tropical climate.

### 3 Results and Discussion
























































The data for the case studies has been collected from the building designers' websites and research articles on the same buildings. The list of case study buildings is shown in Table 1 while the strategies and the associated energy saved is provided in Table 2. A total of 10 tall buildings present in Tropical climatic regions were selected. Most buildings were used either as offices or as residential apartments.

**Table 1.** Case study buildings

No.	Name of building	Usage	City	Country	Plan shape	Annual energy saving (%)
1	Menara Umno	Office	Penang	Malaysia	Oval	25
2	Torre Cube	Office	Guadalajara	Mexico	Circular	100
3	1 Bligh Street	Office	Sydney	Australia	Oval	63
4	Capitagreen	Office	Singapore	Singapore	Rectangle	30
5	One Central Park	Mixed-Use	Sydney	Australia	Rectangle	26
6	Skyville@Dawson	Residential	Singapore	Singapore	Polygonal	55
7	Skyterrace@Dawson	Residential	Singapore	Singapore	Rectangle	24.6
8	Magic Breeze Sky Villas	Residential	Hyderabad	India	Rectangle	60
9	Solaris	Office	Singapore	Singapore	Curved	36
10	Parkroyal On Pickering	Office	Singapore	Singapore	Rectangle	30

Table 1 shows that most tall buildings are designed to use a mixed mode system as the main ventilation system while cross ventilation seems to be the most efficient type of NV for tall buildings in tropical and subtropical climate. Most effective external building form/shape for effective air flow rate in tall buildings is the circular form that can lead to least cooling load i.e. Torre Cube. 5 out of 10 buildings are using vegetated terraces/balconies and NV as cooling strategies and 4 are using Sky-Gardens and NV and the best result is seen in the latter case.

**Table 2.** Case studies used for the research (Where :<sup>1</sup>NV = Natural Ventilation; <sup>2</sup>BIV; Vegetation; <sup>b</sup>Natural Ventilation; <sup>c</sup>Mechanical Ventilation; <sup>d</sup>Mixed Mode Ventilation System; <sup>e</sup>Single sided Ventilation; <sup>f</sup>Cross Ventilation; <sup>g</sup>Stack effect; <sup>h</sup>Green Wall; <sup>i</sup>Sky-Garden; <sup>j</sup>Green Terrace/Balconies; <sup>k</sup>Green Roof)

No.	Segmentation	Ventilation type			NV type <sup>1</sup>			BIV type <sup>2</sup>				Ref.
												
1												[13]
2												[14]
3												[15]
4												[16]
5												[17]
6												[18]
7												[19]
8												[20]
9												[21]
10												[22]

In short, the combined effect of NV and SG on energy saving of tall buildings in tropical/subtropical climate is showing combination is sky-gardens and NV as most suitable as it offers the maximum reduction in cooling load that can reach to zero. There is not much difference in the design of residential and office buildings with reference to these strategies (i.e. NV & BIV), however use of vegetative balconies/terrace seem more popular for residential buildings as compared to office buildings.

## 4 Conclusions

The two main lessons learned from this study are:

- Building form/shape has a great impact on energy savings through NV and the best building shapes for this purpose seem to be twisted oval and circular form and it is being implemented in the design of tall buildings in tropical climate i.e. Torre Cube, 1 Bligh street, Solaris.
- Sky/Gardens help accelerating the wind speed causing effective air flow through the buildings and provides better psychological situation for the users at top floors. The best practical application of this strategy is found be Torre Cube building with 100% annual energy saving. All the buildings with Sky gardens are using segmentation concept as well.

This study observed the building physics’ rules regarding the implementation of NV and BIV as cooling strategies considered for the practical implementation in the design of tall buildings. However, each building has a different urban context so a real comparison cannot be made for having a best solution. i.e. Oval/circular and twisted

building form may not always be the best option for all types of urban context. Furthermore, by studying each case with its own context can give a glimpse into how a better solution can be developed using the same strategies. These generic strategies might be used by designers at early design stages as rules of thumb to follow. Based on these conclusions from case studies data analysis building models can be developed to further simulate the effect of different parameters and design variables on energy performance of multistory buildings.

## References

1. Safarik, D., Ursini, S., Wood, A.: Megacities and tall buildings: symbiosis. In: E3S Web Conference 2018, vol. 33, p. 01001 (2018)
2. Santamouris, M., Asimakopoulos, D.N.: Energy and climate in the urban built environment. James X James (2001)
3. Santamouris, M., Kolokotsa, D.: Urban Climate Mitigation Techniques. Routledge (2016)
4. Godoy-Shimizu, D., et al.: Energy use and height in office buildings. *Build. Res. Inf.* **46**(8) (2018)
5. Aslan, G., Sev, A.: Natural Ventilation for the sustainable tall office buildings of the future. *Int. J. Civil Environ. Struct. Constr. Archit. Eng.* **8**(8) (2014)
6. Oldfield, P., Trabucco, D., Wood, A.: Five energy generations of tall buildings: an historical analysis of energy consumption in high-rise buildings. *J. Arch.* **14**(5), 591–613 (2009)
7. Al-Kodmany, K.: New Suburbanism: Sustainable Tall Building Development. Routledge (2016)
8. Raji, B., Tenpierik, M.J., van den Dobbelsteen, A.: The impact of greening systems on building energy performance: a literature review. *Renew. Sustain. Energy Rev.* **45**, 610–623 (2015)
9. Elshaer, A., Bitsuamlak, G., El Damatty, A.: Aerodynamic shape optimization for corners of tall buildings using CFD. In: 4th International Conference on Wind Engineering (2015)
10. Wang, B., Malkawi, A.: Genetic algorithm-based building form optimization study for natural ventilation potential. In: BS2015: 14th Conference of International Building Performance Simulation Association (2015)
11. Etheridge, D.W., Ford, B.: Natural ventilation of tall buildings—options and limitations. In: CTBUH 8th World Congress (2008)
12. Mohammadi, M., Calautit, J.K.: Numerical investigation of the wind and thermal conditions in sky gardens in high-rise buildings. *Energies* **12**(7), 1380 (2019)
13. Ismail, L.H.: An Evaluation of Bioclimatic Skyscrapers in a Tropical Climate: Energy Audit and User's Satisfaction in Selected Office Buildings in Malaysia. University of Liverpool, United Kingdom (2016)
14. e-architect. <https://www.e-architect.co.uk/mexico/cube-tower-guadalajara>. Accessed 19 June 2019
15. Lochhead, H., Oldfield, P., Lochhead, D.H.: The role of design competitions in shaping sydney's public realm architecture/design. *CTBUH* **4** (2017)
16. Parakh, J.: The space between: urban spaces surrounding tall buildings. *CTBUH*, 184–191 (2016)
17. Wood, A., Bahrami, P., Safarik, D.: Green Walls in High-Rise Buildings: An Output of the CTBUH Sustainability Working Group (2014)



18. Samant, S., Menon, S.: Exploring new paradigms in high-density vertical hybrids high-rise buildings exploring new paradigms in high-density vertical hybrids. *Int. J. High-Rise Build.* 7(2), 111–125 (2018)
19. CTBUH. <http://www.skyscrapercenter.com/building/skyterrace-dawson-block-91/19968>. Accessed 21 June 2019
20. Aasarchitecture. <https://aasarchitecture.com/2016/07/magic-breeze-sky-villas-penda.html>. Accessed 06 June 2019
21. Yeang, K.: *The green skyscraper: the basis for designing sustainable intensive buildings*. Prestel (1999)
22. de-zeen. <https://www.dezeen.com/2013/10/10/parkroyal-on-pickering-by-woha/>. Accessed 19 June 2019

**Design**



# Improve Engineering Skills in Digital Manufacturing for New Products

C. Relvas<sup>(iD)</sup> and A. Ramos<sup>(✉)</sup><sup>(iD)</sup>

Department of Mechanical Engineering, Centre for Mechanical Technology and Automation, University of Aveiro, Aveiro, Portugal  
a.ramos@ua.pt

**Abstract.** The 3D printing technologies has changed the reality of manufacturing processes and today to prepare future engineers and designers, we need to think which are the best skills and scientific knowledge and also technical know-how capable to promoting and accelerating changes on companies to improve their competitiveness. How we can develop a consistent method to improve the skills for future engineers to deal with it.

The methodology focus is in the development of an integrative project for a new product. The project aim to prepare students to develop an product from the initial idea to the final prototype and involve diverse competences like 3D modelling, physical models, CNC machining and 3D printing process.

The results of the methodology and tasks established are adequate and possibility to improve the individual and group performance. The evaluation model implemented permit the valorization of the final work and that preserves the context of the workgroup and individual commitment.

**Keywords:** 3D printing · Digital products · Digital manufacturing · CAD/CAM/CNC

## 1 Introduction

There seems to be no doubt about the impact 3D printing will have in the future. There are many examples of the use of this technology and how it may change our day-to-day. With 3D printing it is possible to dream, design and build in any place or circumstance, even in our own home, with just a computer with software and a printer. However, we must bear in mind that the use and impact of 3D printing in an industrial context will be substantially different from its adoption in a domestic context. This printing technology offers multiple benefits, such as: fast and effective communication of design ideas; effective design validation; formal or functional analysis. It also offers greater design flexibility, allowing multiple iterations to be performed quickly, in order to validate the concept; correct defects and improve the quality of production and final products. One of his realities seems to be the indispensability of a digital model to obtain a physical model by 3D printing. Where sometimes “the physical and tangible” is easier to acquire, such as machines and equipment, but in order to obtain “good results”, the most technical aspects, namely those related to digital manufacturing processes, can not be forgotten today (CAD), reverse engineering, CNC machining and

high-speed machining, among others. It is therefore necessary to prepare future engineers and designers, not only with scientific knowledge, but also with technical know-how capable of promoting and accelerating change, in order to help companies improve their skills and increase competitiveness. Allowing you to look at and face the challenges of the future so that you are prepared for the future instead of waiting for it, otherwise it will be too late to react.

## **2 Project in Digital Manufacturing**

### **2.1 Objectives and Learning and Challenges**

In the area of Digital Manufacturing and its respective training aims to develop the skills in Project of Mechanical Engineering, namely in its component of models development and prototypes framed in the New Product Development Process. In addition to guiding and disseminating knowledge in the scientific and technological environment, and the development of new methods of rapid prototyping and rapid manufacturing processes and technologies as well as providing interfaces with the market and the improvement of their products and services.

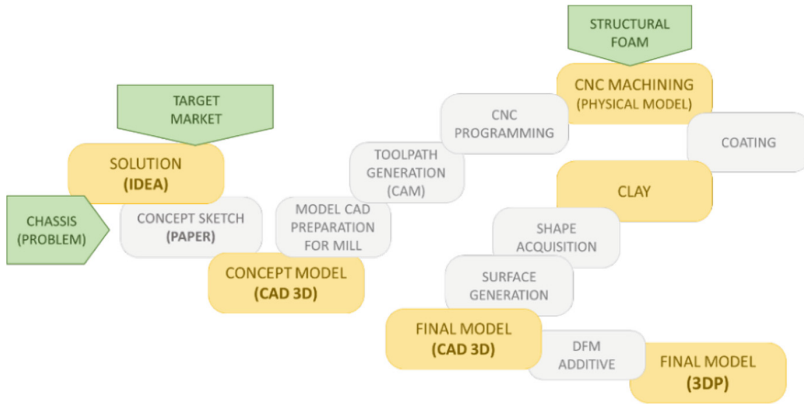
The project consists of developing the bodywork and interior of a small “electric” city car from a previously defined chassis.

### **2.2 The Methodology**

The work presented here tries to report in a summarized way the methodology developed and implemented in the module designed Rapid Prototyping Technique (Mechanical Engineering Department of University of Aveiro - Portugal). This course addresses the materials, processes and technologies associated with product development and digital manufacturing. The students are expected to perceive and prepared to do a concept or product proposal from the initial idea to the final product. The methodology allows a quickly perceive the results in a physical way and through models, in order to increase the possibility to assess the impact of the concept presented [1, 2].

The student begins by defining his market segment and target audience, develops the first conceptual sketches up to the 3D CAD modeling. Once the first 3D CAD models has obtained, it prepares to obtain a concept model 1:20 scale model in structural foam by CNC machining. This foam model is a basis for the development of CLAY and refinement of the concept. Once CLAY is obtained, its shape survey (reverse engineering) is performed in order to obtain a faithful 3D CAD model of this new proposal. This CAD model should be as representative as possible of a viable product, so observe all ergonomic and anthropometric principles.

At the end, the student should make a cost survey of all the developed process, materials and resources used. The methodology is centered in the development of an integrative project of the diverse competences to be acquired during the semester. The project was carryout by a group of 3 to 5 elements following the methodology (Fig. 1).



**Fig. 1.** The methodology and processes

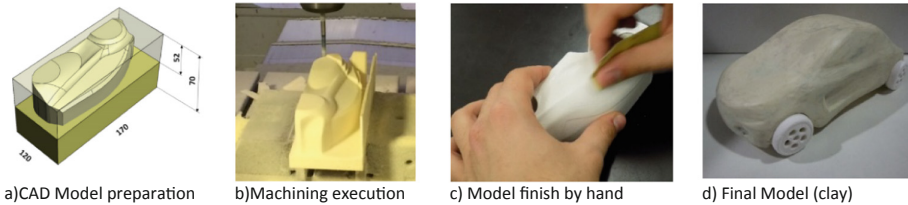
### 2.3 Initial Market Analysis, Concept and 3D CAD Model

After the choice of the topic of concept, the group begins to develop its proposal in conceptual and geometric terms and for this it realizes the first drafts in paper. The concept must guide the elaboration in the computer of the 3D CAD model. It is intended that the 3D CAD model be created in a free form and representative of the existing proposal on paper, containing regular geometric elements, but also organic forms. It is well known that the lack of mastery of 3D modeling skills often leads students defining the simplified and geometrically regular shapes that are not representative of their initial idea or their design intent.

### 2.4 The Volumetric Model, CNC Machining and Clay

To develop and refine the initial concept is usual the use of a clay. In order to obtain the clay, it is necessary, firstly, to obtain a volumetric model that is the core for coating in technical clay. This volumetric model is obtained by CNC machining, firstly because it allows a more accurate approximation of the model created in CAD 3D, second feel the size and volume of object and then because it allows the students a contact and learning of a relevant technology in terms of digital manufacturing to obtain physical models directly from a computer. Computer numerical control (CNC) machining is a technology that enables the rapid fabrication of physical models in a consistent and accurate mode and a quick approximation to the geometry projected in 3D CAD system [3–5]. It is also useful to learn the design for manufacturing (DFM) use of this technology and all the procedure and steps associated with obtaining a physical model with CNC. We refer to the preparation of the CAD model for the machining, definition of the technological parameters, namely the cutting tool selection, the CNC programming and pos-processing, transfer and machining run [6]. The creation of the CNC program was done automatically using a CAM (Computer Aided Manufacturing) application, PowerMill software (AutoDesk). The model is machined in two symmetrical parts

(Fig. 2) that are glued and coated with plasticine or technical clay. After machining the finishing process starts, the clay model was obtained and the process is represented in Fig. 2.



**Fig. 2.** Machining and finishing parts to obtain the clay model

## 2.5 Data Shape Acquisition e 3D Modelling (CAD)

In digital manufacturing and 3D printing, it is imperative to use 3D digital models, hence the importance of the development of these skills, both in terms of direct, inverse and detail modeling, aiming at aspects of functionality and manufacturing. The digital design has 3 steps, a first of 3D modeling, representative of the concept outline. A second 3D modeling obtained by CLAY shape survey and subsequent surface treatment. Finally, the modeling of detail in order to obtain the final model for 3D printing, considering adaptations of the model according to DFM recommendations. [7–9].

## 2.6 Prototyping and Design for Additive Manufacturing

The constraints/limitations in the manufacture of a part or component by 3D printing must be considered during the project. At this stage of the project, the student modifies some of the non-critical geometric characteristics of the model to facilitate its manufacturing and reduce the cost and time of manufacture considering the specificities of each one of the additive manufacturing processes, ensuring that the model is suitable for be obtained through a specific process or technology. The constraints/limitations in the manufacture of a part or component by 3D printing should be considered during the project, we refer to aspects such as obtaining completely closed solid models and tight water model, the use of recommendations of minimum wall thickness, correction of ambiguities on the surrounding surfaces [10, 11].

## 2.7 3D Printing

Many 3D printing equipment provides its own software, namely the additive manufacturing equipment for metallic materials, but there are currently a set of free or low cost solutions that a cost-saving option can be used. In this context and within the scope of the project the students proceed to the preparation of the model and elaboration of the manufacturing program [8]. The manufacturing can be done internally, using

the existing equipment in the Laboratory of the Department or be executed by out-sourcing. It should be noted that more than 90% of the works have presented a final of semester the model obtained by 3D printing by resources external to the Department and sometimes using their own means since they have a 3D printer at home [8].

The Fig. 3 presents some examples of models produced by 3D printing during the course where was used a FFF technology and a binder jet printing technology.



**Fig. 3.** Examples of models produced by 3D printing.

## 2.8 Estimating Cost of Prototyping

Knowing the cost is critical and although the company can be equipped with digital manufacturing resources, equipment and technologies and thus be perfectly capable of internally satisfying a wide range of needs for the manufacture of parts, models or prototypes, by CNC machining or by additive manufacturing. Subcontracting allows the company to choose the best methods for any particular need. Since this situation can be triggered for example when the company does not have a specific technology or because of work overload or because the project involves the use of several different methods of prototyping. Therefore, in the scope of this work, the costs associated with the use of the existing CNC equipment in the department, as well as 3D printing (internal costing) should be calculated and compared with budgets obtained by consulting external companies or online consultation.

## 3 Final Considerations

Project-centered teaching, although through design and manufacturing simulation processes, allows in an academic context the identification of the methods, tools and techniques that must be integrated in the development phase [12–14] for the transformation of an idea into a product through a digital process. This working model allows teaching and learning to compensate and anticipate eventual anomalies and possible manufacturing difficulties in the realization of ideas. These are in our understanding very valid attributes that attest our commitment to the training and qualification of engineers, designers and technicians of today and for the future. The methodology presents as an added value the iteration between the idealization and the conception of products and physical prototypes through the use of digital manufacturing, as a way of assessing its materialization and definition of concept, proving to be a knowledge tool of great applicability in the industry of the future.

**Acknowledgments.** Acknowledgments to Program Compete 2020, Portugal 2020 and Fundos Europeus e Estruturais e de Investimento da União Europeia, Projeto em co-promoção n. 33325 – BrickITsmart.

To the students of the integrated master's degree in mechanical engineering and of the master's degree in engineering and product design of the University of Aveiro.



## References

1. Hamon, C., Green, M. Dunlap, B., Camburn, B, Crawford, R., Jensen, D.: Virtual or physical prototypes? Development and testing of a prototyping planning tool. In: ASEE Annual Conference & Exposition, Design In Engineering Education Division, Indianapolis (2014)
2. Hilton, P.D.E., Jacobs, P.F.: Rapid Tooling: Technologies And Industrial Applications. Marcel Dekker, New York (2000)
3. Davis, J.R.: Metals Handbook, 9th edn., vol. 16, Machining. ASM International (1989)
4. Kalpakjian, S.: Manufacturing Engineering and Technology, 3rd edn. Addison-Wesley, Reading (1995)
5. Oberg, E., Jones, F.D., Horton, H.L.: Machinery's Handbook, 23rd edn. Industrial Press Inc., New York (1998)
6. Boboulos, M.A.: CAD-CAM and Rapid Prototyping Application Evaluation. Bookboon Publisher, Ebook (2010). ISBN-13: 9788776816766
7. Relvas, C., et al.: Accuracy control of complex surfaces in reverse engineering process. *Int. J. Precis. Eng. Manuf.* **12**(6), 1035–1042 (2011)
8. Relvas, C.: O Mundo da Impressão 3D e o Fabrico Digital. Ed.: Publindustria (2018)
9. Soni, K., Chen, D., Lerch, T.: Parameterization of prismatic shapes and reconstruction of free-form shapes in reverse engineering. *Int. J. Adv. Manuf. Technol.* **41**(9), 948–959 (2009)
10. Bourell, D.L., Beaman, J.J., Leu, M.C., Rosen, D.W.: A Brief History of Additive Manufacturing and the 2009 Roadmap for Additive Manufacturing: Looking Back and Looking Ahead, Us – Turkey Workshop on Rapid Technologies, pp. 5–11 (2009)
11. Wong, K.V., Hernandez, A.: Review of additive manufacturing. *ISRN Mech. Eng.* **2012**. Article Id 208760 (2012)
12. Doppelt, Y.: Implementation and assessment of project-based learning in a flexible environment. *Int. J. Technol. Des. Educ.* **13**(3), 255–272 (2003)
13. Perrenet, J.C., Bouhuijs, P.A.J., Smits, J.G.M.M.: The suitability of problem-based learning for engineering education: theory and practice. *Teach. High. Educ.* **5**(3), 345–358 (2000)
14. Bell, S.: Project-based learning for the 21st century: skills for the future. *Clear. House J. Educ. Strat. Issues Ideas* **83**(2), 39–43 (2010)





# Geometry-Based Process Adaption to Fabricate Parts with Varying Wall Thickness by Direct Metal Deposition

Daniel Eisenbarth<sup>1</sup> , Fabian Soffel<sup>1</sup> , and Konrad Wegener<sup>2</sup>

<sup>1</sup> inspire AG, Technoparkstrasse 1, 8005 Zürich, Switzerland  
eisenbarth@inspire.ethz.ch

<sup>2</sup> Institute of Machine Tools and Manufacturing, ETH Zürich,  
Leonhardstrasse 21, 8092 Zürich, Switzerland

**Abstract.** The process of direct metal deposition gains recently high attention in the additive manufacturing community, but its capabilities to fabricate complex geometries is still limited. Especially for thin-walled structures, heat accumulation can disturb the process significantly. An adaption of process parameters, for instance by a semi-empirical model, is able to stabilize the process. Herein, an algorithm is proposed that creates a digital twin of the part from a given NC code, analyses the massiveness of the part by calculating a local geometric factor, and alters the laser power accordingly: The heat flux in a thin wall is limited compared to a massive plate due to its smaller cross section and requires therefore less laser power to generate a comparable melt pool, especially if waiting times shall be avoided. The algorithm correlates experimentally determined process parameters to the local geometric factor. Since no physical simulation is performed, it is fast, easy to use, and enables a clearly defined and repeatable process. The buildup of a demonstrator part reveals the potential of the parameter adaption to fabricate arbitrary geometries.

**Keywords:** Additive manufacturing · Direct metal deposition · CAM programming · Parameter adaption

## 1 Introduction

Direct metal deposition (DMD) is an additive manufacturing (AM) technology that blows metallic powder into a melt pool that is created by a laser beam. It emerges from traditional laser cladding, which has been used for decades to apply wear- and corrosion-resistant coatings. Compared to powder-bed fusion, DMD has a higher buildup rate and the design space is only limited by the axis range of the robot or CNC machine. DMD aims to provide all advantages of AM such as “complexity for free”, but its capabilities to build geometrically complex structures are still limited.

Many researchers such as Wirth and Wegener [1] model the melt pool in detail, but validation can only be performed with single tracks, since they provide constant, measurable boundary conditions such as the workpiece temperature, geometry, and surface roughness. Thermomechanical models as proposed by Huang et al. [2], which are able to predict the shape of multi-layer structures, were validated by building

straight, thin walls. DebRoy et al. [3] state that the lack of reliable predictions for the additive fabrication of large, complex parts is due to missing temperature dependent thermo-physical material properties, the high computational effort, and missing experimental data for multi-layer structures.

Alternatively, the DMD process could be mastered by experimental approaches. However, constant input parameters can only create a constant process if the boundary conditions remain also constant. For complex parts, there are various influencing factors besides the workpiece temperature such as the surface shape and roughness, oxide layers, and local heat transfer conditions. Therefore, adapted process parameters are required that account for these changes. One common approach is the application of closed-loop control systems. Brueckner et al. [4] fabricated 40 mm high turbine blades by a temperature monitoring system. Sammons et al. [5] scan the height of each layer and adapt the position of the tool path for the subsequent layer accordingly. However, closed-loop control systems show certain drawbacks: The NC code of traditional CNC machines cannot be altered during execution due to their system architecture, and control systems rely on sensors that are often costly, bulky, and sensitive to errors. This paper proposes a semi-empirical model that neither relies on closed-loop control nor on sophisticated simulations, but uses experimentally gained data in combination with the actual part geometry to adapt parameters in advance.

## 2 Modelling Approach

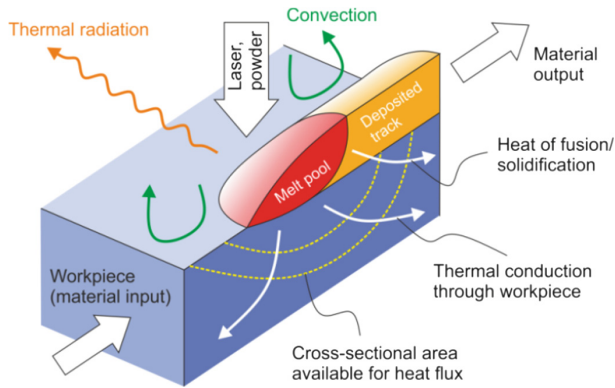
### 2.1 Parameter Influence

By the NC code, all parameters such as laser power  $P_L$ , scan speed  $v_s$ , powder flow rate  $\dot{m}_i$ , and the tool path are fixed before manufacturing. The powder flow rate is not suited as adaptable parameter, since there is typically a lag of several seconds until a changed powder flow rate reaches the processing head. Therefore, the only two parameters that can be changed instantaneously are the laser power and scan speed, in combination with the tool path. As shown by the authors in [6], one outer contour path together with a raster filling turned out to be a suitable tool path for most geometries and is applied in here. The scan speed is used to compensate deviations of the powder efficiency to obtain a homogeneous layer height as further outlined in [7].

For an ideal DMD process, the melt pool maintains a defined steady-state balance of energy input and output. The laser power and the absorptivity of the work piece and the melt pool determine the energy input during the process. Thermal conduction in the workpiece, convection, thermal radiation, and latent heat of fusion are responsible for the energy output. As these processes interact with each other, thermomechanical simulations are required to model the DMD process in detail.

Suitable parameters for one combination of workpiece and powder material to create a crack- and pore-free track, layer, or volume can be obtained experimentally in practice, treating the melt pool as a “black box”. The question raised herein is, if process parameters, which were developed for specific geometries such as massive plates and thin walls, can be interpolated to fabricate arbitrary geometries with reasonable microstructure and geometric accuracy.

Regarding heat conduction in a solid body, the available cross-sectional area through which heat can flow is a determining factor for the total heat flux from the melt pool. A thin wall or column provides a much smaller cross-sectional area for heat flux compared to a massive plate. The geometry of the workpiece surrounding the melt pool has the highest impact on heat flux, and its influence decays with increasing distance, since the heat distributes or dissipates by thermal radiation and convection. Thus, the required amount of laser power to create a comparable melt pool depends on the local geometry, even if processing starts at the same temperature. Figure 1 illustrates the DMD process with the melt pool, deposited track, workpiece, as well as the energy and material inputs and outputs.



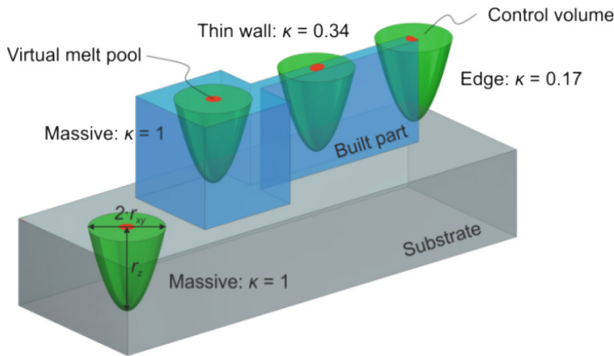
**Fig. 1.** Cut through the processing zone, showing the melt pool, deposited track, workpiece, and energy as well as material inputs and outputs

## 2.2 Geometry Recognition

A CAM software has been developed in MATLAB that creates the tool path for a given CAD model and adds points in a constant distance, typically the size of the melt pool. For each point on the path, an adapted laser power is assigned to the NC-code. Since the algorithm as described hereafter relies only on pointwise motion commands, NC-codes from any CAM software can be used as input for the tool path, as long as the melt pool width and height are known.

First, the design space of the part is discretized into a three-dimensional matrix with default value 0, which means “void”. By simulating the tool path, a virtual melt pool changes the respective matrix entries to 1 in order to indicate deposited material and to generate a digital twin of the part that is built. Simultaneously, the algorithm spans a larger control volume around the melt pool as an indication for the available cross-sectional area for heat flux as described above. Figure 2 illustrates the principle with a combined massive and thin-walled part in blue built on a grey substrate. The control volume in green has a circular shape in lateral direction in order to be direction-independent. Downwards, it forms a parabolic shape. Thus, there are only three simulation parameters, namely the step size of discretization as well as the lateral radius  $r_{xy}$

and the depth  $r_z$  of the control volume. For each point, the algorithm calculates the fraction  $\kappa$  of the substrate or deposited material inside the control volume, using the matrix of the digital twin that represents the geometry built up to this point. The fraction  $\kappa$  is therefore a measure for the massiveness of the surrounding workpiece and is called “geometric factor”. Figure 2 depicts control volumes at different positions. The control volume in the substrate is completely surrounded by material, thus  $\kappa$  equals 1 when the DMD process starts. The built block is massive enough in order that  $\kappa$  remains 1 in its center. When the melt pool reaches the thin wall,  $\kappa$  decreases to 0.34 here. At the edge of the thin wall, the heat flux through the part is most limited and  $\kappa$  decreases further to 0.17.



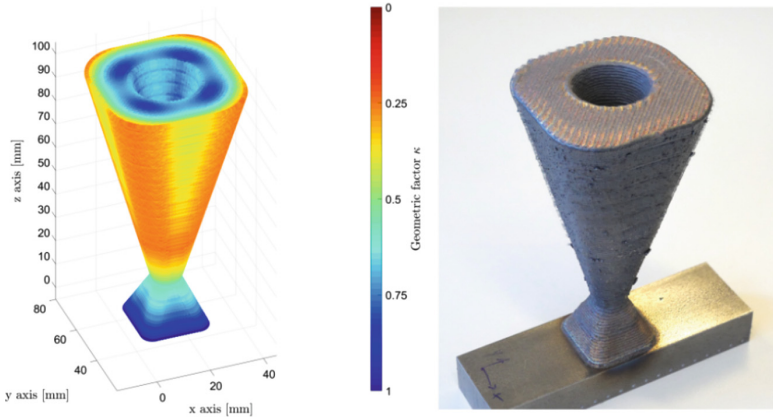
**Fig. 2.** Schematic part (blue) built on a substrate (grey). The control volume (green) follows the melt pool (red) and determines the geometric factor depending on the massiveness of the geometry at a specific point

### 3 Results and Discussion

The CAM software has been validated by the buildup of various geometries. Monitoring of the DMD process with an infrared camera revealed that a linear relation of the geometric factor  $\kappa$  and laser power  $P_L$  results in a comparable melt pool size and temperature. Thus, it is sufficient to determine a maximum and minimum laser power for the two geometric extrema of  $\kappa = 0$  and  $\kappa = 1$ . The required laser power is then interpolated for each point depending on the local geometric factor.

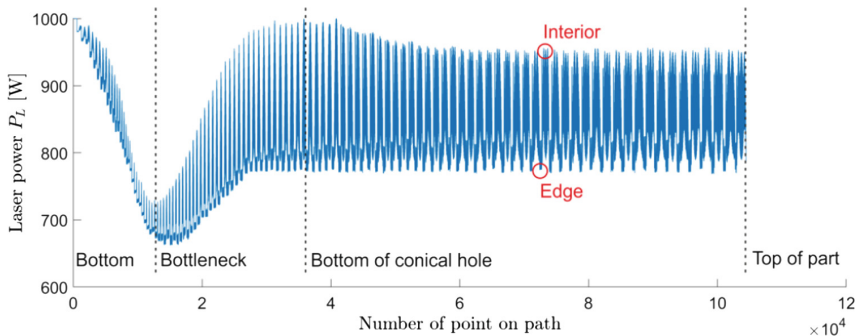
A 100 mm high overhanging demonstrator has been fabricated from steel 1.4404 with a prototype machine for combined DMD and milling, which is based on a 5-axis machining center type “Mikron HPM 450U” from the Swiss company GF Machining Solutions. The tool path for the demonstrator was divided into 104000 points. Due to the absence of physical simulations, computation of the geometric factor takes 15 min, whereas the fabrication of the part takes 150 min. Figure 3 shows a 3D plot of the geometric factor and the final part. The first layer has a constant geometric factor of one due to the heat-dissipating substrate. Up to the bottleneck in a height of 16 mm,  $\kappa$  decreases gradually from 1 to 0.5. Above, the build area and  $\kappa$  increase again, but the

algorithm distinguishes the massive interior from the edge, where  $\kappa$  decreases to 0.25 at minimum. The hole in the middle is conical, thus  $\kappa$  is greater at the tapered inner edge compared to the overhanging outer edge.



**Fig. 3.** 100 mm high demonstrator part made from steel 1.4404, showing the plot of the geometric factor  $\kappa$  on the left and the final part on the right

The assigned laser power as a function of the tool path point is depicted in Fig. 4. It starts at 1000 W, which is the maximum power as experimentally determined, and decreases down to 660 W at the bottleneck. The power oscillates during the raster path within one layer by up to 330 W, depending on the local value of  $\kappa$ . With the conical hole starting in a height of 62 mm, the build area and the mean power per layer remain approximately constant up to the top of the part.



**Fig. 4.** Assigned laser power as a function of all tool path points during buildup

## 4 Conclusion

An algorithm is proposed that adapts the laser power according to the massiveness of a part during CAM programming. It spans a control volume around the current melt pool position with the filling degree as a representation of the local heat flux conditions. This geometric factor  $\kappa$  is then correlated to the experimentally determined laser power. Since the algorithm neither relies on physical simulations nor on closed-loop control systems, it enables a fast, simple, and automated fabrication of various geometries as soon as the basic process parameters for a specific combination of machine and material have been developed and the melt pool size is known. The adapted parameters for the tool path can serve as a basis for further fine tuning of the process, until the desired part properties are obtained.

In the future, the algorithm shall be extended to five-axis-processing and undergo a validation campaign in order to be able to guarantee a certain microstructure and geometrical accuracy for any geometry.

**Acknowledgements.** The authors would like to acknowledge the contribution of the funding agency Innosuisse (grant number 25498) and of the companies GF Machining Solutions, GF Precicast, and ABB Turbo Systems Ltd.

## References

1. Wirth, F., Wegener, K.: A physical modeling and predictive simulation of the laser cladding process. *Addit. Manuf.* **22**, 307–319 (2018)
2. Huang, Y., Khamesee, M.B., Toyserkani, E.: A new physics-based model for laser directed energy deposition (powder-fed additive manufacturing): From single-track to multi-track and multi-layer. *Opt. Laser Technol.* **109**, 584–599 (2019)
3. DebRoy, T., Wei, H.L., Zuback, J.S., Mukherjee, T., Elmer, J.W., Milewski, J.O., Beese, A. M., Wilson-Heid, A., De, A., Zhang, W.: Additive manufacturing of metallic components – process, structure and properties. *Prog. Mater Sci.* **92**, 112–224 (2018)
4. Brueckner, F., Seidel, A., Straubel, A., Willner, R., Leyens, C., Beyer, E.: Laser-based manufacturing of components using materials with high cracking susceptibility. *J. Laser Appl.* **28**(2), 022305 (2016)
5. Sammons, P.M., Gegel, M.L., Bristow, D.A., Landers, R.G.: Repetitive process control of additive manufacturing with application to laser metal deposition. *IEEE Trans. Control Syst. Technol.* **27**(2), 566–575 (2019)
6. Eisenbarth, D., Wirth, F., Spieldiener, K., Wegener, K.: Enhanced toolpath generation for direct metal deposition by using distinctive CAD data. In: *Industrializing Additive Manufacturing - Proceedings of Additive Manufacturing in Products and Applications - AMPA2017*, pp. 152–161 (2018)
7. Eisenbarth, D., Borges Esteves, P.M., Wirth, F., Wegener, K.: Spatial powder flow measurement and efficiency prediction for laser direct metal deposition. *Surf. Coat. Technol.* **362**, 397–408 (2019)



# Design and Printing Parameters Effect on PLA *Fused Filament Fabrication* Scaffolds

R. Baptista<sup>1,2(✉)</sup> and M. Guedes<sup>1,3</sup>

<sup>1</sup> CDP2T e Departamento de Engenharia Mecânica,  
Escola Superior de Tecnologia de Setúbal, Instituto Politécnico de Setúbal,  
2910-761 Setúbal, Portugal

{ricardo.baptista, mafalda.guedes}@estsetubal.ips.pt

<sup>2</sup> IDMEC, Escola Superior de Tecnologia de Setúbal,  
Instituto Politécnico de Setúbal, 2910-761 Setúbal, Portugal

<sup>3</sup> CeFEMA, Instituto Superior Técnico, ULisboa,  
Av. Rovisco Pais, 1049-001 Lisbon, Portugal

**Abstract.** The *Fused Filament Fabrication* technique was used to build PLA scaffolds for bone tissue replacement. Scaffolds with 100% interconnectivity were fabricated using different printing parameters and geometry design. Two temperature values and two extrusion speeds were combined with two different layer thicknesses. The influence of these parameters upon produced scaffold morphology and compressive mechanical properties was assessed. Afterwards, two different geometries were fabricated considering only the best performing parameters, to assess the influence of the main and lateral pores dimension on scaffolds mechanical properties. Specimen morphology was analysed by scanning electron microscopy, to assess the geometrical quality of the produced parts. It was verified that the higher tested temperatures combined with the lower printing speeds increased the overall mechanical strength of produced scaffolds. Low temperatures and high printing speeds were found to limit the amount of material possible to be extruded due to viscosity issues, and introduced scaffold defects. Creating staggered scaffolds with offsets between layers, decreased the resulting scaffold mechanical performance.

**Keywords:** Scaffolds · *Fused Filament Fabrication* · Tissue replacement · Mechanical properties

## 1 Introduction

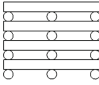
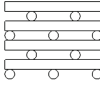
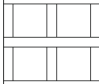
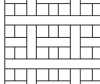
When bone tissue is damaged by disease or trauma it must be replaced, permanently or temporarily until enough regeneration has occurred. Permanent substitution is mainly achieved using autografts. Yet, this technique has major disadvantages regarding supply limitation, risk of rejection and other morbidities. Metal implants can also be used for permanent replacement, but they are non-degradable, cause stress shielding and display fatigue and fracture issues. Scaffolds, manufactured in natural or synthetic polymers are a valid and interesting alternative. Several features are demanded for a functional scaffold, including biocompatibility and biodegradability (in order for gradual replacement by regenerating tissue); interconnected pore structure (to allow cell

proliferation, oxygen and nutrient diffusion and waste removal); osteoconductivity; and geometric customization with the specific patient bone defect to be fulfilled [1]. In this context, additive manufacturing can produce scaffolds using different materials and techniques. As new *Fused Filament Fabrication* (FFF) 3D printers reach the market, with higher resolution and lower price, FFF becomes one of the most noticeable scaffold production techniques. Major advantages include the ability to fabricate scaffolds with customized and complex geometries, while using biocompatible polymers such as poly(lactic acid) (PLA) or poly(caprolactone) (PCL) eliminates potential toxicity introduced by organic solvents in other AM techniques [2]. This paper aims to assess the influence of the major FFF parameters on mechanical behavior and geometric performance of produced scaffolds.

## 2 Materials and Methods

PLA filament with  $\varnothing$  1.75 mm (BQ) was used in all the experiments. Scaffolds design steps comprised drawing a  $12.7 \times 12.7 \times 25.4$  mm block in Solidworks (Dassault Systèmes) CAD software, which was then processed in Cura (Ultimaker) slicing software and transformed into a scaffold, using no top, bottom or lateral walls. Different infill parameters were used to fabricate PLA scaffolds, devised with 100% interconnected 400  $\mu$ m pores. A first series of scaffolds was designed using a line pattern with infill density of 50% (corresponding to 800  $\mu$ m filament spacing), to produce a regular orthogonal 0/90° (*Ortho*) lattice. Layers were built in a single motion, printing each filament in alternate direction. Eight configurations were manufactured, combining different temperatures (200 °C and 220 °C), extrusion speeds (30 and 45 mm/s) and layer thicknesses (200 and 300  $\mu$ m) (Table 1). After determination of the best parameter configuration, a second series of scaffolds was design by manually altering the *gcode* files previously produced in Cura. Each alternating layer was displaced by 400  $\mu$ m, creating a staggered configuration (*Displ*). All scaffolds were printed in a Blocks Zero (Blocktec) 3D Printer.

**Table 1.** *Fused Filament Fabrication* parameters and geometries.

Parameters		
Extrusion temperature (°C)	200	220
Extrusion speed (mm/s)	30	45
Layer thickness ( $\mu$ m)	200	300
Scaffold density (%) / filament spacing ( $\mu$ m)	50 / 800	
Scaffold geometry	Ortho	Displ
Lateral Pores		
Main Pores		



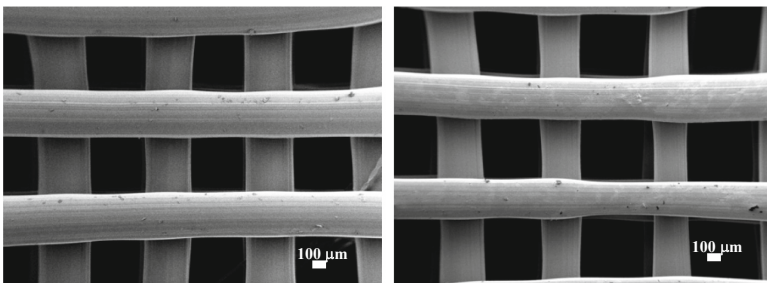
A smaller sample of each series was also printed for microscopy, and coated with Au-Pd alloy to assure adequate electrical conductivity during observation. Scanning electron microscopy (JSM-7001F, Jeol) allowed to assess scaffolds morphology, pattern defects, final pore dimension and overall compliance to projected dimensions.

All produced configurations were submitted to compression test using an electromechanical test machine (TS300, Impact Test Equipment), to assess the influence of manufacturing parameters and resulting scaffold defects upon mechanical properties. Deformation was set at 1 mm/min, until deformation reached 40% of initial length. The apparent compressive stress was calculated as the applied load  $F$  divided by the total area  $A$  of specimen's apparent cross section ( $12.7 \times 12.7 \text{ mm}^2$ ). Strain  $\varepsilon$  was calculated as the ratio of length variation  $\Delta L$  by the initial specimen length  $L$  (25.4 mm). Compressive modulus was determined as the linear slope of the  $\sigma$ - $\varepsilon$  curve, and yield stress as the point at which the curve levels off.

### 3 Results and Discussion

#### 3.1 Specimen Morphology

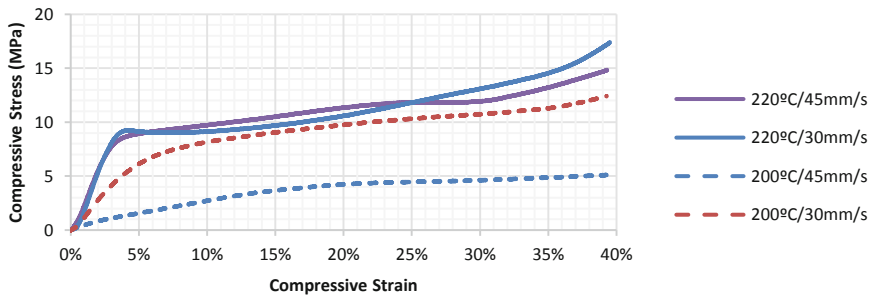
Measured scaffold and pore dimensions show that filament spacing is not dependent on the tested manufacturing parameters or scaffold geometry, since attained and projected values are very close. Pore dimensions were thus expected to be a function of filament extruded diameter, corresponding to nozzle diameter (400  $\mu\text{m}$ ). However, the diameter of all extruded filaments was smaller, mainly from 360 to 380  $\mu\text{m}$  (Fig. 1a), but reaching as low as 320 and 290  $\mu\text{m}$  in scaffolds printed at 200  $^\circ\text{C}$  and 45 mm/s (Fig. 1b). These conditions produced the worst quality scaffolds, suggested to result from high material viscosity hindering the 3D printer to extrude the necessary amount of filament to fulfill the designed dimensions. As a result, final pore size was always higher than the designed 400  $\mu\text{m}$ , reaching 500  $\mu\text{m}$  on the worst-case manufacturing conditions (Fig. 1b). These results conflict a previous report by Guduric et al. [3], suggesting that future development should take into account the flow correction parameter (available in most slicing software) as a route to correct filament diameter and pore size [4].



**Fig. 1.** Low magnification micrographs of patterns printed using (a) 220  $^\circ\text{C}$  and 30 mm/s; and (b) 200  $^\circ\text{C}$  and 45 mm/s printing parameters.

### 3.2 Mechanical Properties

The influence of printing parameters on scaffold final mechanical properties was assessed by compressive stress. Figure 2 shows  $\sigma$ - $\epsilon$  curves for 300  $\mu\text{m}$  layer thickness samples. All scaffolds show similar behavior, in good agreement with results by Gong et al. [5]. The curve can be divided in three sequential stages: (1) linear elastic behavior, where each scaffold layer is equally compressed; (2) a region of almost constant stress level; followed by (3) the exponential increases of curve slope. The plateau in region (2) plays a major role in scaffold mechanical behavior, and is a consequence of repeated layer buckling, taking place until collapse of all lateral pores [6].



**Fig. 2.** Compressive  $\sigma$ - $\epsilon$  curve for all manufacturing parameters combinations (300  $\mu\text{m}$  layers).

Figure 2 summarizes the obtained mechanical properties and the major manufacturing parameters influencing performance. Layer thickness has clear impact. When increasing thickness from 200 to 300  $\mu\text{m}$ , not only the geometry of the scaffold is altered (by increasing the size of lateral pores), but also the compressive modulus and the yield stress of the scaffold are reduced. When printing at 45 mm/s and 220  $^{\circ}\text{C}$  the compressive modulus is reduced by 42%, while at 200  $^{\circ}\text{C}$  the decrease reaches 95%. Yield stress follows a similar behavior. Increasing layer thickness increases the distance between equal layers, therefore the columns supporting these layers will buckle and collapse more easily. Contrary results have been reported by Germain et al. [7], yet those authors increased the size of the lateral pores and of the distance between layers by adding more layers with the same orientation, therefore creating weak boundaries within each column. Regarding the temperature parameter, increasing temperature from 200  $^{\circ}\text{C}$  to 220  $^{\circ}\text{C}$  increases the overall mechanical performance. Temperature is especially important for the scaffolds with 300  $\mu\text{m}$  layer thickness. Decreasing the 45 mm/s printing temperature decreases the compressive modulus about 92%. Low temperature (and high speed) influence material viscosity, decreasing the amount of printed material and increasing pore dimensions. For the 200  $\mu\text{m}$  scaffolds the compressive modulus decrease is only 10%. In this case, the lower amount of material to be extruded per layer allows the printer to be able to supply enough material to print the designed quality. Finally, higher printing speed decreases scaffolds mechanical performance. Again, high thickness and low printing temperature are the most affected parameters, with a difference reaching 81%. Domingos et al. [8] reported similar

behavior for PCL printed scaffolds, with printing speed having higher influence on mechanical properties, but with overall interconnection of all parameters.

**Table 2.** Mechanical properties of the different produced scaffold configurations.

Type	Infill (%)	Layer ( $\mu\text{m}$ )	Speed (mm/s)	Temperature ( $^{\circ}\text{C}$ )	Compressive modulus (MPa)	Yield stress (MPa)
Ortho	50	200	45	220	510.5	14.4
Ortho	50	300	45	220	295.3	8.4
Ortho	50	200	30	220	555.0	15.7
Ortho	50	300	30	220	374.1	10.1
Ortho	50	200	45	200	479.9	13.0
Ortho	50	300	45	200	23.2	1.4
Ortho	50	200	30	200	500.5	13.6
Ortho	50	300	30	200	124.3	5.3
Displ	50	200	30	220	191.9	6.5
Displ	50	300	30	220	230.7	8.2

Table 2 suggests that optimal manufacturing parameters are printing temperature of  $220^{\circ}\text{C}$  and printing speed of  $30\text{ mm/s}$ , with compressive modulus reaching  $555\text{ MPa}$ , similar [5] or higher [9] than reported values for scaffolds with equal porosity.

Staggered samples were also produced because this geometry has been reported to increase cell adhesion to the scaffold, by limiting vertical cell movement [4]. However, when using offsets the intersections will be suspended, allowing fiber bending, increasing overall scaffold deformation and decreasing mechanical performance [10, 11]. These results were confirmed in the current work. Table 2 shows a 65% compressive modulus decrease for  $200\ \mu\text{m}$  scaffolds, and of only 38% for  $300\ \mu\text{m}$  scaffolds, when compared to the non-staggered configuration. In fact, the  $300\ \mu\text{m}$  displaced scaffold has higher compressive modulus. This can be attributed to the increased amount of material supporting the bending load between layers [12].

## 4 Conclusions

*Fused Filament Fabrication* was used to build PLA scaffolds. The effect of design (line pattern and thickness) and manufacturing (printing temperature and speed) parameters upon geometrical compliance and mechanical performance of produced scaffolds was assessed. Attained results show that low extrusion temperature and high printing speed hinder efficient extrusion due to insufficient material flow, leading to uneven line diameter and decreased mechanical strength.

**Acknowledgements.** This work was supported by FCT, through IDMEC-LAETA (project UID/EMS/50022/2019) and CeFEMA (contract Pest-OE/CTM/UI0084/2014).

## References

1. Roseti, L., Parisi, V., Petretta, M., Cavallo, C., Desando, G., Bartolotti, I., Grigolo, B.: Scaffolds for bone tissue engineering: state of the art and new perspectives. *Mater. Sci. Eng., C* **78**, 1246–1262 (2017). <https://doi.org/10.1016/j.msec.2017.05.017>
2. Do, A.V., Khorsand, B., Geary, S.M., Salem, A.K.: 3D printing of scaffolds for tissue regeneration applications. *Adv. Healthc. Mater.* **4**(12), 1742–1762 (2015)
3. Guduric, V., Bareille, R., Latour, S., Gr, A.: Characterization of printed PLA scaffolds for bone tissue engineering Characterization of printed PLA scaffolds for bone tissue engineering (2017). <https://doi.org/10.1002/jbm.a.36289>
4. Gregor, A., Filová, E., Novák, M., Kronek, J., Chlup, H., Blahnová, V., Barto, M., Ne, A., Ho, J.: Designing of PLA scaffolds for bone tissue replacement fabricated by ordinary commercial 3D printer 1–21 (2017). <https://doi.org/10.1186/s13036-017-0074-3>
5. Gong, B., Cui, S., Zhao, Y., Sun, Y., Ding, Q.: Strain-controlled fatigue behaviors of porous PLA-based scaffolds by 3D-printing technology. *J. Biomater. Sci. Polym.* **28**, 2196–2204 (2017)
6. Moroni, L., De Wijn, J.R., Van Blitterswijk, C.A.: 3D fiber-deposited scaffolds for tissue engineering: Influence of pores geometry and architecture on dynamic mechanical properties. *Biomaterials* **27**, 974–985 (2006)
7. Germain, L., Fuentes, C.A., Van Vuure, A.W., Dupont-gillain, C.: 3D-printed biodegradable gyroid scaffolds for tissue engineering applications. *Mater. Des.* **151**, 113–122 (2018). <https://doi.org/10.1016/j.matdes.2018.04.037>
8. Domingos, M., Gloria, A., Ambrosio, L.: Effect of process parameters on the morphological and mechanical properties of 3D Bioextruded poly (1-caprolactone) scaffolds **1**, 56–67 (2012), <https://doi.org/10.1108/13552541211193502>
9. Esposito Corcione, C., Gervaso, F., Scalera, F., Padmanabhan, S.K., Madaghiele, M., Montagna, F., Sannino, A., Licciulli, A., Maffezzoli, A.: Highly loaded hydroxyapatite microsphere/PLA porous scaffolds obtained by fused deposition modelling. *Ceram. Int.* **45**, 2803–2810 (2018)
10. Szojka, A., Lalh, K., Andrews, S.H.J., Jomha, N.M., Osswald, M., Adesida, A.B.: Biomimetic 3D printed scaffolds for meniscus tissue engineering. *Bioprinting* **8**, 1–7 (2017). <https://doi.org/10.1016/j.bprint.2017.08.001>
11. Korpela, J., Kokkari, A., Korhonen, H., Malin, M.: Biodegradable and bioactive porous scaffold structures prepared using fused deposition modeling 610–619 (2012). <https://doi.org/10.1002/jbm.b.32863>
12. Serra, T., Planell, J.A., Navarro, M.: High-resolution PLA-based composite scaffolds via 3-D printing technology. *Acta Biomater.* **9**(3), 5521–5530 (2013)



# Strategies for Obtaining Porous Media Through the Process Planning in Material Extrusion Additive Manufacturing

Marcelo Okada Shigueoka<sup>(✉)</sup>, Elis Cassiana Nakonetchnei,  
and Neri Volpato

Additive Manufacturing and Tooling Group (NUFER),  
Federal University of Technology - Paraná, Curitiba, Brazil  
mshigueoka@gmail.com, elisan@alunos.utfpr.edu.br,  
nvolpato@utfpr.edu.br

**Abstract.** Porous materials or porous media (PM) are found in many applications. The design of the porous structures for specific applications presents challenges that involve their geometric modeling and manufacturing. Additive Manufacturing (AM) has a great potential in this area since it allows porosity planning. In particular, the AM based on the material extrusion principle allows obtaining PM with a planned macro porosity without the need to model it geometrically. This is possible because this principle allows varying a number of manufacturing parameters in the production of lattice geometries. Although there are parameters that allow the creation of PM, the current process planning software still have limitations on the level of customization of the part filling. This work presents the potential of the process planning software called RP3 (Rapid Prototyping Process Planning) to obtain PM with the material extrusion AM technologies. For this, some specific filling strategies were developed such as the staggered raster and the joined filaments. The efficiency of the process planning system was evaluated by manufacturing PM in an open source printer.

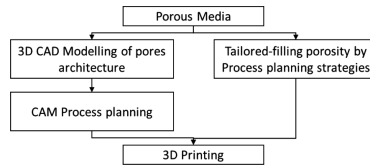
**Keywords:** Additive manufacturing · Porous media · Material extrusion · Process planning · Tailored filling

## 1 Introduction

Porous materials or porous media (PM) are found in applications related to power generation, vibration suppression, thermal insulation, sound absorption, fluid filtration, and others. One of its main mechanical characteristics is to have structural rigidity with low mass density [1]. The design of the porous structures for specific applications presents challenges related to their geometric modeling and manufacturing.

Additive Manufacturing (AM) has a great potential in this area, as it allows the production of planned porosity [2]. In particular, the AM based on the material extrusion principle allows obtaining PM by varying a number of manufacturing parameters to produce lattice-type geometries, without the need to model each filament of this structure [3]. This is possible because the deposition of material directly generates the “bars” of lattice structures in the deposition plane.

There are two main routes to design and produce a PM through a material extrusion AM. The first one is to model the porous structures in a CAD system and then follow the traditional manufacturing process (left path in Fig. 1). The drawback of this option is the difficulty of the geometric modelers (CAD) to generate this 3D model. The second one is to design the pores directly by controlling the process parameters, without any PM detailed model (right path in Fig. 1). For instance, a raster strategy (also known as rectilinear filling), which is a zigzag path formed with parallel lines, with a positive road gap and variation between the raster angle generates different pores geometries [3–8]. Some variation of this option is the possibility to apply a staggered raster, which consists of generating a lateral displacement of the raster between the layers with the same raster angle, maintaining the road gap initially defined [9–11].



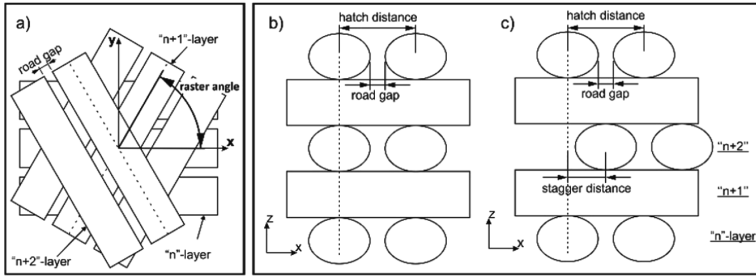
**Fig. 1.** Routes to obtain PM via material extrusion AM

Although there are parameters that allow the creation of PM, the process planning software currently available still have limitations on the level of customization of the part filling. This work presents the potential of the software called RP3 (Rapid Prototyping Process Planning) to produce PM by process planning strategies in material extrusion AM technologies (right path in Fig. 1).

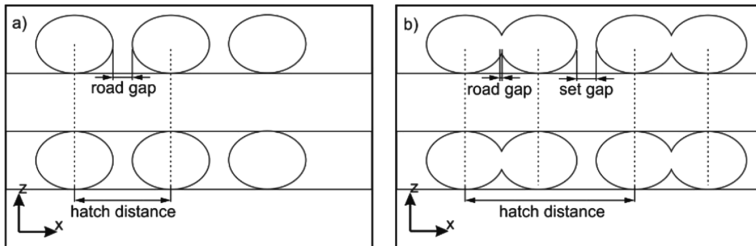
## 2 Proposed PM Design for Material Extrusion AM

Although there are different filling strategies for material extrusion AM, the raster filling was selected as it was more suitable for the objective of this work. Some specific filling strategies combining the rotation of the raster angle between layers, the staggered raster and the joined filaments, which is a new strategy not explored so far, were developed.

Figure 2a shows schematically the parameters raster angle, its rotation and the road gap, which together create a basic lattice PM. The staggered raster concept is shown in Fig. 2b and c, and Fig. 3 illustrates the joined filaments idea. Joined filaments is a new strategy where two or more filaments (raster lines) are printed together (side-by-side) forming a set, and a gap is left between successive lines sets (Fig. 3b). This pattern is then repeated forming the path filling. A zero or negative road gap can be used inside the lines sets to ensure that there will not be holes along the contact areas. It is worth mentioning that these parameters and strategies can be used separately or can be combined to generate new variations of PM.



**Fig. 2.** Schematic of PM varying raster angle (a) and stagger parameter (b)



**Fig. 3.** Schematic of PM obtained with a new joined filaments strategy

## 2.1 RP3 (Rapid Prototyping Process Planning)

The filling strategies specifically designed to obtain PM by the material extrusion AM proposed in this study were implemented in the RP3 (Rapid Prototyping Process Planning) software. The RP3, which is an AM process-planning tool, was then used to generate the process data to build the proposed geometries. This is a research tool that allows testing new filling or scanning strategies, combining different process parameters in order to tune it to a specific case, and can even be applied to different AM technologies [12]. The RP3 was developed using Microsoft Visual C ++ 6.0 compiler, following the Object Oriented Programming (OOP). This implementation allows the freedom to position each filament in the layer, without the need to model filament-to-filament as done in 3D CAD programs.

In Fig. 4 is shown the Advanced Filling option interface developed to plan the PM. The parameters and strategies mentioned are highlighted and identified by “a”, “b” and “c” in this figure. The parameters controlling the road gap and the rotation of the raster angle, which varies from  $0^\circ$  to less than  $180^\circ$ , are obtained in item “a”. Parameters “b” refer to the joined filaments strategy. To differ these parameters from those used in the traditional raster, it was decided to name the joined filaments as raster lines sets. Therefore, the Line Gap is responsible to control the road gap inside the sets (joined filaments) and the Set Gap defines the distance between the joined filaments (lines sets). Parameters “c” were developed for the Staggered Raster. The Stagger Distance was defined as a percentage of the Raster/Road Gap (single filament) or the Set Gap (joined filaments).

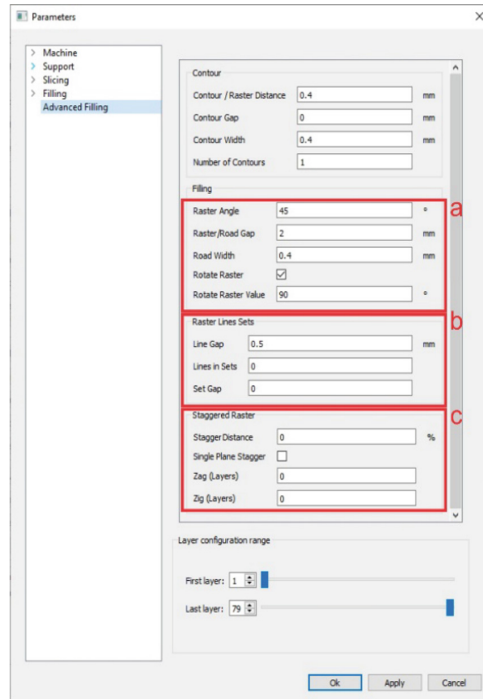


Fig. 4. RP3’s interface to plan PM

## 2.2 Printed PM

Using an open source desktop printer and the RP3, some PM design variations listed in Table 1 were manufactured in PLA (Poly(lactic acid)). The main build parameters for all designs were extrusion temperature 195 °C, bed temperature 50 °C, extrusion nozzle diameter 0.4 mm, layer height 0.3 mm, road width 0.4 mm and print speed 25 mm/s. The main objective of this study was not to explore all design possibilities, but to test the implementation done in the RP3. To prove the efficiency, two of the PM designs were digitally reconstructed by X-ray micro tomography (Table 1).

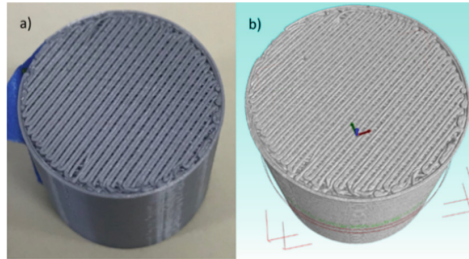
Table 1. PM designs

Designed PM	Joined filaments (lines in set)	Rotate raster value	Staggered distance	Raster/road gap or line gap (mm)	Set gap (mm)
L01A90S00	1	90°	0%	0.2	–
L01A90S50	1	90°	50%	0.2	–
L02A90S00	2	90°	0%	0	0.2
L02A90S50	2	90°	50%	0	0.2
L02A60S00	2	60°	0%	0	0.2
L02A60S50	2	60°	50%	0	0.2

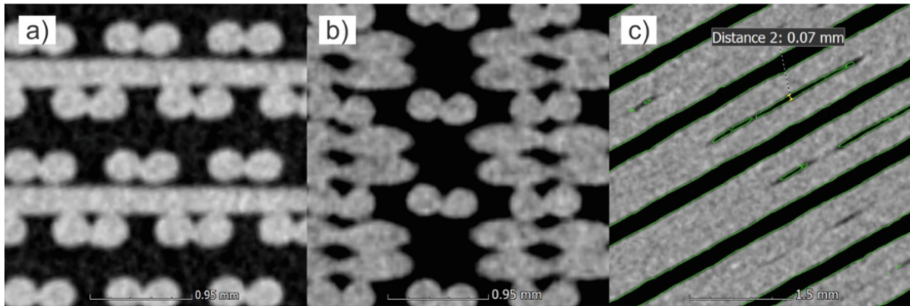


### 3 Results and Discussion

The L02A60S00 printed (a) and digitally reconstructed from the X-ray micro tomography (b) is shown in Fig. 5. In Fig. 6 some layers of the cross sections of the L01A90S50 (a) and L02A60S00 (b) obtained by cutting the 3D geometric models are displayed. As can be seen, the PM with the joined filaments and the staggered raster were manufactured as planned (designed) by the RP3. In addition, as shown in Fig. 6a and b, the joined filaments hold the elliptical shape.



**Fig. 5.** L02A60S00 printed (a) and digitally reconstructed from the X-ray micro tomography (b)



**Fig. 6.** Cross section of the L01A90S50 (a) and L02A60S00 (b) and insufficient filament bonding (c)

The analysis of the 3D models showed that the parameter line/road gap planned as “0” produced regions where the joined filaments did not touch each other (Fig. 6c). This result is not an implementation problem in the RP3, but an indication that the 3D printer was not well adjusted, causing a deviation in the printing process. A machine adjustment prior to print or a negative line/road gap will correct this effect.

## 4 Conclusions

The strategies implemented in the RP3 system to design PM with lattice structures in the material extrusion AM were successful. The results showed that it was able to produce these structures taking into account raster angle rotation, staggered raster and joined filaments strategies. A similar idea can be applied to other AM principles in the future, since RP3 is not tied to the material extrusion AM.

**Acknowledgments.** To Repsol Sinopec Brasil S.A. for supporting this research carried out according to ANP's research, development and innovation incentive law (No. 9478, 08/08/1997).

## References

1. Liu, P., Chen, G.-F.: *Porous Materials Processing and Applications*. Butterworth-Heinemann, Waltham (2014)
2. Michailidis, N., Tsouknidas, A., Lefebvre, L., Hipke, T., Kanetake, N.: Production, characterization, and applications of porous materials. *Adv. Mater. Sci. Eng.* **2014**, 1–2 (2014)
3. Kalita, S.J., Bose, S., Hosick, H.L., Bandyopadhyay, A.: Development of controlled porosity polymer-ceramic composite scaffolds via fused deposition modeling. *Mater. Sci. Eng., C* **23**, 611–620 (2003)
4. Too, M.H., Leong, K.F., Chua, C.K., Cheah, C.M., Ho, S.L.: Feasibility of tissue engineering scaffold fabrication using fused deposition modelling. In: *The Seventh Australian and New Zealand Intelligent Information Systems Conference*, pp. 433–438. IEEE (2001)
5. Zein, I., Hutmacher, D.W., Tan, K.C., Teoh, S.H.: Fused deposition modeling of novel scaffold architectures for tissue engineering applications. *Biomaterials* **23**, 1169–1185 (2002)
6. Chin Ang, K., Fai Leong, K., Kai Chua, C., Chandrasekaran, M.: Investigation of the mechanical properties and porosity relationships in fused deposition modelling-fabricated porous structures. *Rapid Prototyp. J.* **12**, 100–105 (2006)
7. Moroni, L., De Wijn, J.R., Van Blitterswijk, C.A.: 3D fiber-deposited scaffolds for tissue engineering: Influence of pores geometry and architecture on dynamic mechanical properties. *Biomaterials* **27**, 974–985 (2006)
8. Olubamiji, A.D., Izadifar, Z., Si, J.L., Cooper, D.M.L., Eames, B.F., Chen, D.X.: Modulating mechanical behaviour of 3D-printed cartilage-mimetic PCL scaffolds: influence of molecular weight and pore geometry. *Biofabrication* **8**, 025020 (2016)
9. Sobral, J.M., Caridade, S.G., Sousa, R.A., Mano, J.F., Reis, R.L.: Three-dimensional plotted scaffolds with controlled pore size gradients: effect of scaffold geometry on mechanical performance and cell seeding efficiency. *Acta Biomater.* **7**, 1009–1018 (2011)
10. Lee, J.S., Cha, H.D., Shim, J.H., Jung, J.W., Kim, J.Y., Cho, D.W.: Effect of pore architecture and stacking direction on mechanical properties of solid freeform fabrication-based scaffold for bone tissue engineering. *J. Biomed. Mater. Res., Part A* **100 A**, 1846–1853 (2012)
11. Woo Jung, J., Yi, H.-G., Kang, T.-Y., Yong, W.-J., Jin, S., Yun, W.-S., Cho, D.-W.: Evaluation of the effective diffusivity of a freeform fabricated scaffold using computational simulation. *J. Biomech. Eng.* **135**, 084501 (2013)
12. Volpato, N., Foggianto, J.A.: The development of a generic rapid prototyping process planning system. In: *Proceedings of VR@P4, Leiria, Portugal*, pp. 381–387. Taylor & Francis Group, London (2009)



# Programming 4D Printed Parts Through Shape-Memory Polymers and Computer-Aided-Design

Eujin Pei<sup>(✉)</sup>, Giselle Hsiang Loh, Seok Woo Nam,  
and Ezrin Faten Azhar

Department of Design, Brunel University London,  
Kingston Lane, Uxbridge UB8 3PH, UK  
eujin.pei@brunel.ac.uk

**Abstract.** This paper aims to provide an overview about 4D Printing (4DP), the use of Shape Memory Polymers (SMP) and how Computer-Aided Design (CAD) can be applied to programme shapes to perform controlled behaviors of 4DP parts when subject to environmental stimuli, leading to potential applications and outlining future challenges for this emerging field of multi-disciplinary science. One of the main barriers outlined in this work concerns the early stages of Design for 4DP (Df4DP), in which communicating the intent and the shape change behavior is important for designers, engineers and manufacturers.

**Keywords:** 4D Printing · 5D Printing Additive Manufacturing · Shape Memory Polymers · Computer-Aided-Design · Stimuli Responsive Materials

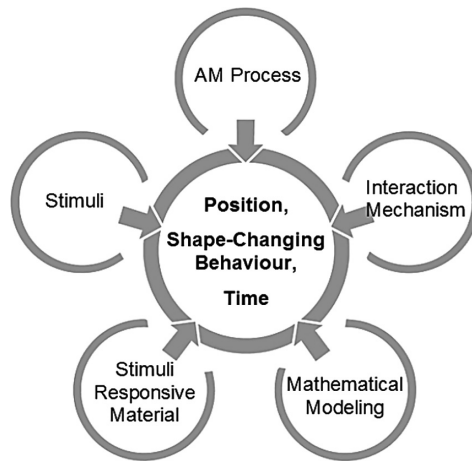
## 1 Introduction

### 1.1 The Concept of 4D Printing

4D Printing (4DP) combines the use of Additive Manufacturing (AM) to produce freeform components with Stimuli Responsive Materials (SRMs) so that printed parts can transform over a pre-determined duration of time (Nam and Pei 2019). As more SRMs and suitable AM processes become available, the widespread application of 4DP is expected to rise. In the near future, the 4DP industry will have a major impact into sectors such as aerospace, defense, healthcare, automotive, clothing and construction (Markets and Markets 2017). For example, in the review of 4DP prospects for the aerospace industry, Ntouanoglou et al. (2018) and other researchers claimed that morphing structures could become a reality for parts such as auxetic honeycomb structures that have ultra-high strength and ductility, variable-rigidity and multi-stable tube structures, and corrugated structures. 4DP could also be suited for space applications, including deployable structures and foldable antennas where sending payloads to space are constrained by the availability of space in the launch vehicle and the weight of the cargo. Zolesi et al. (2012) also claimed that 4DP parts could be built individually and then re-assembled into a net-like structure, or self-deploy into a much larger solar panel. Bakarich et al. (2015) and Tibbits et al. (2013) claimed that another

major application for 4DP is the area of soft robotics that could make use of flexible shells and printable actuators to reduce and remove heavy, expensive, error-prone and complex electro-mechanical parts such as motors, sensors and electronics.

One of the early fundamentals of 4DP was proposed by Farhang et al. (2017) who suggested that there are five elements of 4DP, including the AM process, the stimuli-responsive material (SRM), the stimuli, the interaction mechanism and mathematical modelling. The AM process is necessary to produce the physical components and the stimuli triggers the printed part into a new form. Exposure to water or changes in temperature are most commonly used as the activation stimuli. Other less-exploited means such as magnetism, UV light, electricity and pH levels are also possible. In addition, combined methods of stimuli using different SRMs can allow a 4DP part to exhibit a plurality of functions and display distinct controllable reconfigurations. (Kuksenok 2016). Most AM processes can be used for 4DP as long as the selected SRM is compatible with the machine (Pei and Loh 2018). The interaction mechanism is the programming process in which the material is deformed into a temporary shape. Lastly, the mathematical modeling process defines the material distribution and its structure needed to achieve the desired change in shape. The mathematical modelling process is intrinsically linked to the design of the Computer-Aided-Design model. Taking a step further, Nam and Pei (2019) suggested that within the five fundamental elements of 4DP, it is also important to consider the location of the deformation (the position), the type of shape-change effect (the shape-changing behavior), and the given duration for the 4DP effect to occur (time) as illustrated in Fig. 1.



**Fig. 1.** A conceptual framework of 4D Printing (Nam and Pei 2019)

4DP enables different structural shapes to be activated in a timely, controlled and coordinated way when exposed to external stimuli. We define that a timely approach refers to the specific moment in time for the trigger and initiation of the shape-changing behavior; while a controlled approach enables a pre-programmed deformation process

to take place across the specified amount of time; and lastly, a coordinated way refers to synchronizing the part (or parts) that behave during the shape changing process.

## 2 Materials, Computer-Aided-Design and Behaviour

### 2.1 Materials and Computer-Aided-Design for 4D Printing

4DP requires the use of active SRMs, including Shape Memory Alloys (SMAs) and Shape Memory Polymers (SMPs) that are most commonly used, although other work has also shown that conventional polymeric materials can have a notable Shape Memory Effect (SME) (Zhou et al. 2015). Organic materials such as wood and paper can be used as bio-responsive materials and this also occurs nature, such as the scales of seed-bearing pine cones that respond to changes in the environment. During a warm and dry climate, the scales open up to release the seeds; and conversely, during a cold or wet season, the scales close to protect the seeds (Song et al. 2015). Rigid materials, often known as passive materials, can be integrated within a 4DP part to demonstrate different types of shape-change behavior (Tolley 2014). For 4DP, specific materials are chosen to harnesses the unique properties to activate the shape changing process. For example, the expansion of water-absorbing materials have the ability to provide energy to trigger a deformation (Pei 2014).

SMPs possess at least two phases. A stable phase stabilizes the polymer and this is also used to return the part back to its original shape; as well as a second and temporary phase (Huang et al. 2010). Such parts can remain in a temporary shape until an external stimuli is applied and then it reverts back to its original shape. This entire process is known as the Shape Memory Effect (SME) which can be reversible or irreversible. A reversible SME requires reprogramming after each recovery. The mechanism of SMPs are achieved through the thermo-responsiveness or chemo-responsiveness of the material. Thermo-responsive SMPs use a glass transition as the threshold temperature to evoke a shape change effect. For chemo-responsive SMPs, immersing the part into a chemical solution stimulates the plasticizing effect of the polymer (Roos and Karel 1991). Thermo-responsive SMPs are usually produced using material extrusion, material jetting, sheet lamination and vat polymerization. Chemo-responsive SMPs usually as hydrogels are produced using material extrusion and sheet lamination (Lee et al. 2017). The choice of the material is the biggest determining factor in the appearance and function of the 4DP part. An efficient SRM should have a good shape fixity for programming and reprogramming, an excellent shape memory effect with fast shape change velocity and can undergo multiple cycles of recovery without losing its functionality. A shape memory test using basic geometrical programming such as folding and bending can be carried out to study the characteristics of a SRM.

Through the use of Computer-Aided-Design (CAD), and simulation, scientists are able to predict the shape change of a 4DP part. Ge et al. (2014) also developed equations to predict the behaviour of self-assembled parts and foldable origami structures. Mao et al. (2015) produced a multi-material layered composite that could achieve a reversible shape changing effect, using the properties of each material that reacts differently to the stimuli. This allows the parts to efficiently switch between a

stable and rigid configuration without the need for manual or mechanical loading. The smart hinge system consists a lower layer made up of a hydrogel being sandwiched between two columns of elastomers while the top layer consists of thermo-responsive SMPs. Small holes are located within the elastomeric layer to permit water for expansion. The difference in rigidity between the materials allows the strip to bend only inwards and in one direction and the design restricts the swelling of the hydrogel in the Z direction, allowing the shape change to only occur in the X-Y direction. Other attempts to create smart 4DP hinges include those proposed by Ge et al. (2014) (Fig. 2a), and those by Tolley et al. (2014) and Na et al. (2015) (Fig. 2b).

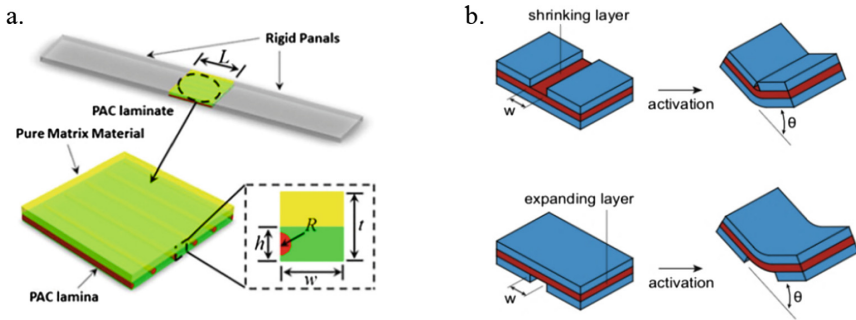


Fig. 2. Examples of smart hinges (a. Ge et al. 2014; b. Tolley et al. 2014; Na et al. 2015)

Other researchers including Kim et al (2012) (Fig. 3a), Wu et al. (2013) (Fig. 3b) and Thérien-Aubin et al. (2015) (Fig. 3c) experimented with the use of CAD to determine the arrangement, location and amount of materials using patterns as opposed to the method of uniform stacking, so that different effects such as swelling ratios could be generated upon activation when exposed to water as the stimuli.

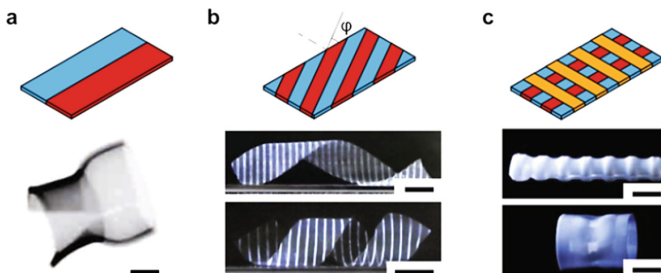


Fig. 3. Arrangement of multiple materials to achieve different shape-changing effects (a. Kim et al. 2012; b. Wu et al. 2013; c. Thérien-Aubin et al. 2015)

4DP has started to gain mainstream popularity as more AM processes and suitable materials are beginning to become commercially available. Photopolymer composites, such as Vero White which is a rigid plastic polymerized with ink; and Tango Black

which is an active rubbery material polymerized by monomers have been demonstrated to be suitable for 4DP (Vaezi et al. 2013). The Stratasys Objet Connex machines use the material jetting process to mix and vary the composition of Vero White and Tango Black before UV hardening, leading to different thermo-mechanical properties for the 4DP parts (Mao et al. 2015). Other researchers such as Zarek et al. (2015) demonstrated the use of photopolymers for vat polymerization using the Asiga Pico Plus 39 Printer. Monzón et al. (2017) explored the use of TPU materials with shape memory properties in a pelletized form and subjecting the material with an extrusion-based AM system. They developed an experimental extruder and a measurement device to precisely calculate the recovery force to ascertain the quality of the processed parts. Using the results of the recovery force as a baseline, they further improved the geometry and build parameters and demonstrated the potential of this material and by producing a working coil mechanism that could actuate and move in a vertical axis (Fig. 4).





Fig. 4. Programmed part and AM coil in its flat form (Monzón et al. 2017)

### 2.2 Shape Changing Behaviours of 4D Printed Parts



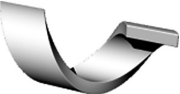



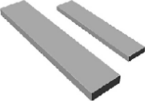


To identify the types of shape change behaviour for 4D Printed Parts, Nam and Pei (2019) analyzed existing literature and identified 11 possible types of shape changing behaviour that could be achieved using 4DP. Taking a step further, they provided definitions of the deformation to distinguish the different types of deformation (Table 1).

Table 1. Definitions of shape-change behaviours (Nam and Pei 2019)

Behaviour	Definition
1. Folding 	“Folding is caused by a stress mismatch between rigid and active materials, which is possible with various swelling ratios” Farhang et al. (2017), Raviv et al. (2014) and Tibbits (2013)
2. Bending 	“Bending is the swelling or shrinkage mismatch between both layers in response to activation stimuli, while sustaining the same strain at the interface between both layers, could result in different types of deformation” Cendula et al. (2009), Gladman et al. (2016), Wu et al. (2016) and Zhang et al. (2016)

(continued)

**Table 1.** (continued)

Behaviour	Definition
3. Rolling 	“Rolling deformation is a normalized curvature that varies depending on both the expansion mismatch and the thickness, which is a nonlinear relationship between the rolling radius of one hand and the ratio of expansion and the sample thickness” Byun et al. (2013), Ge et al. (2013) and Gladman et al. (2016)
4. Twisting 	“Twisting deformation printed the fibers with certain angles to induce twisting, and by adjusting the print angles of active fibers, the final twist angle would be changed” Zhang et al. (2016)
5. Helixing 	“Helixing deformation is made by a uniaxial expanding/shrinking active layer for a nonzero angle between the main straining direction of the active layer and the main axis of the bilayer strip” Janbaz et al. (2016) and Zhang et al. (2016)
6. Buckling 	“Buckling deformation that compressive stresses above a certain critical value will induce out-of-plane buckling of the flat structure” van Manen et al. (2017)
7. Curving 	“Based on the light intensity gradient along the thickness of material, a stress gradient could be created, which results in spontaneous curving of the structure after release from the substrate” Zhao et al. (2017) and Tibbits (2013)
8. Topographical change 	“Mountain and valley features can be generated from concentric circles in the presence of an appropriate stimulus. Surface topography is the representation of local deviations of a surface from a flat plane. These features usually occur under compressive loading conditions” Wang and Zhao (2014), Hu et al. (2017) and Tibbits et al. (2014)
9. Expansion/contraction 	“This mechanism is driven by a variety of expansion ratios between active and rigid materials, which consist of scalable, hydrophobic active materials and rigid materials” Bakarich et al. (2015), Raviv et al. (2014) and Yu et al. (2015)
10. Waving 	“Wave shape deformation could occur in bilayers with comparable stiffness and layer thickness through swelling/shrinkage mismatch in response to activation stimuli” Cendula et al. (2009) and Wu et al. (2016)
11. Curling 	“Curling deformation is enabled by a stress mismatch between rigid and active materials from their different swelling properties” Tibbits et al. (2014)



### 2.3 Communicating the Intent of 4D Printing

Advances in AM processes allow specific materials that possess performance properties to be precisely deposited within a three-dimensional space (Pei 2014). A 4D printed component is time dependent yet predictable. For such predictions to become accurate, specialized software is needed to design specific folds, creases, patterns and to enable the controlled sequence of deformation. The current challenge is to develop software that can control the sequence so that the structure can be designed to behave in a controlled way. Autodesk developed Project Cyborg which is a cloud-based design tool capable of programming matter from nanoparticle to human scale, enabling the simulation of self-assemblies, programmable materials and specifying the optimization parameters for geometrical transformation, shape constraints and the shape changing sequence (Autodesk Research 2019). However, while advancements in CAD, Computer-Aided Engineering (CAE), simulation, materials database and predictive analysis have progressed, one key area that has been rarely investigated is the communication of design intent on paper. Research by Azhar and Pei (2019) have investigated how designers and engineers communicate the design intent of 4DP parts on paper. Using focus groups, interviews and observations, their results show that even though a diverse range of sketches were produced, there were some similarities in which most participants used colours to distinguish different parts and materials; using arrows to indicate the shape changing behaviour and direction of deformation; and using symbols to indicate the stimuli and the sequence of time. More importantly, their work highlighted that even though AM capability has advanced, there is still a need to investigate how to communicate the design of 4DP parts.

### 2.4 Summary and Future Work

This paper provides a conceptual understanding of 4DP which includes aspects of material science, digital manufacturing, CAD, shape changing behaviours and its potential applications. The paper also raises future challenges such as communicating the intent for the Design of 4DP (Df4DP) parts which is an important facet for us to gain a broader understanding of the subject. We are on the cusp of a new industrial revolution with the convergence of different disciplines. 4DP promises opportunities for new markets and industrial applications. As our understanding of material science knowledge grows and the ability to produce new digital materials, another paradigm opens up. What would be the next big thing? Will 5DP or 5D Printing allow living micro-organisms to be embedded within AM parts to enable components to objectively make their own independent decisions or choose how to behave? Some emerging examples could include printing tissues that form living structures, or printing electronic sensors directly onto our body (Heilweil 2018), possibly leading to the field of human augmentation - bring on Human 2.0!

## References

- Autodesk Research: Projects - Project Cyborg and 4D Printing. <https://www.autodeskresearch.com/projects/4dprinting>. Accessed 10 July 2019
- Azhar, F.E., Pei, E.: Investigating the Communication of 4D printing among product designers and manufacturing engineers. In: 16th Rapid Design, Prototyping and Manufacturing Conference, Brunel University London, UK (2019)
- Bakarich, S.E., Gorkin, R., Spinks, G.M.: 4D printing with mechanically robust, thermally actuating hydrogels. *Macromol. Rapid Commun.* **36**(12), 1211–1217 (2015)
- Byun, M., Santangelo, C., Hayward, R.: Swelling-driven rolling and anisotropic expansion of striped gel sheets. *Soft Matter* **9**, 8264–8273 (2013)
- Cendula, P., Kiravittaya, S., et al.: Bending and wrinkling as competing relaxation pathways for strained free-hanging films. *Phys. Rev. B* **79**, 085429 (2009)
- Farhang, M., Seyed, M., et al.: A review of 4D printing. *Mater. Des.* **112**, 42–79 (2017)
- Ge, Q., Qi, H.J., Dunn, M.L.: Active materials by four-dimension printing. *Appl. Phys. Lett.* **103**, 131901 (2013)
- Ge, Q., Dunn, C.K., et al.: Active origami by 4D printing. IOP Publishing Smart Mater. Struct (2014). <http://iopscience.iop.org/0964-1726/23/9/094007/media>. Accessed 10 July 2019
- Gladman, A.S., Matsumoto, E.A., et al.: Biomimetic 4D printing. *Nat. Mater.* **15**(4), 413–418 (2016)
- Heilweil, R.: Wired Magazine - Eyes and Ears 3D-Printed From Flesh Could Boost Our Senses (2018). <https://www.wired.com/story/3d-printed-flesh-body-parts>. Accessed 9 Sept 19
- Hu, G., Damanpack, A., et al.: Increasing dimension of structures by 4D printing shape memory polymers via fused deposition modeling. *Smart Mater* **26**, 125023 (2017)
- Huang, W.M., Ding, Z., et al.: Shape memory materials. *Mater. Today* **13**(7–8), 54–61 (2010)
- Janbaz, S., Hedayati, R., Zadpoor, A.A.: Programming the shape-shifting of flat soft matter: from self-rolling/self-twisting materials to self-folding origami. *Mater. Horiz.* **3**, 536–547 (2016)
- Kim, J., Hanna, J., et al.: Thermally responsive rolling of thin gel strips with discrete variations in swelling. *Soft Matter* **8**, 2375–2381 (2012)
- Kuksenok, O., Balazs, A.C.: Stimuli-responsive behaviour of composites integrating thermo-responsive gels with photo-responsive fibers. *Mater. Horiz.* **3**(1), 53–62 (2016)
- Lee, A., An, J., Chua, C.: Two-way 4D printing: a review on the reversibility of 3D-printed shape memory materials. *Engineering* **3**(5), 663–674 (2017)
- Mao, Y., Yu, K., et al.: Sequential self-folding structures by 3D printed digital shape memory polymers. *Sci. Rep.* **5**, 13616 (2015)
- Markets and Markets: 3D Printing Market by Offering, Process, Application and Geography - Global Forecast to 2023 (2017)
- Monzón, M.D., Paz, R., Pei, E., et al.: 4D printing: processability and measurement of recovery force in shape memory polymers. *Int. J. Adv. Manuf. Technol.* **89**, 1827 (2017)
- Na, J., Evans, A., et al.: Programming reversibly self-folding origami with micropatterned photocrosslinkable polymer trilayers. *Mater* **27**, 79–85 (2015)
- Nam, S., Pei, E.: A taxonomy of shape-changing behavior for 4D printed parts using shape-memory polymers. *Prog. Addit. Manuf.* **4**, 167 (2019)
- Ntounoglou, K., Stavropoulos, P., Mourtzis, D.: 4D printing prospects for the aerospace industry: a critical review. *Procedia Manuf.* **18**, 120–129 (2018)
- Pei, E., Loh, G.H.: Technological considerations for 4D printing: an overview. *Prog. Addit. Manuf.* **3**, 95 (2018)
- Pei, E.: 4D printing – revolution or fad? *Assem. Autom.* **34**(2), 123–127 (2014)

- Raviv, D., Zhao, W., et al.: Active printed materials for complex self- evolving deformations. *Sci. Rep.* **18**(4), 7422 (2014)
- Roos, Y., Karel, M.: Plasticizing effect of water on thermal behavior and crystallization of amorphous food models. *J. Food Sci.* **56**(1), 38–43 (1991)
- Song, K., Yeom, E., et al.: Journey of water in pine cones. *Sci. Rep.* **5**, 09963 (2015)
- van Manen, T., Janbaz, S., Zadpoor, A.A.: Programming 2D/3D shape-shifting with hobbyist 3D printers. *Mater. Horiz.* **4**, 1064–1069 (2017)
- Thérien-Aubin, H., Moshe, M., et al.: Shape transformations of soft matter governed by bi-axial stresses. *Soft Matter* **11**, 4600–4605 (2015)
- Tibbits, S.: 4D Printing. MIT self-assembly lab and Stratasys (2013). <http://www.selfassemblylab.net/4DPrinting.php>. Accessed 10 July 2019
- Tibbits, S., Papadopoulou, A., et al.: Self-Assembly Lab (2013). <http://www.selfassemblylab.net>. Accessed 10 July 2019
- Tibbits, S., McKnelly, C., et al.: 4D printing and universal transformation (2014). [http://papers.cumincad.org/data/works/att/acadia14\\_539.content.pdf](http://papers.cumincad.org/data/works/att/acadia14_539.content.pdf). Accessed 10 July 2019
- Tolley, M., Felton, S., et al.: Self-folding origami: shape memory composites activated by uniform heating. *Smart Mater. Struct.* **23**, 094006 (2014)
- Vaezi, M., Chianrabutra, S., et al.: Multiple material additive manufacturing - Part 1: a review. *Virtual Phys. Prototyp.* **8**, 19–50 (2013)
- Wang, Q., Zhao, X.: Phase diagrams of instabilities in compressed film-substratesystems. *J. Appl. Mech.* **81**, 051004 (2014)
- Wu, Z., Moshe, M., Greener, J., et al.: Three-dimensional shape transformations of hydrogel sheets induced by small-scale modulation of internal stresses. *Nat. Commun.* **4**, 1586 (2013)
- Wu, J., Yuan, C., et al.: Multi-shape active composites by 3D printing of digital shape memory polymers. *Sci. Rep.* **6**, 24224 (2016)
- Yu, K., Dunn, M.L., Qi, H.J.: Digital manufacture of shape changing components. *Extrem. Mech. Lett.* **4**, 9–17 (2015)
- Zarek, M., Layani, M., et al.: 3D printing of shape memory polymers for flexible electronic devices. *Adv. Mater.* **28**, 4449–4454 (2015)
- Zhang, Q., Zhang, K., Hu, G.: Smart three-dimensional lightweight structure triggered from a thin composite sheet via 3D printing technique. *Sci. Rep.* **6**, 22431 (2016)
- Zhao, Z., Wu, J., et al.: Origami by frontal photopolymerization. *Sci. Adv.* **3**(4), e1602326 (2017)
- Zhou, Y., Huang, W.M., et al.: From 3D printing to 4D printing: approaches and typical applications. *J. Mech. Sci. Technol.* **29**(10), 4281–4288 (2015)
- Zolesi, V.S., Ganga P.L., et al.: On an innovative deployment concept for large space structures. In: 42nd International Conference on Environmental Systems, pp. 1–14 (2012)

# **CAD and 3D Data Acquisition Technologies**



# Modeling and Simulation of a Novel Functional Brace for Large Bone Defects

Mohammed S. Alqahtani<sup>1,2</sup>(✉), Abdalla M. Omar<sup>2</sup>, Glen Cooper<sup>2</sup>,  
and P. J. Bartolo<sup>2</sup>

<sup>1</sup> Mechanical Engineering Department, College of Engineering,  
King Saud University, Riyadh, Saudi Arabia

<sup>2</sup> School of Mechanical, Aerospace and Civil Engineering,  
The University of Manchester, Manchester, UK  
mohammed.alqahtani-4@postgrad.manchester.ac.uk

**Abstract.** The treatment of large bone defects often requires the use of an external fixator. However, these fixators present some limitations in terms of pain, morbidity and risk of infection. This paper presents a novel functional brace, being designed to be an alternative to current external fixation devices. Main design requirements are presented in this paper aiming at improving performance and comfort, and reducing costs and weight. The functional brace was tested under impact using finite element analysis (FEA).

**Keywords:** Additive manufacturing · Brace · External fixation device · Finite element analysis · Prostheses · Stress concentration

## 1 Introduction

Musculoskeletal disorders and bone diseases resulting from the ageing population, accidents, wars and natural disasters represent one of the major health concerns in the world [1]. Bone defects with non-union and large bone loss often results in extended healing periods, higher complications rates and long-term morbidity [2]. Moreover, the inoculation of microbial pathogens at the time of initial trauma during the initial fixation surgery or during the healing process may lead to a delay of fracture union, loosening of fixation and chronic osteomyelitis [3]. The treatment of these defects is complex and expensive, placing a burden on the public health system. The costs resulting from the patient's inability to work and mental conditions such as depression as a consequence of the post-traumatic psychological distress are also significant.

A number of surgical techniques are being used to treat large defects but they require multiple procedures and induce significant morbidity. Amputation is in most cases the clinical approach as it provides short recovery time but with significant loss of limb function. Other techniques include internal fixation, bone shortening, external fixation (distraction osteogenesis) and induced membrane. Internal fixation methods such as intramedullary plates to stabilise bone gaps after septic conditions are prone to infection [4]. Recent developments in the field of prosthesis design and manufacturing allows surgeons to replace entire limbs using megaprosthesis. These prostheses, initially developed for the treatment of severe oncological bone loss have been also used in

non-oncological conditions such as acute trauma in severe bone loss and poor bone quality, periprosthetic failures, aseptic and septic post-traumatic failures etc. [5, 6]. However, the use of megaprotheses requires complex surgery and can only be considered in extreme and selected cases. Bone shortening (acute and gradual), with excision of the non-united bone, enables bone healing to begin immediately and assists soft tissue coverage by reducing the defect size on soft tissue tension. The degree of shortening depends on several factors such as the type of bone and the location [7].

External fixation (such as the Ilizarov system) is a versatile method of treating non-union, particularly in the presence of infection and bone loss. They can be used to lengthen and correct deformity, but it usually requires prolonged application time and pin-track infection may require urgent medical or surgical treatment. Moreover, external fixation are heavy and painful to use [8, 9].

This paper presents an alternative method, based on the use of active lightweight functional brace. This brace is being designed under the EPSRC Bone Bricks project aiming to develop and implement a novel low cost osseointegrated modular prosthetic solution to treat large bone loss injuries to enable limb salvage.

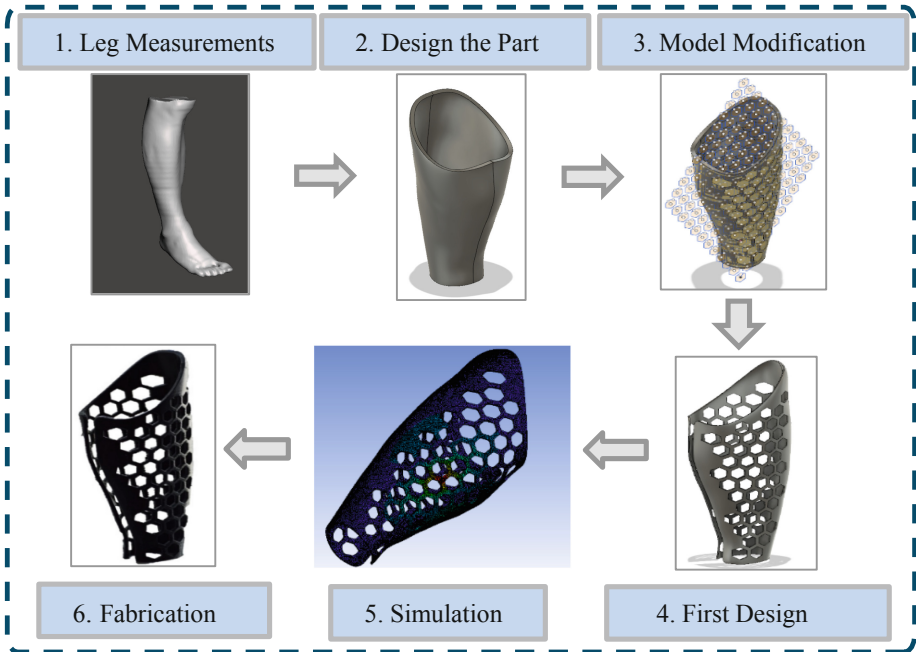
## 2 Product Development Process

The functional brace has been designed considering the following characteristics:

- Customisable (mass personalisation): made to fit for an individual patient, hence maximising functionality.
- Weight and cost reduction: through the use of lightweight materials, less parts and produced using additive manufacturing.
- Enhancing comfort: through a lightweight design and a combination of biocompatible materials with appropriate moisture absorption properties, low friction and good mechanical properties.
- Minimising the risk of infection: by reducing the number of wires.
- Porous structure: to reduce the weight, providing easy access to the wound for treatment, monitoring, air circulation and hygienic purposes.
- Active: as bone is piezoelectric tissue, the device will have two electrodes on the top and the bottom of the wound for electrical stimulation therapy accelerating bone regeneration.

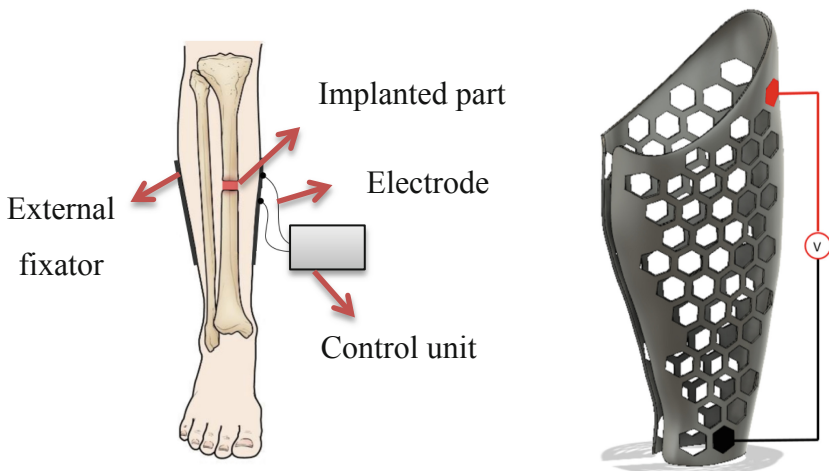
Parametric design will be considered to allow personalisation. Individual braces will be defined from individual leg measurements using anatomic data. Once defined the key geometric parameters (e.g. length and diameters) a light weight geometry will be created using topology optimisation. Proposed designs will be evaluated using FEA. Finally, they will be produced using additive manufacturing. The information flow is briefly presented in Fig. 1.

Previous studies showed that bone regeneration can be strongly enhanced by applying electrical stimulation. Therefore, the brace will incorporate two electrodes and a power source to promote bone regeneration (Fig. 2).



**Fig. 1.** The development steps of the design.

This paper considers three different brace designs based on three different types of holes used to reduce the weight. The first geometry is based on hexagonal holes with rounded edges to reduce stress concentration. The second design is based on ellipse shape and the final design is based on circular holes. In all cases the same volume reduction (32%) was considered.



**Fig. 2.** Functional brace with electrodes for bone electrical stimulation.

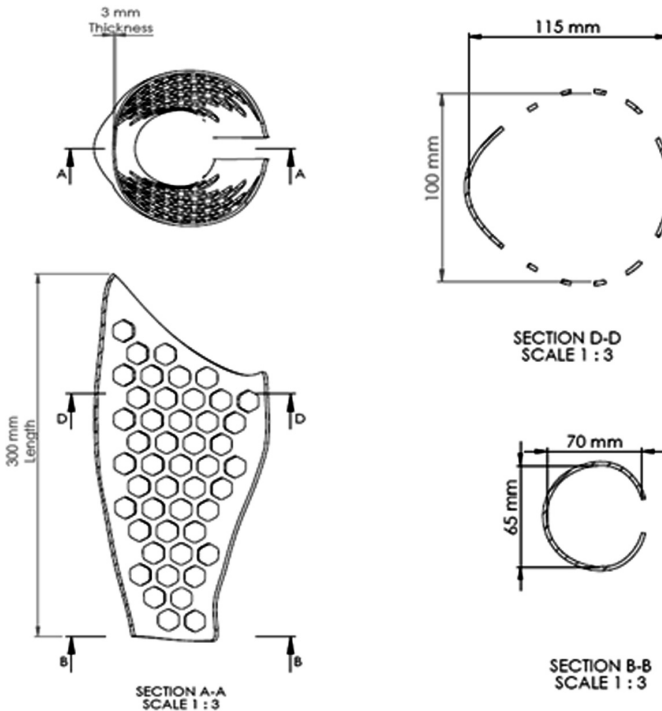
### 3 Modeling and Simulation

Computer Aided Design (CAD) models of the braces were created using SolidWorks. The dimensions of the brace are presented in Fig. 3. Braces are assumed to be made of polyamide (Nylon 6), with properties indicated in Table 1. In a previous paper, we investigated the use of three different materials: Acrylonitrile butadiene styrene (ABS), Polylactic acid or polylactide (PLA) and Polyamide (PA) [10]. Preliminary results show that among these materials, PA is the most suitable material as it shows high flexibility, toughness and capability to absorb high energy during fracture [10].

Different lattice-like brace designs were investigated under impact and considering different load values, representing the loads that might accidentally hit the brace. The areas for the applied load were created on the model with the help of the splint line command of SolidWorks. Numerical simulations were performed using the Ansys Workbench software using tetrahedral elements. The brace was considered to be fixed from the proximal and distal ends to simplify the simulation process and to decrease computational time.

**Table 1.** Material properties of the Nylon (PA).

Young's of modulus (GPa)	Poisson ratio	Yield strength (MPa)	Density ( $\text{g/cm}^3$ )
0.58	0.35	27.8	1.14



**Fig. 3.** The dimensions of the brace.



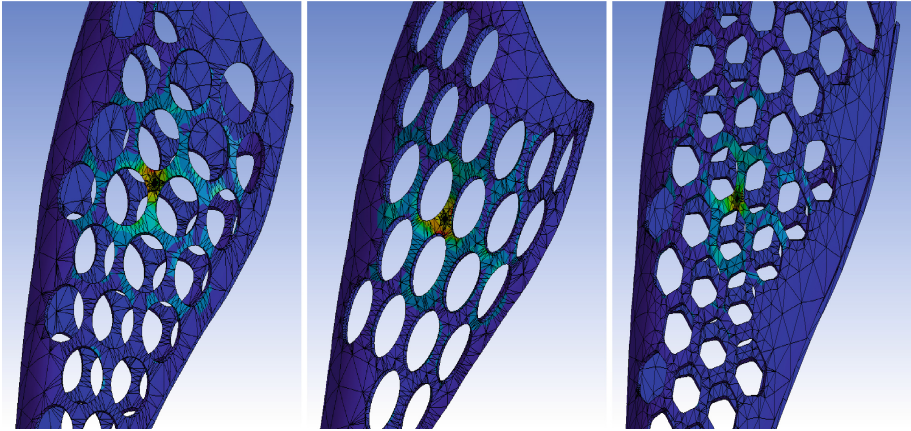
### 4 Results and Discussion

Numerical results for all brace designs are presented in Table 2, showing the maximum deformation and maximum stress as a function of applied load, weight, critical force and specific critical force.

**Table 2.** Numerical results for all brace designs.

		Max. deformation (mm)	Max. Stress (MPa)
<i>Circular pattern</i>			
Applied force (N)	10	1.0376	3.4193
	20	2.0753	6.8386
	30	3.1129	10.258
Weight (g)	290		
F <sub>critical</sub> (N)	81.3		
F* <sub>critical</sub> (N/g)	0.28		
<i>Elliptical pattern</i>			
Applied Force (N)	10	1.4401	4.1221
	20	2.8802	8.2443
	30	4.3204	12.366
Weight (g)	290		
F <sub>critical</sub> (N)	67.44		
F* <sub>critical</sub> (N/g)	0.23		
<i>Hexagonal pattern</i>			
Applied force (N)	10	1.032	5.2157
	20	2.0639	10.431
	30	3.0959	15.647
Weight (g)	290		
F <sub>critical</sub> (N)	53.3		
F* <sub>critical</sub> (N/g)	0.18		

As observed, the weight of all braces is the same as the same volume reduction was imposed to all designs. Maximum stresses increase with the applied load being higher in the hexagonal lattice design due to high stress concentration. Similarly, the critical force, which is the force at which the design will fail, and the specific critical force decrease by moving from the circular design to the elliptical design, and from this to the hexagonal design. Circular and hexagonal designs present similar deformation. Figure 4 shows stress results for all brace designs.



**Fig. 4.** The contours of stress results for circular, elliptical and hexagonal designs (left to right)

Braces were printed using the Ultimaker S5 3D printer. Polyvinyl alcohol (PVA) was used for the supports. The printing temperature at the nozzle was 220 °C and at the platform was 70 °C. The feed rate was set to 60 mm/min, and the layer thickness was 0.2 mm. Figure 5 shows an example of a printed brace, in this case considering the hexagonal lattice geometry.



**Fig. 5.** The printed brace with hexagonal shape without any polishing.

## 5 Conclusion

A novel functional brace for large bone defects is presented. Different lattice-type structures were considered and simulated under impact, using finite element analysis. Results show that among the different configurations, the circular configuration provides better results.

**Acknowledgement.** The first author greatly acknowledges the support received by The King Saud University to conduct his Ph.D. studies.

## References

1. Laurencin, C.T., Ambrosio, A.M.A., Borden, M.D., Cooper Jr., J.A.: Tissue engineering: orthopedic applications. *Annu. Rev. Biomed. Eng.* **1**(1), 19–46 (1999)
2. Knothe, U.R., Springfield, D.S.: A novel surgical procedure for bridging of massive bone defects. *World J. Surg. Oncol.* **3**(1), 7 (2005)
3. Oryan, A., Alidadi, S., Moshiri, A.: Current concerns regarding healing of bone defects. *Hard Tissue* **2**(2), 1–12 (2013)
4. Scholz, A.O., Gehrmann, S., Glombitza, M., Kaufmann, R.A., Bostelmann, R., Flohe, S., Windolf, J.: Reconstruction of septic diaphyseal bone defects with the induced membrane technique. *Injury* **46**, S121–S124 (2015)
5. Parvizi, J., Sim, F.H.: Proximal femoral replacements with megaprotheses. *Clin. Orthop. Relat. Res.* **1976–2007**(420), 169–175 (2004)
6. Calori, G.M., Colombo, M., Ripamonti, C., Malagoli, E., Mazza, E., Fadigati, P., Bucci, M.: Megaprosthesis in large bone defects: opportunity or chimaera? *Injury* **45**(2), 388–393 (2014)
7. Ashman, O., Phillips, A.M.: Treatment of non-unions with bone defects: which option and why? *Injury* **44**, S43–S45 (2013)
8. Solomin, L.: *The Basic Principles of External Skeletal Fixation Using the Ilizarov Device*. Springer, Milan (2008)
9. Fragomen, A.T., Rozbruch, S.R.: The mechanics of external fixation. *HSS J.* **3**(1), 13–29 (2007)
10. Alqahtani, M.S., Omar, A.M., Cooper, G., Bartolo, P.J.: Modeling of a functional brace using the finite element method. In: *Additive manufacturing meets medicine*, Lübeck, Germany, 12–13 September 2019



# AM Tooling for the Mouldmaking Industry

João Carreira<sup>1</sup>, Joel Vasco<sup>1,2</sup> , and Henrique Almeida<sup>1,3</sup> 

<sup>1</sup> School of Technology and Management, Polytechnic Institute of Leiria,  
Leiria, Portugal

joel.vasco@ipleiria.pt

<sup>2</sup> Institute for Polymers and Composites, University of Minho,  
Guimarães, Portugal

<sup>3</sup> CIIC, Polytechnic Institute of Leiria, Leiria, Portugal

**Abstract.** Additive Manufacturing (AM) has proven its value both on the supply-chain and process tooling. Concerning the mouldmaking industry, many studies have been conducted, providing useful information about this manufacturing approach on the mould insert's effectiveness on the mould's cooling stage. Therefore, it is important to assess the feasibility of the use of AM in other mould components where temperature also plays an important role on cycle time. Furthermore, the freeform capacity of the manufacturing process also enables innovative and/or optimized solutions for mould components, providing a significant economic impact, resulting both from mould operation (reduced cycle time) and component's production (conventional manufacturing vs. AM). This work aims also to evaluate the concept of mass customization by developing a common geometry for a hot-runner nozzle bushing, enabling its automatic customization depending on the hot-runner nozzle manufacturer and the cooling requirements of the nozzle. Additionally, generative design is also used to optimize the bushing's volume, reducing build time and costs, providing a more effective cooling of the hot-runners nozzle tip.

**Keywords:** Additive manufacturing · Mould making · Generative design

## 1 Introduction

### 1.1 Additive Manufacturing

Additive manufacturing (AM) has proven its value both on the supply-chain and process tooling and it can be an alternative for moulding components due to its freeform capacity for generating complex geometries with no compromise on tool mechanical properties. Selective Laser Melting (SLM) is one of the most relevant processes on AM technology nowadays, where hot-work steel powder is processed layer-by-layer, by one or more lasers. The process comprehends total fusion of the metal powder, resulting on near 100% solid parts with almost no compromise concerning mechanical properties (Frazier 2014; Gao et al. 2015). Its use on the mouldmaking industry has provided excellent results due to its freeform capacity to build

conformal cooling channels to optimize the injection moulding process by allowing a more uniform and quicker heat removal during the injection moulding cycle (Park and Dang 2012).

## 1.2 Mould Making and Injection Moulding

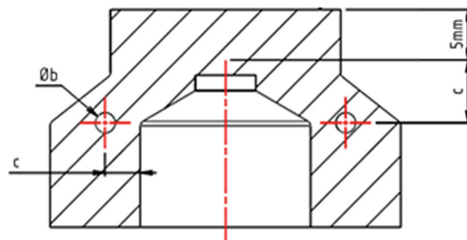
The conventional manufacturing techniques used for cooling channels are limited to linear channels and planar cooling circuits, preventing cooling channels to keep constant distance to the moulding surface for an effective heat transfer, sometimes resulting on unavoidable hot spots. The cooling system design is, therefore, highly dependent on the compromise between temperature uniformity and the duration of the injection moulding cycle (Nickels 2009; Agazzi et al. 2013).

This work aims to evaluate the concept of mass customization by developing a common geometry for a hot-runner nozzle bushing, enabling its automatic customization depending on the hot-runner nozzle manufacturer and the cooling requirements of the nozzle (Bikas et al. 2019). The reengineering of the mould component is the key to a successful introduction of the AM technology into this application domain (Klahn et al. 2014; Vaneker 2017).

Additionally, generative design is also used to optimize the bushing's volume, reducing build time and costs, providing a more effective cooling of the hot-runners nozzle tip.

## 2 Case-Study: Injection Nozzle Bushing

The injection moulding process presents several benefits when AM tooling is used. In this particular case, a bushing which is typically used on the tip of plastic injection nozzles to increase cooling efficiency. This mould component is used to prevent hot spots generated by excessive heat due to the presence of a hot runner nozzle, especially on the direct gating to the plastic parts. The nozzle bushing geometry is simple, although, it enables cooling channels around the sprue, shortening significantly its cooling time. Figure 1 shows the cross-section of a typical bushing nozzle.



**Fig. 1.** Cross-section of a typical nozzle bushing.

The bushing geometry is adapted for each nozzle type, meaning that the mould designer must know in advance the hot-runner nozzle type, dimensions and assembly tolerances to design this component. Although it is not a mandatory component used in mould design, it is often required to prevent hot spots, therefore, suitable for a build-on-demand approach. Considering the thermal and mechanical operating conditions, the nozzle bushing requires operation temperature and surface hardness provided by metals, making SLM a suitable AM technique to produce it.

The metallic freeform building capacity given by SLM enables the build of conformal cooling channels in the nozzle bushing, allowing component design optimization, both in terms of functionality and building costs. The methodological approach for the design optimization of this mould component is depicted in Fig. 2.

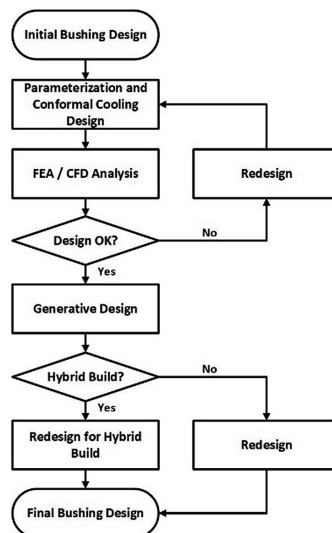
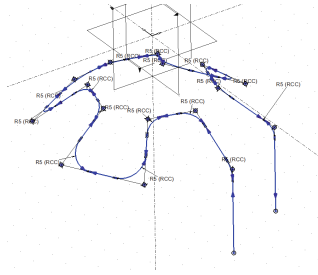


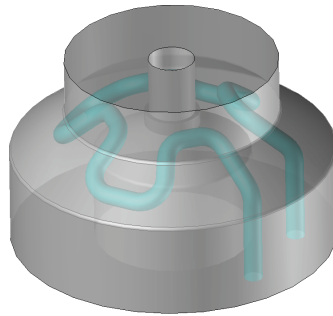
Fig. 2. Methodological design workflow.

## 2.1 Bushing Design for Conformal Cooling

The 3D model of the nozzle bushing was parametrized, enabling quick change of critical dimensions. In particular, the conformal cooling channel dimensional parameters enable validation of distances between the cooling channels and critical distances to the component walls. Figure 3 illustrates the cooling channel's centrelines where the critical relations between dimensions were pre-imposed to respect the best design practices concerning cooling design in moulds. Figure 4 shows the shaded 3D model of the initial nozzle bushing.



**Fig. 3.** Conformal cooling channel's centrelines.

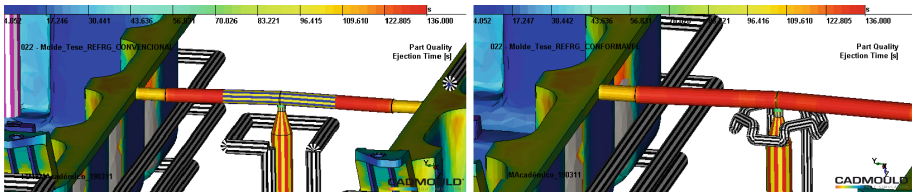


**Fig. 4.** Conformal cooling channels.

## 2.2 Numerical Simulation

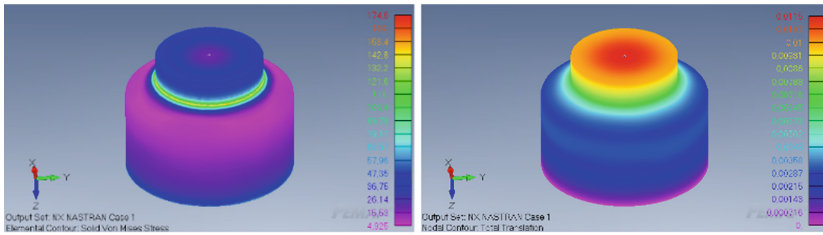
Numerical analysis was conducted to validate the benefits obtained concerning temperature uniformity and to evaluate mechanical performance. Thermal behaviour was evaluated with CADmould<sup>®</sup> 3D-F (SIMCON Kunststofftechnische Software GmbH, Germany) and mechanical performance was assessed with FEMAP<sup>®</sup> NX NASTRAN (Siemens PLM Software, Inc., Plano, USA).

The thermal impact, in this case, has no direct influence on the plastic part, however, it may possess a significant influence on the cooling stage due to the nozzle's tip temperature. The comparison of a conventional cooling strategy vs. a conformal cooling approach (Fig. 5) shows that the runner temperature is kept within the processing window with conformal cooling. Furthermore, the cooling time of the sprue is reduced by 5 s, due to the use of a  $\text{Ø}6$  mm diameter channel, enabling a much more effective positioning of the cooling channel. Conventional cooling channels are limited by tool access and mould plates geometry, enabling the additive approach to succeed.



**Fig. 5.** Runner temperature uniformity for hot-runner nozzle conventional cooling (left image) and for hot-runner nozzle conformal cooling (right image).

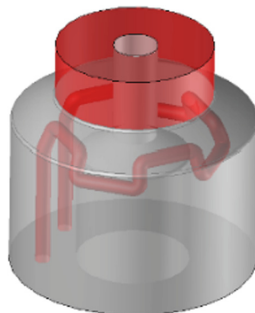
Structural analysis used injection pressure as the most significant mechanical effort imposed. A typical value of 50 MPa, common to most thermoplastic materials, was applied on the back of the nozzle bushing. Stresses are concentrated on a smaller radius area, a geometrical issue easy to correct. The maximum deformation is slightly above 0,01 mm which is acceptable for most moulding applications (Fig. 6).



**Fig. 6.** Stress analysis of nozzle bushing (left image) and deformation (right image).

### 2.3 Generative Design

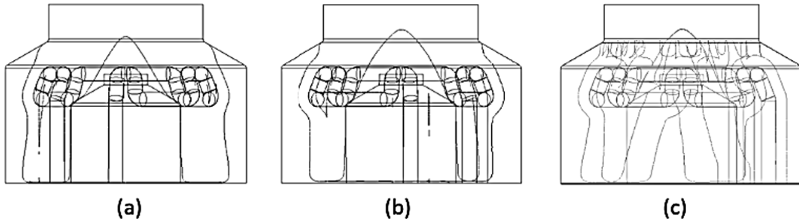
The build-on-demand approach gives way to component optimization through generative design. This technique enables material savings and building time reduction, with a consequent overall costs reduction. Considering the assembly premises for the nozzle bushing, the constraints were defined on the cooling channels, on the top face and the adjacent cylindrical face, as shown on Fig. 7.



**Fig. 7.** Constraints definition for generative design.

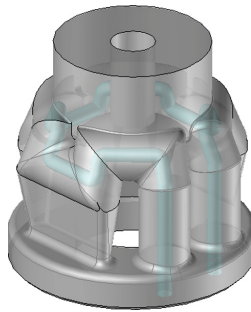


The software used for the generative design approach was SolidEdge® ST10 (Siemens PLM Software, Inc., Plano, USA). Three possibilities were considered for material topological optimization: 35%, 50% and 75%, as depicted on Fig. 8.



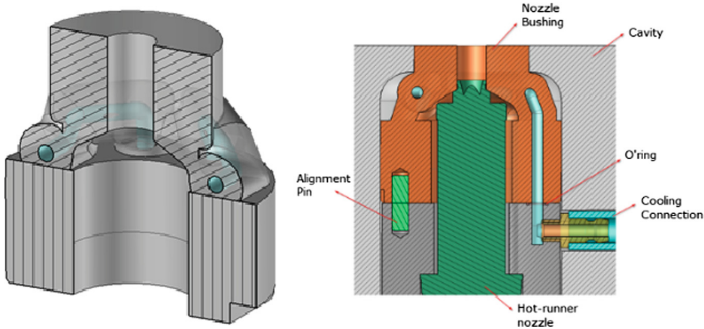
**Fig. 8.** Mass reduction of the nozzle bushing: (a) 35%, (b) 50% and (c) 75%.

Functionality of the component was preserved, even for the highest mass reduction percentage, thus, allowing the geometry to be selected to proceed to production. Concerning SLM building time and costs, the material mass saved provides a competitive edge for a non-standard mould component. Despite the material savings, it's still required to keep the base of the component for cooling connections. The final aspect of the optimized component is shown on the 3D model views (Fig. 9).



**Fig. 9.** 3D model view of the nozzle bushing topologically optimized at 67% mass reduction.

A hybrid building approach was also considered. This approach also provides benefits in terms of feasibility since it combines conventional manufacturing up to the component's height where geometrical complexity begins with additive manufacturing, providing all the design freedom to comply with the final application. Costs are optimized through parallel processing, less building time and less raw material for the most expensive manufacturing process. The cross-section of the hybrid nozzle bushing and its application on an injection mould are shown on Fig. 10.



**Fig. 10.** Cross-section model view of the hybrid nozzle bushing (left image) and its application on an injection mould (right image).

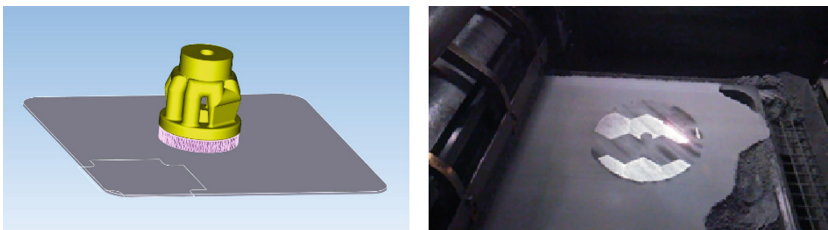
### 3 Manufacture of Injection Nozzle Bushing

The SLM job was prepared on a ProX<sup>®</sup> DMP300 (3D Systems, Rock Hill, USA). The main equipment features are summarized on Table 1.

**Table 1.** ProX<sup>®</sup> DMP300 equipment features.

Equipment feature	Values
Laser power	500 W
Laser type @wavelength	Fiber laser @1070 nm
Build volume	250 × 250 × 300 mm
Layer thickness	10–100 μm (preset 40 μm)
Minimum feature size	100 × 100 × 20 μm (XYZ)
Accuracy	±50 μm

The building job was setup on the equipment’s processing software for a single build of each model to enable processing time evaluation. The evaluated models were the original nozzle bushing (ONB), the topologically optimized nozzle bushing (TONB) and the hybrid nozzle bushing (HNB). Figure 11 shows the job setup and building of the TONB model.



**Fig. 11.** Job setup of the topologically optimized nozzle bushing (left image) and the SLM building chamber (right image).

The comparison between the different nozzle bushing models clarifies the material volume processed to produce each model and the consequent build time and support removal time (Table 2).

**Table 2.** Processing data.

Nozzle bushing model	Preparation time [h]	Processed volume [mm <sup>3</sup> ]	Material saving [%]	Build time [h]	Support removal time [h]	Post-processing time [h]
ONB	0,5	156 424	—	26,4	1,2	1,4
TONB	0,5	102 086	35%	21,0	1,1	1,3
HNB	1,9	51 344	67%	9,8	—	0,5

## 4 Results and Discussion

The three nozzle bushing models analysed in this study enable important preliminary conclusions concerning the use of SLM for the production of an injection mould standard component. The build-on-demand possibility is particularly important to ensure compatibility of the nozzle bushing solution with any hot-runner nozzle type and dimensions, from any hot-runner supplier. On the other hand, preparation, building and post-processing costs must be addressed properly to ensure minimum feasibility, since it can be a single build and not a batch production.

The ONB model consists on the largest processed volume for a nozzle bushing equipped with conformal cooling. Thus, it exhibits the highest values on raw material spent, building time and support removal time.

The TONB model suffered a material reduction, less 35% compared to the ONB model. Such action resulted on a significant decrease on the building time (less 20,5%). Support removal is similar as well as post-processing time.

The HNB model has a significantly higher preparation time compared to the previous models due to its hybrid building approach, however, involving less expensive manufacturing processes, such as CNC machining or WEDM. This model shows the highest processed powder material saving as well as the lowest building time (less 53%). Concerning post-processing, support removal is not required and post-processing operations are limited to surface enhancement on the top face and adjacent cylindrical face to ensure proper assembly of the nozzle bushing.

## 5 Conclusions

The development of components by metal additive manufacturing demonstrates a wide range of possibilities in terms of industrial production. By joining unconventional design methods, using a “additive” mindset, it reveals a substantial reduction in costs and production times, optimizing the process and promoting a faster response in terms of time-to-delivery.

In this case, it is not possible to reduce the mass of the part in terms of performance. In this case, the topological optimization results only in the reduction of manufacturing costs, since the main implication in the cost of production is not the reduction in the volume of raw materials, but rather in the reduction of the processing. On the other hand, the possibility of using a hybrid manufacturing methodology dramatically reduces production costs by substantially reducing processing costs by cutting processing time to more than half in case studies.

With respect to the conformal cooling nozzle bushing, this component was obtained and tested with very satisfactory results by reducing the ejection time of the part in the numerical study carried out for the example mould. This reduction was about 5% of the ejection time, which in this case were removed 5 s of cycle time. Usually, in the automotive industry, injection moulds will have a life of approximately 1 million injections. Generalizing this value for this case study, it can withdraw a reduction of about 1400 h of production, throughout the useful life cycle of the injection mould.

The conformal cooling nozzle bushing occupies much less space than the current solutions available in the market and its format makes its assembly more accessible. The importance of topological optimization and the use of hybrid production methodologies in the development of components by metallic additive manufacturing, both in terms of use of the components and in economic terms, namely in the reduction of cost and time of production, is revealed.

## References

- Agazzi, A., LeGoff, R., Truc-Vu, C.: On the use of topology optimization for improving heat transfer in molding process. In: ESAFORM 2016 Proceedings of the International Conference in Nantes, France, p. 40002. AIP Publishing, Melville (2016)
- Bikas, H., Lianos, A.K., Stavropoulos, P.: A design framework for additive manufacturing. *Int. J. Adv. Manuf. Technol.* (Table 1) (2019). <https://doi.org/10.1007/s00170-019-03627-z>
- Frazier, W.E.: Metal additive manufacturing: a review. *J. Mater. Eng. Perform.* **23**(6), 1917–1928 (2014). <https://doi.org/10.1007/s11665-014-0958-z>
- Gao, W., et al.: The status, challenges, and future of additive manufacturing in engineering. *Comput. Aided Des.* **69**, 65–89 (2015). <https://doi.org/10.1016/j.cad.2015.04.001>
- Klahn, C., Leutenecker, B., Meboldt, M.: Design for additive manufacturing - supporting the substitution of components in series products. *Procedia CIRP* (2014). <https://doi.org/10.1016/j.procir.2014.03.145>
- Nickels, L.: Channelling quality for moulded parts using fast manufacturing. *Met. Powder Rep.* **64**(8), 8–12 (2009)
- Park, H.-S., Dang, X.-P.: Design and simulation-based optimization of cooling channels for plastic injection Mold. In: Volosencu, C. (ed.) *New Technologies - Trends, Innovations and Research*, pp. 19–44. InTechOpen (2012)
- Vaneker, T.H.J.: The role of design for additive manufacturing in the successful economical introduction of AM. *Procedia CIRP* **60**, 181–186 (2017). <https://doi.org/10.1016/j.procir.2017.02.012>



# 3D Printing: An Innovative Technology for Customised Shoe Manufacturing

Tatjana Spahiu<sup>1</sup>(✉), Erald Piperi<sup>2</sup>, Andrea Ehrmann<sup>3</sup>,  
Henrique A. Almeida<sup>4,5</sup>, Rita M. T. Ascenso<sup>4,5</sup>,  
and Liliana C. Vitorino<sup>4</sup>

<sup>1</sup> Faculty of Mechanical Engineering, Textile and Fashion Department,  
Polytechnic University of Tirana, Tirana, Albania  
tspahiu@fm.edu.al

<sup>2</sup> Faculty of Mechanical Engineering,  
Department of Production and Management, Polytechnic University of Tirana,  
“Mother Tereza” Square, No. 1, Tirana, Albania

<sup>3</sup> Faculty of Engineering and Mathematics, Bielefeld University of Applied  
Sciences, Interaktion 1, 33619 Bielefeld, Germany

<sup>4</sup> School of Technology and Management,  
Polytechnic Institute of Leiria, Leiria, Portugal

<sup>5</sup> Research Center for Information Technology and Communications,  
Polytechnic Institute of Leiria, Leiria, Portugal

**Abstract.** Nowadays, consumers are changing the market dynamics. They have become more critical, active and informed. They pursue more personalised products/services and like to be involved in the design process. Additive manufacturing technologies allows this personalisation of products and new business models should embrace these trends to differentiate and gain competitive advantages. The application of 3D technology is widely spread in different areas including textile and apparel manufacturing. From a physical model, it is possible to create a digital model using 3D scanning technology for redesigning purposes. Among the various applications, the apparel industry has expanded with relevant gains, namely fitting and customisation. Several applications of 3D printing for garment, fashion accessories and footwear are described. These applications are based on 3D models that are digitised through 3D scanning and then modelled using CAD software. A case study of shoe redesign is presented in which engineering design tools are implemented, namely, topological and lattice structural design.

**Keywords:** Personalisation · 3D scanning · 3D printing · Apparel industry · Footwear · Design optimisation

## 1 Introduction

Currently, 3D technology is widely spread in different areas of production. Its application can be found almost everywhere as in architecture, cultural heritage, automotive industry, aerospace, medicine, garment, footwear, fashion accessories, among others. Creating a Computer-Aided Design (CAD) model from an existing physical object

depends on the use of 3D scanning technology. After having a virtual 3D model, replicas are made by 3D printing technology, through an automated additive manufacturing process.

The first Additive Manufacturing (AM) was introduced by Kodama in the 1980s [1]. Although, the first AM technique, commonly called Stereolithography, was developed in 1986 by Charles Hull [2]. A variety of 3D printing technologies boomed after 1990s, developing new materials and manufacturing processes to fulfil a wide range of product specifications such as geometric, mechanical and optical requirements. Generally, the 3D printing technology, also known as AM, can be defined as a group of technologies used to quickly fabricate a scale model of a component or full assembly using 3D CAD data [3–5].

Businesses should pursue in personalisation an opportunity to create differentiation and improve consumer traffic and conversation. Personalisation could be a path to sustainable growth, a way to improve efficiency and reduce costs [6]. Being competitive and fulfilling customers' requirements means accelerating production and producing customised products. For instance, Reverse Engineering (RE) plays a key role in assisting the apparel industry since it converts a tested physical model into digital data for mass production or optimisation. Industry gains competitiveness thanks to speed accuracy, quality and product dimension fitting and fulfilling individual customer's requirements, accelerating full-scale production and producing customised products.

In the shoe manufacturing industry, several RE hardware and software tools have been developed and aided to improve the design and aesthetics of the products [7, 8]. This paper focuses on the following stage of the design process, namely, processing and optimising the initial design that was obtained from the 3D scanned models. Topological optimisation and lattice optimisation was implemented into the design process.

## 2 3D Printed Textile Structure and Apparel

3D printing of textile fabrics is not new in the apparel industry. It was demonstrated using Selective Laser Sintering (SLS) [9, 10] and Fused Deposition Modelling (FDM) technology [11, 12] or direct printing of different geometries on textile fabric [13–15]. Mainly of these tests are performed using FDM printers. This technology enables adding new functionalities that cannot be achieved by conventional textile fabrics, such as point-wise defined mechanical properties, design features or other single-item production properties. Different designers and research groups reported on new materials which can be seen as fabric-like, even without complex micro- or meso-structures creating the feeling of flexibility [16]. Other groups have fabric or combined knitted or woven fabrics with 3D printed geometries [17]. Combining 3D printed forms with textiles structures has been investigated by various researchers to achieve different properties or applications which could not be reached by one of these materials alone [18, 19].

But how strongly do these structures adhere to the textile? Exploring the limitations has led to investigation of adhesion strengths of various 3D printing polymers on textile fabrics [20, 21] and the effect of 3D printing parameters on the adhesion forces between both materials [22]. Various applications of 3D printing on textile fabric are considered as new possibilities for smart and functional textiles which avoid the conventional

printing process [23]. 3D printed objects used as connections between textile and small electronic components have shown the suitability of this technique for electrical and mechanical connections [24] of the resulting multi-material objects [25]. Examples of 3D printing in the garment industry are given by introducing 3D printed parts into garment production as dress [26], corset connector and corset [27, 28]. The first fully functional 3D printed dress, the elegant Drape Dress, was designed by Jiri Evenhuis and Janne Kytanen, both industrial designers. The dress was created using an SLS process with nylon powder [29].

The first attempt to create a 3D printed garment was made by Guy Bingham. The CAD model required two months to construct and shows the possibility to generate complex 3D textile fabrics. Then garment was manufactured using an SLS system [30]. The company Electroloom has created the world's first 3D fabric printer which uses an electro spinning process to convert liquid solutions into solid fibres which are then deposited onto a 3D mould. This process is called Field Guided Fabrication. Essentially an internal electric field inside the machine's chamber guides fibres onto a 3D shape where they are bound together [31]. The first 3D printed fashion collection made at home was presented by Danit Peleg, a fashion student, using printers that anyone could get [32]. One of the main problems with 3D printed garments remains the material, which is rather stiff, when compared to textile fabrics which are light and flexible, allowing body movements. This disadvantage has to be overcome by sophisticated connections of the small parts building up the garment.

Successful case studies in applications for garments, footwear, show the adoption of this technology as part of the process from designing to manufacturing. Among the various applications of 3D printing technology, jewellery production has a growing interest, mainly related with the freedom and easiness in production of complex geometries. Jewellery products when comparing Additive manufacturing technology, namely DMLS, with conventional processes, shows a significant advantage related with the waste of material, freedom in terms of the concept, geometries and achieving high levels of quality [33].

Application of different 3D printing geometries on textile fabric used for skirt production shows new possibility for personalised garment [34] and shoes production [35]. Another use of 3D printing technology in garment industry is testing garment fit on scaled 3D printed models as a first stage before real garment production [36].

Personalised logos or designs can also be produced with the use of 3D printing. Due to the problems with the adhesion of 3D printing materials, several tests are performed to regarding printing parameters to achieve a better adhesion of 3D printing materials on textile fabrics.

Another case and important one is for shoes production, as soles, heels or last production. Figure 1 depicts different objects 3D printed starting from garments, shoes or different objects.

Various applications of 3D printing technology with successful case studies shows the raised impact. These applications apart from creating personalised or customised products or applications, reducing the amount of material waste is one of the main issues. Possible use of 3D printing for clothing and shoe manufacturing has to do with the use of 3D printing as a support for designers, shoe and clothing technologists.



**Fig. 1.** The dress and the bag with 3D printed geometries on the textile fabric [37] and sole for shoes production.

## 2.1 Consumer Personalisation Preferences and 3D Printed Footwear

The market is changing, since the 90's, the market is characterised by heterogeneous consumers' desires, unstable demand, product consciousness, the buyer power increase as well as the competition intensity [38]. Kumar [39] refers that we are assisting a shift from mass-customisation to mass-personalisation. Whereas mass-customisation refers to “*product which you do not buy off the shelf or rack in a store – rather you order it directly from a manufacturer, and they tailor make it to your exact requirements or specifications*” [38], mass-personalisation is considered a limiting case of mass customisation [39]. Both strategies pursue the product affordability in consistent with mass production efficiencies, but mass personalisation aims at a market segment of one, while mass customisation aims at a market segment of few [39]. According to the author this shift came from the factors such as new information technology capabilities. For example, peer-to-peer communion technologies, data mining and recommendation engines, consumer relationship management, smart manufacturing systems, mass-customised related factors and the pressure on businesses to deliver personalised products/services at affordable prices. Actually, the social networks and digital devices made consumers more critics and creators, demanding personalised service and expecting to be given the opportunity to shape the products/services that they like [6]. The Deloitte report concludes that more than 50% of consumers have interest in purchasing customised products/services and the majority states willing to pay more for these products and they also like to be involved in all the process.

Hence, marketing managers face strategic choices including the possibility to personalize their offerings [40], or risk losing revenue and consumer loyalty [6]. Businesses should develop capabilities to measure what each individual consumer wants and the processes and resources to provide it. 3D printing enable mass-personalisation at lower costs and allow manufacturers to rethink their supply chain [6].

Having shoes that fit perfectly to your feet now is possible by the use of 3D printing technologies. Companies like Adidas, Rebook, Nike, New Balance, and Under Armour are using 3D printing for producing different shoe parts or whole shoes [41]. Producing footwear by combining 3D printing with craftsman skills is presented by shoe designers [42]. Adidas announced to 3D print 100,000 shoe soles of its Future Craft 4 shoe in 2018 [43]. High heels are a problem, but with the aid of 3D printing technology



more comfortable solutions can be offered for fashionable footwear [44]. Several authors present the combination of traditional patterns in geometric shapes with modern aesthetics using 3D printing technology [45], which can be implemented in a fashionable footwear collection [46].

### 3 Case Study – Shoe Redesign with Topological and Lattice Design

In order to demonstrate the potential of combining several digital and physical technologies, a shoe design case study will be presented. The case study focuses on two different sole models that were previously designed and scanned for this case study. After obtaining the 3D models, the following step consisted in implementing engineering design schemes. The two 3D sole models are illustrated in Fig. 2.

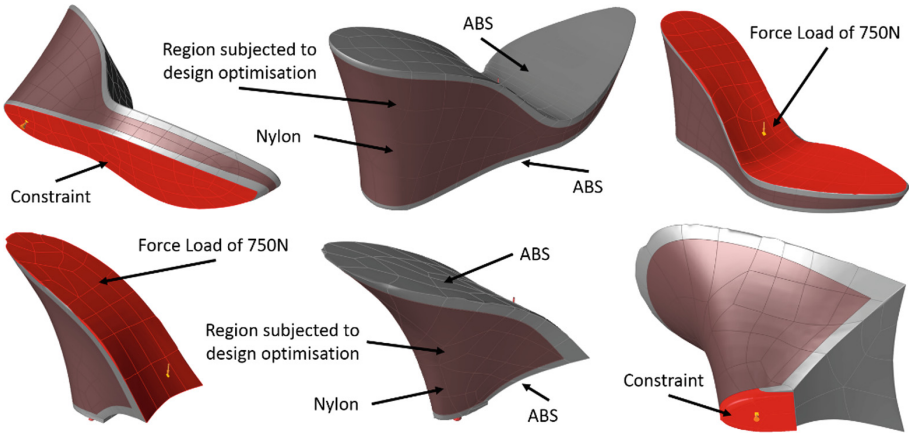


Fig. 2. The two 3D scanned shoe models.

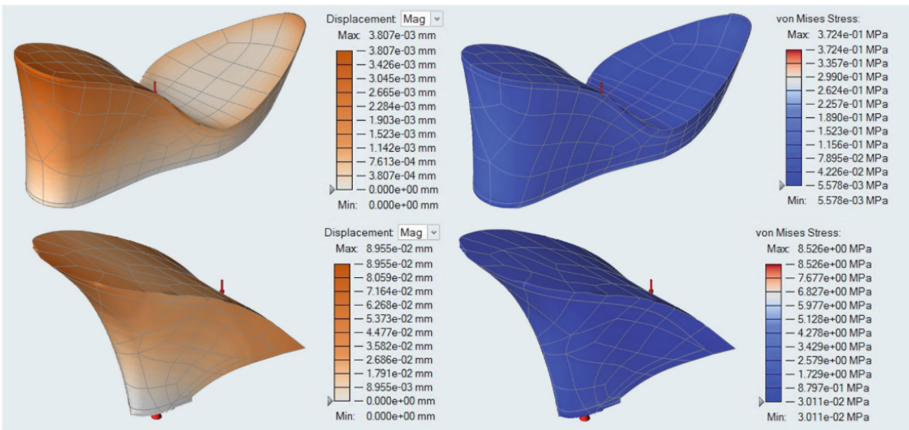
The first step begins with material definition and numerical simulations to validate the selected material. Considering that AM is to be used for the fabrication of the same soles with more affordable systems to guarantee that the price of both soles is similar when compared to other regular designed shoes in the market. Bearing this in mind, the selected option was polymeric materials, namely Acrylonitrile Butadiene Styrene (ABS) and Nylon. These two polymers present high mechanical strength and are both processed by more than one AM system. After defining the material properties, the next step consisted in undergoing structural numerical simulations validating the material selections. Figure 3 illustrates the loads and constraints considered in both soles models. In this particular case, the load considered was of 75 kg and the constraints was fully fixed.

Figure 4 illustrates the numerical results that were obtained from the numerical simulations, namely the displacement and the von Mises stress which validate the material selection indicating its capability of withstanding the loads.

After performing the numerical simulations and validating the material selection, topological optimisation was performed. Topological optimisation is by definition an optimisation scheme based on a mathematical method that optimizes the material layout within a given design space, for a given set of loads, boundary conditions and constraints with the goal of maximizing the system performance. The topological optimisation scheme took into account the loads and constraints defined in the previous



**Fig. 3.** The two sole models indicating the material, loads and constraints.



**Fig. 4.** Displacement and von Mises Stress values for both shoes.

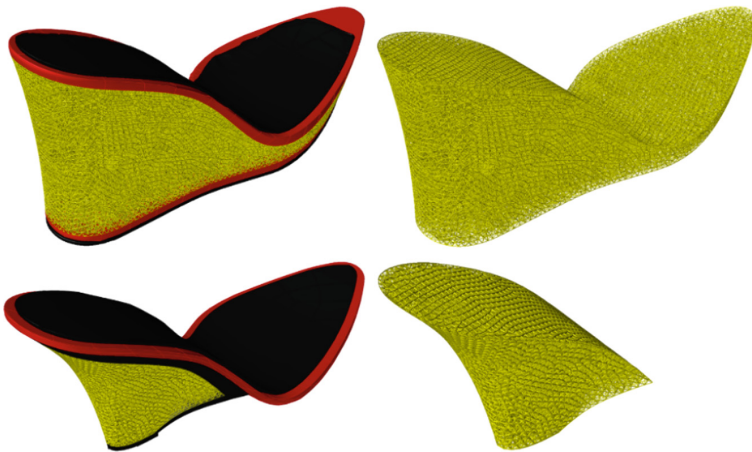
numerical simulations. The material percentage reduction for both soles was of 30% and the area selected in which the topological optimisation will occur is illustrated in Fig. 3. Figure 5 illustrates the optimised topological design for both shoes.

Additionally, a lattice design was also implemented in order to obtain a design fully differentiated from existing shoes available in the market. Similar to the topological optimisation scheme, the loads, constraints and percentage of material reduction was similar to the previous simulations. Figure 6 illustrates the optimised lattice design for both soles.

From the work presented, it is possible to observe that engineering design schemes may be introduced in shoe design with an additional characteristic of numerical simulations in order to predict the product’s mechanical performance. To end the product design cycle, the following step is to produce both designs for consumer approval, which may suffer new iterations according to the consumer’s preferences.



**Fig. 5.** Topological optimisation solutions for both shoes.



**Fig. 6.** Lattice optimisation solutions for both shoes.

## 4 Conclusion

Personalisation helps to improve the efficiency and reduce costs, offering the companies a sustainable growth with differentiated products and services in a profitable manner. This is already possible due to the advanced digital and physical manufacturing systems and distribution technologies. This allows the creation of personalised or customised pieces of garment, reducing the amount of material waste and increasing the consumer's satisfaction.

3D scanning can be used as a support for shoe and clothing designers since it permits the product personalisation, being able to accommodate certain unique personal

characteristics. These 3D technologies propel garment industry to a high level; allowing competitiveness, diversity, customisation and better fit, which contributes to increase consumer satisfaction and profitability.

In this paper, a case study focused on two different sole models that were previously designed and 3D scanned for redesigning is presented. After obtaining the 3D models, engineering design schemes was implemented, namely topological and lattice design. From the framework presented, it is possible to observe that engineering design schemes can be introduced in shoe design with an additional characteristic of numerical simulations in order to predict the product's mechanical performance while maintaining a tailored aesthetic appearance.

## References

1. Kodama, H.: Device of three-dimensional fabrication. Japanese Patent 56-144478 (1981)
2. Hull, C.W.: Apparatus for production of three-dimensional objects by stereolithography. Patent US Patent 4 575 330, 8 August 1984
3. efunda. [http://www.efunda.com/processes/rapid\\_prototyping/intro.cfm](http://www.efunda.com/processes/rapid_prototyping/intro.cfm). Accessed 22 July 2017
4. Dickens, P.M.: Research developments in rapid prototyping. *J. Eng. Manuf.* **209**(4), 261–266 (1995)
5. Mahindru, D.V., Priyanka Mahendru, S.R.M.G.P.C., Ganj, T.: Review of rapid prototyping-technology for the future. *Glob. J. Comput. Sci. Technol.* **13**(4) (2013)
6. Deloitte: The Deloitte Consumer Review: Made-to-order: The rise of mass personalisation Contents (2019)
7. Goehrke, S.A.: 3D Printing Keeps German Shoe Company a Step Ahead with Shoe Lasts 3D Printed In-House, 26 July 2017. <https://3dprint.com/182190/german-reprap-oberle-shoes/>. Accessed June 2019
8. White, C.: Disrupting Global Footwear Market with Tech, 1 July 2019. <https://3dshoes.com/blogs/news>. Accessed July 2019
9. Beercroft, M.: 3D printing of weft knitted textile based structures by selective laser sintering of nylon powder. In: *Global Conference on Polymer and Composite Materials* (2016)
10. Timmermans, M., Grevinga, T., Brinks, G.J.: Towards 3D printed textiles. In: *15th AUTEX World Textile Conference*, Bucharest, Romania (2015)
11. Patsch, L., Vassiliadis, S., Papageorgas, P.: 3D printed of textile structures. In: *5th International Istanbul Textile Congress*. Istanbul, Turkey (2015)
12. Melnikova, R., Ehrmann, A., Finsterbusch, K.: 3D printing of textile-based structures by Fused Deposition Modelling (FDM) with different polymer materials. In: *IOP Conference Series: Materials Science and Engineering* (2014)
13. Pei, E.: Direct 3D printing of polymers onto textiles: experimental studies and applications. *Rapid Prototyp. J.* **21**(5), 556–571 (2015)
14. Spahiu, T., Fafenrot, S., Grimmelsmann, N., Piperi, E., Shehi, E., Ehrmann, A.: Varying fabric drape by 3D-imprinted patterns for garment design. In: *17th World Textile Conference AUTEX 2017- Textiles - Shaping the Future*, Greece, Corfu (Kerkyra) (2017)
15. Rivera, M.L., Moukperian, M., Ashbrook, D., Mankoff, J., Hudson, S.E.: Stretching the bounds of 3D printing with embedded textiles. In: *Conference on Human Factors in Computing Systems*, Denver, Colorado, USA (2017)

16. Mikkonen, J., Kavioja, S., Suonsilta, H., Myllymäki, R., Vanhakartano, S.: Printed material and fabric. In: Nordic Design Research Conference, Copenhagen-Malmö (2013)
17. Döpke, C., Grimmelsmann, N., Ehrmann, A.: 3D printing on knitted fabrics. In: Textile Finishing, pp. 97–98 (2017)
18. Sabantina, L., Kinzel, F., Ehrmann, A., Finsterbusch, K.: Combining 3D printed forms with textile structures – mechanical and geometrical properties of multi-material systems. In: IOP Conference Series: Materials Science and Engineering (2015)
19. Julius, A., Lutz, M., Finsterbusch, K., Ehrmann, A.: Integration of woven fabrics in 3D printed elements to enhance the mechanical properties. Melliland International (2017)
20. Neuß, J., Kreuziger, M., Grimmelsmann, N., Kroger, M., Ehrmann, A.: Interaction between 3D deformation of textile fabrics and imprinted lamellae. In: International Textile Conference, Aachen Dresden Denkendorf (2016)
21. Malengier, B., Hertleer, C., Cardon, L., Van Langenhove, L.: International Conference on Intelligent Textiles and Mass Customisation (ITMC 2017), Het Pand, Onderbergen 1, 9000 Gent, Belgium (2017)
22. Spahiu, T., Grimmelsmann, N., Ehrmann, A., Piperi, E., Shehi, E.: Effect of 3D printing on textile fabric. In: 1st International Conference on Engineering and Entrepreneurship. Tirana, Albania (2017)
23. Sanatgar, R.H., Campagne, C., Niertrasz, V.: Investigation of the adhesion properties of direct 3D printing of polymers and nanocomposites on textiles: Effect of FDM printing process parameters. *Appl. Surf. Sci.* **403**, 551–563 (2017)
24. Grimmelsmann, N., Martens, Y., Schäl, P., Meissner, H., Ehrmann, A.: Mechanical and electrical contacting of electronic components on textiles by 3D printing. *Procedia Technology* **26**, 66–71 (2016)
25. Ehrmann, A.: Combining 3D-Printing with Fibrous Materials - Approaches to Novel Multi-Material Objects. The Masterbuilder, pp. 170–172 (2016)
26. Sun, D., Valtas, A.: 3D printing for garments production: an exploratory study. *J. Fash. Technol. Text. Eng.* **4**(3), 2016 (2016)
27. Mikkonen, J., Kavioja, S., Suonsilta, H., Myllymäki, R., Vanhakartano, S.: Printed material and fabric. In: Nordic Design Research Conference, Copenhagen-Malmö (2013)
28. Lussenburg, K., Van Der Velden, N., Doubrovski, Z., Karana, E.: Designing with 3D printed textiles. In: International Conference on Additive Technologies, Vienna, Austria (2014)
29. Yap, Y.L., Yeong, Y.: Additive manufacture of fashion and jewellery products: a mini review. *Virtual Phys. Prototyp.* **9**(3), 195–201 (2014)
30. Bingham, G.A., Hague, R.J.M., Tuck, C.J., Long, A.C., Crookston, J.J., Sherburn, M.N.: Rapid manufactured textiles. *Int. J. Comput. Integr. Manuf.* **20**(1), 96–105 (2007)
31. The World's First 3D Fabric Printer. Electroloom. <https://www.kickstarter.com/projects/electroloom/electroloom-the-worlds-first-3d-fabric-printer/description>. Accessed July 2017
32. Krassenstein, E.: Danit Peleg Creates First 3D Printed Fashion Collection Printed Entirely at Home, 22 July 2015. <https://3dprint.com/83423/danit-peleg-3d-printed-fashion/>. Accessed June 2019
33. Ferreira, T., Almeida, H.A., Bártolo, P.J., Campbell, I.: Advanced Strategies for Jewellery Production
34. Spahiu, T., Grimmelsmann, N., Ehrmann, A., Piperi, E., Shehi, E.: Effect of 3D printing on textile fabric. In: 1st International Conference Engineering and Entrepreneurship, Tirana, Albania (2017)
35. Spahiu, T., Piperi, E., Grimmelsmann, N., Ehrmann, A., Shehi, E.: 3D printing as a new technology for apparel designing and manufacturing. In: Aachen-Dresden-Denkendorf International Textile Conference, Dresden, Germany (2016)

36. Spahiu, T., Grimmelsmann, N., Ehrmann, A., Shehi, E., Piperi, E.: On the possible use of 3D printing for clothing and shoe manufacturing. In: 7th International Conference of Textile, Tirana, Albania (2016)
37. Spahiu, T., Piperi, E., Ehrmann, A., Shehi, E., Rama, D.: 3D printed geometries on textile fabric for garment production. In: Progress in Digital and Physical Manufacturing, Leiria, Portugal (2019)
38. Pine, B.J.: Mass Customization: The New Frontier in Business Competition. Harvard Business School Press, Boston (1993)
39. Kumar, A.: From mass customization to mass personalization: a strategic transformation. *Int. J. Flex. Manuf. Syst.* **19**, 533–547 (2008)
40. Ji, Y., Jiao, R.J., Zhou, F.: Affective and cognitive design for mass personalization: status and prospect. *J. Intell. Manuf.* **24**, 1047–1069 (2013)
41. <https://www.3dprintingmedia.network/five-footwear-industry-leaders-using-3d-printing-for-production-today/>
42. <https://all3dp.com/shoe-designer-katrien-herdewyn-creates-beautiful-3d-printed-footwear/>. Accessed Oct 2017
43. If the Shoe Fits: 3D Printing and the Future of Manufacturing Footwear. <https://3dprint.com/174833/3d-printing-future-of-footwear/>. Accessed July 2017
44. 98HT works with Chinese students to design convertible 3D printed high-heeled shoes. <http://www.3ders.org/articles/20171011-98ht-works-with-chinese-students-to-design-convertible-3d-printed-high-heeled-shoes.html>. Accessed Oct 2017
45. Sun, L.H.: Development of 3D printed shoe designs using traditional muntin patterns. *Fash. Text. Res. J.* **19**(2), 134–139 (2017)
46. Šafka, J., Mendřický, R., Zelený, P.: Use of reverse engineering methods in the field of fashion design. *Appl. Mech. Mater.* **693**, 189–194 (2014)
47. Spahiu, T., Fafenrot, S., Grimmelsmann, N., Piperi, E., Shehi, E., Ehrmann, A.: Varying fabric drape by 3D-imprinted patterns for garment design. In 17th World Textile Conference AUTEX 2017- Textiles - Shaping the Future, Corfu (Kerkyra), Greece (2017)

# **Materials**



# Polymer Matrix Nanocomposites for 3D Printing

Mylene S. Cadete<sup>(✉)</sup>, Tiago E. P. Gomes, Alfredo Costa,  
Maria Fonseca, João Dias-de-Oliveira, and Victor Neto

Centre for Mechanical Technology and Automation (TEMA),  
Department of Mechanical Engineering of Aveiro, Aveiro, Portugal  
{mylene, tiago.emanuel.gomes, alfredonunodacosta,  
mfonseca, jalex, vneto}@ua.pt

**Abstract.** Additive manufacturing has a great potential since it allows the production of objects with complex geometries, often without auxiliary tools, while still using a wide range of materials. An example is Fused Filament Fabrication (FFF), one of the technologies frequently referred to as 3D printing. One of the most widely used thermoplastic material in FFF is poly(lactic acid) (PLA). This polymer has superior mechanical properties compared to common polymers, in particular the modulus of elasticity, becoming a good substitute in agricultural applications and packaging. However, in sectors such as automotive and electronics, the application of PLA has some disadvantages, such as: low thermal resistance; low thermal deflection temperature; low crystallization rate and reduced impact resistance. With the rising demand for 3D printing solutions, especially for small size parts with specific properties, the development of new materials to suit those demands became of the utmost importance. Thus, one solution that has been adopted in recent years is the incorporation of nanoparticles in the thermoplastics. In this paper, an experimental setup was developed regarding the processing and characterization of two sets of PLA nanocomposites, one with carbon nanotubes (CNT) and another with graphene. The processed nanocomposites' properties were tested through mechanical and melt flow index characterizations to study their suitability for 3D printing.

**Keywords:** Fused filament fabrication · PLA · Nanocomposites · Graphene · Carbon nanotubes

## 1 Introduction

In recent years, 3D printing has undergone a marked evolution, becoming more and more accessible. It has been used in a variety of engineering disciplines, from medicine to aeronautics, with applications ranging from prostheses and prototypes to applications requiring complex geometries. In addition to the ability to produce a wide variety of geometries, through this technology it is possible to obtain parts with high precision, durability and good stability. Various materials of different colors can be 3D printed, including acrylonitrile butadiene styrene (ABS), acrylonitrile styrene acrylate (ASA), polycarbonate (PC), nylon, casting wax and elastomers, and even non-toxic materials with reduced environmental impact such as poly(lactic acid), PLA [1]. Production



times are short and it is possible to locally control properties such as porosity and density [2]. With continued development, the application of 3D printing has been expanded, increasingly demonstrating the ability to compete with other rapid manufacturing techniques.

Due to its mechanical, thermal and physical characteristics one of the polymers most used in 3D printing is PLA. When compared with other common polymers such as polyethylene (PE), polypropylene (PP), polystyrene (PS) and polyethylene terephthalate (PET) [3], PLA's mechanical properties are superior, in particular the modulus of elasticity, and make it a good substitute of other polymers in agricultural applications and packaging. In addition, PLA has good processability and low production costs. With the increasing environmental and sustainability problems associated with oil resources, PLA's potential has been extended to long-term use in the automotive and electronics sectors. However, in these applications this biopolymer has some disadvantages, among them: low thermal resistance; low thermal deformation temperature; low crystallization rate; and reduced impact resistance. These characteristics hamper its use in some consumer products that sometimes require properties such as oxidation resistance and ultraviolet radiation, good durability, electrical conductivity and antibacterial properties [4].

One solution that has been adopted over the last few years to reinforce the material is to incorporate nanoparticles into the polymer matrix. Several types of nanoparticles have been used to reinforce PLA in order to increase its thermal and mechanical properties. Since pioneering work by Toyota Central Research Laboratories in the 1990s [5, 6], research in the field of polymer nanocomposites has achieved substantial improvements in material's properties through the use of low concentrations of nanoparticles, allowing the design and creation of new nanocomposites and structures with improved mechanical, electrical, optical, thermal or magnetic properties and significant industrial impact. In this work we intend to study the feasibility of the use of nanocomposites in 3D printing, using PLA as polymer matrix reinforced with graphene particles and carbon nanotubes (CNT).

## 2 Experimental

### 2.1 Materials

The thermoplastic used for the present experimental work was PLA, characterized by a density of  $1.24 \text{ g/cm}^3$ , a melting temperature between  $145$  and  $160 \text{ }^\circ\text{C}$  and a degradation temperature of  $250 \text{ }^\circ\text{C}$ . As reinforcing nanoparticles to be added to the polymer matrix, two types of carbon nanoparticles with different geometries were used: carbon nanotubes (CNT) and graphene.

The CNTs used have a density of  $2.16 \text{ g/cm}^3$ , diameters between  $20$  and  $40 \text{ nm}$  and a length in the range of  $1$  and  $2 \text{ }\mu\text{m}$ , are multiple walled, and have been functionalized through an acid treatment in order to favor chemical bonding between the nanoparticles and the polymer matrix. [7] The graphene used has between  $3$  and  $8$  layers and is characterized by a thickness of less than  $3 \text{ nm}$ , side dimensions between  $2$  and  $8 \text{ }\mu\text{m}$ , a melting point of  $3652\text{--}3697 \text{ }^\circ\text{C}$  and a density of  $2.25 \text{ g/cm}^3$ .

## 2.2 Nanocomposites

The most common techniques in polymer matrix nanocomposites processing are solution mixing melt blending and in situ polymerization [8–10]. The technique used in this work was fusion mixing, which is more practical, versatile and more suitable when thinking about industrial implementation.

The process was carried out in a Brabender Plastograph EC mixer, which has a processing capacity of 20 cm<sup>3</sup> of material. The nanoparticles were dried in an oven at 100 °C for 24 h to remove moisture. The mixing conditions used were: speed of 50 rpm, at a temperature of 190 °C, for 8 min. The temperature chosen is higher than the melting point (145–160 °C) to allow the polymer to be in a suitable state for mixing, and favor inclusion of the nanoparticles in its matrix. Subsequently, the obtained nanocomposite was cut into pellets.

Nanocomposites were prepared with the two types of nanoparticles and with different volume concentrations. In the table is represented the set of samples prepared (Table 1).

**Table 1.** Prepared samples.

	Nanoparticle	% volume
PLA pure	–	–
P0.5C	CNT	0.5
P1C	CNT	1.0
P0.5G	Graphene	0.5
P1G	Graphene	1.0
P1.5G	Graphene	1.5

## 2.3 Filament Extrusion

The extruder used was an ExtrusionBot, which is typically used in the extrusion of filaments for melt-filament manufacture and is therefore more suitable for the processing of PLA. The extrusion was made at temperature of 190 °C. However, it was necessary to adapt the temperature in the case of nanocomposites with higher fluidity, to allow the extrusion speed to be the same for all, and thus to obtain more accurately the dimensions of the various filaments. During extrusion, particular care was taken to obtain a filament with constant diameter and without curvatures.

## 2.4 Characterization

To study the mechanical properties of prepared nanocomposites, tensile tests were performed. The filaments' mechanical properties depend on the methods used in the tests. The most suitable test for this case is described by ASTM D3379 [11], which is typically used to measure tensile strength and Young's modulus of filaments with high mechanical properties.

To perform the tensile tests, the Shimadzu Autograph AGS-X universal machine was used, and a video-extensometer was used to determine the displacement, the speed used in all tests was 2 mm/min. For each sample the tensile strength was determined by Eq. (1), where  $F_{max}$  represents the maximum force applied to the filament and A the cross-sectional area.

$$\sigma_{max}(MPa) = \frac{F_{max}}{A} \quad (1)$$

The modulus of elasticity was calculated in 3 steps. Using the values obtained in the tests of samples with different lengths, a Force-Displacement plot was plotted and the elastic domain corresponding to 20% and 40% of the maximum force of each test was determined. The conformity value,  $C_a$ , is given by Eq. (2), where D corresponds to the displacement of the material in the tensile test and F to the force applied on the filament.

$$C_a(mm/N) = \frac{D}{F} \quad (2)$$

Knowing the value of  $C_a$  at different lengths, it is possible to sketch a  $C_a$  graph according to the various lengths used and to plot the trend line from the data points through linear regression. The intersection of the trend line with the y-axis allows the identification of the  $C_s$  value, corresponding to the deformability of the equipment, which can be used to calculate true deformability through Eq. (3).

$$C(mm/N) = C_a - C_s \quad (3)$$

Finally, by applying expression (4), it is possible to determine the modulus of elasticity, E, where L is the length of each sample and A is the mean cross-sectional area.

$$E(MPa) = \frac{L}{C \times A} \quad (4)$$

To study the mechanical strength of each filament type were used stress-strain curves. Rupture deformation was determined by measuring the deformation value at the moment before the material reached the break point.

### 3 Results and Discussion

Before proceeding to the analysis and discussion of results, it should be noted that there were two main factors that could induce errors in the results. First, given the extrusion conditions, it was not possible to obtain a perfectly constant filament. An average variation of approximately 6% in diameter was measured. In addition, the stresses induced by the grips were not completely minimized, contributing to premature rupture.

The mechanical properties for the filaments of CNT and graphene nanocomposites are summarized in Table 2.

**Table 2.** Results obtained by tensile tests on nanocomposites.

	Tensile strength (MPa)	Modulus of elasticity (GPa)	Rupture deformation (%)
PLA pure	58.82 ± 3.39	3.525 ± 0.131	6.69 ± 1.35
P0.5C	53.24 ± 5.77	4.519 ± 0.193	2.40 ± 0.14
P1C	55.05 ± 2.08	4.170 ± 0.439	3.20 ± 0.35
P0.5G	52.63 ± 1.75	4.047 ± 0.283	2.24 ± 0.03
P1G	50.93 ± 0.68	3.988 ± 0.135	2.90 ± 0.35
P1.5G	55.17 ± 3.25	4.645 ± 0.330	2.22 ± 0.05

The tensile strength of the filaments with carbon nanotubes and graphene decreased with respect to the PLA pure ones, suggesting that these nanocomposites are more brittle. However, these results may have been influenced by stresses induced by the grips of the test machine, reducing the strength of the material, since rupture was observed in the tightening region in most cases. The fact that the material has been processed several times may have influenced the tensile strength. With the exception of the PLA pure filament, the materials went through processes such as melt blending, injection and extrusion, contributing to the decrease in their tensile strength. Through Table 2 it is possible to verify that the greatest decreases are observed in the filaments with graphene. Tensile strength of the P0.5C and P1C filaments decreased by 9.49% and 6.41% respectively, relative to PLA. As for the P0.5G, P1G and P1.5G these decreased 10.5%, 13.4% and 6.2%. These results lead one to conclude that there may be a decrease in the filament's strength.

Regarding modulus of elasticity, there was an increase of this property compared to PLA pure. The results suggest that processing the filament material can positively affect the modulus of elasticity. The P0.5C filing recorded a considerable increase of 28.2% in relation to that of PLA, whereas with P1C there was an increase of 18.3%. A tendency to increase the modulus of elasticity in graphene containing filaments was theoretically expected because of the high stiffness of graphene. The increases in relation to PLA filing were 14.8%, 13.1% and 31.8% respectively for P0.5G, P1G and P1.5G. Prior to the filament tensile tests, the material was extruded 3 times. These re-processes may have contributed to a significant improvement in the dispersion of the nanoparticles in the matrix, resulting in the increase of the modulus of elasticity. Peinado et al. [12] also defend this justification.

The results of rupture deformation show a generalized reduction in all filaments of nanocomposites of CNT and graphene. This reduction is favored, mainly, by the high rupture deformation verified in the PLA filament. The increased weakness in the filaments of nanocomposites can be explained by the fact that the nanocomposites used are materials of a fragile nature, and therefore their incorporation into the PLA matrix increases the fragility of the polymer.

## 4 Conclusions



In the study of the influence of the filament extrusion process on the mechanical properties, it was concluded that it does not significantly change the tensile strength of pure PLA and that it decreases slightly for P0.5C and P1C. The same was observed in the filaments of graphene nanocomposites. The filaments' modulus of elasticity was determined from the stress-strain curves and an increase of this property was verified in comparison with PLA pure. Finally, the rupture deformation decreased dramatically for both filaments. P0.5C and P1C registered decreases of 64.1% and 52.2% and P0.5G, P1G and P1.5G, decreases of 66.5%, 56.7% and 66.9%, respectively. With the method used, a difficulty in ensuring a good dispersion of nanocomposites with higher concentrations was verified and the high shear stresses that the thermoplastic underwent during the process may have impaired the cohesion of the material.

## References

1. Pham, D.T., Gault, R.S.: A comparison of rapid prototyping technologies. *Int. J. Mach. Tools Manuf* **38**, 1257–1287 (1998)
2. Sun, Q., Rizvi, G.M., Bellehumeur, C.T., Gu, P.: Effect of processing conditions on the bonding quality of FDM polymer filaments. *Rapid Prototyp. J.* **14**(2), 72–80 (2008)
3. Mark, J.E.: *Polymer Data Handbook*. Oxford University Press, London (2009)
4. Raquez, J., Habibi, Y., Murariu, M., Dubois, P.: Polylactide (PLA)-based nanocomposites. *Prog. Polym. Sci. J.* **38**, 1504–1542 (2013)
5. Alexandre, M., Dubois, P.: Polymer-layered silicate nanocomposites: preparation, properties and uses of a new class of materials. *Mater. Sci. Eng.* **28**, 1–63 (2000)
6. Bordes, P., Pollet, E., Avérous, L.: Nano-biocomposites: biodegradable polyester/nanoclay systems. *Prog. Polym. Sci.* **34**, 125–155 (2009)
7. Esumi, K., Ishigami, M., Nakajima, A., Sawada, K., Honda, H.: Chemical treatment of carbon nanotubes. *Carbon* **34**, 279–281 (1996)
8. Al-Saleh, M.H., Al-Saidi, B.A., Al-Zoubi, R.M.: Experimental and theoretical analysis of the mechanical and thermal properties of carbon nanotube/acrylonitrile-styrene-butadiene nanocomposites. *Polymer* **89**, 12–17 (2016)
9. Moniruzzaman, M., Winey, K.I.: Polymer nanocomposites containing carbon nanotubes. *Macromolecules* **39**, 5194–5205 (2006)
10. Coleman, J.N., Khan, U., Blau, W.J., Gun-ko, Y.K.: Small but strong: a review of the mechanical properties of carbon nanotube-polymer composites. *Carbon* **44**, 1624–1652 (2006)
11. Standard Test Method for Tensile Strength and Young Modulus for High-Modulus Single-Filament Materials (D 3379). ASTM International, West Conshohocken, USA (1989)
12. Peinado, V., Castell, P., García, L., Fernández, Á.: Effect of extrusion on the mechanical and rheological properties of a reinforced poly(lactic acid): reprocessing and recycling of biobased materials. *Materials* **8**, 7106–7117 (2015)



# Morphology and Thermal Behaviour of New Mycelium-Based Composites with Different Types of Substrates

Rafael M. E. Alves<sup>1</sup>, M. L. Alves<sup>1</sup> , and Maria J. Campos<sup>2</sup> 

<sup>1</sup> School of Technology and Management,  
Polytechnic Institute of Leiria, 2411-901 Leiria, Portugal  
leopoldina.alves@ipleiria.pt

<sup>2</sup> MARE—Marine and Environmental Sciences Centre,  
Polytechnic Institute of Leiria, 2520-641 Peniche, Portugal

**Abstract.** The need for new green and sustainable materials has been fostering the development, research and introduction of biodegradable materials from natural and renewable sources. Commercially available biodegradable plastics, while minimizing their environmental impact and exhibiting a set of properties that enable the obtainment of industrial components, usually require complex processing methods, are costly and have limited applicability.

A new growth of natural resources based paradigm applied as production process is increasing its relevance as an alternative production process. New materials that combine fungal mycelium with waste materials as coffee grounds or wood waste can be considered as promising to fulfill this new paradigm.

This new biomaterial mycelium based composites present controllable and adjustable properties during their growth, being able to grow and penetrate organic substrates, thus forming a tangle of branched fibers and a structure that presents some thermo-mechanical properties similar to the ones of plastics.

The aim of the present study was the selection of the optimal inoculation temperature, light, humidity and the best substrate for the fastest and consistent mycelium growth. Four types of mycelium were incubated, namely *Pleurotus ostreatus* (382), *Hypsizygus ulmarius* (420), *Ganoderma lucidum* (560) and *Trametes versicolor* (620). The influence of the three substrates (coffee grounds, pine waste and general wood waste) on the growth was analyzed both morphologically and thermo-mechanically by means of differential scanning calorimetry (DSC) and X-ray micro computed tomography (microCT).

**Keywords:** Mycelium-composite · Biomaterials · Differential scanning calorimetry

## 1 Introduction

### 1.1 The Use of Mycelium-Based Biomaterials

The need for new ecological and sustainable materials has been fostering the research, development and introduction of biodegradable materials from natural and renewable sources. Commercially available biodegradable plastics, although they may offer a

panoply of different properties, usually require difficult and complicated processing methods. Its production and development are characterized by high cost, time-consuming and low processing yield. For these reasons, and even considering that they can resolve various environmental problems, these biodegradable materials continue to be expensive and with limited applications.

One solution to these problems is the development of composite biomaterials with controllable and adjustable properties during their growth, without the need for sophisticated and costly processes. The use of fungal mycelium based materials ensures compliance with this strategy [1].

Mycelium is the vegetative part of fungi. It grows and penetrates organic substrates from which it draws nutrients, thus forming a tangle of branched fibers [2]. The filaments of these fibers are called hyphae consisting of elongated cells with diameters between 1–30  $\mu\text{m}$  [3]. Cell walls are composed of chitin, beta-glucans and proteins [4]. The microfibrils of chitin are responsible for the rigidity and mechanical strength of the hyphae, while the elastic properties, orientation and connections of the hyphae characterize the behavior of the mycelium to mechanical stresses [3].

The mechanical properties of the advanced mycelium-based composite materials can vary consistently due to the alteration of factors such as: fungus species; substrate in which it grew; environmental conditions during its growth and also genetic changes in the mycelium [1, 5]. It is possible to obtain properties similar to materials of plant origin such as wood, cork or bamboo, thermoplastics such as polyethylene, polypropylene or polyvinyl chloride (PVC) and also open cell foams [3, 5].

The production or 'cultivation' of advanced mycelium-based materials is by itself innovative and sustainable. As a basic raw material, it requires organic compounds, often organic residues, with a high availability of renewable resources or agricultural residues for use as a substrate [5]. The whole process has a low energy dependency being only essential to provide a small increase in temperature for a short time so that the mycelium stops its growth and becomes inert [1].

The composite mycelium-based materials are totally constituted by biological components and totally biodegradable, being possible to discard these products at the end of their life cycle with little or no economic and environmental costs [6].

## 1.2 Mycelium Based Material Production

Mycelium-based products require a production process that differs significantly from traditional industrial processes in the materials production. The process can be divided into several growing stages, which were based on the existing industrial cultivation of mushrooms, and at specific stages for the manufacture of mycelium-based materials [6].

The first step is choosing the substrate. The substrates must be formed by organic material, so that the mycelium can, through the secretion of enzymes, degrade the polymers present in the substrate and convert them into molecules that can be absorbed as nutrients [5]. The most suitable composition of the substrate will depend on the fungus in question as well as the material application [6].

The second step is the preparation of the substrate in order to prevent other organisms such as bacteria, insects or other fungi from hindering the growth of the desired fungus. There are four possible methods for the important cleaning of the substrate [6]:

(i) sterilization; (ii) pasteurization; (iii) chemical treatment; (iv) natural composting. Each method has its own advantages and disadvantages, and the main factors to be considered are the protection of the substrate to the reappearance of unwanted organisms, the energy consumption involved in the process, the necessary equipment and the use of chemicals or release of harmful gases into the environment [6–9].

After the elimination of microorganisms from the substrate it can be inoculated with the desired fungus. The mycelium can be transferred to the substrate by homogeneously mixing previously developed spores [6, 10], or by deposition of a small inoculum of cultures grown on agar medium [1, 5].

The fourth step is the conformation to geometry. The substrates already with the presence of the mycelium are more often placed in molds in order to acquire the desired geometry. These molds can be produced on a large scale [11, 12]. However, in order to overcome the difficulties that the use of molds involves, it is also possible to resort to layered deposition of the substrate already with the mycelium using different 3D printing technologies [13].

The fifth stage affects the growth of the mycelium, that is, the proliferation of hyphae through the substrate. Depending on the type of fungus and the intended application, it is important to choose the most appropriate growth conditions. Factors such as CO<sub>2</sub> concentration and luminosity are quite important in the properties of the material [5]. The growth time of the fungus, also, varies with the species, substrate, environment and application as a final product, and six to thirty days are normally required [6].

Finally, it is necessary to stop the growth of the fungus. With the heating the colonized substrate the fungus becomes inert, stopping its growth. The composite mycelium material can finally be taken off the molds. If necessary, as a way of improving the properties, a protective material layer can be applied [6].

## 2 Methods

### 2.1 Fungi and Substrates

The fungus species *Pleurotus ostreatus* (382), *Hypsizyguus ulmarius* (420), *Ganoderma lucidum* (560) and *Trametes versicolor* (620) were used in the present work and were purchased from a company specializing in the commercialization of fungi mycelia. Cultures were purchased as cultures grown in solid culture media on 90 mm petri dishes and were stored in the dark at 5 °C before use.

The substrates used were pine sawdust, mixed sawdust and coffee grounds. Pine sawdust was supplied by the company EMMAD, S.A. as excess of cut of untreated pinewood. Mixed sawdust was provided by a large DIY store of Leiria (Portugal) as a cut surplus of several uncharacterized commercial woods. The coffee grounds were provided by a local cafeteria.

Potato Dextrose Broth (PDB) and Potato Dextrose Agar (PDA) medium were used to supplement the substrate.



## 2.2 Preparation of Substrates

In order to sterilize all substrates, culture media and materials were placed in an autoclave (VWR, VAPOR-Line Lite) at 120 °C for 15 min. Handling and preparation of culture media and substrates was performed in a Class II biological safety laminar flow cabinet (Telstar, Bio II Advance).

The PDB medium was prepared by dissolving 26.5 g of dehydrated PDB in 1L of distilled water. The three solid substrates were prepared by adding 10 ml of PDB liquid medium for each 2.30 g of pine sawdust, 2.75 g of mixed sawdust and 17.00 g of coffee grounds, creating a substrate of a more pasty consistency. The obtained substrates were then placed in 90 mm petri dishes each containing 30 g of substrate / medium.

The PDA culture medium was prepared by dissolving 6 g of PDB and 3.75 g of agar in 250 ml of distilled water. After cooling for 30 min, after autoclaving, 15 ml of the medium was plated in 90 mm petri dishes. The petri dishes with the PDA medium were stored at 5 °C for a maximum period of 1 week.

**Inoculation of Substrates.** The substrates prepared as indicated in Sect. 2.2 were inoculated with a mycelium growth agar disc on its surface. The inoculum were removed from the ends of the active growing cultures. All petri dishes with the inoculated substrates were sealed with parafilm to prevent desiccation of the substrate, and were grown in an incubator (Memmert-IPP 110) at 25 °C for 49 days. At the end of the growth stage the petri dishes were uncovered and placed in a incubator with natural convection (Binder - Series BD) at 70 °C for 8 h in order to dry the material and cease its growth.

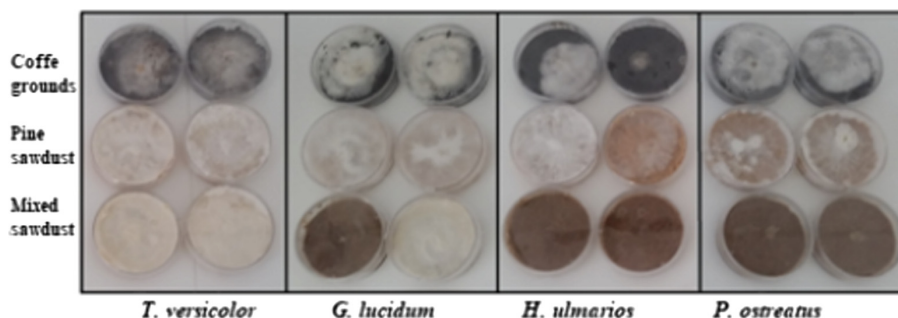
## 2.3 Thermal Tests

The thermogravimetry assay was performed using PerkinElmer's Simultaneous Thermal Analyzer (STA) 6000, heating samples from 30 °C to 600 °C at 10 °C/min and in a nitrogen atmosphere. The Differential Exploratory Calorimeter test was performed on the DSC131 equipment, heating samples from 22 °C to 320 °C at 5 °C/min. Samples in both assays had a mass of  $7 \pm 1$  mg.

# 3 Results and Discussion

## 3.1 Morphological Characterization

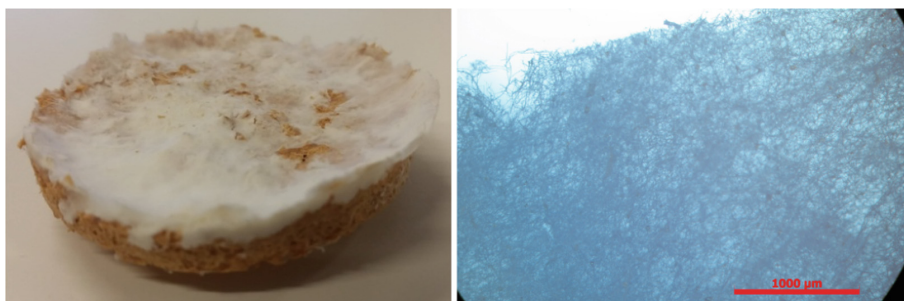
Figure 1 shows the growth of the various fungi after 22 days of the first inoculations performed on all combinations of fungi and substrates used. It is possible to observe that the mycelium of *T. versicolor* grew in the three substrates, in a faster and more consistent way than the other fungi. The mycelium of *T. versicolor* was capable to grow on the mixed sawdust substrate, although this substrate presented major problems for the development of the mycelium of the remaining fungi. The fungi *G. lucidum*, *H. ulmarios* and *P. ostreatus* were unable to grow in the mixed sawdust obtained from mixed commercial woods, often treated/stabilized with chemicals that could inhibit the



**Fig. 1.** Growth of the fungi after 22 days of the first inoculations on the various substrates used.

growth of fungi. In the coffee grounds and pine sawdust substrates all the mycelia from all species grew with no apparent limitations.

Due to the growth pattern of the mycelium on the different substrates, *T. versicolor* were analyzed in more detail on the three substrates and all the other fungi on the pine sawdust substrate. In order to guarantee further growth of the fungi all samples were grown for another 27 days making a total of 49 days. First analysis showed that there is a difference between the hyphae grown in contact with the air and those grown in contact with the substrate (Fig. 2-Left). The aerial mycelium (part of the sample that did not interconnect with the substrate) is characterized by the growth of hyphae outside the substrate, forming a white film. The mycelium that has developed and penetrated the substrate was observed as the result of the agglomeration of the substrate (Fig. 2-Left).



**Fig. 2.** (Left) Pine sawdust and *H. ulmarios*; (Right) Microporous structure of pine sawdust and *H. ulmarios* (bar – 1000 µm)

The aerial mycelium of the chosen combinations was analyzed under the optical microscope. It is possible to observe in all combinations the formation of a compact and microporous structure (Fig. 2-Right). However, two types of structure are clearly visible: one with shorter tubular and grouped hyphae in one small area, and the other with hyphae of greater length, more lagged and in the form of filament (Figs. 3 and 4).

Among the different species that grew in the pine sawdust the mycelia of *G. lucidum* and *P. ostreatus* only developed the filament structure, while the mycelium of *T. versicolor* and *H. ulmarios* presented both structures. The *H. ulmarios* mycelium that grew on the pine substrate demonstrated the greatest hyphae binding and the formation of large knots in the junctions of multiple hyphae ( $>0.8 \mu\text{m}$ ). The mycelium of *T. versicolor* obtained a similar structure of hyphae regardless of the substrate in which it grew. However the mycelium network of *T. versicolor* in the coffee substrate presents a lower density of hyphae and in the mixed sawdust substrate a higher density of hyphae.

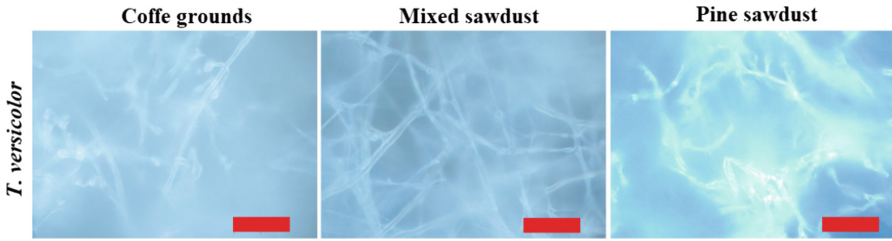


Fig. 3. Microporous structure of *T. versicolor* in different substrates (bar – 2  $\mu\text{m}$ )

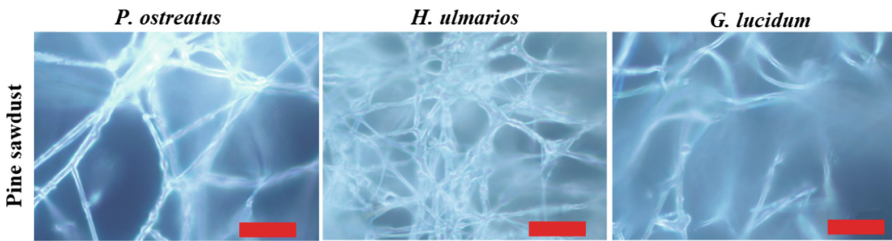


Fig. 4. Microporous structure of different fungi in Pine sawdust (bar – 2  $\mu\text{m}$ )

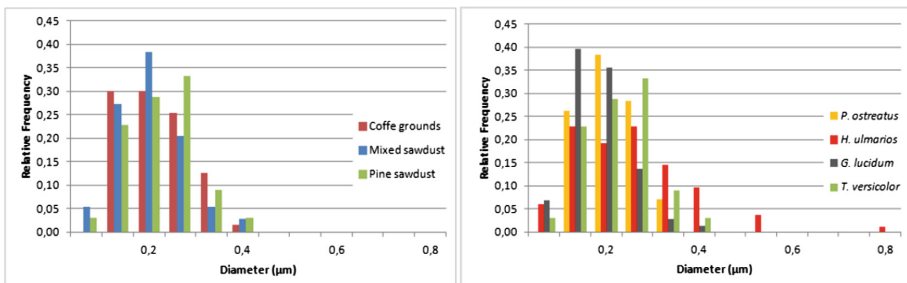
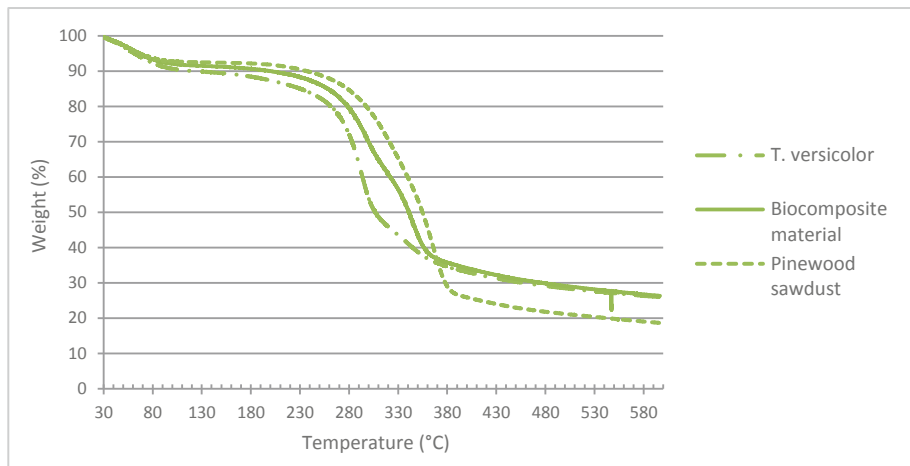


Fig. 5. Diameter analysis of the hyphae for different substrates (left) and species (right).

The hyphae of *T. versicolor* present a diameter of 0.2  $\mu\text{m}$  in the 3 substrates. The hyphae of *P. ostreatus*, *G. lucidum* and *H. ulmarios* that grew on the pine substrate also present diameters of approximately 0.2  $\mu\text{m}$ , however, the *H. ulmarios* species presents a higher density of hyphae (Fig. 5).

### 3.2 Thermal Characterization

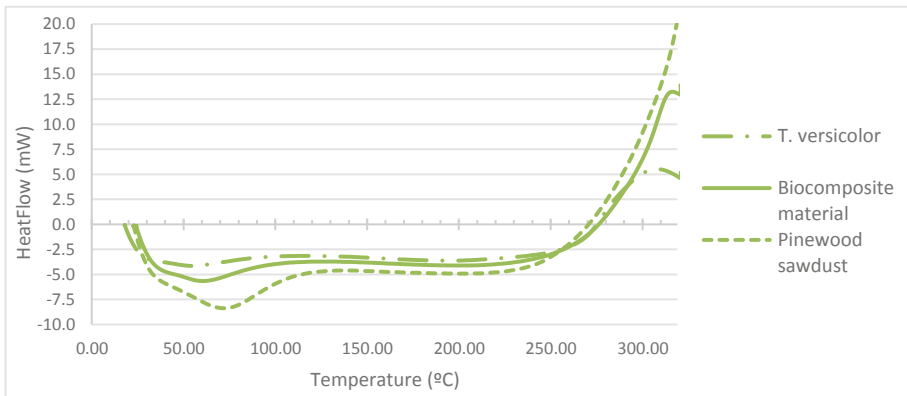
The thermogravimetric analyses (TGA) was performed on the *T. versicolor* species that grew on the pine sawdust substrate during a period of 49 days. Samples of the aerial mycelium structure, the agglomerated substrate with the mycelium structure and only the substrate were analyzed (Fig. 6). The three degradation curves as a function of temperature do not show significant differences, presenting two stages of degradation. The first step, at a temperature below 100 °C, consists of evaporating the moisture from the samples, and in the three samples they lose about 10% of their weight. The second step consists of material degradation or combustion reaction. The pinewood substrate started degradation at 275 °C and ended at 365 °C. The aerial mycelium started its degradation at 265 °C and ended at 290 °C. The pinewood substrate agglomerated with the mycelium structure present intermediate results, initiating the degradation at 270 °C and ending at 345 °C. The mycelium material demonstrated a high thermal stability at high temperatures and a high mass of the products of the combustion reaction, about 28% of the initial weight.



**Fig. 6.** Thermogravimetric analysis of Pinewood sawdust substrate, *T. versicolor* and biocomposite material

The analysis of Differential Scanning Calorimetry (DSC) was performed on the *T. versicolor* species with the Pinewood sawdust substrate after 49 days of growth. Samples of the aerial mycelium structure, the agglomerated substrate with the mycelium structure and the substrate itself were tested similar procedure as the one used for

the TGA. In Fig. 7, 3 events or phases can be identified. The initial phase, up to 100 °C, indicates a higher energy absorption and is attributed to the energy required to the evaporation of the remaining moisture in the sample. The second phase, from 100 °C to 220 °C, represents the energy absorbed by the sample as a function of the temperature increase. Aerial mycelium has been shown to absorb the least amount of energy, while the base pine substrate absorbs the highest amount of energy. The substrate sample agglomerated with the mycelium absorbed an intermediate amount of energy, demonstrating that the presence of the micellar structure improves the thermal insulation capacity of the pinewood sawdust. The third phase is characterized by the end of the endothermic events and by the beginning of the exothermic events of degradation of the samples, at 270–275 °C. It is also noticeable that the aerial mycelium sample releases a lower amount of energy at its degradation. At 320 °C it only emits 5 mW of energy while the base pine substrate emits 20 mW. The sample of pinewood substrate with developed mycelium presented an intermediate energy emission, with 12,5 mW at 320 °C.



**Fig. 7.** Differential Exploration Calorimetry of Pinewood sawdust, *T. versicolor* and biocomposite material

## 4 Conclusion

This study allowed us to validate the use of mycelium, a vegetative part of the fungus, as a new solution for natural and biodegradable materials. It was possible to observe two suitable forms of growth: a bio-composite, where the mycelium penetrates and agglomerates the substrate, from which it obtains the nutrients necessary for its growth; or as a pure material, where a film is formed composed only of an array of mycelia hyphae.

The production of mycelium-based materials is simple and inexpensive. Fungi proliferated well in substrates of industrial waste with low economic value and few applications (pinewood and mixed sawdust and coffee grounds). The growth is guaranteed with a constant temperature of 25 °C, and the highest energy consumption is

used to make the material inert and thus stopping the development of the fungus. During the development of the fungus on the substrate, conditions are created that can become susceptible to various types of contaminations of bacteria or other fungi. This implies the need to ensure a clean workspace as well as sterilized material and base products, which from the industrial point of view can lead to the creation of “white areas” within the company.

Mycelial growth varied with the fungus species and with the selected substrates. Microstructures of hyphae of the mycelium were obtained with different diameters, with numbers of bonds between them and densities.

The mycelium-based materials presented a stable behavior with increased temperature, undergoing degradation in terms of mass values above 270 °C. The mycelium-based materials were heated at the same time as the wood-based base material. There was initially a loss of the residual moisture present in the materials, followed by a constant absorption of energy with increased temperatures, and finally an exothermic peak referring to the combustion reaction at the time of the mass degradation. It should also be noted that the mycelium exhibits a lower thermal conductivity and emits less energy at the degradation point off the pinewood sawdust base material.

## References

1. Haneef, M., Ceseracciu, L., Canale, C., Bayer, I.S., Heredia Guerrero, J.A., Athanassiou, A.: Advanced materials from fungal mycelium: fabrication and tuning of physical properties. *Sci. Rep.* **7**, 41292 (2017)
2. Bonfante, P., Genre, A.: Mechanisms underlying beneficial plant – fungus interactions in mycorrhizal symbiosis. *Nature communications* **1**, 48 (2010)
3. Islam, M.R., Tudryn, G., Bucinell, R., Schadler, L., Picu, R.C.: Morphology and mechanics of fungal mycelium. *Sci. Rep.* **7**(1), 13070 (2017)
4. Ruiz-Herrera, J.: *Fungal Cell Wall; Structure, Synthesis, and Assembly*, 2nd edn. CRC Press, Boca Raton (2016)
5. Appels, F.V.W., Dijksterhuis, J., Lukasiewicz, C.E., Jansen, K.M.B., Wösten, H.A.B., Krijghsheld, P.: Hydrophobin gene deletion and environmental growth conditions impact mechanical properties of mycelium by affecting the density of the material (2018)
6. Lelivelt, R.J.J.: The mechanical possibilities of mycelium materials, Eindhoven university of technology (TU/e) (2015)
7. van der Horst, C.: Interviewee, company visit to CNC substrate productions. [Interview by Lelivelt, R.J.J.] (2014)
8. Wösten, H.: Interviewee, Alternate mycelium applications. [Interview by Lelivelt, R.J.J.] (2014)
9. <https://www.mushroom-appreciation.com/pasteurize.html>. Accessed 8 Nov 2018
10. *Grow-It-Yourself-Instruction-Manual-v1.0 – Ecovative* (2018)
11. A Walck Through the Evolution of a New Product. <https://ecovatedesign.com/blog/166>. Accessed 8 Nov 2018
12. How to Make Your Own Growth Forms. <https://ecovatedesign.com/blog/183>. Accessed 8 Nov 2018
13. <http://www.ericklarenbeek.com/>. Accessed May 2018



# Developing Sustainable Materials for Marine Environments: Algae as Natural Fibers on Polymer Composites

Gleiciane dos Santos Silva<sup>1</sup>, Carlos Capela<sup>1,2(✉)</sup>,  
and Marcelo Gaspar<sup>1</sup>

<sup>1</sup> Mechanical Engineering Department,  
Instituto Politécnico de Leiria, Leiria, Portugal  
carlos.capela@ipleiria.pt

<sup>2</sup> CEMMPRE, Department of Mechanical Engineering,  
University of Coimbra, Coimbra, Portugal

**Abstract.** There is an increasing demand for the use of sustainable materials in marine applications. Thus, the ability of using raw-materials directly from ocean waste effectively contributes to enhance circularity by design in these sensitive ecosystems. Considering the favorable strength-to-weight ratio of composite materials, they usually tend to get selected for nautical applications. In these polymer composites, glass fibers and carbon fibers are usually chosen as reinforcements due to their specific strength and ease of manipulation. However, the use of natural fibers as fillers for composites in marine applications would be beneficial due to the fact that they are biodegradable and have a much lower environmental impact than glass or carbon fibers. Thus, the purpose of current research is to test and assess the use of red algae as filler for polymer composites in marine applications.

**Keywords:** Natural fibers · Composite materials · Red algae · Marine applications

## 1 Introduction

On the quest for developing sustainable products and solutions, a growing trend of natural fibers are being used as fillers in composite materials, as can be identified in recent literature review [1, 2]. Many vegetable origin types of fibers have been used for the reinforcement of thermoplastic and thermoset polymers, such as flax [3], sisal [4] or jute [5].

Algae, as a marine environment raw-material also represent a vast and cheap source of potential fillers for making polymer-matrix composites [6, 7]. Considering also the wide proliferation of algae that occur in many coastlines due to environmental problems [8], the use of these raw materials would be considered beneficial as it would contribute for the circularity by design in engineering applications. Nonetheless, the knowledge on the properties of algae-filled composites is, even today, very scarce [7].

Considering the favorable strength-to-weight ratio of glass or carbon fiber-reinforced composite materials, they can be considered a good material to be used in marine

environments. In this sense, there is a search for fibers that can act as a more sustainable reinforcement than glass fibers and carbon fibers. Natural fibers such as coconut [9], jute [5] and ramie [10] make composites lighter and reduce production costs. Nonetheless, these fibers are absorbent and require investment in planting, harvesting and processing. Such scenario pushes for a search of new alternative natural fibers.

In parallel, the extraction of agar in Portugal generates an immense amount of red algae fiber residues that could be used to produce composites with fiber reinforcement. Thus, the purpose of the following research is to process the red algae fibers as filler in polymer composites and investigate the use of such material in marine environments.

## 2 Materials and Methods

In current study, the composite samples were processed from the algae fibers and SR GreenPoxy 56 resin as the matrix. According to the manufacturer [11], 56% of the resin is of vegetal origin. Additionally, SD Surf hardener was added to the resin in a proportion of 100:37 (weight ratio), according to the manufacturers' specification. The curing process was done in three stages: the first stage was of 24 h at 23 °C, followed by a 4 h stage at 40 °C and a final stage of 8 h at 60 °C.

The method to obtain the algae natural fibers was divided into four distinct stages: cleaning, extraction, bleaching and drying. The main goal of such treatment was to preserve the cellulose fiber content of the red algae *Gelidium Corneum*, harvested in shore of São Martinho do Porto, Portugal.

The collected algae fibers were cleaned, boiled, bleached, dried and cut. The size of the fibers used in the final samples was of 15 mm, which can be classified as of short fiber reinforcements. As a reagent, a chemical bleaching agent was used to remove some of the pigments from the fibers.

To manufacture the composite samples, a compression moulding process was used. On what refers to the fibrous composition of the samples, due to the difficulty of impregnating the fibers with the resin, optimal samples presented a content of 20% algae fiber volume ratio.

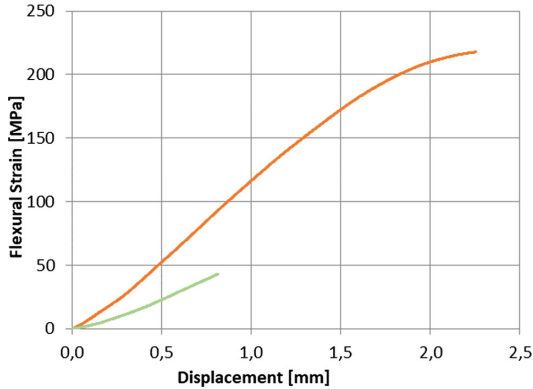
## 3 Results

In order to assess the algae composite mechanical behaviour in seawater environment, dedicated samples (with and without algae fibers) were tested in various conditions to derive the corresponding properties in such severe environment.

### 3.1 Mechanical Properties

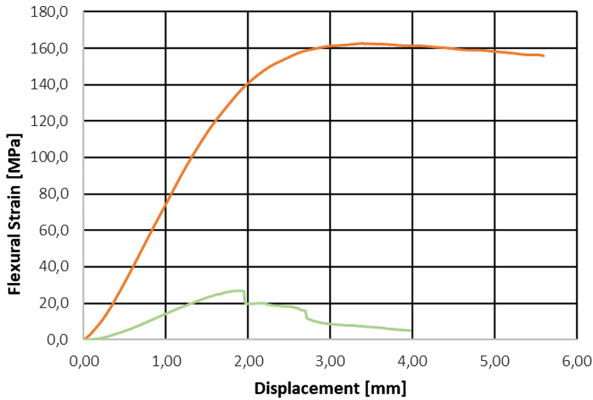
To obtain the algae composite main mechanical properties in seawater, some samples were immersed in such environment up to 30 days. In Fig. 1 the results from the Three-point bending test are presented for the day zero of water immersion. It can be observed that the maximum flexural strain for the plain SR GreenPoxy 56 Resin is significantly higher than that of the 20%  $V_m$  algae resin.





**Fig. 1.** Flexural Strain vs. Displacement of the algae fiber composite (green – lower curve) and the SR GreenPoxy 56 Resin (red – upper curve) – without seawater immersion.

After 30 days of seawater immersion, the maximum flexural strain of both resin and algae composite were lower than those without immersion (see Fig. 2). For the SR GreenPoxy 56 Resin, the maximum flexural strain lowered approximately 13%, whereas for the 20%  $V_m$  algae composite, the maximum flexural strain reduction was of approximately 40%.



**Fig. 2.** Flexural Strain vs. Displacement of the algae fiber composite (green – lower curve) and the SR GreenPoxy 56 Resin (red – upper curve) – after 30 days of seawater immersion.

These results show that the plain SR GreenPoxy 56 Resin has a better performance in seawater conditions than the resulting 20%  $V_m$  algae composite, when submitted to Three-point bending tests.

On Table 1, the three-point bending test results of the SR GreenPoxy 56 Resin and algae fiber composite are presented. These results show the average values of the maximum flexural strain, the corresponding load and elastic modulus for 0 and 30 days of seawater immersion.

**Table 1.** Three-point bending test results: SR GreenPoxy 56 Resin and algae fiber composite – 0 and 30 days of seawater immersion.

Material type	Seawater Immersion	$V_m$ [%]		$\sigma_{flex.m\acute{a}x}$ [MPa]	Load [N]	$E_{flex}$ [MPa]
Resin	0 days	0	Average	221,6	1908,9	5525,0
			Standard deviation	10,9	220,7	480,0
	30 days	0	Average	192,8	1822,0	4284,0
			Standard deviation	26,8	164,8	883,3
Algae Composite	0 days	20	Average	47,5	570,3	2700,7
			Standard deviation	5,9	70,7	257,4
	30 days	20	Average	28,3	340,0	835,59
			Standard deviation	5,8	69,1	130,78

The 20%  $V_m$  algae composite presented an (average) value of 2700 MPa for the modulus of elasticity, which is approximately half of the plain resin before water submersion. Moreover, the 30 days seawater immersion caused a 70% reduction of the same property in the algae composite, whilst for the same time of immersion, the elasticity modulus of the plain resin lowered only approximately 23%.

These results are in line with those presented by Wei *et al.* [12], who also refer a loss of mechanical properties for basalt fiber and glass fiber/epoxy resin composites in seawater. In such study, Wei *et al.* [12], identified a degradation of 30% in the mechanical properties of basalt fiber and glass fiber/epoxy resin composites after 30 days of seawater immersion.

In current research, such degradation may be enhanced by the algae composite porosity, the fibers' hydrophilic behaviour or the composite's surface resulting from the samples mechanical cutting process, which exposed the algae fibers directly to the environment. When considering such scenario, due to the cellulose of the algae fibers, water absorption of the fibers may have affected the mechanical properties of the resulting 20%  $V_m$  composite.

Macroscopic analysis of the fibers allowed identifying significant modifications in the composites' algae surface, which may have been induced by the material's porosity. However, it is necessary to analyse the seawater absorption to obtain more precise conclusions.

### 3.2 Seawater Absorption

To characterize the physical properties of both algae composite and the plain resin in seawater, dedicated samples were immersed in such environment up to 30 days. Every 10 days the main properties were measured and analysed towards the corresponding properties without water immersion.

Comparatively, the resin maintains its integrity, whereas the composite apparently undergoes degradation after long periods of seawater immersion. This conclusion is in agreement with the behaviour predicted, as according to Marinelli *et al.* [13], because of the natural fibers, which have hydrophilic and hygroscopic characteristics, the seawater will affect the fiber-matrix interfaces.

Table 2 shows the results of seawater absorption of the tested materials, based on time and weight variation of the samples.

**Table 2.** Seawater absorption: SR GreenPoxy 56 Resin and algae fiber composite – 0 to 30 days of seawater immersion.

			Seawater Absorption [%]				
Material type	$V_m$ [%]	Sample number	0 days	1 day	10 days	20 days	30 days
Resin	0	1	0	0,32	0,65	0,98	1,08
	0	2	0	0,24	0,74	0,99	1,12
	0	3	0	0,34	0,68	0,90	1,13
Algae composite	20	1	0	6,96	14,17	17,5	18,86
	20	2	0	5,17	10,90	13,98	15,10
	20	3	0	6,31	12,77	15,79	16,89

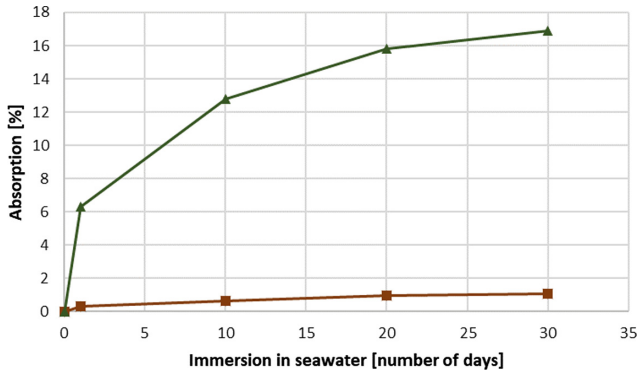
Although the results of seawater absorption are increasing with time, a stability trend may be observed after approximately 20 days of immersion on the composite samples. On average, in the first 10 days of seawater immersion there was an absorption of 12.6% and, at the end of 30 days, of 16.9%.

The plain resin showed a less severe increase of water absorption, as can be observed in Fig. 3. This shows that the natural algae fibers tend to contribute/enhance the water absorption of the resulting composite, whereas the water absorption of the related resin is significantly lower.

Even though the algae composite reached an average of 17% seawater absorption, such results show to be similar to those obtained with other natural fibers used as natural reinforcement in polymer composites. To such end, Nair *et al.* [9], identified approximately 20% absorption of distilled water and seawater in samples of composite materials reinforced with 15% long coconut fibers.

In summary, seawater absorption increases significantly with time in natural fiber polymer composites. Nevertheless, algae fibers may exhibit better performance than other natural fibers, such as coconut fibers.

To contribute to the seawater absorption some of the causes may be the poor adhesion of the matrix to the fibers, excess fiber volume in the composite or the absence of pre-treatment to minimize the hydrophilic behaviour of the algae fibers.

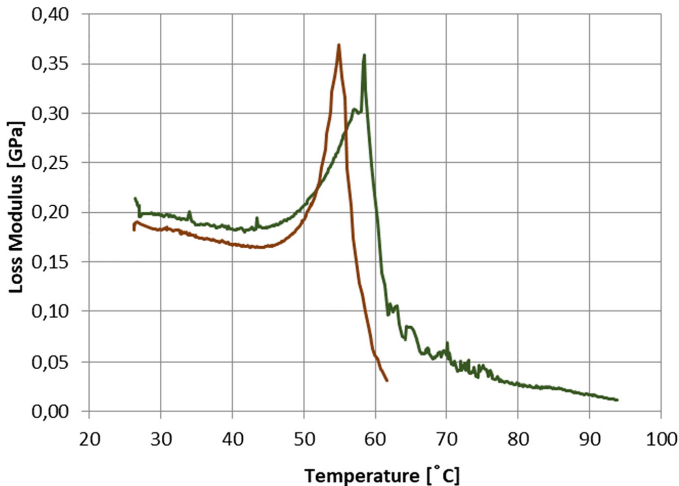


**Fig. 3.** Seawater absorption vs. days of immersion for algae fiber composite (green – upper curve) and SR GreenPoxy 56 Resin (red – lower curve).

### 3.3 Dynamic Mechanical Analysis

Dynamic mechanical analysis (DMA) is one of the most common methods employed to study the materials' composition and properties [14]. The increase in temperature during these experimental tests allows drawing a thermal and mechanical profile of the material developed.

In Fig. 4 a shift between the  $T_g$  value corresponding to the plain SR GreenPoxy 56 Resin and the one of the algae fiber composite can be observed. This displacement of both curves is justified by the insulating characteristics of the algae fiber.



**Fig. 4.** DMA test: Loss modulus vs. Temperature for the algae fiber composite (green – right peak curve) and SR GreenPoxy 56 Resin (red – left peak curve).

The loss modulus of Fig. 4 indicates the energy dissipated by the material, with composite and resin having similar values, 0.34 GPa and 0.36 GPa, respectively. In addition, the  $\tan \delta$ , when marking the mechanical loss factor of the materials, was of 0.28 for the resin and 0.51 for the composite.

The  $\tan \delta$  value of the composite differs from the usual as, usually, composites have lower values than plain resins. Pothan *et al.* [15] argue that fiber incorporation may cause  $\tan \delta$  to decrease, since fiber hinders molecular movement and energy dissipation. If the composite has a good adhesion between fiber and matrix,  $\tan \delta$  is smaller with the addition of the fibers.

## 4 Summary and Conclusions

This study analysed the use of red algae fibers to act as a fibrous reinforcement in an epoxy composite. A method to obtain the algae fiber was developed and applied to extract the cellulosic fibers from the red algae. The corresponding composite samples were manufactured and tested before and after the analysis of seawater absorption.

In summary, the mechanical properties of the composite, determined by Three-point bending tests, showed to be less promising than the thermal performance resulting from the dynamic mechanical analysis. The algae fibers do not enhance the strength of the material. The composite presented values of maximum tension and modulus of elasticity lower than the plain resin.

In conclusion, the poor adhesion of the resin to the algae fibers, the irregular distribution of the fiber in the matrix and the high absorptivity of the algae reduced the possibilities of using the composite in a structural marine environment product.

On the other hand, the alga fibers present great potential as thermal insulation in the same marine environment, as, when subjected to temperature oscillation, the algae composite showed to have better properties than the plain resin.

## References

1. Balla, V.K., Kate, K.H., Satyavolu, J., Singh, P., Tadimeti, J.G.D.: Additive manufacturing of natural fiber reinforced polymer composites: processing and prospects. *Compos. Part B Eng.* **174**(May), 106956–106984 (2019)
2. Campilho, R.D.S.G.: Natural fiber composites, *Nat. Fiber Compos.* pp. 1–340 (2015)
3. Lu, M.M., Van Vuure, A.W.: Improving moisture durability of flax fibre composites by using non-dry fibres. *Compos. Part A Appl. Sci. Manuf.* **123**(April), 301–309 (2019)
4. Senthilkumar, K., et al.: Mechanical properties evaluation of sisal fibre reinforced polymer composites: a review. *Constr. Build. Mater.* **174**, 713–729 (2018)
5. Singh, H., Singh, J.I.P., Singh, S., Dhawan, V., Tiwari, S.K.: A brief review of jute fibre and its composites. *Mater. Today Proc.* **5**(14), 28427–28437 (2018)
6. Arrieta, M.P., López de Dicastillo, C., Garrido, L., Roa, K., Galotto, M.J.: Electrospun PVA fibers loaded with antioxidant fillers extracted from *Durvillaea antarctica* algae and their effect on plasticized PLA bionanocomposites. *Eur. Polym. J.* **103**(February), 145–157 (2018)
7. Bulota, M., Budtova, T.: PLA/algae composites: morphology and mechanical properties. *Compos. Part A Appl. Sci. Manuf.* **73**, 109–115 (2015)

8. Chiellini, E., Cinelli, P., Ilieva, V.I., Martera, M.: Biodegradable thermoplastic composites based on polyvinyl alcohol and algae.pdf. *Biomacromol* **9**(3), 1007–1013 (2008)
9. Nair, M.M., Kamath, M.S., Shetty, N.: Study on distilled / sea water absorption behaviour influenced by non-uniform long piled up coir fiber composites. *Int. J. Innov. Res. Sci. Eng. Technol.* **5**(9), 15–21 (2016)
10. Matsunaga, T., Sato, Y., Goda, K.: Major cause of strength improvement of a ramie/PA composite with low fiber contents. *Adv. Ind. Eng. Polym. Res.* **1**(1), 93–98 (2018)
11. Cen, X.P., Greenpoxy, S.R., Greenpoxy, S.R.: SR GreenPoxy 56 / SZ 8525 Clear epoxy system for compression moulding Resin SR GreenPoxy 56. **33**(0), 1–7 (2015)
12. Wei, B., Cao, H., Song, S.: Degradation of basalt fibre and glass fibre/epoxy resin composites in seawater. *Corros. Sci.* **53**(1), 426–431 (2011)
13. Marinelli, A.L., Monteiro, M.R., Ambrósio, J.D., Branciforti, M.C., Kobayashi, M., Nobre, A.D.: Desenvolvimento de compósitos poliméricos com fibras vegetais naturais da biodiversidade: uma contribuição para a sustentabilidade amazônica. *Polímeros* **18**(2), 92–99 (2008)
14. Henriques, I.R., Borges, L.A., Costa, M.F., Soares, B.G., Castello, D.A.: Comparisons of complex modulus provided by different DMA. *Polym. Test.* **72**(October), 394–406 (2018)
15. Pothan, L.A., Oommen, Z., Thomas, S.: Dynamic mechanical analysis of banana fiber reinforced polyester composites. *Compos. Sci. Technol.* **63**(2), 283–293 (2003)



# On the Effect of Deposition Patterns on the Residual Stress, Roughness and Microstructure of AISI 316L Samples Produced by Directed Energy Deposition

Gabriele Piscopo<sup>1(✉)</sup>, Alessandro Salmi<sup>1</sup>, Eleonora Atzeni<sup>1</sup>, Luca Iuliano<sup>1</sup>, Mattia Busatto<sup>2</sup>, Simona Tusacciu<sup>2</sup>, Manuel Lai<sup>2</sup>, Sara Biamino<sup>3</sup>, Mostafa Toushekhah<sup>3</sup>, Abdollah Saboori<sup>3</sup>, and Paolo Fino<sup>3</sup>

<sup>1</sup> Department of Management and Production Engineering, Politecnico di Torino, Corso Duca degli Abruzzi 24, 10129 Torino, Italy  
gabriele.piscopo@polito.it

<sup>2</sup> IRIS S.r.l., Via Papa Giovanni Paolo Secondo 26, 10043 Orbassano, TO, Italy

<sup>3</sup> Department of Applied Science and Technology, Politecnico di Torino, Corso Duca degli Abruzzi 24, 10129 Torino, Italy

**Abstract.** Despite the extensive capabilities of Laser-Powder Directed Energy Deposition (LP-DED), compared to other metal additive manufacturing processes, the use of LP-DED in industry is still limited as a result of the limited knowledge on the relationships between the process parameters and mechanical behaviour. In this work, the quality of AISI 316L samples, produced by means of LP-DED and evaluated in terms of surface roughness, residual stresses and microstructure, is linked to the scanning strategy. The outcomes confirm that the deposition strategy plays a key role in the definition of the final properties of specimens.

**Keywords:** Laser Powder-Directed energy deposition · 316L · Residual stress · Surface roughness · Microstructure

## 1 Introduction

Metal Additive Manufacturing (AM) processes are currently recognised as the future of manufacturing industries, thanks to their potentialities in terms of design freedom, part functionality and material usage efficiency [1]. Sectors characterised by a huge level of personalisation, high topological complexity and small production volumes, such as the biomedical, aerospace and racing fields, are the ones in which AM processes are used the most [2]. Focusing attention on processes that use lasers as the energy source to melt material, two different categories of processes can be identified: Laser-Powder Bed Fusion (L-PBF) and Directed Energy Deposition (DED).

Producing large metal components is one of the most challenging issues for AM processes [3]. DED processes allow this problem to be overcome and thus make it possible to produce components in a build volume up to one cubic meter [4]. In the

Laser Powder Directed Energy Deposition (LP-DED) process, a focused laser beam is used to produce a melt pool on an existing surface, while a nozzle is used to inject metal powder directly into the generated melt pool. Once the laser moves away, the material rapidly solidifies and a raised track is obtained [5]. The particular LP-DED construction methodology process allows certain unique capabilities, such as the possibility of repairing worn components, of modifying the topology of an existing component and of producing functionally graded materials (FGMs), to be obtained [1, 6]. LP-DED processes are currently considered premature for industrial applications [5]. One of the main reasons is that the properties of the built parts are not sufficiently characterised or optimised. For this reason, it is important to relate the part properties to the main process variables, such as the deposition strategy and process parameters. Smugeresky et al. [7] performed an experimental analysis in order to optimise selected process parameters, that is, the powder size, laser power, scan speed and powder feed rate, with respect to the surface roughness and the microstructure of thin AISI 316L walls produced by means of LP-DED. Pratt et al. [8] used the neutron diffraction method to evaluate the effect of the laser power, scan speed and powder feed rate on residual stresses in thin AISI 410 walls produced by means of LP-DED. Dai and Shaw [9] studied the effects of bi-direction and offset-out scanning strategies on the distortion and residual stresses of single nickel layers produced by means of LP-DED.

The effects of the scanning strategy on the surface roughness, residual stresses and microstructure of AISI 316L stainless steel cubes, produced by means of LP-DED, have been investigated in this work.

## 2 Materials and Methods

The deposition of  $20 \times 20 \times 20 \text{ mm}^3$  AISI 316L stainless steel cubes on a  $100 \times 100 \times 8 \text{ mm}^3$  substrate of the same material was performed using a three-axis machine with a coaxial deposition head. The power source was an ytterbium fibre laser with a maximum operating power of 5 kW. The considered process parameters are listed in Table 1. Two different scanning strategies were adopted:

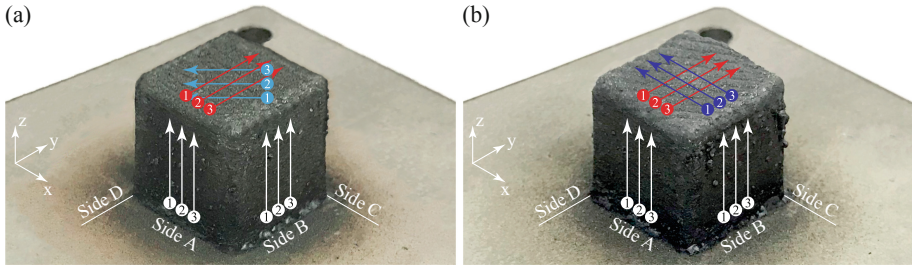
- $0\text{--}90^\circ$ , an orthogonal deposition direction between two adjacent layers;
- $0\text{--}67^\circ$ , the deposition direction is rotated by  $67^\circ$  for each new layer.

Surface roughness was evaluated on the top and the lateral surfaces of each LP-DED cube sample using a RTP80 portable stylus-type surface-roughness tester (SM Metrology Systems S.r.l, Italy). The measurements were taken along a profile length of 10 mm, using a Gaussian filter and a cut-off of 0.8 mm. Figure 1 illustrates

**Table 1.** Process parameters used in the experimental procedure.

Laser power, $P$	Laser speed, $v$	Focus, $h$	Powder feeding rate	Carrier gas flow	Overlap in X	Overlap in Z
900 W	15 mm/s	7.5 mm	3.5 rpm	5 l/min	50%	25%





**Fig. 1.** LP-DED cube samples fabricated using (a) the 0–90° scanning strategy and (b) the 0–67° scanning strategy with lateral surfaces nomenclature and schematic representation of surface roughness measurement directions.

the directions and the measurement positions that were considered in the experimental analysis according to the following rules:

- the roughness was evaluated on the lateral surfaces along the building direction;
- the first measurement direction on the top surfaces, for the cubes fabricated using the 0–90° scanning strategy, was perpendicular to the scanning direction, the second measurement direction was inclined by about  $-45^\circ$  with respect to the x-axis, instead the measurement directions for the cubes built using the 0–67° scanning strategy were along the x-axis and along the y-axis.

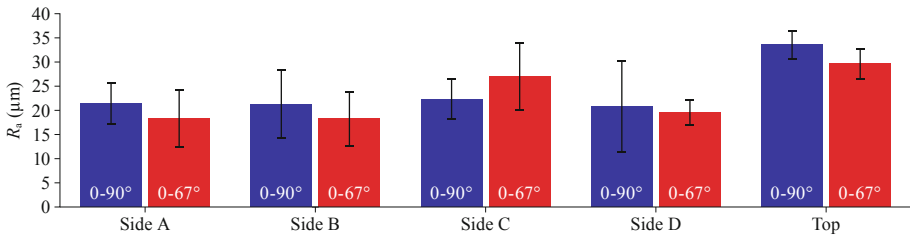
The residual stress behaviour beneath the surface was evaluated using the semi-destructive hole drilling strain gauge method, according to ASTM E837-13a. The RESTAN-MTS3000 (SINT Technology S.r.l., Italy) system was used. The surfaces of the samples were prepared in order to optimise the bonding between the measuring rosettes and the surface. Thus, agglomerated particles were removed using a flat, high carbon, steel file and the surface was then abraded using abrasive paper with different grain dimensions (120, 400 and 600 grit). The strains released by the tested material were acquired for each drilling step and were used to calculate the residual stresses. An acquisition programme was developed, in LabVIEW 2018, in order to automate the data acquisition at each step. The acquired strains were introduced into EVAL (SINT Technology S.r.l., Italy) software to back-calculate the residual stresses in compliance with the ASTM E837-13a standard. A 1.8 mm diameter drill bit was used in the experimental procedure to produce a 1.2 mm deep flat-bottom hole, by executing 24 drilling steps to a depth of 50  $\mu\text{m}$ . The measurements were performed on the top surface and on Side A (Fig. 1).

### 3 Results and Discussion

The results, in terms of surface roughness, in-depth residual stress profiles and microstructure for the cubes fabricated using the two different scanning strategies, are presented hereafter.

### 3.1 Surface Roughness

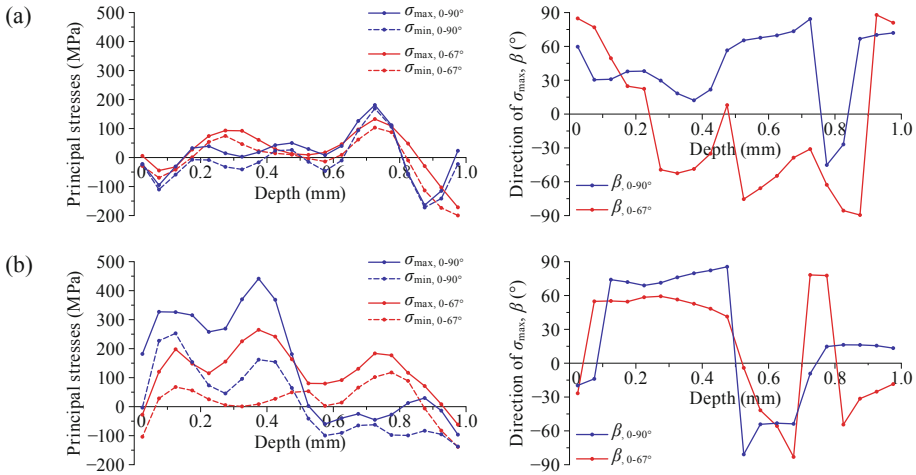
From the graph reported in Fig. 2, it is possible to observe that the surface roughness on the lateral surfaces (Side A, Side B, Side C and Side D) is slightly lower than the surface roughness on the top surface. For the cube built using the 0–90° scanning strategy,  $R_a$  on the lateral surfaces varies between 20.5  $\mu\text{m}$  and 22.5  $\mu\text{m}$  instead  $R_a$  is about 33  $\mu\text{m}$  on the top surface. For the cube built with the 0–67° scanning strategy, the value of  $R_a$  on the lateral surfaces varies between 18  $\mu\text{m}$  and 27  $\mu\text{m}$ , whereas the value of  $R_a$  is about 29  $\mu\text{m}$  on the top surface.



**Fig. 2.** Surface roughness on the analysed surfaces. The red and the blue bars refer to samples produced using the 0–90° scanning strategy and the 0–67° scanning strategy, respectively.

### 3.2 Residual Stresses

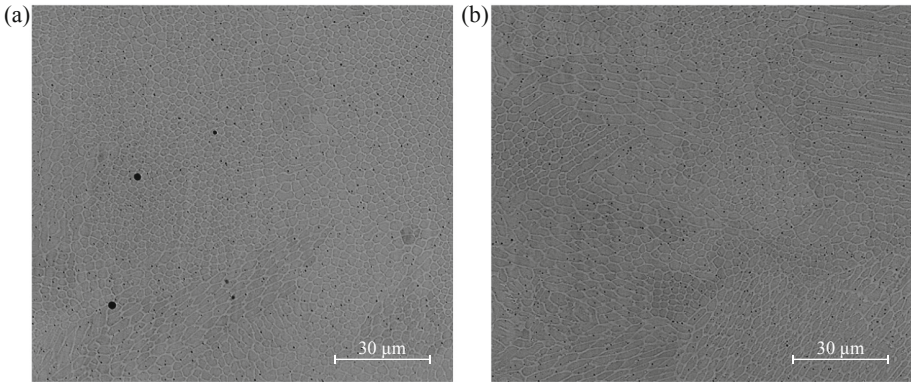
Figure 3a shows the residual stress distribution on the top surface for both cubes. The oscillatory trend of the residual stresses, with respect to the depth, is clearly noticeable. It is possible to note that the stress distribution is similar for both cubes. The peak of the curves is obtained approximately at the same depth, that is, of 0.7 mm, with a value of about 200 MPa. It may be observed that the direction of the principal stress ( $\beta$ ) showed different behaviour when the cubes were fabricated using different scanning strategies. The  $\beta$ -value for the cube produced using the 0–90° scanning strategy is positive for more than half of the analysed depth and then an abrupt variation occurs in correspondence to the maximum stress value. Instead, for the cube produced with the 0–67° scanning strategy, the  $\beta$ -value is prevalently negative, but with an oscillatory trend. Figure 3b shows the stress distribution on Side A of both cubes. The stresses have a similar trend on both cubes. A prevalent tensile stress is observed for a depth of less than 0.5 mm. The maximum stress is obtained at a depth of about 0.4 mm, and it is about 450 MPa in the case of the 0–90° scanning strategy and about 250 MPa with regard to 0–67° scanning strategy. After 0.5 mm, a quite uniform compressive stress, of about 50 MPa, is observed on the cube produced using the 0–90° scanning strategy, instead the stress distribution on the cube produced with the 0–67° scanning strategy shows an oscillatory trend with a predominant tensile state. The trend of the  $\beta$  angle in the two cubes is almost the same. A variation in the  $\beta$ -value occurs at a depth of 0.5 mm. It is possible to relate this behaviour to the value of the residual stress, which crosses the zero-axis and changes in sign from positive to negative.



**Fig. 3.** Stress depth profiles and direction of the principal stress (a) on the top surfaces and (b) on Side A of the cubes.

### 3.3 Microstructure

In general, the microstructure of each layer of both samples is composed of two regions. The bottom part of each layer is basically a columnar structure. The top part of the layer shows a typical fine cellular dendritic structure with classical secondary dendrite arms that change to a columnar structure in the subsequent deposition. In the laser deposition process, the cooling rate of the melt pool, and consequently the solidification velocity, is very high at the bottom part of the layer. The upper part of the layer cools down slowly compared to the bottom part. Owing to the very high solidification velocity of the bottom part of the melt pool, secondary dendrites were not able to grow. As a result, the bottom part of each layer mainly consisted of primary dendrites. Because of the progressive decrease in the cooling rate from the bottom to the top part of the melt pool, a gradual transition of the microstructure from a fully columnar to a cellular dendritic transition was observed. Figure 4 shows the microstructure of the cross-section of the cubes deposited with the 0–90° and the 0–67° scanning strategies, respectively. As can be seen in Fig. 4, the Primary Cellular Arm Spacing (PCAS) of the sample produced using the 0–67° scanning strategy is coarser than the cubes produced using the 0–90° scanning strategy. This difference in the PCAS of the cubes produced using different scanning strategies is related to the general cooling rate associated with each rotation.



**Fig. 4.** Microstructure of the cubes obtained using (a) the 0–90° scanning strategy and (b) the 0–67° scanning strategy.

## 4 Conclusions

In this work, the effect of the adopted scanning strategy on the surface roughness, residual stress and microstructure of cubes produced by means of LP-DED has been investigated. The main results are summarised below:

- the surface roughness on the top surfaces is higher than that on the lateral surfaces. When the 0–90° scanning strategy was used, the surface roughness on the lateral surfaces was about 21  $\mu\text{m}$  and about 33  $\mu\text{m}$  on the top surface, instead when the 0–67° scanning strategy was used, the surface roughness ranged between 18  $\mu\text{m}$  and 27  $\mu\text{m}$  on the lateral surfaces and was about 29  $\mu\text{m}$  on the top surface;
- the residual stresses on the top surfaces were similar for both scanning strategies, although higher stress values were observed on the lateral surfaces of the cubes produced using the 0–90° scanning strategy;
- a coarse microstructure was observed when the 0–67° scanning strategy was used.

**Acknowledgments.** The authors would like to acknowledge the European Horizon 2020 research and innovation programme; grant agreement No. 723795/4D Hybrid–Novel ALL-IN-ONE machines, robots and systems for affordable, worldwide and lifetime distributed 3D hybrid manufacturing and repair operations.

## References

1. Gu, D., Meiners, W., Wissenbach, K., Poprawe, R.: Laser additive manufacturing of metallic components: materials, processes and mechanisms. *Int. Mater. Rev.* **57**(3), 133–164 (2012)
2. Piscopo, G., Salmi, A., Atzeni, E.: On the quality of unsupported overhangs produced by laser powder bed fusion. *Int. J. Manuf. Res.* **14**(2), 198–216 (2019). <https://doi.org/10.1504/ijmr.2020.10019045>

3. Ngo, T.D., Kashani, A., Imbalzano, G., Nguyen, K.T., Hui, D.: Additive manufacturing (3D printing): a review of materials, methods, applications and challenges. *Compos. B Eng.* **143**, 172–196 (2018)
4. ASTM F3187-16, Standard Guide for Directed Energy Deposition of Metals, ASTM International, West Conshohocken, PA (2016). [www.astm.org](http://www.astm.org). <https://doi.org/10.1520/f3187-16>
5. Thompson, S.M., Bian, L., Shamsaei, N., Yadollahi, A.: An overview of Direct Laser Deposition for additive manufacturing; Part I: transport phenomena, modeling and diagnostics. *Additive Manufacturing* **8**, 36–62 (2015)
6. Toyserkani, E., Khajepour, A., Corbin, S.F.: *Laser Cladding*. CRC Press, Boca Raton (2004)
7. Smugeresky, J., Keicher, D., Romero, J., Griffith, M., Harwell, L.: Laser Engineered Net Shaping (LENS [TM]) process: optimization of surface finish and microstructural properties. In: *Advances in Powder Metallurgy and Particulate Materials–1997*, vol. 3, p. 21 (1997)
8. Pratt, P., Felicelli, S., Wang, L., Hubbard, C.: Residual stress measurement of laser-engineered net shaping AISI 410 thin plates using neutron diffraction. *Metall. Mater. Trans. A* **39**(13), 3155–3163 (2008)
9. Dai, K., Shaw, L.: Distortion minimization of laser-processed components through control of laser scanning patterns. *Rapid Prototyping J.* **8**(5), 270–276 (2002)



# A Novel Specimen Geometry for Fatigue Crack Growth in Vacuum

L. M. S. Santos<sup>1</sup>, C. Capela<sup>1</sup>✉, F. V. Antunes<sup>2</sup>, J. A. M. Ferreira<sup>2</sup>,  
J. D. Costa<sup>2</sup>, and R. Branco<sup>2</sup>

<sup>1</sup> Department of Mechanical Engineering, ESTG,  
Instituto Politécnico de Leiria, Leiria, Portugal  
carlos.capela@ipleiria.pt

<sup>2</sup> Department of Mechanical Engineering,  
University of Coimbra, Coimbra, Portugal  
fernando.ventura@dem.uc.pt

**Abstract.** Selective Laser Melting (SLM) is a technology for additive manufacturing consisting in the fusion of a fine metal powder layer by layer. This procedure is very interesting to generate components with complex geometry and eventually composed of different materials. This novel technology opened new opportunities. A cylindrical geometry is proposed here, with an internal circular crack placed at the center of the specimen, as shown in Fig. 1. This new specimen geometry is interesting to study fatigue crack growth (FCG) in vacuum, which is important for a better understanding of FCG mechanisms. The environment inside internal cracks is likely similar to a vacuum environment since it is shut off from air, leading to negligible effect of oxidation or gas absorption. This way, the complex apparatus typically used to develop fatigue studies in vacuum, is avoided.

**Keywords:** Selective Laser Melting (SLM) · Fatigue crack growth · Vacuum · Novel cylindrical specimen with interior crack

## 1 Introduction

Fatigue crack growth (FCG) in metals is typically studied using  $da/dN-\Delta K$  plots obtained experimentally. FCG rate is affected by different physical parameters namely loading parameters ( $\Delta K$ , stress ratio,  $K_{max}$ , variable amplitude loading), geometrical parameters (crack length, specimen geometry) and environmental conditions (temperature and atmosphere).

The effect of environment is particularly relevant for relatively low values of FCG rate, namely in region I of  $da/dN-\Delta K$  curves. In fact, the environmental attack is time dependent, competing with cyclic plastic deformation mechanism. Near-threshold the FCGR is small, giving time for the environmental attack. Sunder [1] proposed the Brittle Micro-Fracture (BMF), as an alternative to the cyclic plastic deformation. This brittle fracture is linked to the surface diffusion of hydrogen, released by the reaction of moisture with the crack tip surface, resulting in oxygen and hydrogen formation. Each load rising increases near-tip stress, acting as a diffusion pump to promote

embrittlement of surface atomic layers. The intensity of this surface diffusion driven mechanism at the beginning of the rising half of the load cycle is controlled by near tip stress, which is a measure of residual elastic strain and therefore of initial inter-atomic spacing of atoms in the surface layers. The increase of this spacing enhances the adsorption of air components. A competition is expected between BMF and cyclic slip. The BMF is restricted to crack tip surface atomic layers and therefore becomes insignificant for relatively large crack growth rates. Zerst *et al.* [2] indicated two main environmental mechanisms: stress assisted anodic material dissolution and hydrogen embrittlement. In the first case, the protective layer is locally destroyed at the crack tip and the exposed material dissolves electro-chemically. In the second case, the hydrogen atoms penetrate into the process zone and modify the deformation and the damage mechanisms at the crack tip. The corrosion damage is a time-dependent process which will occur when the medium is in contact with the crack tip. In the near-threshold regime the crack is almost stationary, reason why the environment has a major influence. Karr *et al.* [3] studied near-threshold fatigue in AZ61 magnesium alloy tested in air and vacuum. They observed that the fracture surfaces were smoother in vacuum than in air. In ambient air, the fracture surfaces showed facets and fine steps typical of brittle fracture.

The effect of environment is typically studied using vacuum chambers, which eliminates environmental effects at the crack tip. However, this is a complex and expensive equipment which is not available in all laboratories. Therefore, we propose here new specimen geometry, with internal crack, which is expected to have vacuum conditions at the crack tip. The cylindrical specimen is to be produced by selective laser melting. Note that there is a plane strain state along all crack front, which is interesting. Internal cracks also occur in Very High Cycle Fatigue, but the initiation position is not controlled.

## 2 Specimen Production

Figure 1 presents the geometry proposed for the specimen. It is a cylindrical geometry with screws at the extremities for the fixation in the testing machine. In the working area the specimen has a diameter of 10 mm. The interior crack is circular, having a initial diameter of 1 mm and a thickness of 0.2 mm.

A second geometry very similar was defined for comparison, as illustrated in Fig. 2. In this geometry a small tunnel was included, with a diameter of 0.4 mm, to provide access of air to the crack front region. The objective is to compare FCG results from both specimens, in order to evaluate the effect of vacuum.

The specimens were synthesized by Lasercusing® with layers growing towards the direction of loading application. The samples were processed using a The ProX DMP 320 high-performance metal additive manufacturing system, incorporating a 500 w fiber laser. Powders were deposited and deposited layer by layer with approximately sixty microns thickness. Metal powder was the Titanium Ti6Al4V Grade 23 alloy. After

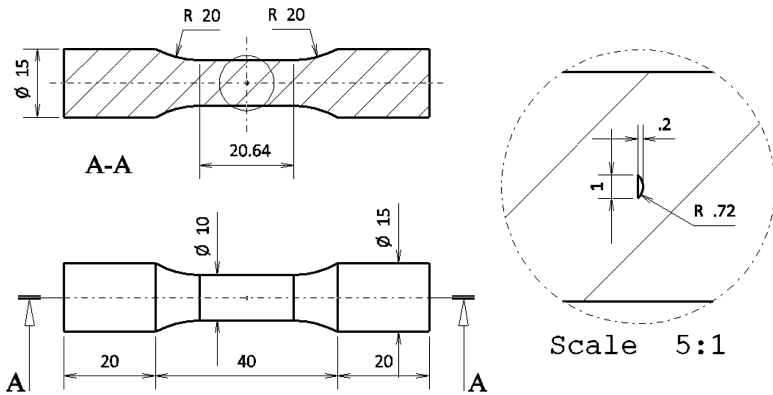


Fig. 1. Cylindrical specimen with internal crack.

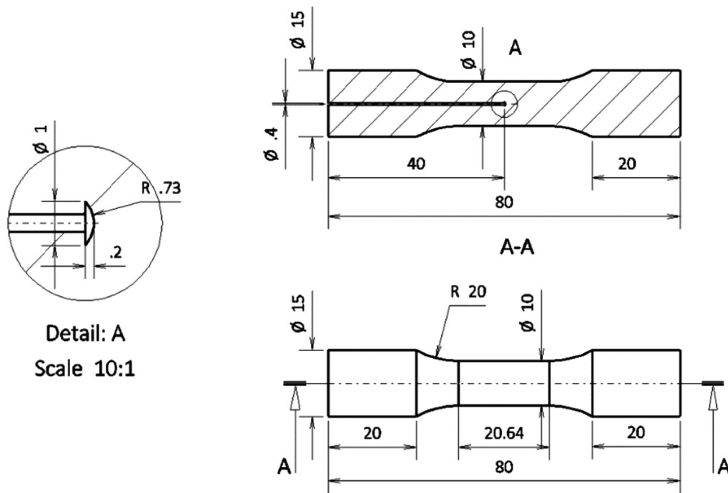
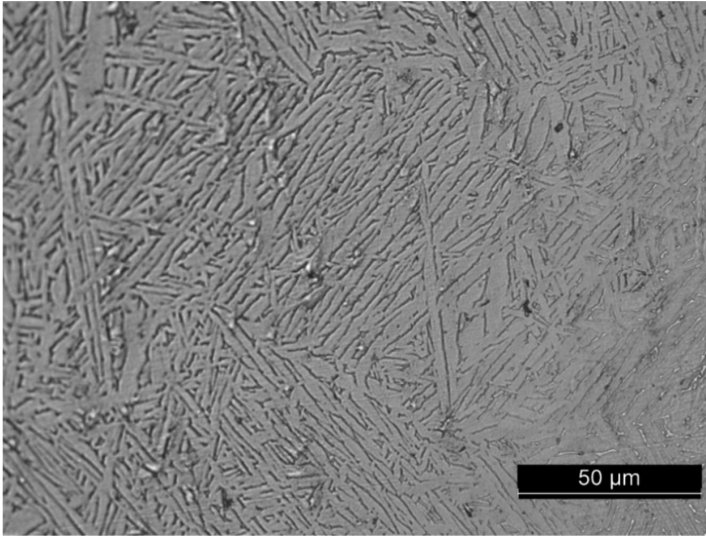


Fig. 2. Cylindrical specimen with internal crack and access to external environment.

manufactured by SLM the specimens are machined and polished for the final dimensions. This approach permits the inclusion of a crack at the center of specimen.

Faces of the specimen were prepared according to the standard metallographic practice and observed using a Leica DM4000 M LED optical microscope. Figure 3 presents the microstructure showing an acicular morphology where it is identified two phases material with a martensitic phase  $\alpha$  (or  $\alpha'$ ), due to the fast solidification. Only a small amount of internal micro pores was observed.





**Fig. 3.** Material microstructure.

### 3 Numerical Analysis

This specimen geometry imposes some technical difficulties, namely in terms of measurement of crack length. The crack is supposed to attain a perfectly circular shape and keep this shape along all crack growth. Since it is not possible to measure optically the crack length, as is proposed in standards for through-thickness specimens [8], an alternative must be found. One option would be to use tomography, however this is a complex equipment which is not available for the research team. Additionally, it would not be easy to place the mechanical device needed to apply load, inside the tomography equipment. A second alternative would be use of potential drop. This approach is used in high temperature tests of nickel base superalloys. Since the tests are made inside a furnace, it is not possible to measure directly the crack length using optical methods. A third alternative is to analyse specimen's compliance, which is supposed to depend on crack length. This solution is also proposed in ASTM standard [4] for the measurement of crack length in CT and MT specimens. The compliance is the reciprocal of the load-displacement slope. Finally, it is possible to do marking on fracture surfaces and use this to measure crack length on the fracture surfaces after the final fracture of the specimen.

The cylindrical specimen is symmetrical relatively to the central axis and the load is independent of the angular position, therefore an axisymmetric model was assumed to quantify stress intensity factor and the compliance. In the software used, which was Marc-Mentat, the symmetry axis is the x-axis and the radial axis is in the y-direction. Only one half of the geometry of the cross-section must be modeled and it must be located in the half-space  $y > 0$ . Figure 4 presents the physical model of the specimen. Symmetry boundary conditions were placed at  $x = 0$  and a fixed displacement of

0.0001 mm was applied at the head of the specimen ( $x = 20$  mm). A homogeneous, isotropic and linear elastic behavior was assumed for the material with  $E = 110$  GPa and  $\nu = 0.3$ . Figure 5 shows the finite element mesh considered in the numerical analysis. It is composed of 1875 quadrilateral linear elements with full integration.

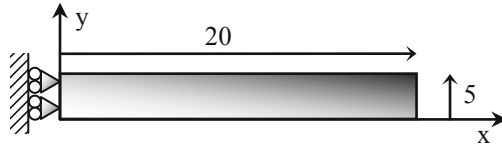


Fig. 4. Axisymmetric model.

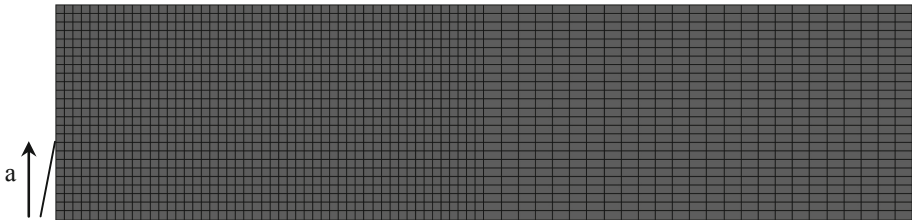


Fig. 5. Finite element mesh.

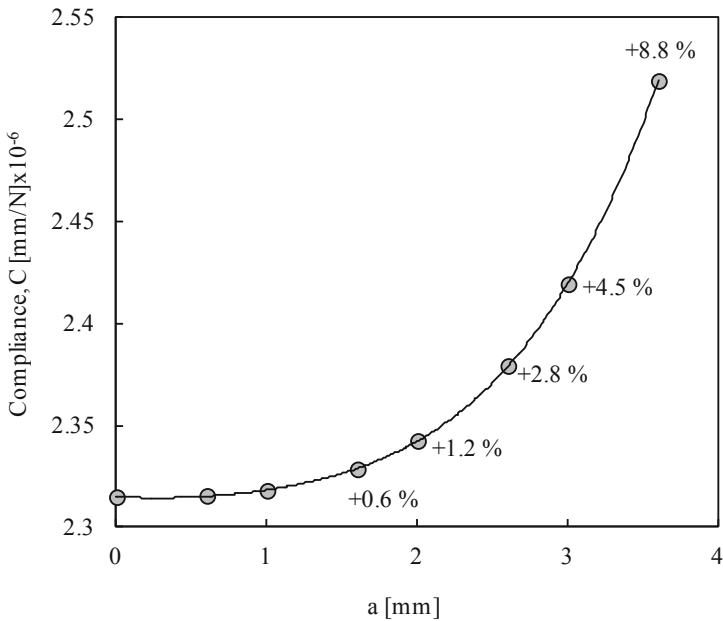


Fig. 6. Variation of compliance with crack length.

## 4 Numerical Results

Figure 5 presents the variation of compliance with crack length,  $a$ . The cracks have a circular shape and their crack length is the radius of the circle. As can be seen, the compliance increases with crack length. The rate of variation also increases progressively with crack length, being quite small for the shortest crack lengths. The variation of compliance relatively to a non-cracked specimen ( $a = 0$ ) was calculated and is presented in the form of percentage in Fig. 6. For crack lengths lower than 2 mm the percentage variation is lower than 1%. This imposes limitation to the experimental detection of crack length using variations of compliance. The following expression is proposed for the compliance, which was obtained by polynomial regression:

$$C = 0.0001234a^6 - 0.0008711a^5 + 0.0027319a^4 - 0.0005364a^3 + 0.0023806a^2 - 0.0007103a + 2.3149811 \quad (1)$$

where the units of  $C$  and  $a$  are mm/N and mm, respectively.

## 5 Conclusions

A novel specimen geometry is proposed here to study fatigue crack growth in vacuum. This is a cylindrical specimen, made by Selective Laser Melting with an interior crack. The crack keeps a circular shape during propagation and a plane strain state exists along all crack front. A numerical study was developed to obtain specimen's compliance. It was found that for crack lengths lower than 2 mm the variation of compliance is lower than 1%. Therefore, for relatively small cracks the measurement of crack length using compliance is not easy and alternatives are needed.

**Acknowledgements.** The authors would like to acknowledge the sponsoring under the project no. 028789, financed by the European Regional Development Fund (FEDER), through the Portugal-2020 program (PT2020), under the Regional Operational Program of the Center (CENTRO-01-0145-FEDER-028789) and the Foundation for Science and Technology IP/MCTES through national funds (PIDDAC).

## References

1. Sunder, R.: Unraveling the science of variable amplitude fatigue. *J. ASTM Int.* **9**(1), 1–32 (2012)
2. Zerst, U., Vormwald, M., Pippan, R., Gänser, H.-P.: Sarrazin-Baudoux C, Madia M. About the fatigue crack propagation threshold of metals as a design criterion – a review. *Eng. Fract. Mech.* **153**, 190–243 (2016)
3. Karr, U., Schönbauer, B.M., Mayer, H.: Near-threshold fatigue crack growth properties of wrought magnesium alloy AZ61 in ambient air, dry air, and vacuum. *Fatigue Fract. Eng. Mater. Struct.* **41**, 38–47 (2018)
4. ASTM E 647-11: Standard test method for measurement of fatigue crack growth rates. Philadelphia: American Society for Testing and Materials, ASTM (2011)



# Fatigue Life Prediction in Selective Laser Melted Samples Under Variable Amplitude Loading Based on Two Constant-Amplitude Tests

L. Santos<sup>1</sup>, R. Branco<sup>1</sup>(✉), J. D. Costa<sup>1</sup>, C. Capela<sup>1,2</sup>,  
and J. A. Martins Ferreira<sup>1</sup>

<sup>1</sup> CEMMPRE, University of Coimbra, Coimbra, Portugal  
ricardo.branco@dem.uc.pt

<sup>2</sup> Department of Mechanical Engineering, Polytechnic Institute of Leiria,  
Leiria, Portugal

**Abstract.** This paper addresses the fatigue behaviour of selective laser melted samples subjected to variable amplitude loading. In a first stage, a series of low-cycle fatigue tests is performed to identify an energy damage parameter able to correlate the load history with the fatigue lifetime. In a second stage, an energy-life curve is established on the basis of two tests performed under pulsating loading conditions. Finally, fatigue lifetime of samples tested at variable-amplitude loading are successfully predicted using the energy-life curve previously established along with an adequate fatigue damage accumulation law.

**Keywords:** SLM · SED · 18Ni300 · Lifetime prediction · Variable amplitude

## 1 Introduction

Maraging steels are outstanding materials to meet the current demands of aerospace, nuclear, and mould industries, among others, due to their superior mechanical properties, such as ultra-high strength, excellent ductility, good fracture toughness, optimal corrosion resistance and weldability. These industries face a constant pressure for the production of a high variety of low-volume products at a minimum cost. In this context, selective laser melting is an ideal technique to compete in such environment. This laser-based additive manufacturing technique enables the production of complex physical objects, difficult or impossible to produce via conventional subtractive processes, in an industrial environment, directly from three-dimensional computer models, in short timeframes, and at low cost [1].

Critical engineering components, in the above-mentioned sectors, are often subjected to variable amplitude loading. Thus, the cumulative fatigue damage analysis plays an important role in the fatigue lifetime design. Particularly in the case of selective laser melted components made of maraging steels, recent studies have been mainly focused on the evaluation of the of processing and post-processing parameters on mechanical properties. In the field of fatigue, research has been mainly focused on high-cycle fatigue regime under constant-amplitude loading histories [2–4].

Studies dealing with variable amplitude loading, so far, are scarce [5]. Therefore, the main goal of the present paper is the analysis of fatigue lifetime in additively manufactured samples undergoing variable-amplitude loading. In a first stage, low-cycle fatigue tests are performed in order to identify a suitable energy-based parameter able to correlate the loading scenario with the lifetime expectancy. In a second stage, constant-amplitude fatigue tests are performed under pulsating conditions in order to establish an energy-life relationship. Finally, fatigue life predictions under variable-amplitude loading are performed using the energy-life curve developed in the previous stage along with an adequate linear fatigue damage accumulation law.

## 2 Experimental Procedure

The material used in this research was the AISI 19Ni300 maraging steel produced by selective laser melting. Samples were manufactured using a Concept Laser M3 linear printing system at a sintering scan of 200 m/s. Layers were deposited vertically, on a base plate, in the direction of load application. After production, all samples were machined and polished to a scratch-free condition [6].

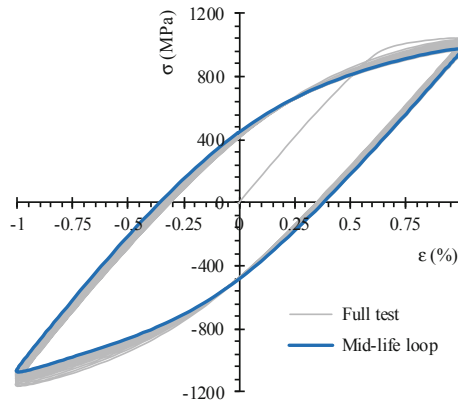
Low-cycle fatigue tests were performed under fully-reversed strain-controlled conditions ( $R_\epsilon = -1$ ), at a constant strain rate ( $d\epsilon/dt = 8 \times 10^{-3}$  s) and with sinusoidal waveforms, using cylindrical cross-section specimens with a 6 mm-diameter gauge section, considering strain amplitudes ( $\Delta\epsilon/2$ ) in the range 0.3 to 1.0%. The stress-strain response was acquired via an axial extensometer clamped directly to the gauge section. Tests were interrupted when the specimen reached the total failure [6].

Constant-amplitude (CA) axial fatigue tests were done under displacement control mode, at pulsating loading conditions, using 4 mm-diameter cylindrical cross-section specimens, and stress ranges ( $\Delta\sigma$ ) between 300 and 700 MPa. Variable-amplitude (VA) axial fatigue tests were carried out at pulsating load conditions, under load control mode, using the same geometry of the former tests. The block load spectra consisted of three stress levels with stress ratios ( $\sigma/\sigma_{\max}$ ) of 0.5, 0.75 and 1.0 applied for 1000 cycles. The maximum stresses ( $\sigma_{\max}$ ) varied in the interval 450 and 700 MPa. Sinusoidal waveforms and cyclic frequencies of 15–20 Hz were used in CA and VA tests.

## 3 Results

The first goal of the present study was the identification of a reliable energy damage parameter able to correlate the loading history with the lifetime expectancy. This identification was done on the basis of the low-cycle fatigue tests. Figure 1 shows the typical stress-strain response recorded in the fully-reversed strain-controlled tests for the AISI 18Ni300 maraging steel produced by selective laser melting ( $\Delta\epsilon/2 = 1.0\%$ ). Cyclic strain-softening behaviour is clearly observed, since the peak tensile stress decreases with the number of loading cycles until a stable behaviour is achieved (see the mid-life loop representative of the stable behaviour). This transient response occurs only at the first few cycles. After that, the stress-strain response stabilises and, in a final stage, for life ratios ( $N/N_f$ ) greater than 90%, the tensile stress drops rapidly culminating in fatigue failure.

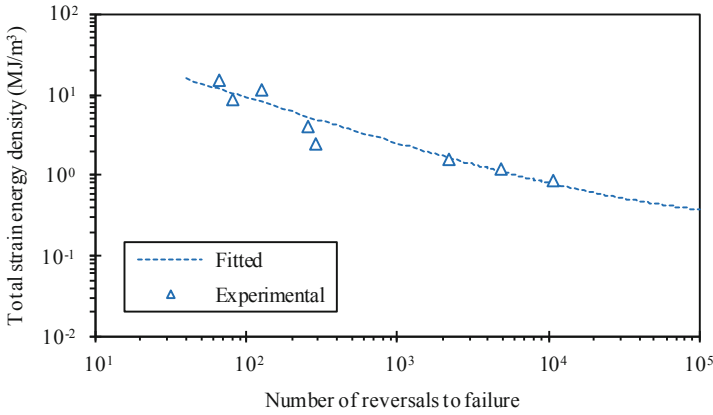
The area of the hysteresis loops, which represents the plastic strain energy per cycle, can be regarded as a main contribution to the fatigue damage process taking place in each cycle. According to Fig. 1, although there are changes during the test, this energy is almost constant. Nevertheless, this parameter is difficult to measure at small values of strain amplitude which makes difficult its application in the high-cycle fatigue regime. At lower strain amplitudes, the total strain energy density (defined as the sum of both the elastic positive and plastic components) is more reliable. Additionally, the use of the elastic positive component makes it sensitive to the mean stress effect which is another advantage. Figure 2 presents the variation of the total strain energy density of the mid-life loop (which is expected to be representative of the stable behaviour) with the number of reversals to failure for various strain amplitudes. In fact, despite some scatter which can be explained by the nature of the fatigue phenomenon, there is very good correlation between both variables. Based on this observation, the total strain energy density seems to be a reliable parameter to deal with the fatigue life prediction of additively manufactured samples.



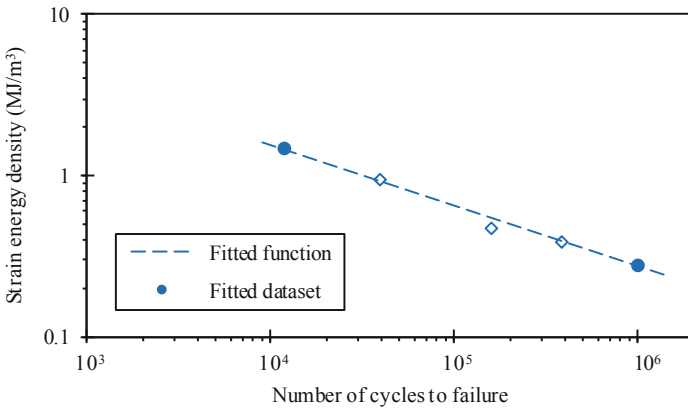
**Fig. 1.** Typical stress-strain response acquired in the fully-reversed strain-controlled test performed in AISI 18Ni300 samples produced by selective laser melting ( $\Delta\epsilon/2 = 1.0\%$ ).

Then, the second goal was the definition of an energy-life relationship. Since the variable-amplitude loading tests were conducted at pulsating conditions, the energy-life curve was established at the same stress ratio. Here, the approach proposed in reference [7] has been adopted. Briefly, the energy-life relationship was established from only two tests conducted at different loading levels (see Fig. 3). The fitted function was computed assuming a power law. Only the two extreme points (filled in circles) were used. The other points (hollow circles) were added to investigate the quality of the proposed relationship. As can be seen, the fitted function is representative of the entire range of tests.

The final goal was the fatigue life prediction under variable-amplitude loading. Fatigue damage accumulation has been computed by the Miner's law. The damage accumulation induced by each loading block was estimated from the energy-life

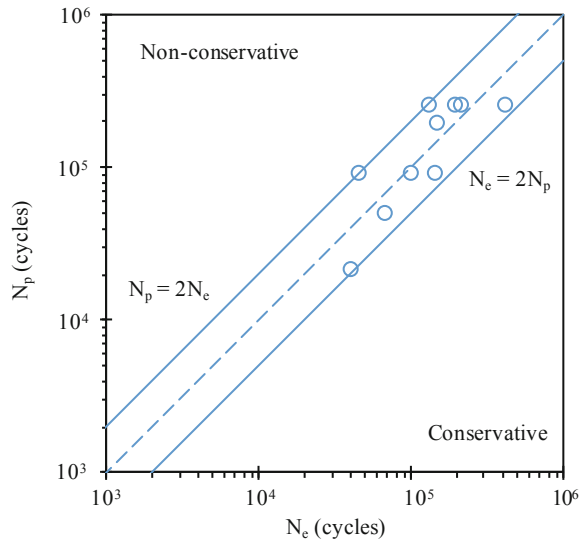


**Fig. 2.** Strain energy density of the mid-life circuits against the number of reversals to failure for the AISI 18Ni300 samples produced by selective laser melting.



**Fig. 3.** Strain energy density versus number of reversals to failure defined from two constant-amplitude tests for the AISI 18Ni300 samples produced by selective laser melting.

relationship as the ratio of the applied number of cycles to the fatigue lifetime associated with this loading block. Figure 4 compares the experimental lives with those predicted via the proposed methodology. As can be seen, there is a very good correlation in the entire range, with all the points within scatter bands of two (i.e.  $N_p = 2N_e$  and  $N_e = 2N_p$ ) which is satisfactory. Furthermore, in general, predictions are conservative, which is also interesting. Therefore, these results show that the proposed methodology can be successfully applied to analyse the fatigue lifetime in of additively manufactured samples undergoing variable amplitude loading histories.



**Fig. 4.** Comparison of experimental versus predicted lives in AISI 18Ni300 samples produced by selective laser melting subjected to variable-amplitude loading.

## 4 Conclusions

This paper has addressed the applicability of energy-life curves to deal with fatigue life prediction of additively manufactured samples subjected to variable amplitude loading. The following conclusions can be drawn:

- The total strain energy density (defined as the sum of both the elastic tensile and the plastic strain components) is a stable parameter almost constant through the entire life of the samples when subjected to strain-controlled conditions;
- An energy-life curve, established on the basis of the mid-life circuits and the number of reversals to failure, is able to correlate the fatigue damage with the fatigue lifetime;
- The definition of an energy-life relationship from two constant-amplitude tests has been sufficiently reliable. In addition, it reduced the time and cost associated with the determination of the fatigue properties;
- Fatigue life predictions under variable-amplitude loading agreed with the experimental results, with all the tests within a scatter band of two. Fatigue life predictions were, in general, conservative.









## References

1. Schmidt, M., Merklein, M., Bourell, D., Dimitrov, D., Hausotte, T., Wegener, K., Overmeyer, L., Vollertsen, F., Levy, G.: Laser based additive manufacturing in industry and academia. *CIRP Ann. Manuf. Technol.* **66**, 561–583 (2017)
2. Mooney, B., Kourousis, K., Raghavendra, R.: Plastic anisotropy of additively manufactured maraging steel: influence of the build orientation and heat treatments. *Addit. Manuf.* **25**, 19–31 (2019)
3. Suryawanshi, J., Prashanth, K., Ramamurty, U.: Tensile, fracture, and fatigue crack growth properties of a 3D printed maraging steel through selective laser melting. *J. Alloy. Compd.* **725**, 355–364 (2017)
4. Croccolo, D., Agostinis, M., Fini, S., Olmi, G., Robusto, F., Ćirić-Kostić, S., Morača, S., Bogojević, N.: Sensitivity of direct metal laser sintering Maraging steel fatigue strength to build orientation and allowance for machining. *Fatigue Fract. Eng. Mater. Struct.* **42**, 374–386 (2019)
5. Santos, L., Ferreira, J., Jesus, J., Costa, J., Capela, C.: Fatigue behaviour of selective laser melting steel components. *Theor. Appl. Fract. Mech.* **85**, 9–15 (2016)
6. Branco, R., Costa, J., Berto, F., Razavi, S., Ferreira, J., Capela, C., Santos, L., Antunes, F.: Low-cycle fatigue behaviour of AISI 18Ni300 maraging steel produced by selective laser melting. *Metals* **8**(1), 32 (2018)
7. Branco, R., Prates, P., Costa, J., Berto, F., Kotousov, A.: New methodology of fatigue life evaluation for multiaxially loaded notched components based on two uniaxial strain-controlled tests. *Int. J. Fatigue* **111**, 308–320 (2018)



# Study of Laser Metal Deposition (LMD) as a Manufacturing Technique in Automotive Industry

F. Q. Ramalho<sup>1</sup> , M. L. Alves<sup>1</sup> , M. S. Correia<sup>1,2</sup>  ,  
L. M. Vilhena<sup>2</sup> , and A. Ramalho<sup>2</sup> 

<sup>1</sup> School of Technology and Management,  
Polytechnic Institute of Leiria, Leiria, Portugal

mario.correia@ipleiria.pt

<sup>2</sup> Centre for Mechanical Engineering, Materials and Processes,  
University of Coimbra, Coimbra, Portugal

**Abstract.** The last few decades in the automotive industry have been marked by a heavy concern with the environment, saving energy and reducing material wastage, while aiming to maintain good mechanical properties, essential in the components usage. Additive manufacturing (AM) techniques present themselves as a viable option in the matter, with Laser Metal Deposition (LMD), rising as one of the most promising techniques within this category, capable of producing near-net shape components, with a layer upon layer construction of three-dimensional solid parts from a 3D CAD model, with good mechanical properties and acceptable surface finishing. Laser Metal Deposition is a relatively recent technique, which is made noticeable by the lack of clarification about the influence of several parameters in the final components characteristics, ultimately leading to a scarce availability of the process in the market. This paper aims to clarify and evaluate, how LMD produced parts can suit the automotive industry, by measuring and analysing their behaviour under several mechanical tests. These mechanical tests have specific focus on wear and abrasion behaviour, as well as elastic properties determination, as these are the characteristics that allow a better overview over the expected performance of LMD components for automotive applications.

**Keywords:** Laser Metal Deposition · Additive manufacturing · Automotive industry

## 1 Introduction

In the process of researching and developing better and more efficient manufacturing techniques, car manufactures invest significantly large quantities of money and time, which contributed to the development and perfecting of new and undeveloped manufacturing techniques and the manufacturing of components with good mechanical properties, allying with less energy consumption and less material wastage.

Additive manufacturing techniques rise as one of the most promising type of processes, since these allow the construction of components through an additive perspective, opposed to the more conventional ones with subtractive nature.

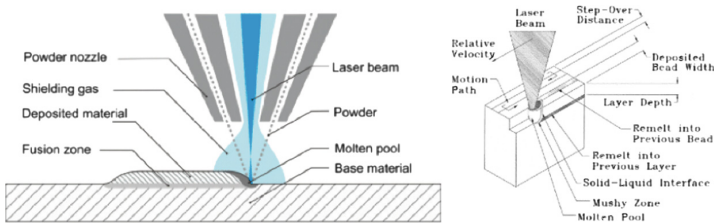
Within additive manufacturing techniques, Laser Metal Deposition (LMD) stands out as one of the main types of additive manufacturing when using metal as a deposition material, which is a key factor on the automotive industry, offering significant energy saving, almost null material waste, lower productions time and good reproducibility.

LMD is a technique capable of producing near-net shape metallic components with good mechanical properties, standing on the good adhesion between layers.

The biggest limitations of the technique stand on the poor surface finishing, which can be corrected with additional processing, and also the somewhat low resolution, since the layer thickness is dependent of the laser beam diameter.

This metallic additive manufacturing process is capable of a layer upon layer 3D part construction, using a high-power laser beam to achieve the fusion of a metallic material, which feeds in the form of either powder or wire through a nozzle, directly into a substrate of metallic nature [1].

Figure 1 (left) illustrates the deposition process, with the laser beam and powder or wire feeding system, as well as the substrate where the layer is deposited.



**Fig. 1.** Illustration of an LMD deposition process [2] (left) and schematic representation of layer deposition in LMD technology [3] (right).

The deposition process is made directly into a surface where a molten pool exists, allowing adhesion between layers through the surface tension, since the metal which is deposited in liquid form is held in place by the already solidified layers that exist on the periphery of the molten pool. This effect also allows the deposition of layers in virtually every direction wanted, including overhead depositions. The morphology of the molten pool area is illustrated on Fig. 1 (right) [3].

The successive vertical layer deposition creates an uneven cooling process of the several layers, which means the mechanical properties of the deposited material can vary throughout the components, since each layer cooling process is distinct from the others [4].

The cooling process can also be influenced by the vertical and horizontal overlap applied between the layers, which also influence the dimensions of the layers and the adhesion between them, and might introduce defects into the final component such as cracks or gaps [5].

The process often uses an inert gas, such as argon, helium or nitrogen that involves the molten pool, preventing oxidation of the parts.

For this the mechanical properties of components produced by LMD process are usually higher than the ones obtained through other conventional processes.

### 1.1 Powder and Wire LMD

The powder LMD was the first type of LMD to be produced and it is slightly more advanced and established than wire LMD, mainly because it offers a more controlled and refined deposition process, with the possibility of robotic control, a much lower dilution rate between the deposited material and the substrate (5% against 20% verified on the wire variety), ending up on a much more refined microstructure due to a more controllable and constant deposition rate [6]. Another advantageous aspect is that the available metallic powder range is much broader than the range of metallic wires.

The downsides of powder LMD are often related to the powder manufacturing processes, which introduce higher costs and bigger health concerns due to the toxicity that the processes generate [7].

Wire LMD on the other hand, is usually a cheaper process to implement and run, and the complexity of the equipment is often lower, is capable of applying high deposition rates without influencing the porosity of the deposited layers and the material usage efficiency is near 100% which is another desirable aspect of the wire variant [8].

However, wire LMD has some downsides, most of which are related to the deposition process itself. The fact that the feed material is on the form of a metallic wire introduces difficulties in its fusion, not being able to function properly under robotic control and encountering several geometrical barriers, which end up meaning that this variant is incapable of depositing thin walls, overhangs and hollow structures [9].

The wire feeding process is not able to maintain a clean and constant stream of wire to the laser focal zone, promoting some defects on the final components, however is significantly simpler to conduct when compared to the powder manufacturing techniques. It represents less cost and almost eliminates the health concerns present on the powder materials, even with an available range of metallic wire materials much more reduced.

## 2 Materials and Methods

### 2.1 Equipment and Material

Given the main goals of this work both powder and wire LMD components were used in order to analyse the feasibility of the process under certain production conditions, but also to achieve data that allows a distinction between the wire and powder variants of this process.

Regarding the powder LMD components, these were produced by IK4-Tekniker, on their facilities, using a 2.2 kW diode pumped continuous wave Rofin DY022 Nd:YAG laser, with the laser beam being guided towards the work area through a 0.6 mm

diameter fiber and an optical head from Precitec. The powder was injected into the molten pool area, using a three-hole coaxial nozzle made by IK4-Tekniker. The movement of the laser head was implemented through a 6-axis ABB 4400 robot.

The powder was fed using a Sulzer Metco Twin-10C powder feeder, with a feed rate of 15 g/min and a translation speed of the laser head stock of 400 mm/min [1].

The several powder LMD components provided present different manufacturing layer shift heights since the distance between the deposition set (laser and powder feeder) and the molten pool was varied (0,3 mm, 0,7 mm, 0,8 mm and 0,9 mm), resulting in components with different characteristics. However, the values of distance between the deposition set and the molten pool do not directly correspond to the layer height itself, since this particular value is a result of the horizontal and vertical overlap, and the amount of deposited material.

The deposition material was Metco 42C Martensitic Stainless-Steel powder, which is identical to AISI 431 grade stainless steel and the substrate plate was C45E Carbon Steel, with 10 mm of thickness.

The wire LMD components were produced using roughly the same equipment, the laser power was lowered to 1,5 kW, the translation speed was increased to 1200 mm/min and the wire feeding rate was of 3 m/min [1].

The wire LMD components, unlike the powder components, were produced using a fixed layer shift height of 0,9 mm.

The metallic wire used was made of AISI 316L austenitic stainless steel and the substrate plate material was also C45E Carbon Steel, with 10 mm of thickness.

Both wire and powder components were manufactured using an overlap between consecutive layers of 40% of a single bead width, which in this case represented a value of 1,3 mm. The deposition process of each layer consists of an external perimeter deposition followed by a zig-zag trajectory that ends up filling the inner section.

The components dimensions are shown in Table 1, with the “Px” being the powder components and the “Wx” being the wire components.

**Table 1.** Powder and Wire LMD components dimensions (x, y, z).

Number identification	x [mm]	y [mm]	z [mm]	Deposition height [mm]
P1	12,55	28,05	78,80	0,3
P2	13,45	29,00	79,00	0,9
P3	11,10	27,00	77,50	0,8
P4	13,00	26,20	80,00	0,7
P5	13,00	27,50	78,70	0,8
W1	30,60	30,60	99,00	0,9
W2	30,60	30,90	60,00	0,9
W3	30,50	30,90	62,10	0,9
W4	30,30	30,90	37,90	0,9
W5	31,00	30,75	47,35	0,9

## 2.2 Mechanical Test Schedule

The planned mechanical tests that were conducted covered several aspects like the elastic properties of the components, surface characteristics and the friction and wear behaviour of the components under different conditions.

In order to achieve those results microhardness, density, impulse vibration tool analysis, friction and wear tests were performed.

The Vickers microhardness test was conducted under the ASTM E92 [13] standard, using a Shimadzu HMV-2 equipment, available on the School of Technology and Management of Polytechnic Institute of Leiria facilities, and was applied to both powder and wire LMD components, with the different layer characteristics. For this tests a load of 4,903 N was applied for 15 s on LMD surfaces.

Before carrying out the test, surface preparation were made by using a Struers RotoPol-21 and sandpaper disks with grits of 500, 800, 1200 and 2400.

In order to obtain a variation profile of the component's microhardness, the test was conducted in sets of 5 point with a 1 mm distance between them, with a distance of 10 mm between the first points of every set.

Through density testing the relation between a components mass and volume is achievable, which, alongside the data reference value for the material density in wrought shape, allows this comparative ratio.

This test was conducted under the Archimedes principle [13], using a Mettler Toledo AG204 scale.

The test consists in two weight measurements of the component, one in a dry condition and another in a submerged condition, which allows the calculation of the density of the component, through the Eq. (1).

$$d_{component} = \left( \frac{m_{dry}}{m_{dry} - m_{submerged}} \right) \cdot d_{H_2O@T_{air}} \quad (1)$$

Additionally, impulse excitation vibration tests were performed to achieve mechanical elastic properties such as Young's modulus, Shear modulus and the Poisson ratio.

Tests were conducted under the ASTM E1876-15 [14] standard.

The measurement of these fundamental resonant frequencies is made by mechanical exciting the component with a singular elastic strike using an impulse tool.

A transducer is then used to sense the resulting mechanical vibrations of the component, transforming them into an electric signal that is later analysed in order to obtain the fundamental resonant frequencies. The laboratorial apparatus is similar to the one presented in Fig. 2.

Knowing the fundamental resonating frequency of the test subject, the following equations are then applied to achieve the aforementioned mechanical properties, namely the values of Young Modulus (E) and the Poisson ratio ( $\mu$ ).

$$E = 0,9465 \cdot \left( \frac{m_f^2}{b} \right) \cdot \left( \frac{L^3}{t^3} \right) \cdot T_1 \quad (2)$$

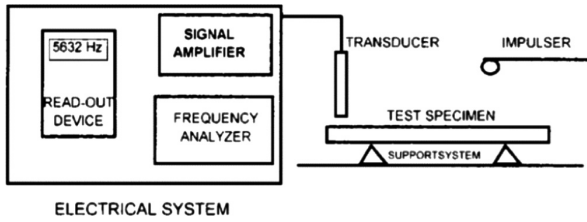


Fig. 2. Impulse excitation of vibration test equipment illustration [14].

$$T_1 = 1 + 6,585 \cdot (1 + 0,0752 \cdot \mu + 0,8109 \cdot \mu^2) \cdot \left(\frac{t}{L}\right)^2 - 0,868 \cdot \left(\frac{t}{L}\right)^4 - \left[ \frac{8,340 \cdot (1 + 0,2023 \cdot \mu + 2,173 \cdot \mu^2) \cdot \left(\frac{t}{L}\right)^4}{1,000 + 6,338 \cdot (1 + 0,1408 \cdot \mu + 1,536 \cdot \mu^2) \cdot \left(\frac{t}{L}\right)^2} \right] \tag{3}$$

$$\mu = \left(\frac{E}{2 \cdot G}\right) - 1 \tag{4}$$

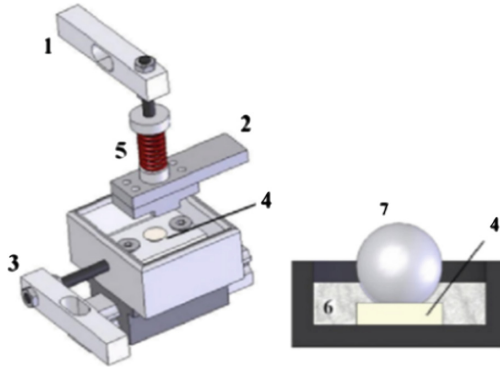
This test was conducted on the ICEMS – University of Coimbra homemade facilities. Both powder and the wire LMD were tested, both specimens with a layer height of 0,9 mm.

The final destructive conducted test was the wear test, which is capable of offering a clearer idea of how a material behaves under specific environmental conditions, with the possibility to reproduce operating conditions such as temperature, fluid interactions, and direction of wear, amongst others.

The selected wear test had a reciprocating nature, allowing a variation in the amplitude of movement, sliding speed and in the normal load value, which ends up giving the possibility to emulate several test conditions that better characterize a real application of a component produced [15].

This test was performed using the ICEMS – University of Coimbra homemade reciprocating tribometer, and although it does not follow any specific standard, it is capable of simulating real conditions, allowing an evaluation of contact wear in both materials under testing.

The used geometry of contact was a ball to plane, being the ball (7) a zirconium sphere with 10 mm of radius, assembled in the moving stage (2), which is in permanent contact with the stationary horizontal plane (4), in the form of LMD components (Fig. 3). The normal load is applied by a spindle-spring (5) which is supported by the normal load cell (1), that measures the normal load applied, which was 3, 5 and 7 N. A harmonic wave generated by an eccentric-and-rod mechanism set with stroke length of 2 mm and frequency of 3 Hz imposes the referred reciprocating movement of the upper sphere carrier. The LMD components were placed in the holder connected to a ball linear bearing slider in order to allow movement in the direction of the sliding reciprocating motion. The stationary load cell (3) is used to equilibrate the lower specimen holder attaining the friction force values along the test.



**Fig. 3.** Wear testing apparatus [15].

Result analysis on the stationary plane side (LMD samples) is made by measuring the area of the wear track and by integration it over the wear track length, obtaining the volume that was stripped away from the surface.

The results regarding the sphere are assessed by measuring directly its diameter. The measurement of the diameter was performed in two orthogonal directions, one along the relative motion direction and another in the perpendicular direction, and then using these two values to calculate the average radius ( $r$ ) of the ball wear scar. Combining this average radius ( $r$ ) and the original ball radius ( $R$ ), it is then possible to obtain the depth ( $h$ ) and volume ( $V$ ) of the ball wear scar created during the test, by using Eqs. (5) and (6). Finally, and using the depth and volume of the wear track, it is then possible to calculate the wear rate ( $k$ ), using Eq. (7), where  $F$  is the normal force and  $L$  the sliding distance.

$$h = r - \sqrt{R^2 - r^2} \quad (5)$$

$$V = \frac{\pi}{3} \cdot h^2 \cdot (3R - h) \quad (6)$$

$$k = \frac{V}{F \cdot L} \quad (7)$$

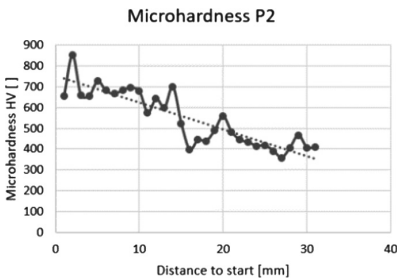
### 3 Results

The results regarding the microhardness test shown that a tendency does exist in both the average value and the variation of microhardness throughout the components, however, the value is somewhat different from the reference value that was expected (Table 2 and Figs. 4 and 5).

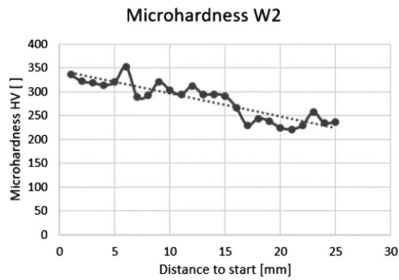


**Table 2.** Average microhardness in each tested component.

Component	Microhardness HV
P1 (0,3 mm)	409
P2 (0,9 mm)	547
P3 (0,8 mm)	485
P4 (0,7 mm)	490
P5 (0,8 mm C.C.)	550
W2 (0,9 mm)	282



**Fig. 4.** Microhardness results for component P2.



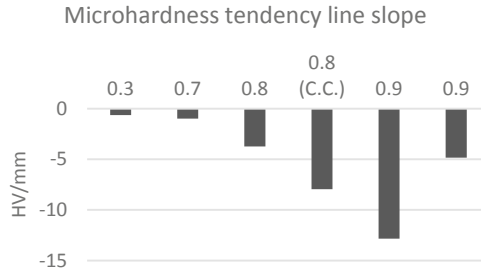
**Fig. 5.** Microhardness results for component W2.

All of the tested components, both powder and wire LMD, showed a tendency to register higher values of microhardness towards the top of the component (last deposited layers) and lower values of microhardness towards the base of the components (first deposited layers), meaning that throughout the component the value of microhardness tends to decrease.

This decrease of microhardness and its magnitude appears to be related to the layer shift, and consequently to the theoretical layer height, at least on the powder LMD components, given that higher values of theoretical layer height, meant that a steeper variation of microhardness happened from the top of the components to the base of it.

The wire LMD component, despite having a 0,9 mm theoretical layer height, showed a behaviour somewhat approachable to the 0,8 mm theoretical layer height powder LMD variant equivalent, in what microhardness is concerned.

The tendency to register a higher variation of microhardness throughout the component, when higher values of layer shift height are used, is confirmed by the value of the slope of the microhardness tendency lines (Fig. 6), which presents a negative value, confirming that the higher values of microhardness are registered near the top of the component, and it also presents a higher absolute value at the higher the layer shift height.



**Fig. 6.** Microhardness tendency line slope, in comparison to the layer shift height.

The test was conducted using deionized water at 20 °C, with a corresponding density of 0,99882 kg/m<sup>3</sup> [16]. The mass of the components in dry and submerged state, as well as their density is presented in Table 3.

**Table 3.** Density test results.

Component	Layer shift height [mm]	Mass in dry condition [g]	Mass in submerged condition [g]	Density [kg/m <sup>3</sup> ]	Variation from reference [10, 11] in %
P1	0,3	6,1624	5,3570	7637,58	2,08% lower
P2	0,7	2,5869	2,2486	7633,00	2,14% lower
P3	0,8	5,6374	4,8938	7567,58	2,98% lower
P4	0,8 CC	7,9109	6,8726	7606,01	2,49% lower
P5	0,9	9,8348	8,5472	7624,34	2,25% lower
W2	0,9	6,4175	5,6157	7989,46	0,01% lower

The density results do not show a clear tendency, with the values for all the powder LMD components being relatively similar, showing that theoretical layer height does not affect density in a significant manner. The wire LMD tested specimens present a density higher than the powder LMD equivalents, however, the difference also occurs because different material was used on both techniques.

Looking at the powder LMD components (P1 to P5) made of Metco 42C, the reference value for density is of 7800 kg/m<sup>3</sup> [11], a value significantly higher than the one registered in the density tests, a tendency that is most likely due to the high porosity.

Regarding the wire LMD component, made with AISI 316L Austenitic Stainless Steel, the registered value is approximately the same as the reference for the material in question, which indicates a lower value of porosity, without significant internal gaps and cracks [11].

The impulse excitation of vibration test was performed on the W2 component, produced by wire LMD, presenting a theoretical layer height of 0,9 mm.

The component to be tested was cut to suitable shape, according to the standard, with a length of  $54,4 \pm 0,22$  mm, a width of  $17,84 \pm 0,026$  mm, a thickness of  $1,77 \pm 0,12$  mm and a mass of 12,80 g.

Figure 7 shows both the experimental and analytical vibrational waves that are created when the component was subject to an elastic strike, with a representation of the amplitude of vibration behaviour over time.

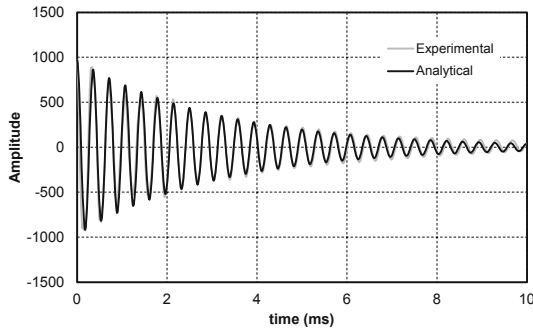


Fig. 7. Experimental and analytical response to the impulse excitation of component W2.

Through the representation of the vibration amplitude over the frequency, it is possible to visualize the fundamental resonant frequency, since the highest amplitude is registered within the area of said frequency, much like it is visible in the image below, with the point “1” being the first mode of bending and the point “2” being the first mode of torsion, both obtained by the excitation in different directions.

The frequency at which the first mode of bending is registered is of 2722 Hz and the one at which the first mode of torsion is registered is of 5177 Hz.

With the value presented on Fig. 8 the mechanical properties are then calculated and the results are presented in the Table 4.

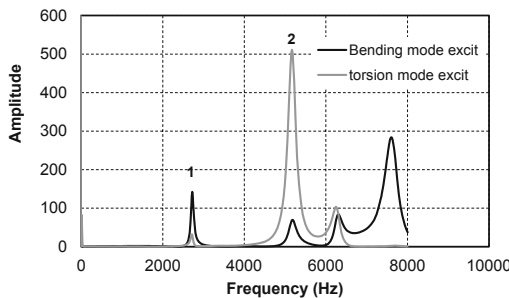


Fig. 8. Vibration spectra of component W2.

**Table 4.** Component W2 mechanical elastic properties, obtained through impulse excitation of vibration testing.

Mechanical property	Value	Variation from reference [11] in %
Young modulus [GPa]	146	24,35% lower
Torsion modulus [GPa]	63,6	17,40% lower
Poisson ratio	0,15	50,00% lower

When comparing the results to the reference values of AISI 316L Stainless Steel, it is possible to register significant differences. This means that the process used to produce this component affects the final mechanical properties significantly.

Some aspects like the thermal cycles suffered by the component during manufacturing as well as the deposition process itself (translation and deposition speeds) end up affecting the material microstructure and the porosity and thus affecting the elastic properties.

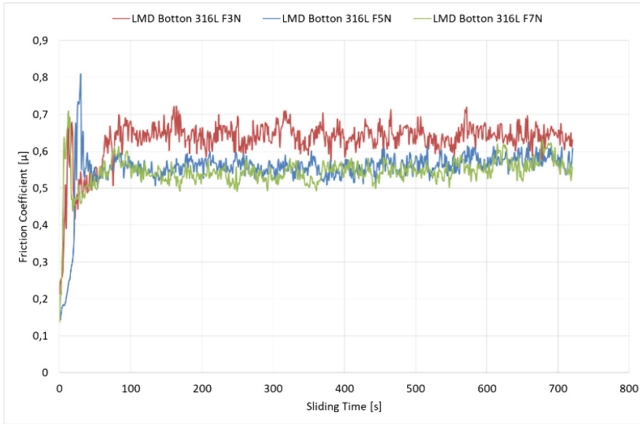
The friction and wear test was performed on the W2 component, produced by wire LMD, presenting a theoretical layer height of 0,9 mm. The selected component was tested under several wear conditions, under the values of normal force of 3, 5 and 7 N, and both the upper portion (last deposited layers) and the lower portion (first deposited layers) of the components also being subject to test. The friction and wear tests were performed at 24 °C and humidity 35%.

According to the friction test results it is possible to understand that there is a clear relationship between the values of the friction coefficient and the normal load applied to the component during the test, either on the upper part of the specimen or at the bottom. This relationship is established in such a way that when friction coefficient attains a steady state regime, which occurred sensibly within the first 100 s of the test, the mean value of friction coefficient was higher for lower normal force values. This relationship can occur due to the wear factor. This means that with the increase of the load it is verified that the wear that occurs in the component is larger, removing a larger quantity of material from the component. Probably, this material is deposited inside the generated crater and most likely will create a tribofilm that provides better sliding conditions between the bodies in contact, which reduces the friction coefficient.

Looking at the variation of the friction coefficient over time (Fig. 9), it is possible to identify an initial phase with running-in effect where this coefficient rises rather quickly, until it stabilizes in throughout the rest of the test, at the value of around 0,55. This value should be then compared to the friction coefficient of cast 316L steel under the same conditions, in order to understand how the LMD process affects this parameter.

It should also be noticed that the differences of coefficient of friction observed between the upper and lower part of the component are not significant, only verifying that the measured friction coefficient at the beginning of the test was slightly higher in the case of the lower part of the specimen, however the differences are minimal and do not allow conclusions to be drawn on this aspect.

Another point of interest resultant from the wear test, is the geometry of the wear track itself.

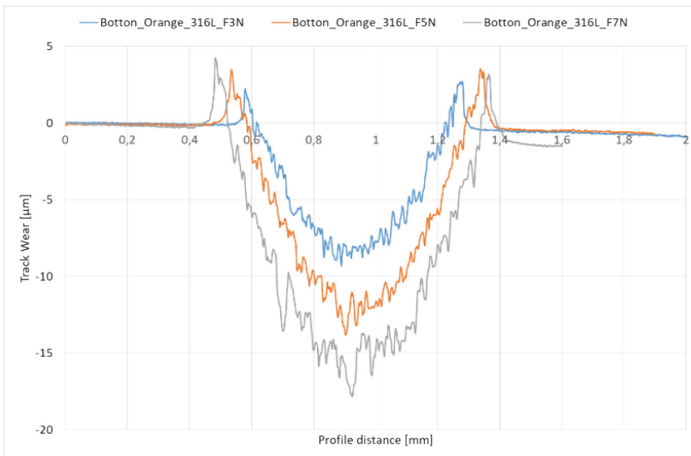


**Fig. 9.** Friction coefficient during reciprocating sliding tests – lower part.

With regard to the analysis of the profile of the wear track resulting on the flat specimen it can be verified that there is also a clear relationship between the transverse area of the cavity with the normal force exerted in the specimen during the test.

It is possible to verify that with the increase of normal force there is also an increase in both the profile depth and the profile width (Fig. 10).

The results of the upper and lower part of the specimen present a similar tendency and range, with higher values of depth and width of the cavity achieved for a normal force exerted in the specimen of 7 N.



**Fig. 10.** Cross section profiles from the wear tracks on the bottom portion of the W2 component, for 3, 5 and 7 N of normal force.

All of the wear tests conducted consisted of 1800 reciprocating cycles that ended up in a sliding distance of 7200 mm.

In order to calculate the wear rate coefficient, the diameter of the sphere needs to be calculated, in order to achieve the depth and volume of the wear track.

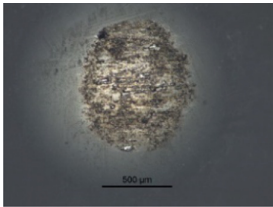
The Fig. 11 in the Table 5 presents the wear on the zirconium sphere, where the radius was measured using an image measurement software, named Digimizer. With this data, it was possible to calculate the depth and the volume of the wear scars, using Eqs. (5) and (6), and also the wear rate through Eq. (7).

Comparing the wear rate coefficients, it is possible to identify a difference between the top and base portions, as it was expected given the microhardness variations throughout the vertical axis of the component.

A significant variation between the base and top portions of the specimen was registered especially for the lower values of the normal force, with the top portion registering a wear rate that almost doubles the one registered on the base portion of the component.

This variation should be related to the fact that, under the highest normal load, the pressure is high enough to deform the metallic material closing the porosity, therefore reducing the porosity influence on the wear.

**Table 5.** Zirconium sphere wear scars diameters, depth (*h*) and volume (*V*) of the wear scars, and wear rate (*k*) of the component W2.

	$F_N = 3 \text{ N}$	$F_N = 5 \text{ N}$	$F_N = 7 \text{ N}$	
Base portion	$d_1 = 597,41 \text{ µm}$ $d_2 = 688,32 \text{ µm}$ $h = 10,34e-3 \text{ mm}$ $V = 16,78e-4 \text{ mm}^3$ $k = 7,8e-5 \text{ mm}^3/\text{N.m}$	$d_1 = 752,43 \text{ µm}$ $d_2 = 820,47 \text{ µm}$ $h = 15,49e-3 \text{ mm}$ $V = 37,65e-4 \text{ mm}^3$ $k = 10,5e-5 \text{ mm}^3/\text{N.m}$	$d_1 = 836,12 \text{ µm}$ $d_2 = 934,07 \text{ µm}$ $h = 19,62e-3 \text{ mm}$ $V = 60,39e-4 \text{ mm}^3$ $k = 12,0e-5 \text{ mm}^3/\text{N.m}$	
Top portion	$d_1 = 689,74 \text{ µm}$ $d_2 = 806,72 \text{ µm}$ $h = 14,02e-3 \text{ mm}$ $V = 30,85e-4 \text{ mm}^3$ $k = 14,3e-5 \text{ mm}^3/\text{N.m}$	$d_1 = 792,46 \text{ µm}$ $d_2 = 823,65 \text{ µm}$ $h = 16,35e-3 \text{ mm}$ $V = 41,95e-4 \text{ mm}^3$ $k = 11,7e-5 \text{ mm}^3/\text{N.m}$	$d_1 = 828,58 \text{ µm}$ $d_2 = 933,75 \text{ µm}$ $h = 19,45e-3 \text{ mm}$ $V = 59,35e-4 \text{ mm}^3$ $k = 11,8e-5 \text{ mm}^3/\text{N.m}$	

**Fig. 11.** Wear scar on the base portion of the W2 component, with 7 N of normal force.

### 4 Conclusion

The main goal set for this study was the understanding of the main mechanical characteristics offered by components produced with powder and wire LMD.

The microhardness values obtain at the tests decrease from the top of the components to the base (both in powder and wire LMD components), which appears to be related to the theoretical layer height. The wire LMD component tested behaves as the 0,8 mm theoretical layer height powder LMD variant equivalent. Both the tendency

hardness gradient and the standard deviation of the microhardness values corroborate the above mentioned conclusions.

It was noticeable that the density of powder LMD components was around 3% lower on all powder LMD specimens, showing that theoretical layer height does not affect the density in a significant manner. With respect to the wire LMD density, similar values were obtained to the reference value, indicating the absence of internal gaps and cracks (low porosity).

By the impulse excitation of vibration test it was possible to conclude that wire LMD component achieved lower results than the reference, namely of Young modulus and Poisson ratio.

The wear test allowed to conclude that the friction coefficient decreases with the increase of normal force used in testing and the wear track geometry is similar for the top and bottom portion of the components, however, the dimensions tend to be higher on the bottom portion, indicating more wear, possibly due to the lower microhardness. It was noticed that on wire LMD under lower loads (3 and 5 N), the top is much more prone to wear than the base portion. However, at higher loads the tendency shifts and the wear rates between the top and base portion are almost identical.

## References

1. Garmendia, I., Leunda, J., Pujana, J., Lamikiz, A.: In-process height control during laser metal deposition based on structured light 3D scanning. 19th CIRP Conference on Electro Physical and Chemical Machining, pp. 375–380, 23–27 de April de 2018
2. Graf, B., Ammer, S., Gumenyuk, A., Rethmeier, M.: Design of experiments for laser metal deposition in maintenance, repair and overhaul applications. In: 2nd International Through-life Engineering Services Conference, pp. 245–248, July de 2013
3. Lewis, G.K., Schlienger, E.: Practical considerations and capabilities for laser assisted direct metal deposition. *Mater. Des.* **21**, 417–423 (2000)
4. Amine, T., Newkirk, J.W., Liou, F.: An investigation of the effect of direct metal deposition parameters on the characteristics of the deposited layers. In: Qiu, E.H. (ed.) *Case Studies in Thermal Engineering*, pp. 21–34. Hong Kong: Elsevier (2014)
5. Oliari, S.H., D'Oliveira, A.S.C.M., Schulz, M.: Additive manufacturing of H11 with wire-based laser metal deposition. *Soldagem & Inspeção* 466–479 (2014)
6. Kaieler, S., Barroi, A., Noelke, C., Hermsdorf, J., Overmeyer, L., Haferkamp, H.: Review on laser deposition welding: from micro to macro. *Phys. Procedia* **39**, 336–345 (2012)
7. Midtgard, U., Jelnes, J.E.: Toxicology and occupational hazards of new materials and processes in metal surface treatment, powder metallurgy, technical ceramics, and fiber-reinforced plastics. *Scand J. Work Environ. Health* 369–379 (1991)
8. Vilar, R.: Laser Alloying and Laser Cladding. *Materials Science Forum*, vol. 301, pp. 229–252 (1999)
9. Hagqvist, P.: Lortek ES. Obtido de Lortek ES, 5 de July de 2019. [http://www.lortek.es/files/merlin/03-P\\_Hagqvist-UW&GKN-Aero-Case-study.pdf](http://www.lortek.es/files/merlin/03-P_Hagqvist-UW&GKN-Aero-Case-study.pdf)
10. Materials, A.: AZO Materials. Obtido de AZO Materials (2019). <https://www.azom.com/article.aspx?ArticleID=1023>
11. Steel eagle commerce, I. (2019). Steel eagle commerce ltd. Obtido de Steel eagle malta: <https://www.steeleaglemalta.com/grades/>

12. ASTM E92-17: Standard Test Methods for Vickers Hardness and Knoop Hardness of Metallic Materials, ASTM International, West Conshohocken, PA (2017)
13. Mazali, I.O. (s.d.). Determinação da densidade de sólidos pelo método de Arquimedes. LQES - Métodos, processos e técnicas
14. ASTM E1876-15: Standard Test Method for Dynamic Young's Modulus, Shear Modulus, and Poisson's Ratio by Impulse Excitation of Vibration, ASTM International, West Conshohocken, PA (2015)
15. Amilcar Ramalho, M.D.: Effects of temperature on mechanical and tribological properties of dental restorative composite materials. *Tribol. Int.* **63**, 186–195 (2013)
16. Toolbox, E.: Engineering Toolbox. Obtido de Engineering Toolbox (2019). [https://www.engineeringtoolbox.com/friction-coefficients-d\\_778.html](https://www.engineeringtoolbox.com/friction-coefficients-d_778.html)



# **Applications**



# Photocurable Alginate Bioink Development for Cartilage Replacement Bioprinting

H. Mishbak<sup>1,2</sup>(✉), Enes Aslan<sup>2</sup>, Glen Cooper<sup>2</sup>, and P. J. Bartolo<sup>2</sup>

<sup>1</sup> Biomedical Engineering Department, School of Engineering,  
The University of Thi-Qar, Thi-Qar, Iraq

<sup>2</sup> School of Mechanical, Aerospace and Civil Engineering,  
Manchester Biomanufacturing Centre, University of Manchester,  
Manchester, UK

hussein.al-hasani@postgrad.manchester.ac.uk,  
paulojorge.dasilvabartolo@manchester.ac.uk

**Abstract.** Bioink design and assessment for tissue engineering replacement is a key topic of research. This article investigates suitable photocurable alginate bioink precursors for bioprinting and the fabrication of 3D constructs for cartilage replacements. Alginate chemically modified with methacrylate anhydride groups is considered and assessed using different techniques. 2% Alginate methacrylate (AlgMA) solutions containing different concentrations of methacrylate and different reaction times were investigated. Nuclear magnetic resonance (NMR) results show the ability to tune the unsaturation degree by changing the reaction conditions. Rheological characterization results show that all alginate methacrylate precursor solutions exhibit a shear thinning behavior. Biocompatibility and cytotoxicity results were no cytotoxicity was observed.

**Keywords:** Alginate polymers · Rheology · Bioprinting · Tissue engineering

## 1 Introduction

Articular cartilage is a non-vascularized tissue, covering the distal ends of the bones, formed by a low density of cells called chondrocytes that maintain the structural and functional integrity of the extracellular matrix [1–3]. Cartilage is characterized by a distinct zonal structure comprising, in descending order, the articular or superficial surface, the middle (or transitional) zone, the deep zone, a tidemark (separates the non-calcified and calcified regions) [4]. However, it lacks inherent self-repair capacity and hence the zonal structure and function are often irreversibly lost following trauma and disease [5]. As a result, cartilage defects are prone to develop into osteoarthritis (OA), which is the predominant cartilage disease, characterized by loss of cartilage, pain and debilitation [6]. Despite the current therapeutic strategies such microfracture, autologous chondrocyte implantation (ACI), matrix-assisted autologous chondrocyte transplantation/implantation (MACT/MACI), autologous matrix-induced chondrogenesis (AMIC), and osteochondral auto- and allografts [7, 8], articular cartilage repair is still a major clinical challenge. Tissue engineering strategy emerged as a potential

therapy through the fabrication of constructs mimicking the ECM structure of articular cartilage [9]. Through this approach different biocompatible and biodegradable materials with or without cells were explored.

This paper focus on the use of photo-curable alginate as a carrier of chondrocyte cells for cartilage repair. Alginate was selected due to its biocompatibility, biodegradability, low cost and mild gelation process [9]. Moreover, photocurable alginate bioinks offer fast gelling, good printability properties [10].

In this case, alginate was functionalized using methacrylate anhydride and the functionalization conditions assessed in terms of reaction time and methacrylate concentration. Rheological properties were assessed in order to guarantee good printability. Finally, cell-laden constructs were produced, and cytotoxicity and cell proliferation tests performed.

## 2 Materials and Methods

### 2.1 Synthesis of Methacrylated Alginate

Methacrylate alginate was prepared following a published protocol [11]. In this study, 2 wt% of sodium alginate powder was completely dissolved in Dulbecco's Phosphate-Buffered Saline (DPBS) (Sigma-Aldrich, UK). Afterward, methacrylate anhydride (Sigma-Aldrich, UK) was added to alginate solution. The pH of the solution was kept around (7–8.0) during the reaction time by adding 5 M of NaOH. After the chemical modification, the polymer solution was precipitated with 100% ethanol, dried in an oven overnight at 40–50 °C, then diluted with distilled water and purified through dialysis for 6 days. The solution was frozen at –80 °C and the polymer recovered by lyophilization. Two different methacrylate concentration (15 and 25 mL for each gram of alginate) were used and two different reaction times (8 and 24 h) were considered for each methacrylate concentration. Crosslinked discs were produced by dissolving the functionalized alginate (AlgMA) polymer in a 1 w/v % photoinitiator solution (PI) VA-086, 2,2'-Azobis[2-methyl-N-(2-hydroxyethyl) propionamide azo initiator (Wako Pure Chemical Industries, USA). The photo-curable material was then pipetting into a custom-made cylindrical Teflon mould (diameter: 8 mm; height 4 mm). Photopolymerisation was conducted using a 365 nm UV light (Dymax 2000-EC, Dymax, Germany) irradiating at 8 mW/cm<sup>2</sup> for 8 min.

### 2.2 <sup>1</sup>H NMR

<sup>1</sup>HNMR was used to characterize the chemical modification of alginate. Methacrylate alginate solution was dissolved in deuterium oxide D<sub>2</sub>O and placed in an NMR tube. The <sup>1</sup>HNMR spectra were recorded using the B400 Bruker Avance III 400 MHz (Billerica, Massachusetts, USA) and the spectra acquired with 128 scans.

### 2.3 Rheological Characterization

The rheological tests were carried out using the DHR2 TA Instrument (USA). Rotational tests were considered, and all measurements were conducted at room temperature.

### 2.4 Cell Viability and Proliferation

The cytotoxicity of the hydrogels was investigated through the encapsulation of human chondrocyte cells (Cell Applications, USA) and a live/dead assessment (ThermoFisher Scientific, UK). Chondrocyte passage 4 were encapsulated at a density of  $0.75 \times 10^6$  cell/mL of sterilized hydrogel precursor solution. 160  $\mu$ L of gel-cell solution was pipetted into a 24-well custom mould and a UV radiation 365 nm emitted by a Dymax 2000-EC Lamp (Dymax 2000-EC, Dymax, Germany) during 8 min with a light intensity of 8 mW/cm<sup>2</sup>. After 3 and 7 days the cytotoxicity was analyzed by removing cell culture media, washing gently in DPBS adding a live dead stain solution, and incubating for 30 min. The hydrogels were then observed using a confocal fluorescence microscope (TCS-SP5, Leica, Germany). The Alamar blue assay was also used to evaluate cell metabolism and proliferation after 1, 3, 5 and 7 days of culture.

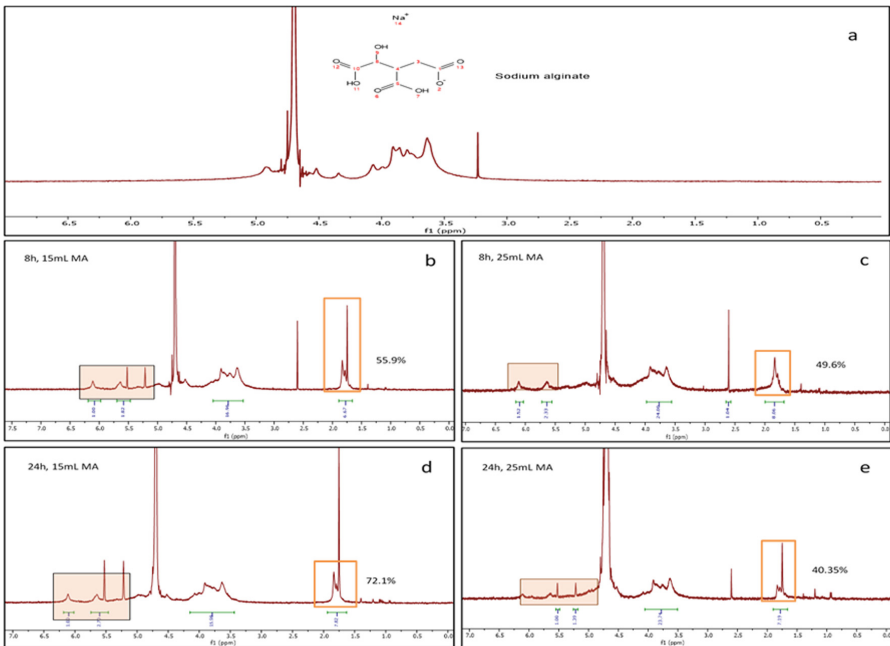
## 3 Result and Discussion

### 3.1 Chemical Modification Through <sup>1</sup>H NMR

<sup>1</sup>HMR results of non-functionalized and functionalized alginate are show in Fig. 1. In the case of functionalized results show that appearance of characteristic peaks of methacrylate (MA) at 5.53 ppm and 6.10 ppm attributed to the methylene group in vinyl bond, and a peak at 1.82 ppm associated to the methyl group. These peaks are not presented in nonmodified alginate (Fig. 1a). The effect reaction time and methacrylate anhydride concentration on the degree of modification (i.e., on the extent of methacrylation) determined by dividing the relative integrations of methylene to carbohydrate protons [12], is shown in Table 1. In the case of 15 ml MA, Results show that the degree of modification increases with increased reaction time, reaching a maximum value of 72.1% at 24 h. However, by increasing the methacrylate anhydride concentration up to 25 ml MA, the degree of modification was decreased, reaching 40.35 for 24 h reaction time. We hypothesized that the reduction on the degree of modification can be a result of the unreacted methacrylate, hydrolysis in aqueous conditions and elevated temperatures (40 °C) during reaction as well as possible reaction between methacrylate groups during dialysis, as previously reported [13]. These results suggest that the modification efficiency with methacrylic anhydride is significantly affected by the methacrylate concentration.

### 3.2 Rheological Characterization of Alginate Methacrylate

Figure 2 shows the variation of both the stress versus shear rate and the variation of viscosity versus shear rate considering different reaction rates and methacrylate concentration. Results show that all samples present a shear thinning behavior making them suitable for printing. It is also possible to observe that by increasing the reaction time the maximum stresses supported by the non-polymerised AlgMA increases. For longer reaction times and high concentration of methacrylate mechanical properties increases. Therefore, low methacrylate concentration (15 mL/g of alginate) will be considered.



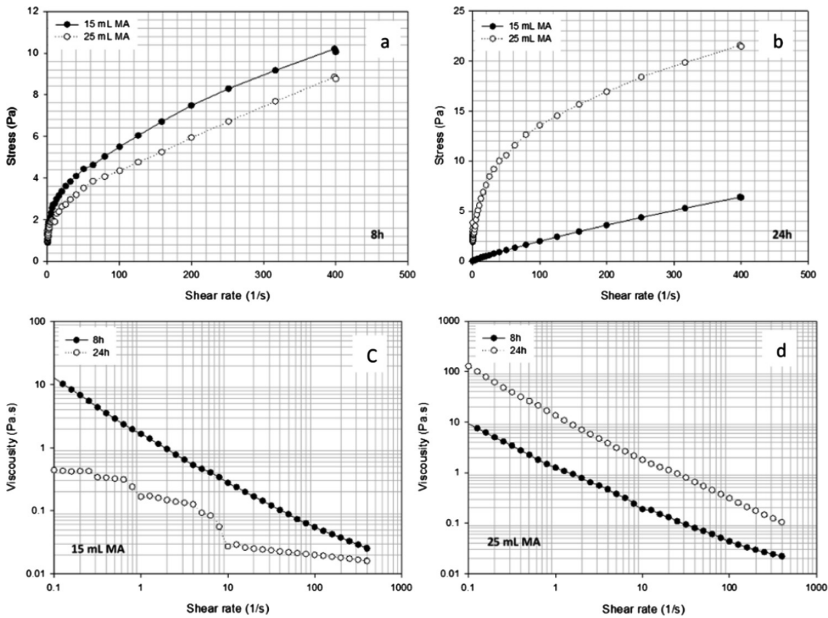
**Fig. 1.** 1H NMR spectra of (a) unmodified alginate and; (b) 2 wt% methacrylate alginate (15 mL MA) after 8 h of reaction; (c) 2 wt% methacrylated alginate (25 mL MA) after 8 h of reaction; (d) 2 wt% methacrylate alginate (15 mL MA) after 24 h of reaction; (e) 2 wt% methacrylate alginate (25 mL MA) after 24 h of reaction.

**Table 1.** Effect of reaction time on the degree of modification

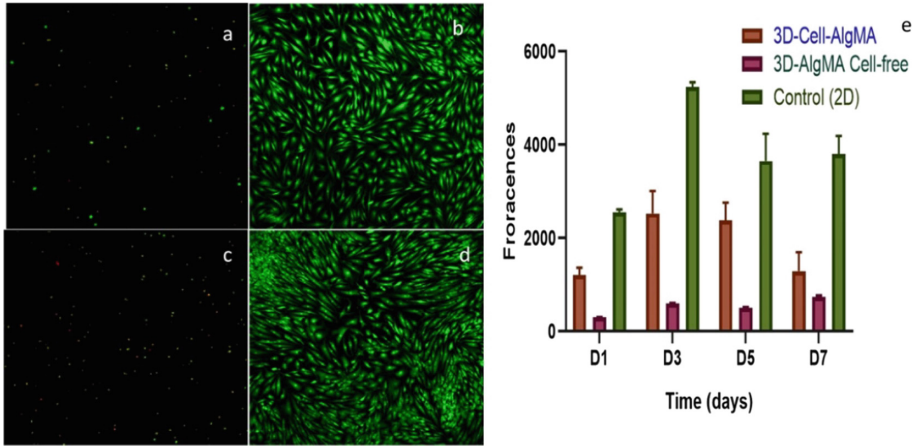
Composition (2 w/v%)	Reaction time (hours)	DoM (%)
AlgMA Low MA (15 ml)	8	55.9
AlgMA Low MA (15 ml)	24	72.1
AlgMA High MA (25 ml)	8	49.6
AlgMA High MA (25 ml)	24	40.35

### 3.3 Cell Viability Assessment

Cell viability assessment was examined using a live/dead assay (Fig. 3 a, b, c and d). As observed for both the 3D cell-laden constructs and 2D cell culture after 3 and 7 days of cell encapsulation, cell viability is higher than 85% with only a few dead cells being observed. The results demonstrate that the functionalized hydrogel presents low cytotoxicity being a suitable bioink materials. The metabolic and proliferation of human chondrocyte cells was also assessed using the Alamar blue assay (Fig. 3e). Results show that the encapsulated cells with AlgMA hydrogels have shown good proliferation rate at day 1 and 3, after day 5, cells proliferation was decreased. This can be explained by the confined space available for cells due to the absence of any degradable sites. Moreover, these results show that photocrosslinkable AlgMA hydrogels are biocompatible and adequately support the encapsulated cells.



**Fig. 2.** Rheological characterization of for 2 wt% methacrylate alginate samples. (a) Stress vs shear rate profile 8 h reaction time with different methacrylate concentrations; (b) Stress vs shear rate profile 24 h reaction time with different methacrylate concentrations; (c) Viscoelastic behavior low methacrylate concentration (15 mL); (d) Viscoelastic behavior high methacrylate concentration (25 mL).



**Fig. 3.** Chondrocyte cell encapsulation (a) day 3-3D cell culture Cell encapsulated in AlgMA; (b) day 3- control 2D cell seeding; (c) day 7- 3D cell culture Cell encapsulated in AlgMA hydrogels; (d) day 7- control 2D cell seeding; (e) Cell proliferation and metabolic activity profile of human chondrocyte cells.

## 4 Conclusions

A bioink for cartilage applications is presented. Alginate were functionalized with methacrylate groups and the effect of reaction time and methacrylation concentrations on the degree of substitution and rheological properties were assessed through NMR and rheological analysis, respectively. NMR data clearly show the ability to tailor the methacrylation degree by changing the reaction time and methacrylate anhydride concentration, enabling us to tailor the properties of the bioink. Successful cell-laden constructs were produced, showing that the bioink is able to support cell proliferation after 7 days of photo-polymerisation. No cytotoxicity emerging from both the alginate or the photoinitiator was observed. The photo-polymerisation was conducted in adequate conditions to guarantee cell survival.

**Acknowledgement.** The authors greatly acknowledge the government of Iraq for their kind support Mr. Hussein Mishbak's PhD through a grant provided by Higher Committee for Development Education Iraq (HCEDIRAQ). Mr. Aslan would like to acknowledge The Republic of Turkey Ministry of National Education for supporting his PhD through grant

## References

1. Buckwalter, J.A., Mankin, H.J.: Articular cartilage: degeneration and osteoarthritis, repair, regeneration, and transplantation. *Instr. Course Lect.* **47**, 487–504 (1998)
2. Simon, T.M., Jackson, D.W.: Articular cartilage: injury pathways and treatment options. *Sports Med. Arthroscopy Rev.* **26**(1), 31–39 (2018)

3. Flik, K.R., Verma, N., Cole, B.J., Bach, B.R.: Articular cartilage. In: Williams, R.J. (ed.) *Cartilage Repair Strategies*, pp. 1–12. Humana Press, Totowa (2007)
4. Guo, T., Lembong, J., Zhang, L.G., Fisher, J.P.: Three-dimensional printing articular cartilage: recapitulating the complexity of native tissue. *Tissue Eng. Part B: Rev.* **23**(3), 225–236 (2017)
5. Nukavarapu, S.P., Dorcemus, D.L.: Osteochondral tissue engineering: current strategies and challenges. *Biotechnol. Adv.* **31**(5), 706–721 (2013)
6. Buckwalter, J.A.: Articular cartilage injuries. *Clin. Orthop. Relat. Res.* **402**, 21–37 (2002)
7. Swieszkowski, W., Tuan, B.H.S., Kurzydowski, K.J., Hutmacher, D.W.: Repair and regeneration of osteochondral defects in the articular joints. *Biomol. Eng.* **24**(5), 489–495 (2007)
8. Redman, S.N., Oldfield, S.F., Archer, C.W.: Current strategies for articular cartilage repair. *Eur. Cell Mater.* **9**(23–32), 23–32 (2005)
9. Fragonas, E., Valente, M., Pozzi-Mucelli, M., Toffanin, R., Rizzo, R., Silvestri, F., Vittur, F.: Articular cartilage repair in rabbits by using suspensions of allogenic chondrocytes in alginate. *Biomaterials* **21**(8), 795–801 (2000)
10. Mishbak, H., Caetano, G.F., Pereira, R.F., Bartolo, P.J.: Photocurable Crosslinked Sodium Alginate and Gelatin based hydrogels for articular cartilage applications, p. 6 (2016)
11. Jeon, O., Bouhadir, K.H., Mansour, J.M., Alsberg, E.: Photocrosslinked alginate hydrogels with tunable biodegradation rates and mechanical properties. *Biomaterials* **30**(14), 2724–2734 (2009)
12. Smeds, K.A., Grinstaff, M.W.: Photocrosslinkable polysaccharides for in situ hydrogel formation. *J. Biomed. Mater. Res. Off. J. Soc. Biomater. Jpn. Soc. Biomater* **54**(1), 115–121 (2001)
13. Billiet, T., Van Gasse, B., Gevaert, E., Cornelissen, M., Martins, J.C., Dubruel, P.: Quantitative contrasts in the photopolymerization of acrylamide and methacrylamide-functionalized gelatin hydrogel building blocks. *Macromol. Biosci.* **13**(11), 1531–1545 (2013)





# Composite Scaffolds for Large Bone Defects

Evangelos Daskalakis<sup>1</sup>(✉), Enes Aslan<sup>1</sup>, Fengyuan Liu<sup>1</sup>,  
Glen Cooper<sup>1</sup>, Andrew Weightman<sup>1</sup>, Bahattin Koç<sup>2</sup>, Gordon Blunn<sup>3</sup>,  
and P. J. Bartolo<sup>1</sup>

<sup>1</sup> School of Mechanical, Aerospace and Civil Engineering,  
University of Manchester, Manchester, UK  
evangelos.daskalakis@postgrad.manchester.ac.uk,  
paulojorge.dasilvabartolo@manchester.ac.uk

<sup>2</sup> Department of Manufacturing Engineering,  
Sabanci University, Instabul, Turkey

<sup>3</sup> School of Pharmacy and Biomedical Sciences,  
University of Portsmouth, Portsmouth, UK

**Abstract.** This paper investigates the use of polymer-ceramic composite scaffolds for bone regeneration. Different ratios between Poly-ε-caprolactone (PCL) and Hydroxyapatite (HA) were considered. Scaffolds were produced using two different lay-down patterns (0/90° and 0/45°), and pore sizes (350 μm, 500 μm and 700 μm). Compressive and cell proliferation tests are reported. Human adipose derived stem cells (hADSCs) were used for the biological characterization.

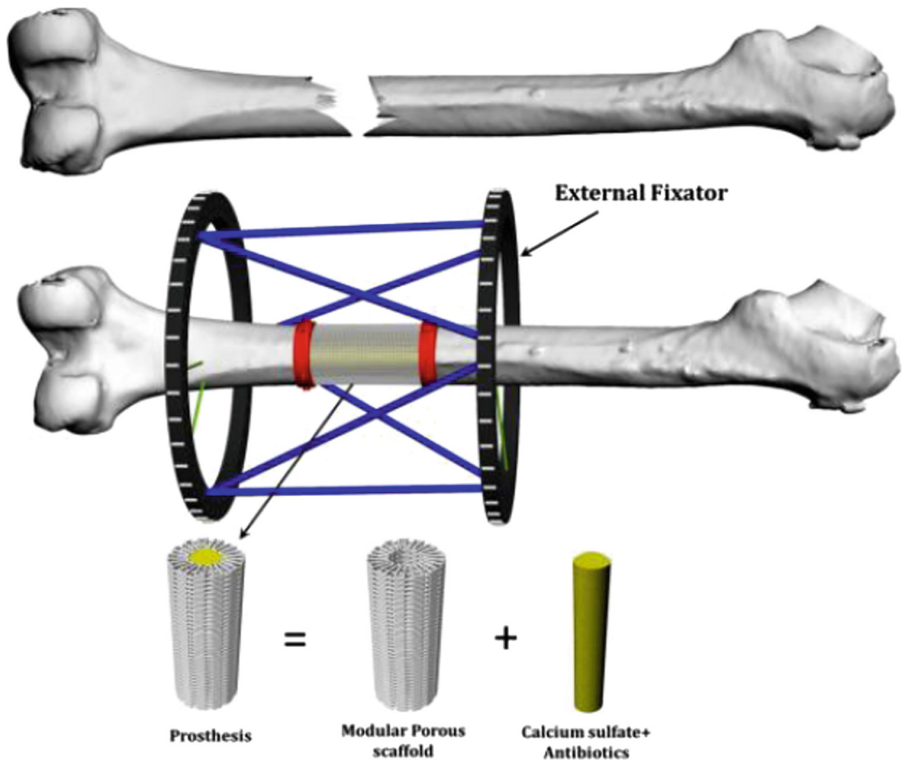
**Keywords:** Hydroxyapatite · Bioprinting · Additive manufacturing · Tissue engineering

## 1 Introduction

Physical and sensory impairments affect one in every five refugees, one in seven is affected by a chronic disease and one in 20 suffers from injury. A 2016 Handicap International report stated that 53% of injuries were due to the use of explosive weapons, among this 47% of refugees had fractures or complex fractures and this includes open fractures of lower and upper limbs. Orthopaedic surgical intervention is a priority after blast injuries to align broken bones, treat infection and implement solution for the associated bone loss. However often the only feasible treatment for these injuries is limb amputation.

As part of an EPSRC/GCRF (Engineering and Physical Sciences Research Council/Global Challenges Research Fund) we are developing a novel low cost osseointegrated modular prosthetic solution to treat large bone loss injuries to enable limb salvage [1]. The immediate application is to treat Syrian refugees who have been displaced to Turkey, but the knowledge can be applied to other conflict or natural disaster area. The project proposes to build on the current treatment of the external fixation but with the addition of an engineering internal prosthetic implant to improve patient outcomes, avoid painful limb lengthening and reduce recovery time. A patient

specific prosthetic to fill the bone lost will be produced using biodegradable and biocompatible modular pieces (Bone Bricks-Fig. 1), from a pellet of shapes and sizes that fit together. This paper investigates different polymer-ceramic compositions, topologies and lay-down pattern strategies. Structures were printed using additive manufacturing and were morphological, mechanical and biological characterized.



**Fig. 1.** Bone bricks approach to treat large bone defects.

## 2 Materials and Methods

### 2.1 Materials

Polycaprolactone (PCL) (CAPA 6500,  $M_w = 50000$  Da) in the form of 3 mm pellets was supplied by Perstorp Caprolactones (Cheshire, UK). It is a semi-crystalline linear aliphatic biocompatible and biodegradable synthetic polymer, with low melting point and easy to process. Hydroxyapatite (HA) ( $M_w = 502.31$  g/mol, MP = 1100 °C) in the form of nanopowder (<200 nm particles size) was supplied by Sigma-Aldrich (St. Louis, USA).

PCL/HA blends were prepared with the use of melt blending creating four different concentrations (5, 10, 15 and 20 wt%). PCL was melted at around 100 °C, in a

porcelain bowl, to guarantee the melting status of the polymer before adding the bioceramic material. The mixing of the material took approximately 1 h to obtain a uniform mixture and then was cut in small pellets after its cooling.

## 2.2 Scaffolds Fabrication

Scaffolds were produced using an extrusion based additive manufacturing machine (3D Discovery from RegenHU, Switzerland). Two lay-down patterns ( $0/90^\circ$  and  $0/45^\circ$ ) and three different pore sizes (350  $\mu\text{m}$ , 500  $\mu\text{m}$  and 700  $\mu\text{m}$ ) were considered. Process parameters were: melting temperature of 90  $^\circ\text{C}$ , screw rotation velocity of 12 rpm and deposition velocity of 20 mm/s. A needle diameter of 330  $\mu\text{m}$  was used.

## 2.3 Morphological Characterization

Scanning electron microscopy (SEM) was used to characterise the morphology of the printed scaffolds. Tests were performed using the HITACHI S-3000 N (Hitachi, Japan) system. The scaffolds were coated using the EMITECH K550X sputter coater (Quorum Technologies, UK) and imaged at an acceleration voltage of 10 kV. The Fiji software was used to analyze the SEM images and to determine pore size, filament width and lay-down pattern angle.

## 2.4 Mechanical Characterization

Compression tests were conducted with the Instron 3344, using the software Bluehill Universal to collect the data. The printed scaffolds were cut into four 4 mm  $\times$  4 mm  $\times$  5 mm samples using a razor blade. The scaffolds were placed in the centre of the machine and were compressed at 5 mm/min rate and with a load of 2000 N.

## 2.5 Water Contact Angle

Water Contact Angle tests are a common procedure for finding the wettability of a surface. The test involves dropping a droplet of water onto a surface, analysing the angle between the surface and droplet edge over a specific time period. If this angle is less than  $90^\circ$  the surface is considered hydrophilic, and if the angle is higher than  $90^\circ$  the surface is considered hydrophobic. Hydrophilic surfaces are desirable as they enhance cell attachment and proliferation.

The water contact angle tests were carried out on the Modular CAM 200, which is a fully computer-controlled instrument, using a video camera to capture the shape of the water droplet to determine the static and dynamic contact angle. The droplet was dropped onto the scaffold by a fixed pipet with the scaffold aligned with the camera. Tests were performed in triplicate.

The results show that by decreasing the angle between the fibres the water contact angle decreases. No significant differences were observed due to the addition of HA. For the considered cases the contact angle ranges between  $72^\circ$  and  $86^\circ$ .

## 2.6 Biological Characterization

Human adipose derived stem cells (hADSCs) (STEMPRO, Invitrogen, USA) were used to investigate the cytotoxicity of the scaffolds. MesenPRO RS<sup>TM</sup> basal media, 2% (v/v) growth supplement, 1% (v/v) glutamine and 1% (v/v) penicillin/streptomycin (Invitrogen, USA) was used for cell culture. Cells were cultured in an incubator (37 °C, 5% CO<sub>2</sub>, and 95% humidity), until an appropriate cell density was achieved and harvested at passage 4 through trypsinization.

Scaffolds were sterilized in 80% Ethanol for 2 h, then washed in Phosphate Buffered Saline (PBS) solution for 3 h and left to dry overnight in a sterile lamina flow cabinet. The sterilized scaffolds were transferred into 24 well plates and kept inside the incubator before the cell seeding. A 70 µl cell suspension containing 50,000 cells was pured on each scaffold at day 0. A tissue culture plastic (TCP) control with the same number of cells was used as the control.

On day 1, the scaffolds were transferred in new 24 well plates and the media was replaced. Cell proliferation was investigated using the Alamar Blue assay that measures cellular metabolic activity. Tests were performed at day 7 and 14 after cell seeding.

On each time point, a 14% of volume (70 µl) of the resazurin solution was added to each scaffold, covered with aluminum foil and placed in the incubator for 4 h. Then 200 µl of each sample was transferred into a 96 well plate for the measurement of the fluorescence intensity (530 nm excitation/590 nm emission wavelength). After the measurement the scaffolds were washed three times with sterilized PBS to remove the resazurin solution and new media was used. Cell media was changed every two days.

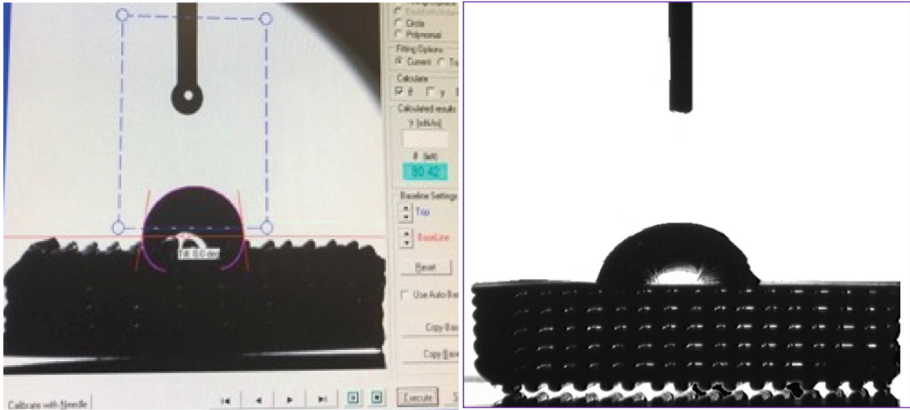
## 3 Result and Discussion

### 3.1 Morphological Characterization

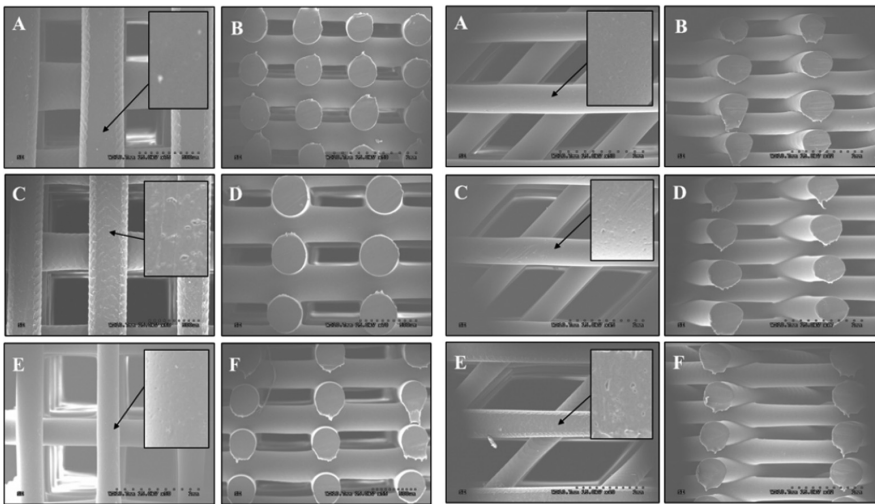
As shown in Fig. 2 produced scaffolds present a regular distribution of pores with uniformed dimensions. Results also show that the printed scaffolds presented pore sizes ( $366.17 \pm 25.81 \mu\text{m}$ ,  $522.60 \pm 5.77 \mu\text{m}$  and  $721.56 \pm 14.36 \mu\text{m}$ ) similar to the designed ones (Fig. 3).

### 3.2 Mechanical Characterization

Compressive modules are presented in Fig. 2. Results show that the compressive modulus decreases by increasing the pore size. For the same pore size and material composition the compressive modulus decreases by decreasing the angle between filaments (moving from 0/90° lay-down pattern to 0/45°). For the same lay-down pattern and pore size compressive modulus increases by increasing the HA concentration. Therefore, the highest value of 80,17 MPa was achieved for a lay-down pattern of 0/90°, pore size 250 µm and 20 wt% HA. The lowest value, 10.5 MPa, was obtained for the 0/45° lay-down pattern, 700 µm of pore size, PCL scaffolds without any HA reinforcement.



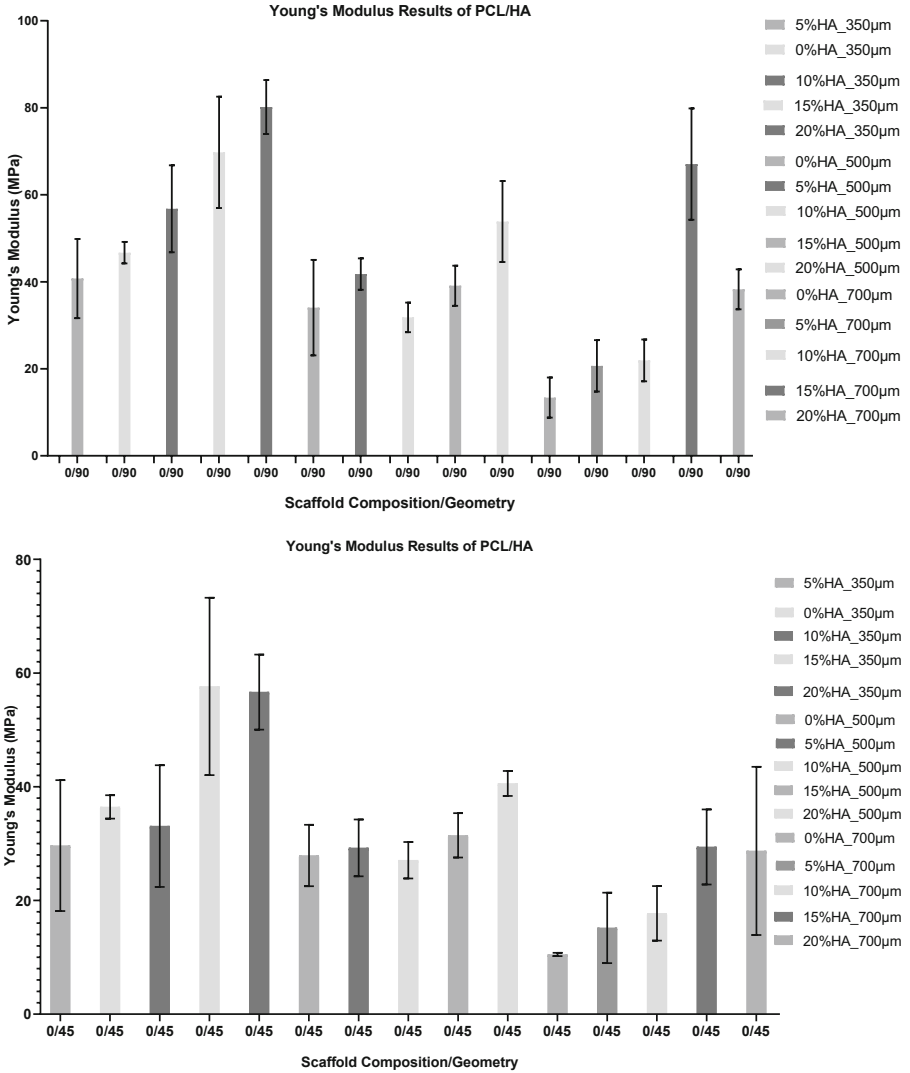
**Fig. 2.** Angle measurement from the captured image (left). Image of scaffold from the fixed camera (Right).



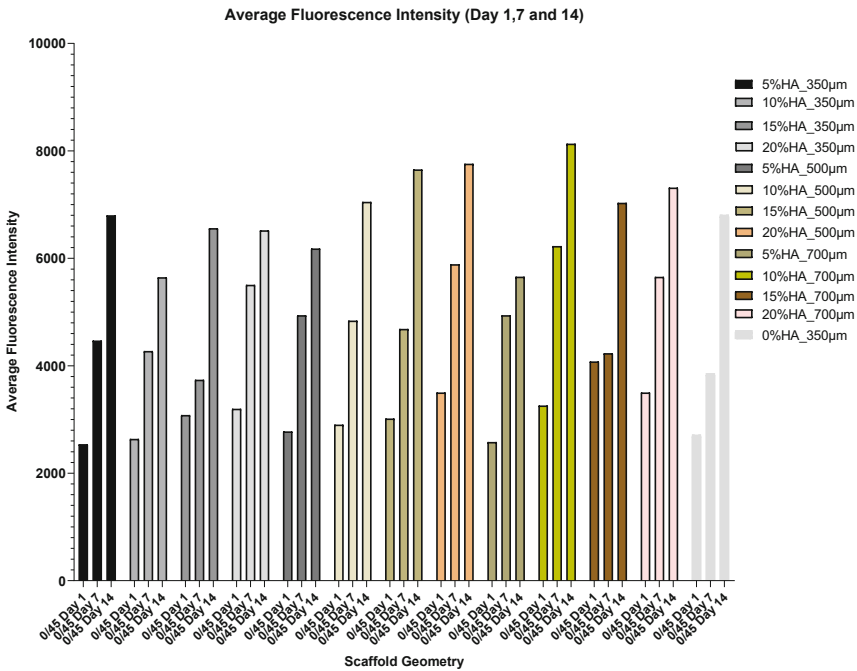
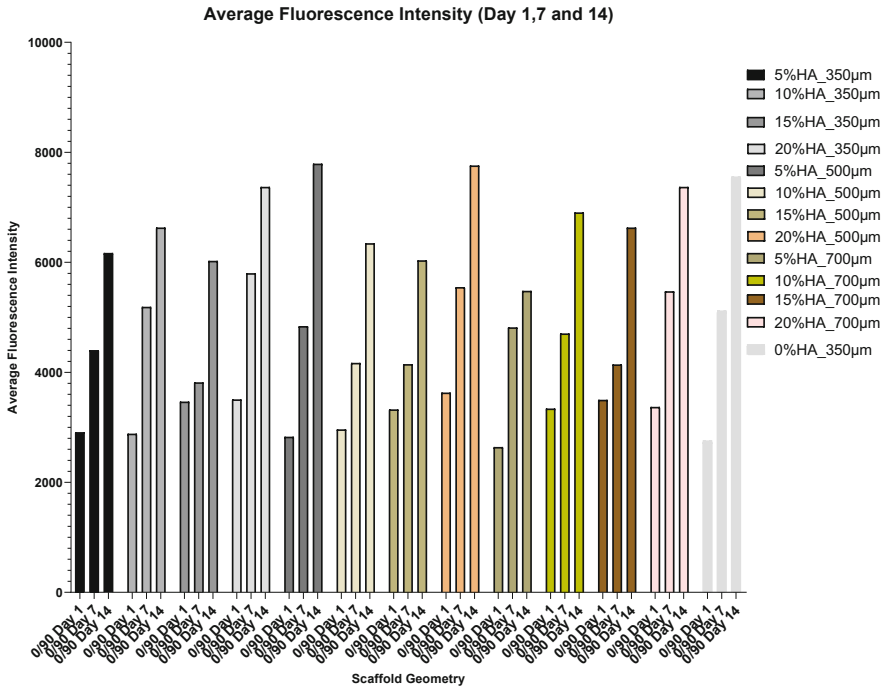
**Fig. 3.** SEM images of (A) PCL/HA scaffolds with 350 μm of pore size, (C) PCL/HA scaffolds with 500 μm of pore size and (E) PCL/HA with 700 μm of pore size. The left images correspond to scaffolds produced with a 0/90° lay-down pattern while the right images to scaffolds produced with a 0/45° lay-down pattern.

### 3.3 Biological Analysis

Fluorescence intensity values as a function of time for the different scaffolds considered in this study are presented in Fig. 4. Results show that in all considered cases scaffolds are able to support cell attachment and proliferation. High cell activity is observed for scaffolds containing HA and produced using a lay-down pattern of 0/45° due to the high surface area provided by this configuration. No significant differences were observed in terms of pore sizes (Fig. 5).



**Fig. 4.** Compressive Modulus as a function of scaffold architecture, pore size and material composition.



**Fig. 5.** Average Fluorescence Intensity as a function of scaffold architecture, pore size and material composition for different days after cell seeding

## 4 Conclusions

PCL and PCL/HA composite scaffolds with different lay-down patterns and pore sizes were produced using a screw-assisted additive manufacturing.

Different HA contents were considered and the composite blends were successfully produced using a melt blending process. Results show that the incorporation of HA increases the mechanical properties, cell attachment and proliferation.

**Acknowledgement.** This project has been supported by the University of Manchester and the Engineering and Physical Sciences Research Council (EPSRC) of the UK, the Global Challenges Research Fund (CRF), grant number EP/R01513/1.

## Reference

1. Bricks, B.: Low cost effective modular osseointegration prosthetics for large bone loss surgical procedures (EP/R01513/1). Funded by Engineering and Physical Sciences Research Council (EPSRC) of the UK, the Global Challenges Research Fund (GCRF) under the call Diagnostics, prosthetics and orthotics to tackle health challenges in developing countries





# Bi-material Electrospun Meshes for Wound Healing Applications

Enes Aslan<sup>1</sup>, Cian Vyas<sup>1</sup>, Carl Diver<sup>2</sup>, Gavin Humphreys<sup>3</sup>,  
and P. J. Bartolo<sup>1</sup>(✉)

<sup>1</sup> School of Mechanical, Aerospace and Civil Engineering,  
University of Manchester, Manchester, UK

paulojorge.dasilvabartolo@manchester.ac.uk

<sup>2</sup> Department of Engineering, Manchester Metropolitan University,  
Manchester, UK

<sup>3</sup> Faculty of Biology, Medicine and Health University of Manchester,  
Manchester, UK

**Abstract.** Skin is a complex and very important tissue, playing a significant protective and regulatory function. It is also prone to a large number of wounds and defects due to external factors such as temperature, chemical agents, and radiation. However, minimizing the risk of infection in the wound area and accelerating the skin healing process are still relevant research challenges. This paper investigates a novel wound dressing based on polycaprolactone (PCL), a synthetic biocompatible and biodegradable polymer, and honey- Surgihoney®. Wound dressing meshes were produced using solution electrospinning. Different polymer solutions were prepared by mixing PCL and Surgihoney® with acetic acid. Process conditions were optimised to create suitable meshes with uniform fiber diameters and minimal presence of beads. Fourier transform infrared spectroscopy analysis (FTIR) was used to investigate the incorporation of Surgihoney® on PCL meshes. Meshes were also biologically assessed using human adipose-derived mesenchymal stem cells. Results show that the presence of Surgihoney® has a positive impact on cell attachment and proliferation.

**Keywords:** Electrospinning · Honey · Polycaprolactone · Wound healing

## 1 Introduction

Skin is the largest organ in the body protecting the internal tissues and organs from the external environment [1]. However, skin is vulnerable to a wide range of injuries induced by acute trauma, burns, chronic wounds, cancer, and other dermatological diseases. Skin has a natural healing capacity; however, this can become compromised in chronic wound environments or if the affected area is too large such as in burns [2]. These non-healing wounds are painful, highly debilitating, and costly [3, 4]. Treatments are limited in these situations. Therefore, novel wound dressings or membranes are required to protect the wound, prevent contamination and dehydration but also to allow tissue regeneration and presenting antibacterial properties.

Electrospinning can manufacture fibers at the nanoscale and has been explored in wound dressings and for tissue engineering applications [1, 5]. The high surface to volume ratio enables better attachment of cells and enhances vascularisation, while the high porosity ensures the transmission of gases and nutrients through the mesh.

Honey has a long history as a medicinal product due to its antibacterial properties [6, 7]. The antimicrobial performance is due to the production of hydrogen peroxide and reactive oxygen species (ROS), high osmolality of sugar, and low pH [7–9]. Furthermore, ROS have been demonstrated to promote wound healing by encouraging cellular repair processes and tail regeneration in tadpoles [10, 11].

This paper investigates for the first time the use of Surgihoney® (SH), a honey with antibacterial properties, for wound dressings. Polycaprolactone/Surgihoney® meshes containing different concentrations of Surgihoney® were produced using solution electrospinning. Meshes were biologically characterised and the results show a positive impact of honey on cell attachment and proliferation.

## 2 Materials and Methods

### 2.1 Materials

PCL (CAPA 6500, Mw 50,000 g/mol) provided by Perstorp Caprolactones (Cheshire, UK) was selected due to its biocompatibility and mechanical properties.

Surgihoney® is a medical grade honey from Matoke Holding (Abingdom, UK) that presents good antibacterial properties. Surgihoney® comprises different natural honey extracts developed by Matoke. Acetic acid ( $\text{CH}_3\text{COOH}$ ) was selected due to its low volatility, non-toxic behaviour and the capacity to dissolve both PCL and honey.

Different PCL/ Surgihoney® solutions were prepared using acetic acid. Firstly, PCL was dissolved in acetic acid by using a hot plate stirrer overnight at 40 °C under the fume cupboard. Then, Surgihoney® was added into the mixture using a conical centrifuge tube and a vortex machine to obtain a homogenous solution. The different material compositions are presented in Table 1.

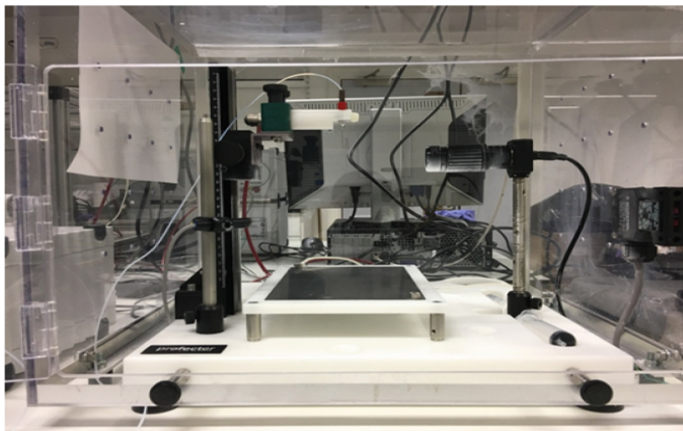
**Table 1.** Materials mixtures used to produce PCL/SH meshes

Weight of PCL (g)	Weight of Honey (g)	Volume of Acetic Acid (ml)	SH Concentration in meshes (%) (w/w)	Mixture Concentration (%) (w/v)
2	0	10	0	20
1.6	0.4	10	20	20
1.4	0.6	10	30	20

### 2.2 Methods

Electrospun meshes were produced using the Prefector system (Spraybase, Ireland). The system (Fig. 1) consists of a high voltage power supply (from 0 kV to 30 kV), software to control a syringe pump system, stainless steel collector and a  $1.8\text{G} \times 25\text{ mm}$

stainless steel emitter (needle). The following processing conditions were considered: 18 kV of voltage, 2 ml/h of flow rate and 165 mm of distance between the needle and the collector.



**Fig. 1.** Electrospinning system used in this research study

Meshes were morphologically characterised using the Hitachi S-3000 N (Hitachi, Japan) scanning electron microscope (SEM) at an accelerating voltage of 15 kV. Samples were coated with platinum. The images were analysed using the Fiji software with the DiameterJ plugin to assess fiber diameter and length [12].

Fourier Transform Infrared Spectroscopy (FTIR), Alpha-P system (Bruker, UK), was used to investigate the incorporation of Surgihoney® on the PCL meshes. The transmittance spectrum was accumulated from  $4000\text{ cm}^{-1}$  to  $400\text{ cm}^{-1}$  with 24 scans resolution for  $4\text{ cm}^{-1}$ .

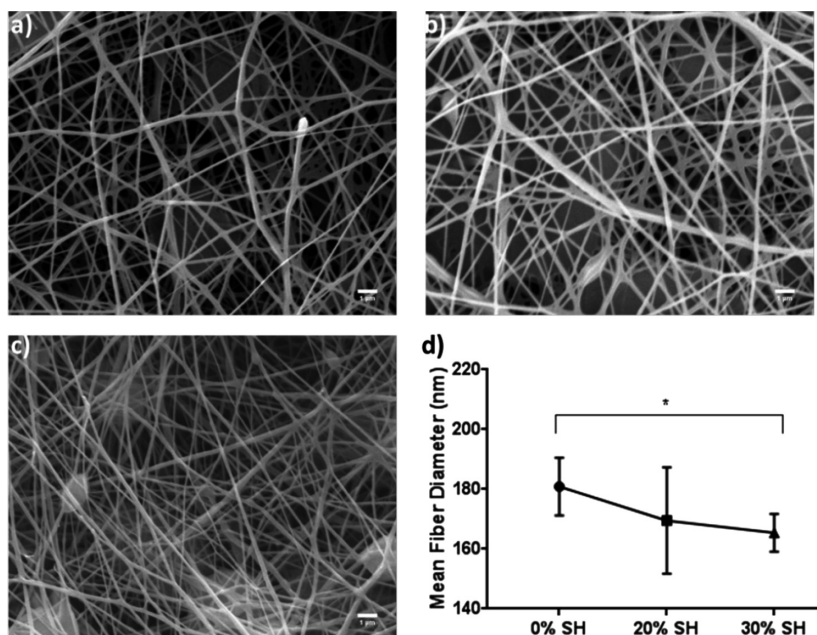
Electrospun meshes were assessed in terms of cell proliferation using human adipose-derived mesenchymal stem cells (hADMSC) (StemPro®, Thermo Fisher Scientific, UK). Cell proliferation was evaluated using the AlamarBlue® assay kit (Sigma-Aldrich, UK) following the suppliers' protocol. The fluorescence intensity was measured on day 3, 7, 10 and 12 after cell seeding. The F-Actin staining was used to observe the cell morphology and cell distribution on the meshes. Tests were performed on Day 12 after cell seeding in triplicate.

### 3 Results and Discussion

#### 3.1 Morphological Analysis of the Meshes

Figures 2a to c show the SEM images of PCL and PCL/Surgihoney® meshes, and Fig. 2d shows the variation of the mean fiber diameter as a function of Surgihoney® concentration. Results show that the mean fiber diameter decreases with the increase of

Surgihoney® concentration, varying from 180 nm for PCL meshes to 170 nm for meshes containing 20 wt% of Surgihoney® and 165 nm for meshes containing 30 wt % of Surgihoney®.

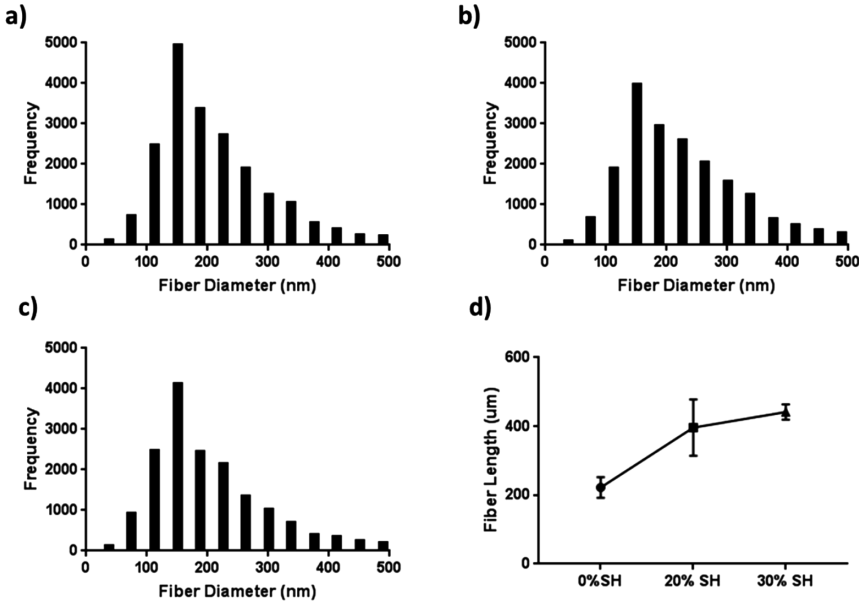


**Fig. 2.** SEM images of the electrospun meshes (a) Pure PCL, (b) PCL/20 wt%SH, (c) PCL/30 wt%SH and (d) Mean Fiber Diameter as a function of honey Concentration (\* $p \leq 0.05$ , Scale: 1  $\mu\text{m}$ )

PCL and PCL/ Surgihoney® meshes exhibit a distribution of fiber diameters ranging from 50 nm to 500 nm (Fig. 3). Contrary, the fiber length of the meshes seems to increase by increasing the Surgihoney® concentration. The reduced fiber diameter leads to much more accumulation of the fibers in the same area, which increases by increasing the Surgihoney® concentration (Fig. 3d).

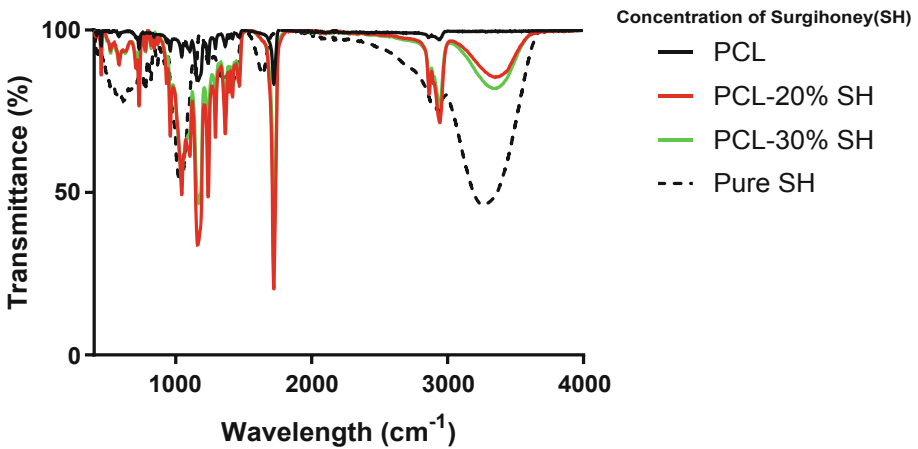
### 3.2 FTIR Analysis of Meshes

Figure 4 shows the FTIR spectrum of Surgihoney®, PCL and PCL/Surgihoney® meshes. As observed the key characteristic peaks of Surgihoney® are also present on the PCL/ Surgihoney® meshes showing the successful incorporation of honey. Results show that the maximum peak intensity in the spectrum increases ( $920 \text{ cm}^{-1}$  and  $1550 \text{ cm}^{-1}$ ) by increasing the Surgihoney® concentration. In this band C-O stretching, C-H bending, -OH bending vibrations, C(O)-O stretching vibrations and also -C-O-H



**Fig. 3.** Distribution of fiber diameters for (a) PCL, (b) PCL/20 wt%SH and (c) PCL/30 wt%SH meshes and (d) fiber lengths as a function of honey concentration.

in-plane bending vibrations can be seen for both Surgihoney® and PCL. Interactions between Surgihoney® and PCL increase the intensity of the spectrum. A similar effect can also be seen at  $3000\text{--}3506\text{ cm}^{-1}$  due to the stretching vibration of bonded and non-bonded -O-H groups [13].



**Fig. 4.** FTIR spectrum of PCL and PCL/Surgihoney® meshes.

### 3.3 Biological Results

Fluorescence intensity values for different time points after cell seeding are presented in Fig. 5. As the fluorescence activity is an indicator of the metabolic activity of cells, it is possible to consider that all meshes are able to sustain cell attachment and proliferation. Significantly better results are obtained for meshes containing 30 wt% of Surgihoney®. Figure 6 shows the nucleus and the shape of the attached cells and their distribution on the meshes on day 12. The results show that cells were able to spread on all samples, creating dense networks, particularly in the case of meshes containing 30 wt% of Surgihoney®.

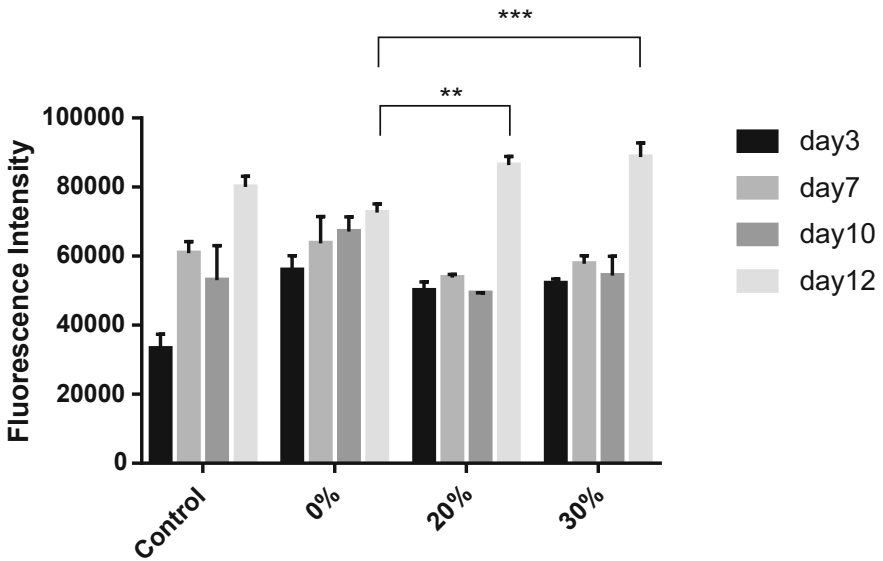


Fig. 5. Fluorescence Intensity as a function of time for different meshes (\*\* $p \leq 0.01$ , \*\*\* $p \leq 0.001$ )

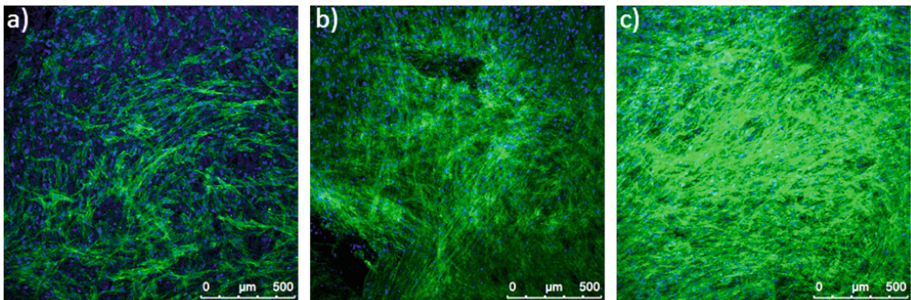


Fig. 6. Cell spreading on (a) PCL, (b) PCL/20 wt%SH and (c) PCL/30 wt%SH meshes at day 12. The blue corresponds to the nucleus and the green the cell cytoskeleton.

## 4 Conclusions

PCL and PCL/Surgihoney® meshes were successfully produced using solution electrospinning. Meshes present fibers with diameters ranging from 50 nm to 500 nm, mimicking the scale of the extracellular matrix (ECM). All meshes supported cell attachment and proliferation with best results obtained for cells containing 30 wt% of Surgihoney®.

**Acknowledgement.** The authors wish to acknowledge the funding provided by the Republic of Turkey Ministry of National Education and the Engineering and Physical Sciences Research Council (EPSRC) and the Medical Research Council (MRC) Centre for Doctoral Training in Regenerative Medicine (EP/L014904/1). We would also like to thank Matoke Holdings for their support.

## References

1. Dias, J.R., Granja, P.L., Bártolo, P.J.: Advances in electrospun skin substitutes. *Prog. Mater. Sci.* **84**, 314–334 (2016)
2. Pereira, R.F., Bártolo, P.J.: Traditional therapies for skin wound healing. *Adv. Wound Care* **5**(5), 208–229 (2016)
3. Gotttrup, F., Apelqvist, J., Price, P.: Outcomes in controlled and comparative studies on non-healing wounds: recommendations to improve the quality of evidence in wound management. *J. Wound Care* **19**(6), 237–268 (2010)
4. Alexiadou, K., Doupis, J.: Management of diabetic foot ulcers. *Diab. Ther.* **3**(1), 4 (2012)
5. Zahedi, P., Rezaeian, I., Ranaei-Siadat, S.-O., Jafari, S.-H., Supaphol, P.: A review on wound dressings with an emphasis on electrospun nanofibrous polymeric bandages. *Polym. Adv. Technol.* **21**(2), 77–95 (2010)
6. Israili, Z.H.: Antimicrobial properties of honey. *Am. J. Ther.* **21**(4), 304–323 (2014)
7. Mandal, M.D., Mandal, S.: Honey: its medicinal property and antibacterial activity. *Asian Pac. J. Trop. Biomed.* **1**(2), 154–160 (2011)
8. Dryden, M., Lockyer, G., Saeed, K., Cooke, J.: Engineered honey: in vitro antimicrobial activity of a novel topical wound care treatment. *J. Glob. Ant. Resist.* **2**(3), 168–172 (2014)
9. Cooke, J., Dryden, M., Patton, T., Brennan, J., Barrett, J.: The antimicrobial activity of prototype modified honeys that generate reactive oxygen species (ROS) hydrogen peroxide. *BMC Res. Not.* **8**(1), 20 (2015)
10. Love, N.R., Chen, Y., Ishibashi, S., Kritsiligkou, P., Lea, R., Koh, Y., Gallop, J.L., Dorey, K., Amaya, E.: Amputation-induced reactive oxygen species are required for successful *Xenopus* tadpole tail regeneration. *Nat. Cell Biol.* **15**, 222 (2013)
11. Dunnill, C., Patton, T., Brennan, J., Barrett, J., Dryden, M., Cooke, J., Leaper, D., Georgopoulos, N.T.: Reactive oxygen species (ROS) and wound healing: the functional role of ROS and emerging ROS-modulating technologies for augmentation of the healing process. *Int. Wound J.* **14**(1), 89–96 (2017)
12. Hotaling, N.A., Bharti, K., Kriel, H., Simon, C.G.: DiameterJ: a validated open source nanofiber diameter measurement tool. *Biomaterials* **61**, 327–338 (2015)
13. Karimi, S., Feizy, J., Mehrjo, F., Farrokhnia, M.: Detection and quantification of food colorant adulteration in saffron sample using chemometric analysis of FT-IR spectra. *RSC Adv.* **6**(27), 23085–23093 (2016)



# Fabrication of Cellulose Hydrogel Objects Through 3D Printed Sacrificial Molds

Hossein Najaf Zadeh<sup>1,3</sup>(✉), Tim Huber<sup>1,2</sup>, Freya Dixon<sup>3</sup>, Conan Fee<sup>2</sup>,  
and Don Clucas<sup>3</sup>

<sup>1</sup> Biomolecular Interaction Centre, University of Canterbury,  
Christchurch, New Zealand

Hossein.Najafzadeh@pg.canterbury.ac.nz

<sup>2</sup> School of Product Design, University of Canterbury,  
Christchurch, New Zealand

<sup>3</sup> Mechanical Engineering Department, University of Canterbury,  
Christchurch, New Zealand

**Abstract.** Effects of mold removal methods in fabrication of cellulose hydrogel objects were investigated in the present work. Cellulose was dissolved in 7 wt% NaOH/12 wt% urea aqueous solution and thermally gelled at 55 °C in three different mold materials, Acrylonitrile Butadiene Styrene (ABS) as a common 3D printing material, Solidscape™ wax, specifically designed as a 3D printing cast material, and sacrificial casting wax (Lost Wax), commonly used for casting. After completion of the gelling process, the molds were removed from the cellulose gel by using a solvent for the ABS mold and melting the waxes in hot water. At the same time, the solvent was extracted from the gel and the cellulose hydrogel regenerated. The results show that mold materials and their associated removal methods have a significant effect on the mechanical properties and microstructure of cellulose hydrogel and cause shrinkage. Larger pore sizes decreased the compression strength and modulus of cellulose hydrogels samples. A balance between the porosity and density for a cellulose hydrogel part must be established for the specific applications.

**Keywords:** Cellulose · Hydrogel · Manufacturing · Mold · Casting

## 1 Introduction

Hydrogel is a class of material described as ‘solid water’ because it maintains properties of liquid water while being physically constrained like a solid. The hydrophilic polymer networks of hydrogels have the strength to absorb and retain a significant amount of water as high as 99% by weight [1]. That is why hydrogel materials have generated considerable interest among scientists for use in a diverse range of applications such as tissue engineering [2] or purification [3]. Natural hydrogels with shown common characteristics such as permeability, nontoxicity, biocompatibility, and biodegradability [4]. are made of natural polymers such as starch [5], alginate [6], and cellulose [7].



Cellulose, a renewable and biodegradable natural polysaccharide, is widely found in wood and plants [8]. The abundant hydroxyl groups in cellulose are essential for making a hydrogel [9]. However, the supramolecular architecture of cellulose makes it insoluble in water, which is due to the strong hydrogen bonding networks [10, 11]. Therefore, it is necessary to break the intermolecular interactions to make it soluble. Aqueous solutions of NaOH/urea are a common solvent for cellulose. By heating or cooling the solution, an irreversible gel forms [12]. Finally, when a non-solvent such as water or acetone is introduced, the cellulose precipitates, and if in the presence of water forms a stable hydrogel. Cellulose hydrogels have various applications such as self-sustaining scaffolds for tissue engineering, chromatography, and viral vector purification [9, 13].

An advanced fabrication technique is necessary to fabricate complex cellulose hydrogel parts [14]. The most common technique used for processing complex geometries hydrogels, including cellulose gels, is cast molding [15]. In this manufacturing method, the cellulose solution is poured into a mold and fills the cavities allowing complex structures to be formed. The solution is gelled and the casting mold can be removed, either by melting or dissolving in a solvent. Any shape and geometries can be fabricated as a mold through a convention processing technique. Different material families, such as thermoplastics and waxes, can be used as a cast mold [16, 17].

## 2 Methodology

### 2.1 Materials

Solidscape™ support material wax and sacrificial casting wax (lost wax) were purchased from Regal Casting, Auckland, New Zealand. Acrylonitrile Butadiene Styrene (ABS) filament was purchased from Stratasy, New Zealand. Cellulose powder, Type 20 Sigmacell particle diameter 20  $\mu\text{m}$ , and Urea (ACS grade) was bought from Sigma-Aldrich (Sigma-Aldrich, St. Louis, MO, USA). Sodium Hydroxide (pellets) with 97% purity was bought from ThermoFisher Scientific (Waltham, MA, USA). All chemicals were used as-received.

### 2.2 Methods

#### Part Design, 3D Printing and Casting

A Stratasy F370 3D printer was used to 3D print molds out of ABS. Simple geometry molds were designed in Solidworks (Dassault systems) to prepare specimens of cellulose hydrogel with a cylindrical shape (20 mm D  $\times$  15 mm H). The first batch of cellulose hydrogel molds was made out of ABS and was directly 3D printed. For Solidscape™ wax, and sacrificial wax molds, a secondary mold was used. Molten wax was injected into this mold and after solidification removed from it. Urethane mold release was used to ease wax part removal.

#### Cellulose Solution Preparation, Casting Cellulose Gel, Mold Removal

A solvent of 12 wt% urea and 7 wt% NaOH in deionized water was prepared and cooled down to 4 °C. 5 wt% Sigmacell cellulose powder was dispersed in the solvent using a Silverson overhead mixer at 6000 rpm for approximately 5 min. The solution

was kept at  $-14\text{ }^{\circ}\text{C}$  for 3–4 h to achieve a clear solution. Then 50 wt% of the initially dissolved cellulose portion was added to the solution and stirred into the solution at 1000 rpm for 5 min until the added powder was dispersed. The solution was stored in a refrigerator at  $2 \pm 1\text{ }^{\circ}\text{C}$ . The added cellulose powder acts as a physical cross-linker and increases the number of hydrogen bonds between suspended cellulose and dissolved cellulose in the solution [14]. For the preparation of the cellulose gel specimens, 2.5 grams of cellulose solution was poured into the prepared molds. It was then placed in a preheated oven at  $55\text{ }^{\circ}\text{C}$  for 60 min to permanently gel the solution [18].

Two methods, dissolving and melting were used to remove molds after gelation. Melting of the ABS mold is impossible as the melting temperature of ABS is  $230\text{ }^{\circ}\text{C}$ , is very close to cellulose decomposition point at  $250\text{--}260\text{ }^{\circ}\text{C}$  [19]. Hence, the ABS was dissolved in Acetone. The wax molds were melted in  $90\text{ }^{\circ}\text{C}$  water bath. At this temperature, wax melts and the cellulose gel does not boil. The cellulose gel was regenerated by a solvent exchange process, replacing NaOH and urea through either Acetone or water.

After removing the wax molds, the cellulose samples were placed in MiliQ water. Samples made through removing the ABS mold in Acetone were rinsed with water and then placed in water to remove the Acetone. This process was repeated 10 times.

#### Mechanical Testing

Compression testing was performed on an MTS Criterion Model 43 Universal Testing machine (MTS, Eden Prairie, MN, USA) with 40 mm diameter clamps, a 0.5 kN load cell and speed of 1 mm/min. The clamps were coated with silicon oil to avoid shear stress. A preload of 0.1 N was applied to the samples, and they were tested to yield.

#### Cross-Section Shrinkage Rate

An optical microscope with a Nikon SMZ-1B camera attached was used to measure the shrinkage of the fabricated samples from different mold materials. ImageJ (Wayne Rasband, National Institutes of Health, USA), was used to measure the diameter of the samples and thus calculate the cross-sectional area. The term shrinkage used in this work is referred to cross-sectional shrinkage of the cellulose gels.

#### Contact Angle

The static contact angle of liquid droplets on the test specimens was measured with a commercial contact angle analyzer software (CAM200, KSV, Helsinki, Finland) and a goniometer (CAM200, KSV, Finland) equipped with a Nikon (Japan) digital camera at ambient temperature  $21 \pm 2\text{ }^{\circ}\text{C}$  and 55% relative humidity.

#### Field Emission Scanning Electron Microscopy

Hydrogel samples were freeze-dried at  $-45\text{ }^{\circ}\text{C}$  for 36 h using a Labconco freeze drier (Labconco Corporation, USA) for SEM analysis. After drying, the samples were manually broken to create fracture surfaces for SEM analysis. The samples were carbon coated for 180 s at 25 mA using an Emitech K975X coater (Quorum Technologies Ltd, United Kingdom). Field emission scanning electron microscopy (FE-SEM) was performed using a JEOL 7000F FE-SEM (JEOL Ltd, Japan) with a probe current of 10 mA and under an acceleration voltage of 5 kV. Pore diameters were randomly selected and measured over 30 measurements. The average diameter was considered as the average pore diameter.

### 3 Results and Discussion

#### 3.1 Effects of Mold Removal Method on Hydrogel Microstructure

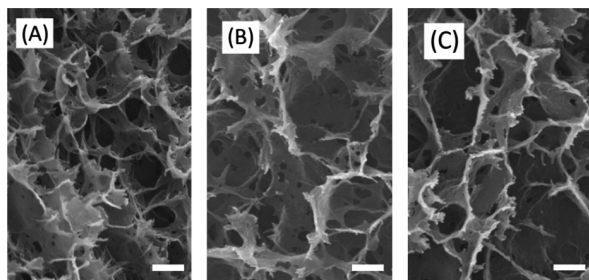
Using a hot water bath as a mold removal method for Solidscape™ and lost wax resulted in the formation of larger microstructures than dissolving ABS mold with acetone (Fig. 1). Using a Solidscape wax mold, the average pore diameter measured 1100 nm, and the part shrank by 6.4%. Lost wax as other mold material resulted in average pore diameters of 800 nm and 9.54% shrinkage of cellulose hydrogel.



**Fig. 1.** Porosity of cellulose hydrogel by measuring internal pore radius of freeze-dried gel samples made with ABS, Lost wax and Solidscape™ wax molds.

Li et al. suggested that in the sol-gel transition of cellulose solution, faster coagulant diffusion results in enhancement of solvent removal from the cellulose solution thus formation of larger pore sizes [20]. The slight difference 3.2% between of Solidscape™ and lost wax molds in shrinkage can be explained by the mold material properties and their interaction with the cellulose gel. Solidscape™ wax has a lower melting point of 48 °C than Lost wax (58 °C). Also, the contact angle between Solidscape™ wax and cellulose gel (114.1°), is higher than the contact angle between lost wax and cellulose gel (110.8°). Having a higher contact angle means that the cellulose gel repels Solidscape™ wax material more than it does Lost wax. Therefore, the lower melting temperature and the higher contact angle of the Solidscape™ wax causes faster wax removal and thus a higher rate of the cellulose hydrogel regeneration. This contributes to a higher rate of solvent removal in cellulose gel and forming smaller pore [20] (Fig. 2).

In contrast with using the hot water bath to remove wax molds, using Acetone to dissolve the ABS mold resulted in cellulose hydrogels with smaller pore diameters of 350 nm and 27.4% part shrinkage. We believe the high concentration of Acetone results in less hydrogel water content, and a part with a higher density [21].



**Fig. 2.** The SEM micrographs of the freeze-dried cellulose hydrogel samples made (A) ABS mold, (B) Lost wax and (C) Solidscape™ wax. The scale equals 1  $\mu\text{m}$  in all images.

### 3.2 Mold Material Effect on Mechanical Properties of Cellulose Gel

The mold material and its removal has a strong effect on the mechanical properties of the cellulose hydrogels. Solidscape™ wax mold resulted in the weakest cellulose hydrogel parts with average compressive strength and modulus values of  $39.25 \pm 5.93$  kPa and  $281 \pm 21.71$  kPa respectively. The cellulose hydrogel parts created using lost wax mold material possess stronger mechanical properties with average compressive strength and modulus values of  $63.25 \pm 8.20$  kPa and  $369.75 \pm 20.63$  kPa respectively. ABS mold material yielded the strongest cellulose hydrogel parts with an average compressive strength of  $133.4 \pm 20.72$  kPa and an average compressive modulus of  $481.4 \pm 28.88$  kPa. As the ratio of water to cellulose in all specimens were constant (1:12), reduction in average pore size caused shrinkage and a denser concentration of hydrogel bonds. This results in a higher compression strength, concordant with results found by Gibson [22]. Ramay suggested that since a higher density usually leads to higher mechanical strength while a high porosity provides a favorable environment for porous media [23], a balance between the porosity and density for a cellulose hydrogel part must be established for the specific applications.

## 4 Conclusion

Sacrificial casting method is used to fabricate cellulose hydrogel objects through thermal gelling. Selection of mold material and therefore mold removal is critical in the fabrication of porous cellulose hydrogel as the gel point, microstructure and mechanical properties of the gel can be affected.

## References

1. Naficy, S., et al.: Progress toward robust polymer hydrogels. *Aust. J. Chem.* **64**(8), 1007–1025 (2011)
2. Kim, Jinku, et al.: Synthesis and evaluation of novel biodegradable hydrogels based on poly(ethylene glycol) and sebacic acid as tissue engineering scaffolds. *Biomacromol* **9**(1), 149–157 (2008)

3. Ha, E.J., et al.: Purification of His-tagged proteins using Ni<sup>2+</sup>-poly(2-acetamidoacrylic acid) hydrogel. *J. Chromatogr. B* **876**(1), 8–12 (2008)
4. Ma, P.X.: Scaffolds for tissue fabrication. *Mater. Today* **7**(5), 30–40 (2004)
5. Li, X., et al.: The swelling behaviors and network parameters of cationic starch-g-acrylic acid/poly(dimethyldiallylammonium chloride) semi-interpenetrating polymer networks hydrogels. *J. Appl. Polym. Sci.* **110**(3), 1828–1836 (2008)
6. Chan, Ariel W., et al.: Semisynthesis of a controlled stimuli-responsive alginate hydrogel. *Biomacromol* **10**(3), 609–616 (2009)
7. Chang, C., et al.: Superabsorbent hydrogels based on cellulose for smart swelling and controllable delivery. *Eur. Polym. J.* **46**(1), 92–100 (2010)
8. Moon, R.J., et al.: Cellulose nanomaterials review: structure, properties and nanocomposites. *Chem. Soc. Rev.* **40**(7), 3941–3994 (2011)
9. Chang, C., Zhang, L.: Cellulose-based hydrogels: present status and application prospects. *Carbohydr. Polym.* **84**(1), 40–53 (2011)
10. Bruno, Medronho, et al.: Rationalizing cellulose (in)solubility: reviewing basic physico-chemical aspects and role of hydrophobic interactions. *Cellulose* **19**(3), 581–587 (2012)
11. Lindman, B., et al.: On the mechanism of dissolution of cellulose. *J. Mol. Liq.* **156**(1), 76–81 (2010)
12. Medronho, B., Lindman, B.: Brief overview on cellulose dissolution/regeneration interactions and mechanisms. *Adv. Colloid Interface Sci.* **222**, 502–508 (2015)
13. Tamayose, K., et al.: A new strategy for large-scale preparation of high-titer recombinant adeno-associated virus vectors by using packaging cell lines and sulfonated cellulose column chromatography. *Hum. Gene Ther.* **7**(4), 507–513 (1996)
14. Huber, T., et al.: 3D printing cellulose hydrogels using LASER induced thermal gelation. *MDPI* **2**(3), 42 (2018)
15. Bakarich, S.E.: 3D/4D printing tough hydrogel composites: a pathway to functional devices. In: *Intelligent Polymer Research Institute. UOW* (2016)
16. Chang, C., et al.: Structure and properties of hydrogels prepared from cellulose in NaOH/urea aqueous solutions. *Carbohydr. Polym.* **82**(1), 122–127 (2010)
17. Shen, X., et al.: Hydrogels based on cellulose and chitin: fabrication, properties, and applications. *Green Chem.* **18**(1), 53–75 (2016)
18. Qin, X., et al.: Stability of inclusion complex formed by cellulose in NaOH/urea aqueous solution at low temperature. *Carbohydr. Polym.* **92**(2), 1315–1320 (2013)
19. Yang, H., et al.: Characteristics of hemicellulose, cellulose and lignin pyrolysis. *Fuel* **86**(12–13), 1781–1788 (2007)
20. Li, R., et al.: Dissolution of cellulose from different sources in an NaOH/urea aqueous system at low temperature. *Cellulose* **22**(1), 339–349 (2015)
21. Saito, H., et al.: Preparation and properties of transparent cellulose hydrogels. *J. Appl. Polym. Sci.* **90**(11), 3020–3025 (2003)
22. Gibson, L.J., Ashby, M.F.: *Cellular Solids: Structure and Properties*. Cambridge university Press, Cambridge (1999)
23. Ramay, H.R., Zhang, M.: Preparation of porous hydroxyapatite scaffolds by combination of the gel-casting and polymer sponge methods. *Biomaterials* **24**(19), 3293–3302 (2003)



# 3D Printed Geometries on Textile Fabric for Garment Production

Tatjana Spahiu<sup>1</sup>(✉), Erald Piperi<sup>2</sup>, Andrea Ehrmann<sup>3</sup>, Ermira Shehi<sup>1</sup>,  
and Dudina Rama<sup>1</sup>

<sup>1</sup> Faculty of Mechanical Engineering, Textile and Fashion Department,  
Polytechnic University of Tirana, Tirana, Albania  
tspahiu@fm.edu.al

<sup>2</sup> Faculty of Mechanical Engineering,  
Department of Production and Management, Polytechnic University of Tirana,  
“Mother Tereza” Square, no. 1, Tirana, Albania

<sup>3</sup> Faculty of Engineering and Mathematics, Bielefeld University of Applied  
Sciences, Interaktion 1, 33619 Bielefeld, Germany

**Abstract.** Within the fashion industry, 3D printing can be used for producing individualized products by 3D printing on textile fabrics. One of the main issues of 3D printed geometries on textile fabrics is the adhesion between both materials. Continuing our previous research, other textile fabrics are used as substrate for 3D printing. Again, washing tests which simulate the real use of the textile fabric for garment production indicate that round shapes and thin objects are uncritical to be washed compared to higher objects and square shapes, which tend to separate after the first or the second washing cycle. For nine textile materials under investigation, no separation was found at all for the first 5 washing cycles for two of them. Finally, a full construction cycle including 2D and 3D design, simulation, 3D printing and garment production is presented.

**Keywords:** 3D printing · Textile fabric · Garments production

## 1 Introduction

3D printing is a form of additive manufacturing where the object is created by laying down successive layers of the material sliced by the 3D printing software to create a 3D model. With the wide spread of 3D printing in different areas of production, the fashion industry is part of these applications. Recently, different products are created by 3D printing starting from garments, shoes, accessories, etc. Fashion designers can express their creations by using 3D printed structures, which sometimes can be difficult by using traditional methods. There are different 3D printing technologies used for garment production such as SLS, FDM, etc., and these applications are presented as whole garment [1–3]. However, these applications are still rare and cannot replace the traditional process of garment production. One of the challenges is the materials used for 3D printing as they are not flexible as textile materials and as a result not comfortable. But attempts to manipulate the bending and deformation properties of 3D printed objects show good results by changing the geometry and size of the print [4].

Apart from the whole garment, parts of garments can be produced by 3D printing using textiles as substrates [5]. Tests have shown significant influence of the distance between printing nozzle and textile surface, the printing material [6, 7]. However, different problems arise during the 3D printing process. Researchers have examined the limitations of materials, modeling programs and 3D printing processes and their development will accelerate the use of 3D printing in fashion industry [8]. This work is part of a project on the application of 3D printing for garment production. Tests results related to the adhesion of 3D printed geometries on textile fabrics conducted in previous research are used [6, 7]. Following these previous results, our experiments are now extended from pure mechanical adhesion tests to washing tests.

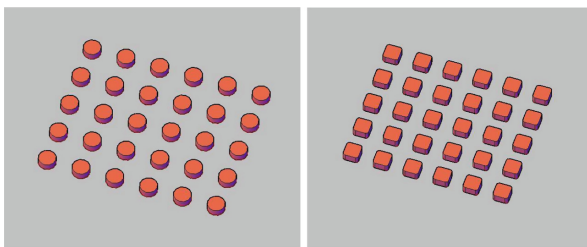
## 2 Materials and Methods

3D printing is realized in different textile fabrics. All textiles used for 3D printing geometries are suitable for garment production. The main characteristics of the textiles are tested and depicted in Table 1.

**Table 1.** Textile fabrics used as base materials for 3D printing.

Samples	Composition	Weave	Thickness	Areal weight	Warp density (1/cm)	Weft density (1/cm)
Fabric 1	Cotton	Plain	0.16 mm	98.83 g/m <sup>2</sup>	46 threads	29 threads
Fabric 2	Wool	Diagonal	0.19 mm	216.41 g/m <sup>2</sup>	36 threads	25 threads
Fabric 3	Polyester	Diagonal	0.23 mm	238.3 g/m <sup>2</sup>	130 threads	26 threads
Fabric 4	Polyester	Plain	0.11 mm	92.9 g/m <sup>2</sup>	44 threads	30 threads
Fabric 5	Polyester	Plain	0.21 mm	110.06 g/m <sup>2</sup>	32 threads	30 threads
Fabric 6	Cotton	Diagonal	0.27 mm	187.26 g/m <sup>2</sup>	69 threads	27 threads
Fabric 7	Polyester	Diagonal	0.26 mm	261.59 g/m <sup>2</sup>	64 threads	36 threads
Fabric 8	Polyester	Plain	0.11 mm	89.5 g/m <sup>2</sup>	42 threads	28 threads
Fabric 9	Cotton	Plain	0.24 mm	179.6 g/m <sup>2</sup>	21 threads	15 threads

For these tests, geometries as rectangles with round corners, circles and triangles are designed on 3D software AutoCAD, with dimensions around 1 cm as given in Fig. 1. Preparing 3D geometries for 3D printing is realized on slicing software CURA 3.4.



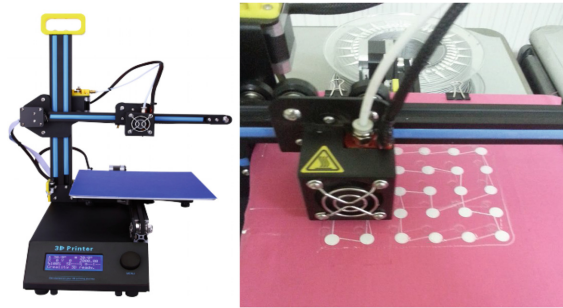
**Fig. 1.** Geometries designed for 3D printing.

The main parameters selected for 3D printing on textile are given in Table 2.

**Table 2.** Main printing parameters.

3D printing parameters	Value
Height	0.1 mm
3D printing temperature	230 °C
3D printing bed	60 °C
Printing velocity	30 mm/s
Polymer flow	100%
Material	PLA (Polylactic acid)

Fused deposition Modeling (FDM) printer is used for 3D printing as shown on the left of Fig. 2. Also, on the right part is shown view during the 3D printing process on textile fabric. For each textile are tested 3 specimen, where are printed 30 circles.



**Fig. 2.** During the 3D printing process in one of the textile fabric.

An investigation of the influence of different fabrics was examined by maintaining the same height for all the geometries printed on textile fabrics. All the textiles with 3D printed objects have undergone the washing process in a washing machine, as in real life. Figure 3 depicts some samples of textile fabrics after after 5 washing cycles.





Fig. 3. 3D printed geometries after 5 washing cycles.

### 3 Results and Discussion

Washing tests reveal the stability of the imprinted 3D objects on the textile fabrics. However visual analyzing of 3D printed geometries on textile is done for all the fabrics. From the visual assessment:

- Textile 3 and 9 has the best adhesion with 0% of partially separated objects.
- Textile 2, 5 and 6 have 2 partially separated objects.
- Textile 1 and 4 has 3 partially separated objects.
- Textiles 7 and 8 have 15 partially separated objects.

As mentioned previously, one of the objectives of this work was producing a garment with 3D printed geometries on the textile fabric. One of the textiles with the best adhesion of 3D printed geometries, textile 9 was chosen for dress production. Garment drape was evaluated during the simulation process on a CLO 3D [9] garment designer software as shown in Fig. 4.

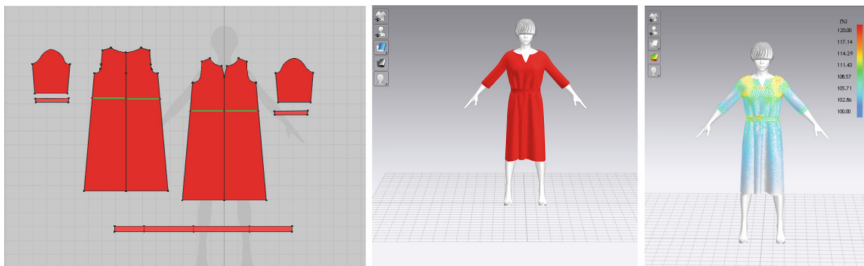
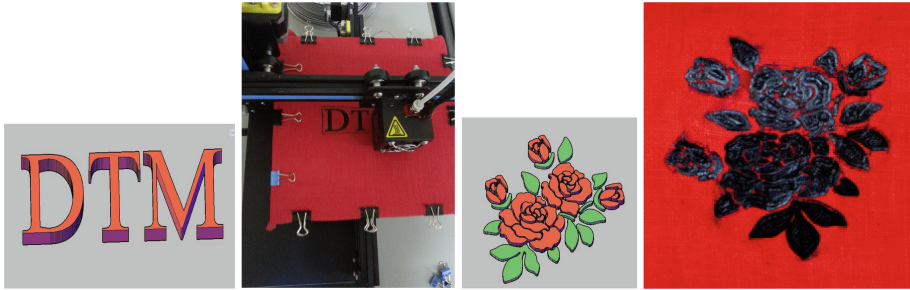


Fig. 4. The main steps during the 3D garment design & simulation process.

After evaluating the virtual garment drape, the dress patterns are printed and cut on the textile fabric used for testing. Prior to the sewing process, dress patterns are used for 3D printing different geometries. Figure 5 depicts views from pattern design and 3D printing process.



**Fig. 5.** Views of 3D design & printing process.

The final dress produced is depicted in Fig. 6. In addition, a bag was produced with a 3D printed Albanian flag on a textile fabric.



**Fig. 6.** The dress and the bag with 3D printed geometries on the textile fabric.

## 4 Conclusions

3D printing on different textile fabrics is depicted in this work. Testing the adhesion of 3D printed geometries is done by washing as in real life to simulate their use for garment production. Washing tests conducted here show that thin 3D printed geometries show a better adhesion on the textile fabric [10]. Based on the results taken, fabric 3 and fabric 9 showed the best adhesion with 3D printed geometries, where all the geometries are on textile fabric. These results can be used by other researchers or fashion designers in the implementation of 3D printing for garment production.


## References

1. August 2018. <http://www.irisvanherpen.com/about>. Accessed Aug 2018
2. August 2018. <https://danitpeleg.com/product/create-your-own-3d-printed-jacket/>. Accessed Aug 2018
3. August 2018. <https://all3dp.com/sri-lankas-first-3d-printed-wedding-dress/>

4. Gürcüm, B., Börklü, H., Sezer, K., Eren, O.: Implementing 3D printed structures as the newest textile form. *J. Fash. Technol. Text. Eng.* **4**, 019 (2018)
5. Spahiu, T., Fafenrot, S., Grimmelsmann, N., Piperi, E., Shehi, E., Ehrmann, A.: Varying fabric drape by 3D-imprinted patterns for garment design. In: *IOP Conference Series: Materials Science and Engineering*, vol. 254, p. 172023 (2017)
6. Grimmelsmann, N., Kreuziger, M., Korger, M., Meissner, H., Ehrmann, A.: Adhesion of 3D printed material on textile substrates. *Rapid Prototyp. J.* **24**, 166–170 (2018)
7. Spahiu, T., Grimmelsmann, N., Ehrmann, A., Piperi, E., Shehi, E.: Effect of 3D printing on textile fabric. In: *1st International Conference Engineering and Entrepreneurship*, Tirana, Albania (2017)
8. Kim, S., Seong, H., Her, Y., Chun, J.: A study of the development and improvement of fashion products using a FDM type 3D printer. *Fashion and Textiles* **6**(9), 1–24 (2019)
9. <https://www.clo3d.com/>
10. Spahiu, T., Piperi, E., Al-Arabiyyat, M., Ehrmann, A., Shehi, E.: Novel 3D shaped garments by 3D printing on textile fabrics. In: *8th International Conference on Textile*, Tirana, Albania (2018)



# Moving Forward to 3D/4D Printed Building Facades

Flávio Craveiro<sup>1,2</sup>, José P. Duarte<sup>3</sup>, Helena Bártoło<sup>1,2</sup>,  
and Paulo Bártoło<sup>4</sup>

<sup>1</sup> CIAUD, Lisbon School of Architecture,  
Universidade de Lisboa, Lisbon, Portugal  
fcraveiro@fa.ulisboa.pt

<sup>2</sup> School of Technology and Management,  
Polytechnic Institute of Leiria, Leiria, Portugal

<sup>3</sup> Stuckeman School of Architecture and Landscape Architecture,  
Penn State University, State College, USA

<sup>4</sup> School of Mechanical, Aerospace and Civil Engineering,  
The University of Manchester, Manchester, UK

**Abstract.** Nearly Zero Energy Buildings will require high-performance building envelopes, though the building sector is currently a major contributor to the world's energy consumption and related CO<sub>2</sub> emissions. Innovative advanced materials, such as smart or functionally graded materials are being developed to better adapt buildings to environmental needs. This paper presents a brief overview of novel advanced materials for passive/kinetic facades. There is a great potential for 3D/4D printing building components to address actual and future built environmental challenges. 3D printing buildings are still in its infancy, several limitations and barriers need to be addressed, though architects and engineers must keep looking forward and the rise of 4D design could bring “life” to buildings.

**Keywords:** 3D/4D printing · Smart materials · Functionally graded materials · Shape memory materials · Phase change materials

## 1 Introduction

The 2030 Agenda for Sustainable Development addresses climate change and the urgent need to reduce CO<sub>2</sub> emissions and minimize its environmental impacts [1]. The global building sector accounts for 46% of energy consumption and 39% CO<sub>2</sub> emissions. A future scenario of Nearly Zero Energy Buildings (NZEB) requires high-performance building envelopes, being the facades a significant part accounting for about 40% of heat loss in winter and over-heating in summer [2]. Today, the construction industry faces huge challenges towards sustainability, by using more durable, lighter, stronger and environmentally friendly materials. Innovative advanced materials, such as smart or functionally graded materials are being developed to better adapt buildings to environmental needs.

On the other hand, additive manufacturing (AM), also called 3D printing, has several advantages regarding traditional construction methods, allowing improved materials' savings and greater design freedom, as well reducing construction time and costs. Research on 3D printing in construction is growing exponentially [3, 4], while 4D printing is emerging as a disruptive technique where a 3D structure can be printed and then transformed into a new shape when exposed to predetermined stimulus (environmental/human) such as temperature, light, or moisture. 4D printing considers not only three spatial dimensions, but also a fourth one, namely time.

This paper presents a brief overview of novel advanced materials for passive/kinetic facades, highlighting the potential of 3D/4D printing for its manufacture. Other advanced materials can also be used in building facades, though lie outside the scope of this work.

## 2 Advanced Materials for Building Facades

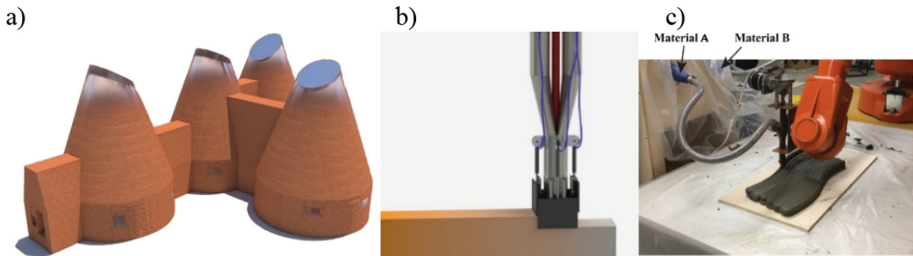
AM is an exceptional technology to precisely place smart materials on desired location, such as: shape memory polymers or metals, reacting to temperature, enabling shading systems opening or close; phase change materials located in strategic areas could also help to control indoor temperature and comfort; or functionally graded materials that seamlessly change its material composition along the structure.

### 2.1 Functionally Graded Materials

Commonly, homogeneous building components respond only to one purpose each, according to different building characteristics. Several material layers are usually applied sequentially along/crosswise building facades, requiring extra labor time and frequently causing energy losses and building pathologies. In buildings composed of a skeleton structure system, the masonry is used to infill walls and cracks frequently occur [5], while the facade insulation, typically comprising layers of insulation materials, internally or externally placed, when inappropriately assembled can originate thermal bridges. On the other hand, windows composed of translucent materials, mechanical frames and bonding agents require different joints between materials, which can cause poor thermal insulation or water infiltration problems. Functionally graded materials (FGM) using AM will allow a seamless and impermeable transition between different materials, a potential good solution optimizing the facade performance from a mechanical, thermal and optical view [6–8] (Fig. 1).

### 2.2 Phase Change Materials

Phase change materials (PCM) can be used to store thermal energy in buildings in a latent form, as they have a greater heat storage capacity compared to conventional building materials. The incorporation of PCM in wall panels or directly mixed in concrete can provide facade cooling and heating by latent heat storage [10]. PCM changes from a solid to a liquid form, with an increase of ambient temperature, absorbing heat (endothermic process), though it reverts to the solid state when the



**Fig. 1.** (a) 3D rendering of a seamless building [8], (b) 3D rendering of a functionally graded wall, and (c) a functionally graded concrete building component produced by AM [9].

temperature decreases again, releasing back the absorbed heat. Materials like salt hydrates, paraffin waxes, fatty acids and eutectics of organic and non-organic compounds have largely been studied [11, 12]. According to Baetens et al. [13], the heat capacity of concrete containing PCM is 10 times higher than gypsum plasterboards, reaching  $8000 \text{ kJ}/(\text{m}^2 \text{ K})$  at the transition temperature. However, its extensive use in a building seems to represent a high initial capital investment, so the use of concrete printing technologies will enable to strategically place PCM in specific areas, this way reducing material costs though optimizing its performance.

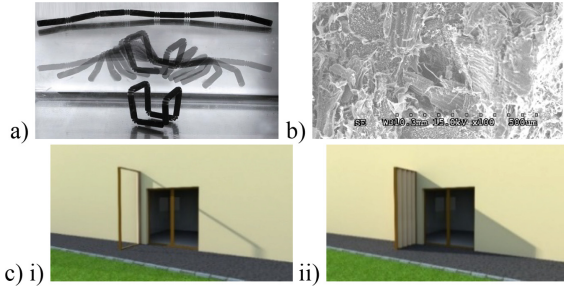
### 2.3 Shape Memory Materials

Kinetic facades are dynamic and adaptable, acting as an outer building skin providing either insulation or solar shading, in response to climatic scenarios and user needs [14, 15]. Commercial systems, usually electrically driven and controlled, are composed of moving surfaces interacting physically with the environment [14]. Conversely, the use of shape memory materials, shape memory polymers (SMP) and shape memory alloys (SMA), need no conventional actuators and controls, as the material itself provides a similar functionality by 4D design.

#### Shape Memory Polymers

SMP represent a group of polymers that can recover their original shape through an external stimuli, such as temperature, lighting or moisture [16]. Time-dependent shape-shifting changes generally requires a step-by-step thermo-mechanical protocol: (i) programming (fixing to the deformed shape) - involving the deformation of the SMP above a transition temperature ( $T_d$ ), subsequently a cooling down below  $T_d$ , followed by unloading; (ii) recovery - comprising heating above  $T_d$  to recover the original shape by entropic elasticity [17].

On the other hand, shading systems can reduce solar radiation transmittance through windows, like external folding shutters sensible to the outside temperature opening whenever the sun heats the system. 3D/4D printing technologies could produce multi-material polymer systems, including panels composed by thermoplastic polymers reinforced with wood fibers [18, 19] and hinges made by SMP with specified thermomechanical behaviors [16, 20, 21] (Fig. 2).

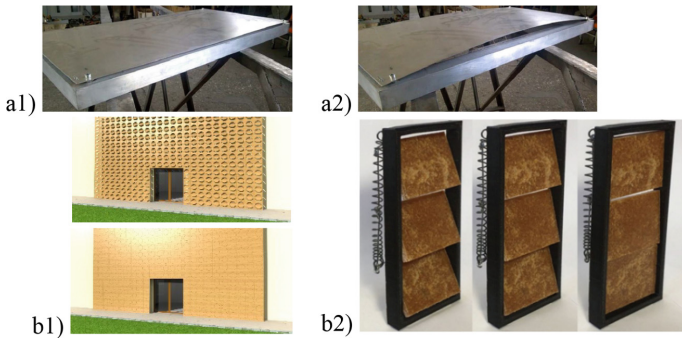


**Fig. 2.** (a) Self-folding of a 4D printed multi-material single strand into a three-dimensional cube [20], (b) Scanning electron microscope image of wood polymer composite made by extrusion technology, and (c) 3D renderings of a self-folding shutter, closed (i) and opened (ii).

**Shape Memory Alloys**

A SMA is a metallic material, such as Nitinol (Ni-Ti) alloy, which can recover from a deformed state to the original shape when subjected to a thermal cycle. Its shape is fixed by a thermal treatment. When SMA are plastically deformed at low temperatures, they can recover its shape just by warming up. In this case, they are named “one-way” SMA. The so-called “two-way” SMA changes shape after a cooling step too [22].

SMA wire can be used for dynamic facades, as proposed by Formentini and Lenci [23], who developed a ventilated facade prototype using a Ni-Ti wire to force aluminum panels bending in summer (30 °C), allowing natural ventilation (Fig. 3a). Figure 3b1 shows a facade using a Ni-Ti spring to kinetically rotate panels with heat. A mockup is presented in Fig. 3b2, which is part of an ongoing work.



**Fig. 3.** Kinetic facades: (a) ventilated facade prototype panel (1) unstressed in a closed position, (2) stressed in an open position [23], (b1) 3D renderings of a kinetic facade and (b2) mockup representing this rendering, closing when the nitinol spring is subjected to temperature variation.

AM has been used to manufacture SMA components, such as rectangular cubes obtained by selective laser melting using powder material [24]. Wang et al. [25] compared different AM technologies to produce parts with premixed Ni-Ti powders, considering directed energy deposition as the best AM technology for this application.

### 3 Conclusions

Building facades are important elements of the building envelope, playing an essential role in energy consumption and comfort in buildings. An improved material design can enhance the potential of a more effective use of the external climate, requiring the minimum energy to keep comfort inside.

There is a great potential for 3D/4D printing building components to address actual and future built environmental challenges. Printing structures that can change its shape over time if exposed to a stimulus as lighting, moisture or heat, could revolutionize the way buildings interact in real time with surrounding environments. 3D printing buildings are still in its infancy, several limitations and barriers need to be addressed, though architects and engineers must keep looking forward and the use of 4D design could bring “life” to buildings, by reducing its operational energy demand and materials usage, and minimizing CO<sub>2</sub> emissions.

### References

1. Global Alliance for Buildings and Construction: 2018 Global Status Report - Towards a zero-emission, efficient and resilient buildings and construction sector. United Nations Environment Programme (2018)
2. Barozzi, M., Lienhard, J., Zanelli, A., Monticelli, C.: The sustainability of adaptive envelopes: developments of kinetic architecture. *Procedia Eng.* **155**, 275–284 (2016). <https://doi.org/10.1016/j.proeng.2016.08.029>
3. Craveiro, F., Duarte, J.P., Bartolo, H., Bartolo, P.J.: Additive Manufacturing as an enabling technology for digital construction: a perspective on Construction 4.0. *Automation in Constr.* **103**, 251–267 (2019). <https://doi.org/10.1016/j.autcon.2019.03.011>
4. Craveiro, F., Bartolo, H.B., Bartolo, P.J., Duarte, J.P.: Fabricating construction elements with varying material composition: a case study. In: *Proceedings of the 39th International MATADOR Conference*. Springer, Manchester (2018)
5. Thomaz, E., Sousa, H., Roman, H., Morton, J., Silva, J.M., Corrêa, M., Pfeiffermann, O., Lourenço, P.B., Vicente, R.S., Sousa, R.: Defects in masonry walls. Guidance on cracking: identification, prevention and repair. In: *International Council for Research and Innovation in Building and Construction* (2015)
6. Craveiro, F., Bartolo, H.M., Gale, A., Duarte, J.P., Bartolo, P.J.: A design tool for resource-efficient fabrication of 3d-graded structural building components using additive manufacturing. *Autom. Constr.* **82**, 75–83 (2017). <https://doi.org/10.1016/j.autcon.2017.05.006>
7. Craveiro, F., Bartolo, H., Bartolo, P.J., Nazarian, S., Duarte, J.P.: Additive manufacturing of functionally graded building parts: towards seamless architecture. In: *4th Biennial Residential Building Design & Construction Conference Proceedings*, pp. 529–540. Pennsylvania Housing Research Center, State College, PA USA (2018)
8. DEN@MARS: Development of Functionally Graded Materials - NASA 3D Printed Mars Habitat Challenge Phase 3 - Penn State - Virtual Construction Level 2 (2019). <https://www.youtube.com/watch?v=iVDY5m2lx3w>
9. Craveiro, F., Bartolo, H., Bartolo, P.J., Nazarian, S., Duarte, J.P.: An automated system for 3D printing functionally graded concrete-based materials. Manuscript submitted for publication (2019)



10. Tang, W., Wang, Z., Mohseni, E., Wang, S.: A practical ranking system for evaluation of industry viable phase change materials for use in concrete. *Constr. Build. Mater.* **177**, 272–286 (2018). <https://doi.org/10.1016/j.conbuildmat.2018.05.112>
11. Kenisarin, M., Mahkamov, K.: Passive thermal control in residential buildings using phase change materials. *Renew. Sustain. Energy Rev.* **55**, 371–398 (2016). <https://doi.org/10.1016/j.rser.2015.10.128>
12. Desai, D., Miller, M., Lynch, J.P., Li, V.C.: Development of thermally adaptive Engineered Cementitious Composite for passive heat storage. *Constr. Build. Mater.* **67**, 366–372 (2014). <https://doi.org/10.1016/j.conbuildmat.2013.12.104>
13. Baetens, R., Jelle, B.P., Gustavsen, A.: Phase change materials for building applications: a state-of-the-art review. *Energy Build.* **42**, 1361–1368 (2010). <https://doi.org/10.1016/j.enbuild.2010.03.026>
14. Johnsen, K., Winther, F.V.: Dynamic facades, the smart way of meeting the energy requirements. *Energy Procedia* **78**, 1568–1573 (2015). <https://doi.org/10.1016/j.egypro.2015.11.210>
15. López, M., Rubio, R., Martín, S., Croxford, B., Jackson, R.: Active materials for adaptive architectural envelopes based on plant adaptation principles. *J. Facade Des. Eng.* **3**, 27–38 (2015). <https://doi.org/10.3233/FDE-150026>
16. Mao, Y., Yu, K., Isakov, M.S., Wu, J., Dunn, M.L., Jerry Qi, H.: Sequential self-folding structures by 3D printed digital shape memory polymers. *Sci. Rep.* **5** (2015). <https://doi.org/10.1038/srep13616>
17. Bodaghi, M., Damanpack, A.R., Liao, W.H.: Adaptive metamaterials by functionally graded 4D printing. *Mater. Des.* **135**, 26–36 (2017). <https://doi.org/10.1016/j.matdes.2017.08.069>
18. Le Duigou, A., Castro, M., Bevan, R., Martin, N.: 3D printing of wood fibre biocomposites: From mechanical to actuation functionality. *Mater. Des.* **96**, 106–114 (2016). <https://doi.org/10.1016/j.matdes.2016.02.018>
19. Henke, K., Treml, S.: Wood based bulk material in 3D printing processes for applications in construction. *Eur. J. Wood Wood Prod.* **71**, 139–141 (2013). <https://doi.org/10.1007/s00107-012-0658-z>
20. Tibbits, S.: 4D printing: multi-material shape change. *Archit. Des.* **84**, 116–121 (2014). <https://doi.org/10.1002/ad.1710>
21. Zhang, Q., Zhang, K., Hu, G.: Smart three-dimensional lightweight structure triggered from a thin composite sheet via 3D printing technique. *Sci. Rep.* **6**, (2016). <https://doi.org/10.1038/srep22431>
22. Otsuka, K., Ren, X.: Physical metallurgy of Ti–Ni-based shape memory alloys. *Prog. Mater. Sci.* **50**, 511–678 (2005). <https://doi.org/10.1016/j.pmatsci.2004.10.001>
23. Formentini, M., Lenci, S.: An innovative building envelope (kinetic facade) with Shape Memory Alloys used as actuators and sensors. *Autom. Constr.* **85**, 220–231 (2018). <https://doi.org/10.1016/j.autcon.2017.10.006>
24. Elahinia, M., Shayesteh Moghaddam, N., Amerinatanzi, A., Saedi, S., Toker, G.P., Karaca, H., Bigelow, G.S., Benafan, O.: Additive manufacturing of NiTiHf high temperature shape memory alloy. *Scripta Mater.* **145**, 90–94 (2018). <https://doi.org/10.1016/j.scriptamat.2017.10.016>
25. Wang, C., Tan, X.P., Du, Z., Chandra, S., Sun, Z., Lim, C.W.J., Tor, S.B., Lim, C.S., Wong, C.H.: Additive manufacturing of NiTi shape memory alloys using pre-mixed powders. *J. Mater. Process. Technol.* **271**, 152–161 (2019). <https://doi.org/10.1016/j.jmatprotec.2019.03.025>

# Author Index

## A

Afonso, Mário, 73  
Almeida, Henrique, 10, 162  
Almeida, Henrique A., 20, 171  
Alqahtani, Mohammed S., 155  
Alves, Bruno, 28  
Alves, M. L., 189, 225  
Alves, Rafael M. E., 189  
Antunes, F. V., 213  
Asai, Satoru, 89, 96  
Ascenso, Rita M. T., 171  
Aslan, Enes, 243, 250, 258  
Atzeni, Eleonora, 206  
Ayvaz, Peter, 28  
Azhar, Ezrin Faten, 143

## B

Baptista, R., 131  
Barros, Ana C., 49  
Bártolo, Helena, 277  
Bartolo, P. J., 155, 243, 250, 258  
Bártolo, Paulo, 277  
Beirão, José Nuno, 102, 110  
Biamino, Sara, 206  
Blunn, Gordon, 250  
Branco, R., 213, 219  
Busatto, Mattia, 206

## C

Cadete, Mylene S., 183  
Campos, Maria J., 189  
Capela, Carlos, 198, 213, 219  
Carreira, João, 162

Carvalho, Alexandre R. F., 57  
Castro, Hélder F., 57  
Clucas, Don, 265  
Cooper, Glen, 155, 243, 250  
Correia, M. S., 225  
Costa, Alfredo, 183  
Costa, J. D., 213, 219  
Craveiro, Flávio, 277

## D

Daskalakis, Evangelos, 250  
Dias-de-Oliveira, João, 183  
Diver, Carl, 258  
Dixon, Freya, 265  
dos Santos Silva, Gleiciane, 198  
Duarte, José P., 277

## E

Ehrmann, Andrea, 171, 271  
Eisenbarth, Daniel, 125

## F

Fee, Conan, 265  
Ferreira, J. A. M., 213  
Fino, Paolo, 206  
Fonseca, Maria, 183  
Fujiwara, Toshihiro, 96

## G

Gaspar, Marcelo, 198  
Gomes, Reinaldo, 65  
Gomes, Tiago E. P., 183  
Gouveia, Helena, 57

Guarda, Fabiana, [73](#)  
 Guardão, Luís, [65](#)  
 Guedes, M., [131](#)

**H**

Hattori, Kazunori, [89](#)  
 Hernández, Elder, [49](#), [65](#)  
 Huber, Tim, [265](#)  
 Humphreys, Gavin, [258](#)

**I**

Iuliano, Luca, [206](#)

**K**

Kampker, Achim, [28](#)  
 Kempton, William, [3](#)  
 Killi, Steinar, [3](#)  
 Klaeger, Uwe, [40](#)  
 Koç, Bahattin, [250](#)

**L**

Lai, Manuel, [206](#)  
 Leal, Fátima, [57](#)  
 Liu, Fengyuan, [250](#)  
 Loh, Giselle Hsiang, [143](#)

**M**

Marques, Alexandra, [65](#)  
 Marrazes, Luís, [73](#)  
 Martins Ferreira, J. A., [219](#)  
 Mishbak, H., [243](#)  
 Mughal, Humera, [110](#)

**N**

Nakonetchnei, Elis Cassiana, [137](#)  
 Nam, Seok Woo, [143](#)  
 Neto, Victor, [183](#)  
 Nomura, Kazufumi, [89](#)

**O**

Ogino, Yosuke, [89](#), [96](#)  
 Omar, Abdalla M., [155](#)

**P**

Pedgley, Owain, [82](#)  
 Pei, Eujin, [143](#)  
 Piperi, Erald, [171](#), [271](#)  
 Piscopo, Gabriele, [206](#)

**R**

Rama, Dudina, [271](#)  
 Ramalho, A., [225](#)  
 Ramalho, F. Q., [225](#)  
 Ramos, A., [119](#)  
 Rebelo, Rui, [49](#), [65](#)  
 Relvas, C., [119](#)

**S**

Saboori, Abdollah, [206](#)  
 Sakamoto, Shin-ichi, [96](#)  
 Salmi, Alessandro, [206](#)  
 Santos, Deborah M., [102](#)  
 Santos, L., [219](#)  
 Santos, L. M. S., [213](#)  
 Senna, Pedro, [49](#)  
 Serrano, Emanuel, [20](#)  
 Shehi, Ermira, [271](#)  
 Shigueoka, Marcelo Okada, [137](#)  
 Silva, Daniela, [49](#)  
 Soares, Ricardo, [65](#)  
 Soffel, Fabian, [125](#)  
 Spahiu, Tatjana, [171](#), [271](#)

**T**

Tamura, Kosuke, [96](#)  
 Telesh, Andriy, [40](#)  
 Toscano, César, [49](#)  
 Toushekhah, Mostafa, [206](#)  
 Tusacciu, Simona, [206](#)

**V**

Vasco, Joel, [10](#), [162](#)  
 Vilhena, L. M., [225](#)  
 Vitorino, Liliana, [20](#)  
 Vitorino, Liliana C., [171](#)  
 Volpato, Neri, [137](#)  
 Vyas, Cian, [258](#)

**W**

Wegener, Konrad, [125](#)  
 Weightman, Andrew, [250](#)

**Y**

Yardim Sener, Sevcan, [82](#)

**Z**

Zadeh, Hossein Najaf, [265](#)